

**MOLECULAR CLONING AND CHARACTERIZATION OF IMPORTANT
STRESS AND REDOX REGULATORY GENES FROM *HYDRA VULGARIS***

A Dissertation

by

BHAGIRATHI DASH

Submitted to the Office of Graduate Studies of
Texas A&M University
in partial fulfillment of the requirements for the degree of

DOCTOR OF PHILOSOPHY

December 2005

Major Subject: Toxicology

**MOLECULAR CLONING AND CHARACTERIZATION OF IMPORTANT
STRESS AND REDOX REGULATORY GENES FROM *HYDRA VULGARIS***

A Dissertation

by

BHAGIRATHI DASH

Submitted to the Office of Graduate Studies of
Texas A&M University
in partial fulfillment of the requirements for the degree of

DOCTOR OF PHILOSOPHY

Approved by:

Chair of Committee,
Committee Members,

Head of Department,

Timothy D. Phillips
Stephen H. Safe
Richard H. Loeppert
Kirby C. Donnelly
Robert C. Burghardt

December 2005

Major Subject: Toxicology

ABSTRACT

Molecular Cloning and Characterization of Important Stress and Redox

Regulatory Genes from *Hydra vulgaris*. (December 2005)

Bhagirathi Dash, B. Sc., Orissa University of Agriculture and Technology at

Bhubaneswar; M. Sc., Punjab Agricultural University at Ludhiana

Chair of Advisory Committee: Dr. Timothy D. Phillips

In this research, important stress and redox regulatory genes present in *Hydra vulgaris* were isolated and characterized to facilitate our understanding of the evolution and mechanisms of stress response. *H. vulgaris* heat shock protein 70 (HvHSP70), extracellular copper zinc superoxide dismutase (HvEC-CuZnSOD), manganese superoxide dismutase (HvMnSOD), phospholipid peroxidase glutathione peroxidase (HvPHGPx) and monofunctional catalase (HvCatalase) were cloned and characterized with regard to stress response, phylogeny and molecular structure.

The HSP70 gene isolated from *H. vulgaris* encodes a polypeptide of 650 amino acids ($M_w=710,037$) and is interrupted by three intron sequences. The 5' non-coding region of the HvHSP70 possessed the canonical heat shock elements. Phylogenetically HvHSP70 formed a distinct lineage. A molecular model generated for the N-terminal fragment of the HvHSP70 displayed the heat shock protein fold and domains of phosphotransferases.

The EC-CuZnSOD cDNA isolated from *H. vulgaris* encodes a protein of 189 amino acids ($M_w=20959.73$); the first 19 amino acids constitute the presumed signal peptide. Phylogenetically HvEC-CuZnSOD is grouped with EC-CuZnSODs from several organisms. A molecular model generated for the HvEC-CuZnSOD displayed the CuZnSOD β -barrel fold.

The MnSOD cDNA isolated from *H. vulgaris* encodes a protein of 219 amino acids ($M_w=24348.75$); the first 21 amino acids constitute the presumed mitochondria-targeting signal peptide. Phylogenetically HvMnSOD is clustered with mollusk and crustacean MnSODs. A molecular model generated for the HvMnSOD displayed the N-terminal long alpha antiparallel hairpin and the C-terminal mixed alpha/beta fold characteristic of MnSODs.

The PHGPx gene isolated from *H. vulgaris* encodes a polypeptide of 168 amino acids ($M_w=18746.51$) including a TGA-encoded selenocysteine at residue 44 and lacks any intron. Phylogenetically HvPHGPx is grouped with PHGPxs from several organisms. A molecular model generated for the HvPHGPx displayed the thioredoxin fold.

The 3'-end of a cDNA sequence encoding for 168 amino acids of the C-terminal end of a catalase was isolated from *H. vulgaris*. Phylogenetically HvCatalase is grouped with heme-containing monofunctional catalases.

Hydrae exposed to thermal, starvation, oxidative and metal stress responded by regulating respective mRNA transcriptions suggesting that these

genes are involved in stress and (anti)oxidative processes and may have potential as molecular biomarkers for assessing aquatic environment quality.

DEDICATION

To my parents Srimati Shantilata Dash and Sri Ananta Charan Dash, my brother Amarendra Kumar Dash and sister-in-law Harapriya Dash.

ACKNOWLEDGEMENTS

I would like to thank my advisor Dr. Timothy D. Phillips for giving me an opportunity to carry out research towards my Ph. D. in Toxicology. I express my gratitude to him for supporting me as a Graduate Assistant (Research) for three years. His support, encouragement and leadership have been instrumental in successfully conducting and concluding the studies. The confidence and competence perfused by him will go a long way in shaping my life.

I sincerely thank my advisory committee members: Dr. Stephen H. Safe, Dr. Richard H. Loeppert and Dr. Kirby C. Donnelly for their valuable input during the course of my research and for critically reading the dissertation and making valuable suggestions for its improvement.

I offer my respectful thanks to Dr. Weston Porter and Dr. Rick Metz for their valuable technical guidance and help during the course of my research.

I am indebted and obliged to lab members (past and present): Dr. Henry Huebner, Dr. Evans Afriyie-Gyawu, Dr. Melinda Wiles, John Taylor, Molly Richardson and Natalie Malek for their help and moral support during the course of my research work.

I express my sincere feelings to my friends Vivek, Binoy, Kabi, Chaitu, Rupak and Woddi for their help and moral support during my stay and study at A&M.

I thank my family members for their love, inspiration and sacrifices during my doctoral work.

TABLE OF CONTENTS

	Page
ABSTRACT	iii
DEDICATION	vi
ACKNOWLEDGEMENTS.....	vii
TABLE OF CONTENTS.....	viii
LIST OF FIGURES	xiv
LIST OF TABLES	xviii
 CHAPTER	
I INTRODUCTION	1
1.1 Hydra: Basic structure, morphology and life	2
1.2 Hydra as an experimental model organism	6
1.2.1 Cell death and cell fate	7
1.2.2 Development and generation of the embryonic body axes and patterning	9
1.2.3 Development and evolution of nervous system .	12
1.2.4 Environmental toxicology and toxicity testing	15
1.2.5 Environmental and oxidative stress	18
1.2.6 A genomic tool kit	19
1.3 Habitat of hydra: Exposure to environmental contaminants and stressors in the aquatic environment ..	20
1.4 Exposure to environmental contaminants and stressors: Stress proteins and antioxidant enzymes	24
1.4.1 Heat shock protein 70.....	29
1.4.2 Superoxide dismutases	29
1.4.3 Catalases and peroxidases	30
1.4.4 Glutathione peroxidases	31
1.5 Stress proteins and antioxidant enzymes in aquatic organisms.....	31
1.6 Stress proteins and antioxidant enzymes in cnidarians...	32
1.6.1 Sea anemones	33
1.6.1.1 <i>Anthopleura elegantissima</i>	33
1.6.1.2 <i>Anemonia viridis</i>	34
1.6.1.3 <i>Aiptasia pulchella</i>	36

CHAPTER	Page
1.6.1.4 <i>Actinia schmidtii</i>	36
1.6.2 Corals	36
1.6.2.1 <i>Montastraea faveolata</i>	36
1.6.2.2 <i>Stylophora pistillata</i>	37
1.6.2.3 <i>Platygyra ryukyuensis</i>	39
1.6.2.4 <i>Plexaura homomalla</i>	39
1.6.2.5 <i>Montastrea annularis</i>	39
1.6.2.6 <i>Tubastrea cocchineae</i>	40
1.6.2.7 <i>Astrangia danae</i>	40
1.6.2.8 <i>Corynactis californica</i>	41
1.6.3 Sea fans	41
1.6.3.1 <i>Leptogorgia virgulata</i>	41
1.6.4 Jelly fish.....	42
1.6.4.1 <i>Aurelia</i>	42
1.7 Research hypotheses.....	43
1.8 Research objectives	46
II MOLECULAR CLONING AND CHARACTERIZATION OF A HEAT SHOCK PROTEIN 70 FROM <i>HYDRA VULGARIS</i>	48
2.1 Materials and methods.....	51
2.1.1 Hydra culture	51
2.1.2 RNA isolation and clean up	51
2.1.3 Oligonucleotides	52
2.1.4 Cloning and identification of a partial fragment of <i>H. vulgaris</i> HSP70 cDNA.....	52
2.1.5 3'-RACE of the HvHSP70 cDNA.....	58
2.1.6 5'-RACE of the HvHSP70 cDNA.....	62
2.1.7 Cloning the 5' non-coding region	64
2.1.8 Determination of the exon/intron structure of the HvHSP70 gene	64
2.1.9 Heat treatment.....	66
2.1.10 Metal treatment.....	68
2.1.11 Oxidative stress treatment.....	68
2.1.12 Starvation treatment	68
2.1.13 Expression analysis of HvHSP70 mRNA in hydrae	69
2.1.14 General bioinformatic analyses	70
2.1.15 Phylogenetics	70
2.1.16 Threading	72
2.1.17 Molecular modeling	73
2.1.18 Analysis of the model.....	73

CHAPTER	Page
2.2 Results	78
2.2.1 Cloning and analysis of HSP70 gene	78
2.2.2 Exon/intron structure of the HvHSP70 gene	81
2.2.3 The 5' non-coding region	81
2.2.4 Sequence conservation in HSP70 proteins	83
2.2.5 Phylogenetic analysis	84
2.2.6 The structural model of HvHSP70	84
2.2.7 HvHSP70 mRNA expression analysis	89
2.3 Discussion	91
III MOLECULAR CLONING AND CHARACTERIZATION OF A MANGANESE SUPEROXIDE DISMUTASE FROM <i>HYDRA</i> <i>VULGARIS</i>	100
3.1 Materials and methods	101
3.1.1 Hydra culture	101
3.1.2 RNA isolation and clean up	102
3.1.3 Oligonucleotides	102
3.1.4 Cloning and identification of a partial fragment of HvMnSOD cDNA	106
3.1.5 3'-RACE of the HvMnSOD cDNA	109
3.1.6 5'-RACE of the HvMnSOD cDNA	109
3.1.7 Heat treatment.....	110
3.1.8 Metal treatment.....	110
3.1.9 Oxidative stress treatment.....	110
3.1.10 Expression analysis of HvMnSOD mRNA in hydrae	111
3.1.11 General bioinformatic analyses	112
3.1.12 Phylogenetic analysis	113
3.1.13 Threading	114
3.1.14 Molecular modeling	116
3.1.15 Analysis of the model.....	116
3.2 Results	120
3.2.1 Cloning and analysis of HvMnSOD cDNA	120
3.2.2 Sequence conservation in MnSOD proteins	123
3.2.3 Phylogenetic analysis	125
3.2.4 The structural model of HvMnSOD.....	125
3.2.5 HvMnSOD mRNA expression analysis.....	126
3.3 Discussion	129

CHAPTER	Page
IV MOLECULAR CLONING AND CHARACTERIZATION OF AN EXTRACELLULAR COPPER ZINC SUPEROXIDE DISMUTASE FROM <i>HYDRA VULGARIS</i>	135
4.1 Materials and methods.....	137
4.1.1 Hydra culture.....	137
4.1.2 RNA isolation and clean up.....	138
4.1.3 Identification of a partial fragment of <i>H. magnipapillata</i> CuZnSOD cDNA.....	138
4.1.4 Oligonucleotides.....	141
4.1.5 Cloning and identification of a partial fragment of <i>H. vulgaris</i> CuZnSOD cDNA.....	141
4.1.6 3'-RACE of the HvCuZnSOD cDNA.....	143
4.1.7 5'-RACE of the HvCuZnSOD cDNA.....	143
4.1.8 Heat treatment.....	145
4.1.9 Metal treatment.....	145
4.1.10 Oxidative stress treatment.....	146
4.1.11 Starvation treatment.....	146
4.1.12 Expression analysis of HvCuZnSOD mRNA in hydrae.....	146
4.1.13 General bioinformatic analyses.....	147
4.1.14 Phylogenetic analysis.....	148
4.1.15 Threading.....	149
4.1.16 Molecular modeling.....	151
4.1.17 Analysis of the model.....	151
4.2 Results.....	155
4.2.1 Cloning and analysis of HvEC-CuZnSOD cDNA.....	155
4.2.2 Sequence conservation in EC-CuZnSOD protein.....	159
4.2.3 Phylogenetic analysis.....	159
4.2.4 The structural model of HvEC-CuZnSOD.....	161
4.2.5 HvEC-CuZnSOD mRNA expression analysis....	163
4.3 Discussion.....	166
V MOLECULAR CLONING AND CHARACTERIZATION OF A PHOSPHOLIPID HYDROPEROXIDE GLUTATHIONE PEROXIDASE <i>HYDRA VULGARIS</i>	172
5.1 Materials and methods.....	173
5.1.1 Hydra culture.....	173
5.1.2 RNA isolation and clean up.....	174
5.1.3 Identification of a partial fragment of <i>H. magnipapillata</i> PHGPx cDNA.....	174

CHAPTER	Page
5.1.4 Oligonucleotides	177
5.1.5 Cloning and identification of a partial fragment of <i>H. vulgaris</i> PHGPx cDNA	177
5.1.6 3'-RACE of the HvPHGPx cDNA	179
5.1.7 5'-RACE of the HvPHGPx cDNA	179
5.1.8 Determination of the exon/intron structure of the HvPHGPx gene	181
5.1.9 Heat treatment.....	182
5.1.10 Metal treatment.....	182
5.1.11 Oxidative stress treatment.....	182
5.1.12 Expression analysis of HvPHGPx mRNA in hydrae	183
5.1.13 General bioinformatic analyses	184
5.1.14 Phylogenetics	185
5.1.15 Threading	187
5.1.16 Analysis of the model.....	188
5.2 Results	188
5.2.1 Cloning and analysis of HvPHGPx cDNA.....	188
5.2.2 Exon/intron structure of the HvPHGPx gene	193
5.2.3 Sequence conservation in PHGPx proteins.....	193
5.2.4 Phylogenetic analysis	195
5.2.5 The structural model of HvPHGPx.....	197
5.2.6 HvPHGPx mRNA expression analysis.....	198
5.3 Discussion.....	201
VI MOLECULAR CLONING AND CHARACTERIZATION OF A CATALASE FROM <i>HYDRA VULGARIS</i>	205
6.1 Materials and methods.....	207
6.1.1 Hydra culture	207
6.1.2 RNA isolation and clean up	207
6.1.3 Identification of a partial fragment of <i>H. magnipapillata</i> Catalase cDNA	208
6.1.4 Oligonucleotides	208
6.1.5 Cloning and identification of a partial fragment of <i>H. vulgaris</i> Catalase cDNA	208
6.1.6 3'-RACE of the HvCatalase cDNA.....	210
6.1.7 Heat treatment.....	213
6.1.8 Metal treatment.....	213
6.1.9 Oxidative stress treatment.....	213
6.1.10 Expression analysis of HvCatalase mRNA in hydrae	214

CHAPTER	Page
6.1.11 General bioinformatic analyses	215
6.1.12 Phylogenetics	215
6.2 Results	219
6.2.1 Cloning and analysis of HvCatalse cDNA.....	219
6.2.2 Sequence conservation in catalase proteins	220
6.2.3 Phylogenetic analysis	222
6.2.4 HvCatalase mRNA expression analysis	222
6.3 Discussion	225
VII SUMMARY AND CONCLUSIONS.....	228
REFERENCES	244
VITA.....	288

LIST OF FIGURES

FIGURE	Page
1. Hydra and its different body parts	3
2. The electron structure and spin restrictions of various forms of oxygen	22
3. Schematic representation of the role of antioxidant enzymes in preventing oxidative stress.....	23
4. Pathways of metal induced oxidative stress.....	25
5. Multiple sequence alignment of HSP70 proteins using the program ClustalW.....	53
6. HSP70 protein sequence comparison of the <i>H. magnipapillata</i> to that of <i>H. oligactis</i>	56
7. Image of electrophoretic gel for degenerate PCR products of HvHSP70 gene	59
8. Nucleotide and deduced amino acid sequence of <i>H. vulgaris</i> HSP70	60
9. Image of electrophoretic gel for 3'-RACE PCR products of HvHSP70 gene	63
10. Images of electrophoretic gels for 5'-RACE PCR products of HvHSP70 gene	63
11. Image of electrophoretic gel for PCR products of 5' flanking sequence of HvHSP70 gene.....	65
12. Image of electrophoretic gel for genomic PCR products of HvHSP70 gene	67
13. Target and template assembly used for generation of HvHSP70 model.....	74
14. A 3D model of the N-terminal fragment of the HvHSP70	75
15. Secondary structural elements of the HvHSP70 model	76

FIGURE	Page
16. Ramachandran plot of model HvHSP70	77
17. Phylogenetic alignment of the amino acid sequences of the HSP70s from different organisms	85
18. Expression analysis of HSP70 mRNA from <i>H. vulgaris</i> exposed to thermal, starvation, metal and oxidative stress	90
19. Expression analysis of HSP70 mRNA from <i>H. vulgaris</i> exposed to metal and oxidative stress for 1 h	92
20. Multiple sequence alignment of MnSOD proteins performed using the program ClustalW	103
21. Images of electrophoretic gels for PCR products of HvMnSOD gene	107
22. Nucleotide and deduced amino acid sequence of <i>H. vulgaris</i> manganese superoxide dismutase	108
23. Phylogenetic alignment of the amino acid sequences of the MnSODs from different organisms	115
24. Target and template assembly used for generation of <i>H. vulgaris</i> MnSOD model	117
25. A 3D model of the <i>H. vulgaris</i> MnSOD	110
26. Secondary structural elements of the HvMnSOD model	119
27. Ramachandran plot of model HvMnSOD	119
28. Expression analysis of MnSOD mRNA from <i>H. vulgaris</i> exposed to thermal, metal and oxidative stress	128
29. Expression analysis of MnSOD mRNA from <i>H. vulgaris</i> exposed to metal and oxidative stress for 1 h	130
30. Multiple sequence alignment of CuZnSOD proteins performed using the program ClustalW	139

FIGURE	Page
31. Images of electrophoretic gels for PCR products of HvEC-CuZnSOD gene.....	142
32. Nucleotide and deduced amino acid sequence of <i>H. vulgaris</i> extracellular CuZnSOD	144
33. Phylogenetic alignment of the amino acid sequences of the CuZnSODs from different organisms	150
34. Target and template assembly used for generation of <i>H. vulgaris</i> EC-CuZnSOD model	152
35. A 3D model of the <i>H. vulgaris</i> EC-CuZnSOD.....	153
36. Secondary structural elements of the HvEC-CuZnSOD model	154
37. Ramachandran plot of model HvEC-CuZnSOD	154
38. Expression analysis of EC-CuZnSOD mRNA from <i>H. vulgaris</i> exposed to thermal, starvation, metal and oxidative stress.....	164
39. Expression analysis of EC-CuZnSOD mRNA from <i>H. vulgaris</i> under metal and oxidative stress for 1 h	165
40. Multiple sequence alignment of PHGPx proteins performed using program ClustalW	175
41. Images of electrophoretic gels for PCR products of HvPHGPx gene.....	178
42. Nucleotide and deduced amino acid sequence of <i>H. vulgaris</i> PHGPx cDNA.....	180
43. Phylogenetic alignment of the amino acid sequences of the glutathione peroxidases from different organisms.....	186
44. A 3D model of <i>H. vulgaris</i> PHGPx	189
45. The secondary structural elements of the HvPHGPx model	190
46. Expression analysis of PHGPx mRNA from <i>H. vulgaris</i> exposed to thermal, starvation, metal and oxidative stress	199

FIGURE	Page
47.Expression analysis of PHGPx mRNA from <i>H. vulgaris</i> under metal and oxidative stress for 1 h	200
48.Images of electrophoretic gels for PCR products of HvCatalase gene.....	211
49.Partial nucleotide and deduced amino acid sequence of <i>H. vulgaris</i> monofunctional catalase	212
50.Multiple sequence alignment of catalase proteins using the program ClustalW.....	216
51.Phylogenetic alignment of the amino acid sequences of the catalases from different organisms	218
52.Expression analysis of catalase mRNA from <i>H. vulgaris</i> exposed to exposed to thermal, starvation, metal and oxidative stress.....	223
53.Expression analysis of catalase mRNA from <i>H. vulgaris</i> exposed to metal and oxidative stress for 1 h	224

LIST OF TABLES

TABLE	Page
1. Representative cnidarians.....	4
2. The minimal stress proteome of cellular organisms	26
3. Antioxidant defense system of cellular organisms	28
4. Oligonucleotides used in the cloning of HvHSP70 gene	57
5. Amino acid composition of the HvHSP70 polypeptide	80
6. Similarities among <i>H. vulgaris</i> HSP70 and 70 kDa heat shock proteins from other organisms	82
7. Comparison of the Ramachandran plot statistics between template 3HSC and the model HvHSP70	88
8. Oligonucleotides used in the cloning of HvMnSOD cDNA	105
9. Amino acid composition of the HvMnSOD polypeptide.....	122
10. Similarities among <i>H. vulgaris</i> MnSOD and Mn-/Fe-SOD proteins from other organisms	124
11. Comparison of the Ramachandran plot statistics between the model HvMnSOD and the template 1LUV: A	127
12. Oligonucleotides used in the cloning of HvEC-CuZnSOD cDNA	140
13. Amino acid composition of the HvEC-CuZnSOD polypeptide.....	157
14. Similarities among <i>H. vulgaris</i> EC-CuZnSOD and (EC)-CuZnSOD proteins from other organisms	160
15. Comparison of the Ramachandran plot statistics between the model HvEC-CuZnSOD and the template 1N18	162
16. Oligonucleotides used in the cloning of HvPHGPx gene	176
17. Ramachandran plot statistics of the 3D model of HvPHGPx.....	191

TABLE	Page
18. Composition of the HvPHGPx polypeptide	194
19. Similarities among <i>H. vulgaris</i> PHGPx and GPx proteins from other organisms	196
20. Oligonucleotides used in cloning of the partial sequence of HvCatalase	209
21. Similarities among <i>H. vulgaris</i> catalase and catalase proteins from other organisms	221

CHAPTER I

INTRODUCTION

Hydrae are an evolutionarily primitive group of invertebrates and belong to the phylum Cnidaria, the second oldest phylum of the animal kingdom (Field *et al.*, 1988) (Figure 1). The Cnidaria phylum is supposed to have diverged about 700 million years ago, preceding the Cambrian explosion, a period when most ancestors to bilaterian species arose (Raff, 1996; Nielsen, 1997; Ayala and Rzhetsky, 1998). Cnidarian species distributed in four distinct groups (or classes) (Table 1), anthozoans (anemones and corals), scyphozoans and cubozoans (jellyfish), and hydrozoans (hydrae), which alternate the polyp and the medusa shape in their life cycle. Most cnidarians are marine animals (e.g., jelly fish, corals; etc.), however, hydra (e.g., *H. vulgaris*, *H. magnipapillata*, *H. oligactis*; etc.) are fresh water cnidarians. Cnidarians display a radial symmetry either as a polyp or as medusa. They are made up of two cell layers, ectoderm and endoderm, separated by an extracellular matrix named mesoglea. Hydrae, members of the class Hydrozoa, are present before the divergence of the protostomes and deuterostomes (Field *et al.*, 1988).

This dissertation follows the style of *Toxicological Sciences*.

1. 1 Hydra: Basic structure, morphology and life

Hydra sp., a simple freshwater cnidarian, is organized as a gastric tube and is very small in size (Figure 1). For example, *H. vulgaris* is a small freshwater polyp, about 1 cm in height, and has a simple morphology (Golstein *et al.*, 2003). The mouth and tentacle ring of hydra are at its head pole and a peduncle and mucous cell disc at its foot pole (Bode, 1996). The gastric tube is considered as the longitudinal axis of the organism. Its body wall along the entire longitudinal axis is structurally reduced to an epitheliomuscular bilayer with an intervening extracellular matrix (Sarras *et al.*, 1991). This bilayer is composed of about 20 cell types, including ectodermal and endodermal epitheliomuscular cells, and various interstitial cells such as nerve cells, gametes and nematocysts (Bode, 1996).

The cells of hydra are in a dynamic state of proliferation and turnover. Because of this extensive cell turnover, hydra is in a perpetual embryonic state and therefore has an extensive regenerative capacity (Bosch, 1998). The interstitial cells arise from interstitial stem cells that reside along the gastric column (Bode, 1996). Epithelial cells continuously proliferate along the body column and migrate toward the poles, where they are eventually shed (Bode, 1996; Bode *et al.*, 1986). Epithelial cells that are displaced into the base of tentacles or the basal disc of the foot process differentiate into phenotypes specific to the head (i.e. squamous battery cells in tentacles) or foot regions (columnar mucous cells in the basal disc) (Bode, 1996; Bode *et al.*, 1986).

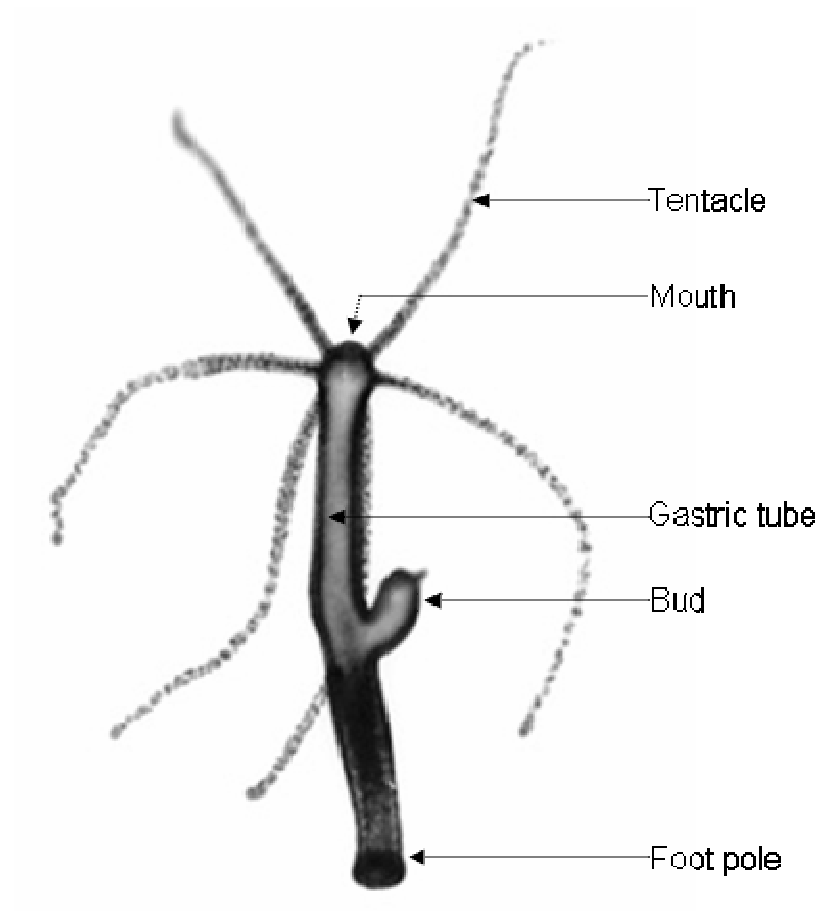


Figure 1. Hydra and its different body parts.

TABLE 1

Representative Cnidarians ^a				
Class	Group	Common name	Scientific name	Family
Anthozoa	Anemones	-	<i>Anemonia viridis</i>	Actiniidae
		-	<i>Aiptasia pulchella</i>	Aiptasiidae
		-	<i>Anthopleura elegantissima</i>	Actiniidae
	Corals	Stony coral	<i>Montastraea faveolata</i>	Faviidae
		boulder star coral	<i>Montastrea annularis</i>	Faviidae
		reef-building coral	<i>Stylophora pistillata</i>	Pocilloporidae
		black coral	<i>Antipathes fiordensis</i>	Antipathidae
		orange cup coral	<i>Tubastrea cocchineae</i>	Dendrophylliidae
		-	<i>Leptogorgia virgulata</i>	Gorgoniidae
	Sea fans	-	<i>Renilla koellikeri</i>	Renillidae
	Sea pens	sea pansy		
	Jellyfish	moon jellyfish	<i>Aurelia aurita</i>	Ulmaridae
		crown jellyfish	<i>Atolla vanhoeffeni</i>	Atollidae
		Stalked jellyfish	<i>Depastromorpha africana</i>	Cleistocarpidae
Cubozoa	Sea wasps	-	<i>Chironex fleckeri</i>	Chirodropidae
Hydrozoa	Hydra	-	<i>H. vulgaris</i>	Hydridae
		-	<i>H. magnipapillata</i>	Hydridae
		-	<i>H. oligactis</i>	Hydridae
		Swiftwater hydra	<i>H. littoralis</i>	Hydridae
	Fire corals	-	<i>Millepora exaesa</i>	Milleporidae

^aCompiled from NCBI taxonomy browser

Interactions between the epithelial and the interstitial cell lineages are highly regulatory. For example the control of nerve cell differentiation is regulated by epitheliopeptides (Shimizu and Fujisawa, 2003).

The interstitial stem cell, otherwise common stem cell, gives rise to four specialized cell differentiation products: neurons, nematocytes, gland cells and gametes (David, 1973; Bode, 1996). Gland cells and gametes are produced when the animal follows the sexual life cycle. The nematocytes undergo four to five synchronous syncytial cell cycle divisions, forming nests of nematoblasts into the ectoderm of the body column. Once proliferation stops, the nematoblasts differentiate their nematocyst vacuole and finally most of them migrate to the tentacles (Campbell, 1988; Campbell and Marcum, 1980). In the tentacles several nematocytes are embedded within large epithelial cells known as battery cells, and these establish synapses with sensory neurons.

The hydra nervous system is formed of sensory-motor neurons, ganglia neurons and mechanoreceptor cells named nematocytes, which all differentiate from common stem cells. Ganglia neurons are the most common type of nerve cells and spread among the mesoglea. Cell bodies of most sensory neurons are located within the ectodermal layer, while their processes reach the surface. Neurons represent about 3 % of the total cell number in hydra (David, 1973) and are organized as a nerve net. This nerve net is not uniform and distinct subsets of neurons with specific spatial distribution could be identified (Grimmelikhuijzen *et al.*, 1989; Koizumi *et al.*, 1992). For example, the RFamide-expressing

neurons are more abundant in the hydra head and foot regions while they are almost absent in the central part of the body column (Grimmelikhuijzen and Westfall, 1995). In addition to the nerve net, a dense anatomical structure named the nerve ring is also identified at the base of tentacles of some hydra species (Koizumi *et al.*, 1992). Similar ring structures are also identified in jellyfish: inner and outer nerve rings at the bell margin of hydrozoan medusae (Grimmelikhuijzen *et al.*, 1989).

Since hydra possesses a reduced number of cell types the differentiated cells in hydra are multifunctional. For example, the muscular system of hydra is organized within the epithelial bilayer and consists of outer longitudinal contractile fibers in the ectodermal cells and inner circular contractile fibers in the endodermal cells. These epithelial cells also function in other processes such as fluid and electrolyte transport (Lum *et al.*, 2003).

Hydra reproduces mostly by a vegetative process, with new polyps budding at a regular rate (every two days in optimal conditions) from the main body column. Hydra does not seem to age and has an amazing capacity for regeneration. If the head or the foot is removed, the remaining polyp rebuilds the missing parts in just a few days (Fujisawa and David, 1984).

1. 2 Hydra as an experimental model organism

Hydra being a basal metazoan is considered as an equally important model organism like: *Trichomonas*, *Trypanosoma*, *Leishmania* and *Dictyostelium* (unicellular eukaryotes); *Caenorhabditis elegans*, *Drosophilla* and

Ciona (multicellular invertebrates); *Danio*, *Xenopus* and *Mus musculus* (multicellular vertebrates); yeast and *Podospora* (fungi); *Volvox* and *Arabidopsis* (plants) (Blair *et al.*, 2002; Golstein *et al.*, 2003). It is studied as a model organism for understanding several biologically relevant processes like generation of the embryonic body axes and patterning, neurogenesis and nervous system development; cell death and cell fate; environmental toxicology and teratology; genomic toolkit (recently); oxidative and environmental stress. Phylogenetically it is relatively positioned between unicellular eukaryotes and multicellular invertebrates (Blair *et al.*, 2002; Golstein *et al.*, 2003).

1.2.1 Cell death and cell fate

It is proposed in that among alternative models of cell death zebra fish might be useful to study embryonic cell death and hydra might help to answer questions related to the energy balance in cell death (= apoptosis). Hydra tissues are in a stage of continual flux. The death of some cells is counterbalanced by the continuous proliferation of others. If the animal is starved constitutive cell turnover in hydra doesn't stop but slows down. So a starved hydra survives for months, slowly decreasing in size. Importantly, this shrinkage is due to a decrease in cell numbers, not in cell size (Bosch and David, 1984). Therefore, the polyps of hydrae are well-accepted animal models for studying cell proliferation, regeneration, differentiation and energy balance.

Hydra exhibits some of the classical hallmarks of apoptosis including chromatin condensation and DNA laddering. It is also associated with caspase

activation (Cikala *et al.*, 1999). Dead cells, which are easily visualized with acridine orange, are always seen in phagocytic vacuoles of neighboring epithelial cells. This phagocytosis of apoptotic cells allows the recycling of energy and other cell constituents, and is therefore linked to the regenerative and starvation-resistance abilities of hydra. It is proposed that hydra can be used to measure the economic efficiency of apoptotic cell death, and perhaps even to compare it with non-apoptotic death if apoptosis can be inhibited with suitable drugs. Hydra can also answer questions regarding how decisions are made as to which cells are to die for the sake of others, and which must be spared (Golstein *et al.*, 2003).

Recently, flow cytometry (FCM) has been used to analyze cell-cycle distribution and mitotic cells in *H. oligactis* and *H. vulgaris* (Ulrich and Tarnok, 2005) and is shown to be an appropriate technique for quantifying proliferation in hydra model. Cell-cycle analysis of different parts of the animals shows low proliferation in the head region and high proliferation in the gastric and foot regions. Cell-cycle analysis of different parts of hydra, comparison of *H. oligactis* and *H. vulgaris*, as well as pharmacological treatment yielded results that are in agreement with prior microscopic analysis. Therefore it has been proposed that hydra can be used for basic research on development, regeneration and differentiation as well as for innovative drug investigation and toxicology studies.

1.2.2 Development and generation of the embryonic body axes and patterning

Cnidaria are assumed to be close to the last common ancestor before the bilateral body plan arose in evolutionary development (Meinhardt, 2004). Cnidarian hydra has now been chosen as a model system to gain understanding of biological pattern formation. Recent studies suggest that hydra could be important in understanding the establishment of the second axis and the evolution of bilateral body plan (Meinhardt, 2004).

Genes involved in the establishment of the body plan in hydra and in higher organisms reveal a relation of the ancestral and the contemporary anteroposterior (AP) axis. Genes that are expressed in the body column of hydra have their counterparts in the head of higher organisms. This suggests that the entire body of a radially symmetrical ancestor evolved into the brain and the heart of higher organisms whereas the trunk is a later addition in evolutionary development (Meinhardt, 2002).

The hydra foot corresponds to the most anterior structure, as indicated by the *Nkx2.5* expression (Grens *et al.*, 1996). The foot can be regarded as an ancestral heart (Shimizu and Fujisawa, 2003). It is under the control of the same gene *NKx2.5* (Grens *et al.*, 1996), initiated at the same (very anterior) position, has pumping activity, and its constriction frequency can be influenced by a peptide that also regulates the beating rate in the mammalian heart.

Contrastingly *Wnt* and *Brachyury* are expressed around the gastric opening (Hobmayer *et al.*, 2000; Technau and Bode, 1999) suggesting that the so-called hydra head corresponds to the most posterior structure (= blastoporus). In hydra, *Gooseoid* and *Brachyury* are expressed in adjacent rings near the opening (Technau and Bode, 1999; Broun *et al.*, 1999). In vertebrates *Gooseoid* is involved in head patterning (Niehrs *et al.*, 1993) and *Brachyury* in tail formation (Kispert *et al.*, 1994). Hence it is understood that the trunk was not yet present in ancestral organisms but instead evolved and differentiated later, next to the posterior end. Early in vertebrate development, both *Gooseoid* and *Brachyury* are expressed in overlapping regions (Artinger *et al.*, 1997), but become separated by the sequentially intercalated trunk. Similarly, in short-germ insects and annelids the head is formed first while the segmented trunk is added later.

Establishment of a second axis orthogonal to the ancestral AP axis is important in the development of the bilateral body plan. All higher organisms use *Chordin* and *BMPs* (*short gastrulation* and *dpp* in *Drosophila*) to specify the dorsoventral (DV) axis (Holley *et al.*, 1995). In hydra *Chordin* is present in the head region, and *BMP5/8* is present in the budding region and in the peduncle (i.e. antipodal to the organizer region) (Meinhardt, 2004). Therefore the systems that pattern the embryonic AP and DV axes in higher organisms were already present in radially-symmetric ancestors.

In hydra the gastric opening (= blastoporus) is very small and the corresponding structure in vertebrates is a large ring (e.g. the marginal zone in *Xenopus* or the germ ring in the fish). Also in vertebrates the ancestral part of the AP axis (brain and heart) is organized from the (large) ring-shaped blastoporus, presumably involving *Wnt* (Kiecker and Niehrs, 2001; Nordstrom *et al.*, 2002). β -catenin/*Wnt* is involved in the generation of the primary body axes in hydra and also in the initiation of insect and vertebrate appendages, feather primordia and teeth (Struhl and Basler, 1993; Parr and McMahon, 1995; Noramly *et al.*, 1999; Pispas and Thesleff, 2003). Thus hydra recruits the same signaling systems as vertebrates for very different steps in development. During budding, local high expression of β -catenin and *Wnt* are formed that initiate outgrowth for asexual reproduction. This is analogous to the development of appendages that result from the reprogramming of outgrowths towards non-detaching appendages.

β -catenin and *Wnt* are expressed in the hydra organizer (Hobmayer *et al.*, 2000). Also β -catenin/*Wnt* pathway plays a crucial role in the formation of the vertebrate organizer (Harland and Gerhart, 1997). In *Drosophila* exists a positive loop in the β -catenin/*Wnt* regulatory pathway (van de Wetering, 1997). The experiments in hydra revealed that β -catenin has a much broader distribution than *Wnt*. The broad β -catenin distribution seems to be the precondition for a narrower *Wnt*-peak, suggesting a more indirect autocatalysis. In the formation of the *Drosophila* wing margin, secreted *wingless* has an inhibitory function on

wingless itself (Rulifson *et al.*, 1996). It is possible that secreted *Wnt* plays an analogous inhibitory role in hydra too.

It is postulated that the hydra foot functions as a secondary organizer antipodal to the primary organizing region (Meinhardt, 1993). The expression of the transcription factor *Nkx2.5* homolog in the foot shows pattern regulation as expected for a foot activator (Grens *et al.*, 1996). It has been also shown that this gene is autoregulatory (Thomsen *et al.*, 2004). A diffusible peptide, *pedibin*, appears to spread the autocatalytic activation. As it is the case for the β -*catenin/Wnt* system mentioned above, no long-ranging inhibition has yet been found.

These molecular evidences suggest that hydra body axes and patterning is controlled by an array of sophisticated and strikingly evolutionarily conserved proteins.

1.2.3 Development and evolution of nervous system

Cnidaria represent the first animal phylum with an organized nervous system and a complex active behavior. They are also the simplest organisms in which movements are governed by a neuromuscular system (Westfall, 1996). Their active feeding behavior relies on coordinated movements of their tentacles. Therefore, cnidarians provide the most appropriate model systems to trace back the first-evolved nervous systems (Anderson and Spencer, 1989).

Many of the basic synaptic mechanisms and properties that are associated with more advanced nervous systems are demonstrated in the

cnidaria (Spencer, 1989). Recently, calcium and potassium channels were characterized in jellyfish with functional features similar to those measured in vertebrate counterparts (Jeziorski *et al.*, 1999; Grigoriev *et al.*, 1999). GABA receptors are also pharmacologically identified in jellyfish (Pierobon *et al.*, 2004). Neurotransmitters like glycine (Pierobon *et al.*, 2004), nitric oxide (Colasanti *et al.*, 1997), endocannabinoid (De Petrocellis *et al.*, 1999) and glutamate (Bellis *et al.*, 1991) are predicted to be playing a physiological role in the feeding response of cnidaria. Morphological effect of dopamine synthesis inhibitors or dopamine antagonists is observed in hydra (Ostroumova and Markova, 2002). However, the presence and function of bioamines and acetylcholine has not yet been proven in hydra.

Cnidarian nervous systems are shown to be strongly peptidergic (Grimmelikhuijzen and Westfall, 1995). This is likely a major difference with bilaterian nervous systems. Putative N-methyl-D-aspartate (NMDA) receptors are also expressed in hydra tissues. Pierobon *et al.* (2004) hypothesized that NMDA-like glutamate receptors may occur in hydra tissues where they may be involved in modulation of the response to glutathione (GSH) with opposite actions to those of gamma-amino-butyric-acid (GABA) and glycine.

The Prd-class homeogene *prdl-b* and the nuclear orphan receptor *hyCOUP-TF* (evolutionarily conserved regulatory genes) are expressed in hydra at strong levels in proliferating nematoblasts and at low levels in distinct subsets of neurons. Interestingly, Prd-class homeobox and COUP-TF genes are also

expressed during neurogenesis in bilaterians. Moreover, the Prd-class homeobox gene *prdl-a*, the Antp-class homeobox gene *msh*, and the thrombospondin-related gene *TSP1* are expressed during early budding and/or head regeneration and in distinct subset of neurons in the adult polyp. These data support for neurogenesis and patterning, a feature also identified in bilaterian related genes (Miljkovic-Licina *et al.*, 2004). The hyCOUP-TF protein is specifically bound onto the evolutionarily conserved DR1 and DR5 response elements, and trans-activates RAR: RXR nuclear receptors in a dose-dependent manner when expressed in mammalian cells. It is also demonstrated that the cnidarian transcription factor COUP-TF is active in vertebrate cells. It implies that functional interactions between COUP-TF and other nuclear receptors were evolutionarily conserved (Gauchat *et al.*, 2004).

The proneural genes of achaete-scute (*ac-sc*) family that encodes the bHLH class transcription factors play a variety of roles in neurogenesis. In hydra, the *ac-sc* homolog CnASH is involved in nematocyte differentiation. CnASH is expressed in the sensory neurons in the tentacles and differentiating nematocytes in the body column of hydra (Hayakawa *et al.*, 2004).

Overall, these structural, biochemical, electrophysiological and molecular data support the view that the cnidarian nervous system exhibits a sophisticated organization, with strikingly evolutionarily conserved properties.

1.2.4 Environmental toxicology and toxicity testing

Several invertebrates and vertebrates are important model organisms for the characterization and risk assessment of different chemicals, pharmaceuticals, toxins and environmental contaminants. They are also important for monitoring environmental conditions and for ecological risk assessment (LeBlanc *et al.*, 1997). Several aquatic organisms are also used in assessing the aquatic environmental conditions and risk assessment. Organisms such as *Pimephales promelas* (Fish), *Daphnia magna* (Crustacea), *Ceriodaphnia dubia* (Crustacea), *Hyalella azteca* (Crustacea), *Hyalella* sp. (Crustacea), *Chironomus tentans* (Insect), *Lumbriculus variegates* (Annelida), *H. vulgaris* (Cnidaria), *Hexagenia* sp. (Mayflies) and *Baetis tibialis* (Mayflies) are successfully used to assess stressor exposure and to determine the effects on survival, growth, feeding, and/or uptake (Burton *et al.*, 2005).

Hydra is used as an ideal environmental toxicological model to study the acute and chronic toxicity effects of several environmental toxicants because of its simplified structure and its high regenerative capacity. As diploblasts, all of the cells of hydra are in close proximity to the aqueous medium and the immediate environment. This particular feature enables hydra to be very sensitive and susceptible to minute amounts of environmental toxicants (Lum *et al.*, 2003). The changes in external gross morphology, anatomy, and physiology are useful as markers of toxicity or toxicity end points in the hydra bioassays.

Previous studies have exploited the use of *Hydra* bioassay to assess the toxicity of various compounds including phenol, chlorinated phenols (CP), CP homologs and their isomers (Mayura *et al.*, 1991; Pollino and Holdway, 1999; Ake *et al.*, 2003); selected phenyl acetates, anisoles, sodium phenates, and tetrachlorobenzoquinones (a total of 38 chemicals) (Mayura *et al.*, 1991); polyaromatic hydrocarbons like B(a)P (Ottinger *et al.*, 1999); mycotoxins including patulin (Huebner *et al.*, 2000), fumonisin B₍₁₎ (Lemke *et al.*, 2001), citrinin (Yang *et al.*, 1993); heavy metals such as copper, cadmium, and zinc (Beach and Pascoe, 1998; Pollino and Holdway, 1999; Karntanut and Pascoe, 2000; Holdway *et al.*, 2001; Karntanut and Pascoe, 2002), and estrogens and estrogen mimics including 17 α -ethinylestradiol (EE2), bisphenol A (BPA), octylphenol (OP) (Pascoe *et al.*, 2002, Segner *et al.*, 2003). The hydra bioassay has also been used to assess the toxicity of pharmaceuticals like ibuprofen, paracetamol, acetylsalicylic acid, amoxicillin, bendroflumethiazide, furosemide, atenolol, diazepam, digoxin, amlodipine (Pascoe *et al.*, 2003); insecticides like endosulfan, Dimilin WP 25 and Torak EC 24 (Pollino *et al.*, 1999; Kalafatic *et al.*, 1991a; Kalafatic *et al.*, 1991b); organophosphate nerve agent analogues isopropyl p-nitrophenyl methylphosphonate (for sarin); pinacolyl p-nitrophenyl methylphosphonate (for soman); and diisopropyl S-(2-diisopropylaminoethyl)phosphorothioate, diethyl S-(2-diisopropylaminoethyl)phosphorothioate, and diethyl S-(2-trimethylaminoethyl)phosphorothioate (for VX) (Lum *et al.*, 2003). Several forms

of vitamin A (retinol, retinyl acetate, retinaldehyde, all *trans*-retinoic acid, and 13 *cis*-retinoic acid) are also tested in the *in vitro* hydra assay for their developmental toxicity hazard potential and site of action on progressive ontogenesis and each was established clearly as being able to perturb development of artificial hydra "embryos" at, or near, adult toxic treatment levels (Johnson *et al.*, 1982).

Endocrine disruptors also have been evaluated in hydra bioassay. Fukuhori *et al.* (2005) examined the effects of bisphenol A (BPA), a weak estrogenic compound (Krishnan *et al.*, 1993), on sexual (testis and egg formation) and asexual (budding) reproduction of *H. oligactis*. BPA at (0.5 - 4 mg/L) had stimulatory as well as adverse effects on asexual reproduction and only adverse effects in sexual reproduction. Pascoe *et al.* (2002) reported the acute toxicity of BPA (> 42 µg/L) and the synthetic estrogen 17α-ethynyl estradiol (> 58 µg/L) to the morphology and regeneration in *H. vulgaris* and concluded that the doses causing these acute toxicities were comparable to those reported earlier in aquatic invertebrates and were much higher than environmentally detected doses which cause disruption of the endocrine system in fishes. All these facts indicate that the adverse effects are the results of general toxicity and may not be due to the estrogenic function of the compound.

Similarly metamizole sodium solution was tested on *H. vulgaris* to evaluate its toxicity. This caused nucleolar structural damage in 90 % of hydra cells as early as after 30 min of exposure and the authors proposed that this

kind of test may be applied for obtaining rapid, cost-efficient and useful supplementary data on different types of toxicity for marketed drugs as well as for drugs under development (Arkhipchuk *et al.*, 2004).

Although the hydra assay has been established as a sensitive indicator of toxicity, some studies have shown only weak relationships between hydra responses (changes in external gross morphology, anatomy, and physiology) and levels of certain toxicants (Pardos *et al.*, 1999).

1.2.5 Environmental and oxidative stress

Sessile aquatic organisms undergo constant direct exposure to the surrounding environmental conditions, including local and global environmental fluctuations that may lead to fatal protein damage. Induction of heat shock proteins (HSPs) constitutes an important defense mechanism that protects these organisms from deleterious stress conditions (Choresch *et al.*, 2004). Bosch *et al.* (1988) reported induction of heat shock proteins in *H. vulgaris*, and lack of its induction in *H. oligactis* in the event of stress. Gellner *et al.* (1992) cloned and characterized HSP70 gene from *H. oligactis* and *H. magnipapillata* and studied their differential stress response. It was observed that (Gellner *et al.*, 1992) both *H. oligactis* and *H. magnipapillata* accumulate HSP70 mRNA after heat shock. However, *H. oligactis* accumulates significantly less HSP70 mRNA after heat shock than *H. magnipapillata* (Gellner *et al.*, 1992) though nuclear run-on experiments suggested that transcriptional induction of HSP70 expression in response to stress is similar in both species (Gellner *et al.*, 1992). Gellner *et al.*

(1992) and Brennecke *et al.* (1998) latter proved that the inability of *H. oligactis* to synthesize heat shock proteins in response to stress is at least in part due to reduced stability of HSP70 mRNA during heat shock.

1.2.6 A genomic tool kit

Deductions about the evolutionary origins and structures of human genes are largely based on comparisons with the genomes of model organisms. These include: insects *Drosophila melanogaster* and *Anopheles gambiae*; nematode *Caenorhabditis elegans*; yeasts *Saccharomyces cerevisiae* and *Schizosaccharomyces pombe*, fish *Danio rerio*, frog *Xenopus laevis*, mouse *Mus musculus*; etc. (Kortschak *et al.*, 2003). In summary a small number of complete genome sequences and large EST (expressed sequence tag) datasets that represent only a few complex animals are very important in advancing our knowledge of metazoan genomic complexity. Given the knowledge that cnidaria is regarded as the sister group to the bilateria (Holland, 1999); cnidarians are likely to be critically important in terms of understanding of the evolution of metazoan genetic and developmental complexity. The limited available data also suggest that cnidarian genes reflect the ancestral intron/exon structures (Schmitt and Brower, 2001; Spafford *et al.*, 1999). Also analysis of decapentaplegic (DPP) pathway genes in cnidarian *Acropora millepora* revealed a remarkable level of conservation between these genes and their vertebrate, rather than their invertebrate counterparts (Samuel, 2001; Hayward *et al.*, 2002). Jellyfish (*Podocoryne carnea*) equivalents of the myogenic genes *Brachyury*, *Mef2*, and

Snail are also more similar to their vertebrate homologs than to their *D. melanogaster* and *C. elegans* counterparts (Spring *et al.*, 2002).

The understanding of the genomic complexity of hydra is unfolding. The genome of hydra is fairly large (1,600 Mb) for such a simple organism (David and Campbell, 1972). In order to understand the genomic complexity of hydra, an EST sequencing programme for *H. magnipapillata* is under way. The result of this collaborative effort is an extensive EST database (with over 100,000 ESTs sequenced corresponding to ~16,000 distinct sequences representing ~13,000 different genes) which is available online at www.hydrabase.org. The EST database has been utilized recently by Sher *et al.* (2005) for a bioinformatic analysis of components of the hydra's allomonal system. The authors have shown that this primitive cnidarian expresses several, but not all, of the known cnidarian toxins, as well as orthologs of highly specific and elaborate reptilian, arachnid and molluscan venom components.

As functional genomic tools, protocols have also been proposed for RNA interference-mediated gene silencing (Lohman *et al.*, 1999) and transient transfection assays (Bottger *et al.*, 2002) in hydra.

1.3 Habitat of hydra: Exposure to environmental contaminants and stressors in the aquatic environment

Hydra is a fresh water sessile organism. Unable to move, it is exposed to contaminants/environmental stressors from sediments, suspended particulate material, water-column, industrial effluents and food-sources. The major routes

exposure to contaminants depends on dietary and ecological lifestyles of the organism (Van Veld, 1990; Livingstone, 1991; Livingstone, 1998).

Exposure to contaminants can cause toxicity to hydrae as previously discussed (environmental toxicology and testing). Contaminants can have many different mechanisms of toxicity, and several mechanisms may exist for a single contaminant, each contributing in various degrees to the final overall deleterious effect (Livingstone, 1991; Rand, 1995; Walker *et al.*, 1996; Livingstone *et al.*, 2000). Contaminants can stimulate the formation of reactive oxygen species (ROS) (superoxide, hydroxyl radicals, hydrogen peroxide, and singlet oxygen) (Figure 2) which subsequently can result in oxidative damage (Figure 3). Oxidative damage is also proposed as a mechanism of toxicity in aquatic organisms exposed to pollution (Di Giulio *et al.*, 1989; Livingstone, 1991; Livingstone *et al.*, 1990; Livingstone *et al.*, 1994; Winston and Di Giulio, 1991; Lemaire and Livingstone, 1993; Rand, 1995).

There are many contaminants that produce ROS and free radicals and those that often occur in aquatic environments include: redox cycling compounds (quinones, nitroaromatics, nitroamines, bipyridyl herbicides), PAHs (benzene, PAH oxidation products), halogenated hydrocarbons (bromobenzene, dibromomethane, PCBs, lindane), dioxins and pentachlorophenol; metal contaminants (aluminium, arsenic, cadmium, chromium, mercury, nickel, vanadium); air contaminants (NO_2 , O_3 , SO_2); peroxides; UV-radiation; hypoxia and hyperoxia (Lemaire and Livingstone, 1993; Rand, 1995; Halliwell

σ^*2p					
π^*2p	\uparrow	\uparrow	$\uparrow\downarrow$	$\uparrow\downarrow$	\uparrow
$\pi2p$	$\uparrow\downarrow$	$\uparrow\downarrow$	$\uparrow\downarrow$	$\uparrow\downarrow$	$\uparrow\downarrow$
$\sigma2p$	$\uparrow\downarrow$	$\uparrow\downarrow$	$\uparrow\downarrow$	$\uparrow\downarrow$	$\uparrow\downarrow$
σ^*2s	$\uparrow\downarrow$	$\uparrow\downarrow$	$\uparrow\downarrow$	$\uparrow\downarrow$	$\uparrow\downarrow$
$\sigma\pi2s$	$\uparrow\downarrow$	$\uparrow\downarrow$	$\uparrow\downarrow$	$\uparrow\downarrow$	$\uparrow\downarrow$
σ^*1s	$\uparrow\downarrow$	$\uparrow\downarrow$	$\uparrow\downarrow$	$\uparrow\downarrow$	$\uparrow\downarrow$
$\sigma1s$	$\uparrow\downarrow$	$\uparrow\downarrow$	$\uparrow\downarrow$	$\uparrow\downarrow$	$\uparrow\downarrow$
Orbitals	Base state (O ₂)	Singlet (¹ O ₂)	Superoxide (O ₂ ⁻)	Peroxide (O ₂ ²⁻)	Singlet

Figure 2. The electron structure and spin restrictions of various forms of oxygen. The basal and singlet states have 16 electrons each. However, the superoxide and peroxide states have 17 and 18 electrons each, respectively. Adapted from Olinescu and Smith (2002) and Halliwell and Gutteridge (1999).

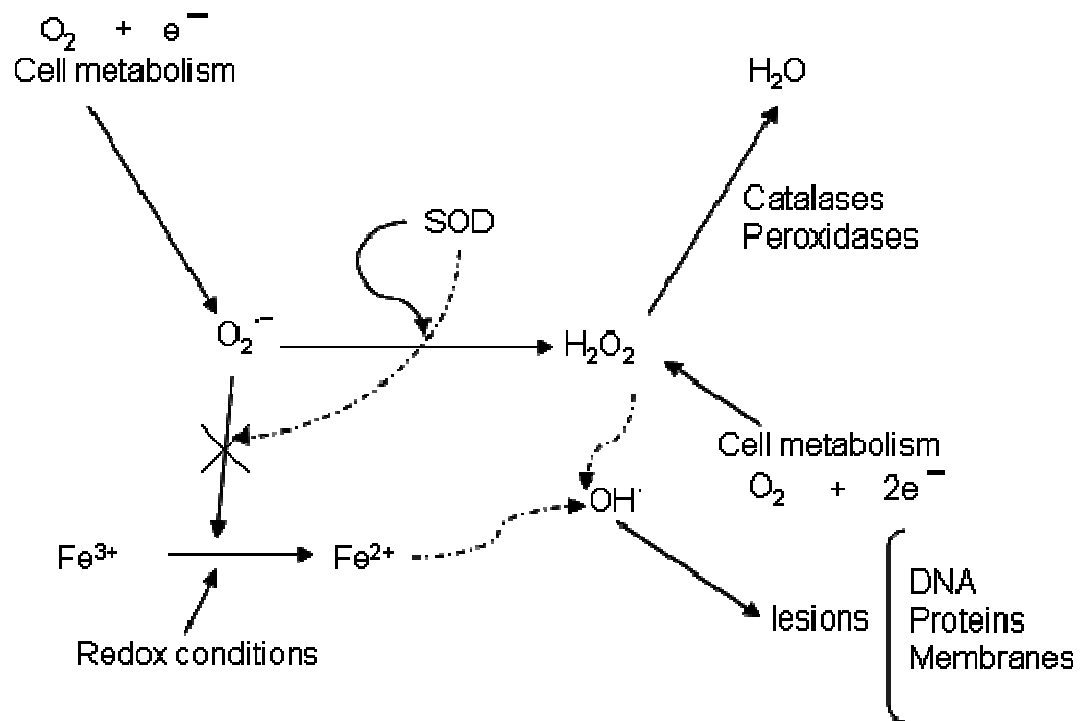


Figure 3. Schematic representation of the role of antioxidant enzymes in preventing oxidative stress. Superoxide dismutases (SOD) disproportionate superoxide ($O_2^{\cdot-}$) to hydrogen peroxide (H_2O_2); and catalases and peroxidases convert H_2O_2 into water. Adapted from Halliwell and Gutteridge (1999).

and Gutteridge, 1999). As an example the pathway of metal induced oxidative stress is illustrated in Figure 4.

1.4 Exposure to environmental contaminants and stressors: Stress proteins and antioxidant enzymes

Environmental stress and oxidative stress (including reactive oxygen species (ROS) formation, lipid peroxidation and oxidative damage to DNA and proteins) affect organisms exposed to environmental pollutants. Organisms respond to stress differently in different situations (Kultz, 2005). There are about 300 proteins involved in stress response. They constitute the stress proteome. About forty stress proteins constitute the minimal stress proteome (MSP) in different organisms (Table 2) and are evolutionarily conserved (Kultz, 2005). For example, organisms exposed to heat or heavy metal ions respond by the immediate synthesis of several stress proteins (e.g., heat shock proteins) (Lindquist, 1986), and often the cessation of synthesis of most other proteins (Hand and Hardewig, 1996).

A sophisticated antioxidant system (Table 3, Figure 3) also protects organisms from oxidative stress. It relies on both water-soluble and fat-soluble low molecular weight free radical scavengers (i.e., ascorbic acid, reduced glutathione (GSH), β -carotene, retinol and α -tocopherol) as well as specific antioxidant enzymes such as CuZn-SOD, Mn-SOD, catalase, Se-dependent glutathione peroxidase (GPx; EC 1.11.1.9), glutathione reductase (EC 1.6.4.2) and DT-diaphorase. Other antioxidant molecules listed in Table 2 (Kultz, 2005;

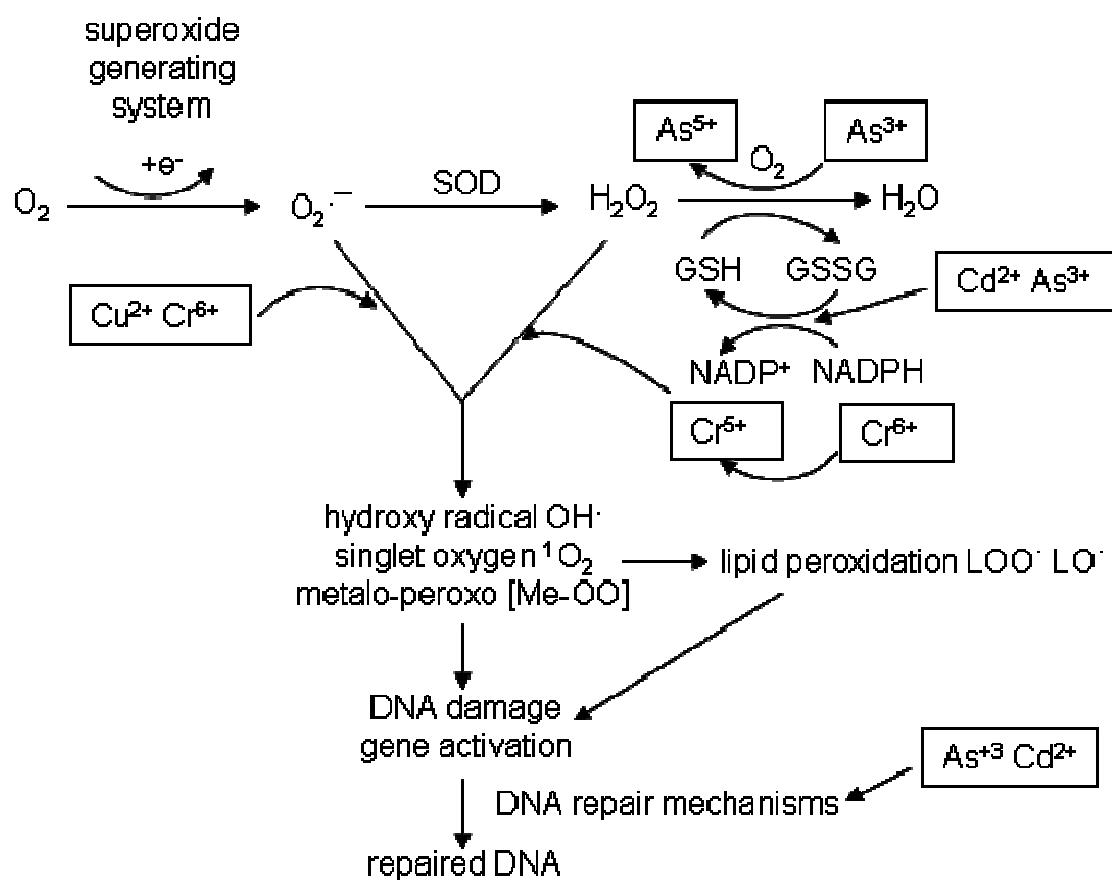


Figure 4. Pathways of metal induced oxidative stress. Hydroxy radical (OH^{\cdot}), singlet oxygen (1O_2) and metalo-peroxide generated as a consequence of metal induced stress cause lipid peroxidation and DNA damage. GSH = reduced glutathione, GSSG = oxidized glutathione, NADP = nicotinamide adenine dinucleotide phosphate, NADPH = reduced NADP. Adapted from Halliwell and Gutteridge (1999) and Valko *et al.* (2005).

TABLE 2**The Minimal Stress Proteome of Cellular Organisms^a**

Pathway	Proteins
Redox regulation	Aldehyde reductase Glutathione reductase Thioredoxin Peroxiredoxin Superoxide dismutase MsrA/PMSR SelB Proline oxidase Quinone oxidoreductase NADP-dependent oxidoreductase YMN Putative oxidoreductase YIM Aldehyde dehydrogenase Succinate seialdehyde dehydrogenase 6 phosphogluconate dehydrogenase Glycerol-3-phosphate dehydrogenase 2-hydroxyacid dehydrogenase Hydroxyacylglutathione hydrolase
DNA damage sensing/repair	MutS/MSH MutL/MLH Topoisomerase I/III RecA/Rad51
Molecular chaperones	Petidyl-prolyl isomerase DnaJ/HSP40 GrpE (HSP70 cofactor) HSP60 chaperonin DnaK/HSP70
Protein degradation	FtsH/proteasome-regulatory subunit Lon protease/protease La Serine protease Protease II/prolyl endopetidase Aromatic amino acid aminotransferase Aminobutyrate aminotransferase

^aAdapted from Kultz *et al.* (2005).

TABLE 2 (Continued)

Pathway	Protein
Fatty acid/lipid metabolism	Long-chain fatty acid ABC transporter Multifunctional beta oxidation protein Long chain fatty acid CoA ligase
Energy metabolism	Citrate synthase (Krebs cycle) Ca ²⁺ /Mg ²⁺ -transporting ATPase Ribosomal RNA methyltransferase Enolase (glycolysis) Phosphoglucomutase
Other functions	Inositol monophosphatase Nucleoside diphosphate kinase Hypothetical protein YKP1

^aAdapted from Kultz *et al.* (2005).

TABLE 3**Antioxidant Defense System of Cellular Organisms^a**

Group		Molecules	
Small molecule antioxidants	Water soluble	ascorbic acid glutathione bilirubin uric acid	
	Lipid soluble	alpha-tocopherol lycopene beta-carotene lutein ubiquinol-10	
Antioxidant proteins	Non-enzymatic	protein thiols albumin transferrin lactoferrin ferritin ceruloplasmin hepatoglobin hemopexin	
	Enzymatic	superoxide dismutases (SOD)	CuZnSOD EC-SOD MnSOD FeSOD
		peroxidases	glutathione peroxidase (=selenium independent) phospholipid hydroperoxide glutathione peroxidase (=selenium dependent)
		catalases	monofunctional catalase bifunctional catalase non-heme catalase

^aAdapted from Frei *et al.* (1992) and Olinescu and Smith (2002).

Dunlap *et al.*, 1999; Dunlap *et al.*, 2000) are also important in oxidative stress defense. A brief discussion and role of a few stress responsive molecules as relevant to the current study is given below.

1.4.1 Heat shock protein 70

Heat shock protein 70 (HSP70) is important in protein chaperoning (Gething and Sambrook, 1992) and acquired tolerance processes (Coleman *et al.*, 1995; Craig, 1985; Lindquist and Craig, 1988; Clegg *et al.*, 1998) and is evolutionarily highly conserved. HSP70 regulate protein structure and function under normal physiological conditions, as well as during and after stress. It assists in reactivating denatured proteins in an ATP-dependent manner (Hartl, 1996). Furthermore, mitochondrial and chloroplastic HSP70 homologs work in concert - an essential multistep pathway for correct conformation of protein structure.

HSP70 levels increase in response to stress, specifically in response to increased protein synthesis and denaturation and indicate that the cell's housekeeping proteins are experiencing denaturing conditions. Thus measurement of these chaperones is an index of the structural integrity of one component of the cell superstructure (Downs *et al.*, 2002).

1.4.2 Superoxide dismutases

Superoxide dismutase (SOD) enzymes are widely observed in biology: even in organisms lacking other antioxidant enzymes, such as catalase or peroxidase, and is expressed without exception (Asada *et al.*, 1977). Superoxide

dismutases catalyze the reaction of superoxide ions and 2 protons to form hydrogen peroxide and oxygen dioxide (Fridovich, 1995) (Figure 3). SODs are classified into three groups. Copper zinc superoxide dismutase (CuZnSOD) is found only in the cytosol of animal cells, while homologs of this enzyme are found in both the cytosol and chloroplast in plants and algae (Fridovich, 1995). Manganese superoxide dismutase (MnSOD) is localized only to the mitochondria in any eukaryotic cell (Fridovich, 1995). MnSODs described are homologous to Fe-dependent bacterial SODs (FeSODs) (Fridovich, 1995). Extracellular copper zinc superoxide dismutases (EC-SOD), as the name indicates, are secreted by many types of cells (Weisiger and Fridovich, 1973; Marklund, 1982; Mantonavi and Dejana, 1989). SODs accumulate in response to stress and are one of the main antioxidant defenses. Increased SOD levels have been linked to increased longevity and tolerance to ischemic or reperfusion events and factors that induce oxidative stress (Fridovich, 1995). SODs indicate that the cell is responding to an oxidative stress; MnSOD specifically shows that the mitochondria are experiencing an oxidative stress (Fridovich, 1995).

1.4.3 Catalases and peroxidases

Catalase is present in all aerobic cells, especially in peroxisomes and mitochondria. Catalases and peroxidases are heme-containing enzymes most commonly used to transform the harmful oxygen compound H_2O_2 into harmless products (oxygen and water) (Halliwell and Gutteridge, 1999) (Figure 3). In

addition to heme-containing catalases and peroxidases, nonheme varieties of these enzymes also exist (Schnellhorn *et al.*, 1994).

1.4.4 Glutathione peroxidases

Glutathione peroxidase (GPx) catalyses the degradation of peroxides, which may include hydrogen peroxide, organic peroxide or lipid peroxides. The specificity of the enzyme for peroxides is low and the specificity for glutathione is high (Halliwell and Gutteridge, 1999). Glutathione peroxidase competes with catalase for hydrogen peroxide, or lipid peroxides. There are two types of glutathione peroxidase based on the metal cofactor present: selenium independent GPx and selenium dependent GPx. Selenium independent peroxidase has a preference for organic peroxides. Selenium dependent peroxidase is found in the cytosol and exhibits a high capacity to decompose hydrogen peroxide. Another form of selenium dependent glutathione peroxidase acts efficiently on lipid peroxides, and is known as phospholipid hydroperoxide glutathione peroxidase (Olinescu and Smith, 2002).

1.5 Stress proteins and antioxidant enzymes in aquatic organisms

It is becoming apparent that environmental stress and oxidative stress affect aquatic organisms. Recent examples of species in which stress and antioxidant defenses have been studied include the freshwater bivalve *Unio timidus* (Doyotte *et al.*, 1997), arctic populations of the clam *Macoma balthica* (Regoli *et al.*, 1998a; Regoli *et al.*, 1998b), the Antarctic scallop *Adamussium colbecki* and Mediterranean scallop *Pecten jacobaeus* (Viarengo *et al.*, 1995),

and the teleost fish species *Ictalurus nebulosus* (Hai *et al.*, 1997) and *Lampanyctus crocodilus* (Capo *et al.*, 1997).

Examples of other types of recently studied antioxidant enzymes include aldehyde dehydrogenase in the mussel *Mytilus galloprovincialis* (Nasci *et al.*, 1998), hepatic DT-diaphorase in *O. mykiss* (Lemaire and Livingstone, 1997), glyoxylase (EC 4.4.1.5) in *M. balthica* (Regoli *et al.*, 1998a), and glutathione S-transferase A in plaice (*Pleuronectes platessa*) which is capable of readily conjugating and detoxifying products (alkenals) of lipid peroxidation (Leaver and George, 1998). Most other types of antioxidants that are found in higher organisms, such as other thiols, purine bases and ubiquinones haven't been found in blood of elasmobranch and teleost fish species examined from the Black Sea (Rudneva, 1997).

1.6. Stress proteins and antioxidant enzymes in cnidarians

The study of stress proteins and antioxidant defense enzymes is more or less advanced in marine and symbiotic cnidarians. Moreover, the evolutionary adaptation of antioxidant defenses of symbiotic cnidarians to O₂ (produced by the symbiont algae) is compared to the antioxidant defenses in plants that protect them from the toxic effects of oxygen radicals produced during photosynthesis (Richier *et al.*, 2005, Apel and Hirt, 2004). No specific report on oxidative stress and antioxidant defense in hydra exists in literature except the report of heat shock proteins (HSP70) (Bosch *et al.*, 1988) in hydra as discussed

above. Environmental and oxidative stress as reported in cnidarians is discussed below.

1.6.1 Sea anemones

1.6.1.1 *Anthopleura elegantissima*

Rossi and Snyder (2001) studied the role of constitutive (HSC) and inducible (HSP) heat shock proteins of the HSP70 family in intra- and interspecific competition for space in sessile Pacific cnidarians *Anthopleura elegantissima*. *A. elegantissima*, an intertidal anemone, expressed HSP70 in the absence of apparent physical stress. HSP70 protein expression was concentrated in the tentacles of *A. elegantissima* when the animal was exposed to contact with other benthic organisms. When two different clones of *A. elegantissima* interacted in the field, the outside polyps (warriors) expressed more HSP70 than the inside ones (2.4 versus 0.6 ng HSP70/microg protein). HSP70 expression was related to the different kinds of aggression encountered by both cnidarians. HSP70 expression is suggested to be involved in the recovery of tissues damaged by the allelochemical, cytotoxic, or corrosive substances produced by different enemies. *A. elegantissima* exhibited differential HSP70 expression depending on the identity of each neighboring intra- or interspecific sessile competitor. It was proposed that stress proteins could be used to quantify space competition or aggression among sessile marine invertebrates.

Early studies conducted in symbiotic anemone *A. elegantissima* demonstrated an increased antioxidant enzymatic capacity in response to hyperbaric oxygen conditions as a result of increased oxygen production from its endosymbiotic algae (Dyken *et al.*, 1992). Enhanced OH[·] production has been observed in *A. elegantissima* and its endosymbiotic zooxanthellae algae (Dyken *et al.*, 1992).

1.6.1.2 *Anemonia viridis*

Choresh *et al.* (2004) reported an immunological detection of a 60 kDa HSP (HSP60) in the symbiotic Mediterranean sea anemone *Anemonia viridis* and studied its expression under a variety of stress conditions. The cloned HSP60 gene from *A. viridis* (1764 bp) encodes for a protein of 62.8 kDa (588 amino acids). The 62.8 kDa protein contained an amino terminal extension that might serve as a mitochondrial targeting signal. It shared a significant identity with mitochondrial HSP60s from several animals but less identity with HSP60s from either bacteria or plants.

Richier *et al.* (2003) studied the mechanism of high tolerance of *A. viridis* to rapid transition between hypoxia and hyperoxia by characterizing superoxide dismutases (SODs) from the three cellular compartments: ectoderm, endoderm and zooxanthellae. The lowest SOD activity was found in ectodermal cells while endodermal cells and zooxanthellae showed a higher SOD activity. Polyacrylamide gel electrophoresis (PAGE) showed two, seven and six SOD activity bands from ectoderm, endoderm and zooxanthellae, respectively. A

CuZnSOD was identified in both ectodermal and endodermal tissues and MnSODs were detected in all compartments with two different subcellular localizations. One band displayed a classical mitochondrial localization and three others were extramitochondrial in localization. FeSODs present in zooxanthellae also appeared in endodermal host tissue. Richier *et al.* (2005) also showed (qualitative analysis of SOD activity on native gel) no change in SOD isoform expression within the compartments of *A. viridis* during endogenous (photosynthetic) hyperoxia or experimental hyperoxia. However, spectrophotometric measurement showed a significant (1.5-fold) increase in SOD activity in the ectodermal fraction. No change occurred in endodermal cells.

The overall SOD pattern of *A. viridis* did not change in its compartments even after 5 days of incubation at a temperature 7 °C above normal. Quantitative measurements detected a slight increase after 24 h incubation in ectodermal and no significant change in endodermal animal cells. Also Richier *et al.* (2005) showed that bleached specimens of *A. viridis* exhibited a global decrease in SOD activities and a loss of some SOD activity bands. The analysis of the three compartments (ectoderm, endoderm and freshly isolated zooxanthellae (FIZ)) from *A. viridis* enabled a more precise localization of modifications in the SOD pattern. While the electrophoretic pattern for ectodermal cells were unchanged, the endodermal host cells lost its major SOD activity bands, representing MnSOD and FeSOD classes as identified by them previously (Richier *et al.*, 2003). Spectrophotometric measurements confirmed five- and threefold

decreases of SOD activity in the ectodermal and endodermal compartments, respectively. However, a MnSOD band and a CuZnSOD band remained in symbiotic specimens (Richier *et al.*, 2005).

1.6.1.3 *Aiptasia pulchella*

Bleached specimens of sea anemone *Aiptasia pulchella* exhibited a global decrease in SOD activities and a loss of some SOD activity bands. In the *A. pulchella* total extract, three SOD activity bands disappeared from the bleached anemone. However a MnSOD band and a CuZnSOD band remained in aposymbiotic specimens (Richier *et al.*, 2005).

1.6.1.4 *Actinia schmidtii*

In non-symbiotic sea anemone, *Actinia schmidtii*, superoxide dismutase (SOD) activities responded strongly to the experimental treatment. The CuZnSOD activity bands (both isoforms AsSODa and AsSODb) disappeared after 2 days and a novel activity band (AsSODe) appeared. After 5 days of incubation, another CuZnSOD activity band (AsSODf) was expressed, and a high-molecular mass smear appeared. Parallel measurements by spectrophotometer showed a global decrease in SOD activity during 5 days of incubation at elevated temperature (Richier *et al.*, 2005).

1.6.2 Corals

1.6.2.1 *Montastraea faveolata*

Downs *et al.* (2001) studied the heat shock protein 70 (HSP70), manganese superoxide dismutase (MnSOD), copper zinc superoxide dismutase

(CuZnSOD) levels in the symbiotic coral (*Montastraea faveolata*) in response to stressors heat, light, or both. CuZnSOD levels of the coral in heat-stressed samples were significantly higher in the light than in the dark. Increased levels of CuZnSOD suggested that oxidative stress was greater in the cytoplasm, where the zooxanthellae reside. MnSOD expression had blunted expression response to oxidative stress, unlike that of MnSOD expression in other invertebrates such as *Drosophila* sp. or nematodes (Fridovich, 1995).

1.6.2.2 *Stylophora pistillata*

Tom *et al.* (1999) cloned the first coral heat shock protein 70 gene (SP-HSP70) from symbiotic scleractinian coral *Stylophora pistillata* genome to use it as a tool for studying coral stress response. The sequenced clone (5212 bp) contained a complete 1953 bp intronless open reading frame and TATA, CAAT, and ATF boxes as well as 11 putative heat shock elements in the SP-HSP70 5'-flanking region. SP-HSP70 protein sequence resembled the cytosolic/nuclear HSP70 cluster. RT-PCR (reverse transcription – polymerase chain reaction) studies confirmed SP-HSP70 mRNA expression in corals grown within their normal physiological conditions.

Downs *et al.* (2002) examined the HSP70, copper zinc superoxide dismutase (CuZnSOD) and manganese superoxide dismutase (MnSOD) levels in bleached *S. pistillata* experiencing oxidative stress. It was found that HSP70 levels increased significantly in bleached corals and Copper/Zinc SOD concentrations varied significantly with the exact combination of sampling date

and depth. Cu/Zn SOD concentrations were significantly higher at the 3 m site than at all deeper sites (sampled from May-August). Manganese SOD showed a similar accumulation pattern. Levels of Mn SOD and Cu/Zn SOD were significantly positively correlated. The authors suggested that superoxide dismutases were significant components of the antioxidant capacity of corals and that these two proteins might play an important role in preventing the process of coral bleaching.

Also, Richier *et al.* (2003) characterized superoxide dismutases (SODs) from *S. pistillata* in order to study tolerance mechanisms during rapid transition between hypoxia and hyperoxia states. SOD activity was observed on native gel in *S. pistillata* cell extracts. The number of bands remained comparable to *A. viridis* but *S. pistillata* revealed its own pattern identified by inhibitors.

Yakovleva *et al.* (2004) studied the susceptibility of *S. pistillata* to oxidative stress mediated by elevated temperature. Activity of superoxide dismutase (SOD) and catalase (CAT) enzymes were measured to assess the physiological response of the coral to elevated temperature stress. In *S. pistillata*, the SOD activity of the coral tissue increased by 4-fold after the first 6 h of stress exposure and remained at that level for the next 6 h. In the coral tissue of *S. pistillata*, the CAT activity was increased by about 1.8-fold of the initial value within 6 h and further by 2.7-fold after 12 h.

1.6.2.3 *Platygyra ryukyuensis*

Yakovleva *et al.* (2004) in order to study the susceptibility of shallow-water scleractinian coral, *Platygyra ryukyuensis*, to oxidative stress mediated by elevated temperature measured the activity of superoxide dismutase (SOD) and catalase (CAT). In *P. ryukyuensis*, the SOD activity of the coral tissue was unaffected by elevated temperature during the whole exposure time. The CAT activity of the coral tissue remained unaffected during the first 6 h of stress treatment, but after 12 h a 2.5-fold increase was observed.

1.6.2.4 *Plexaura homomalla*

Koljak *et al.* (1997) discovered a distant relative of catalase that is specialized for metabolism of a fatty acid hydroperoxide from Caribbean sea whip coral *Plexaura homomalla*. This catalase (=heme peroxidase) occurs in coral as part of a fusion protein, the other component of which is a lipoxygenase that forms the hydroperoxide substrate. The findings expanded upon the known chemistry of catalase-like proteins and revealed a distinct type of enzymatic construct involved in the metabolism of polyunsaturated fatty acids in corals.

1.6.2.5 *Montastrea annularis*

Hayes and King (1995) studied the induction of the 70 kDa family of heat shock proteins (HSP70) in the tissues of zooxanthellate stony coral, *Montastrea annularis*. Experimental tissues fractionated by PAGE indicated that the initial induction of HSP70 occurred rapidly, within one hour of transfer to water of elevated temperature. Thereafter, the level of HSP70 decreased within 12-24 h

to approximately the constitutive level. In field-bleached specimens of *M. annularis*, HSP70 was not detected. Since the coral tissue once bleached to whiteness contained no 70 kDa heat shock protein, the authors concluded that the process of coral bleaching might include, among other metabolic alterations, a failed heat shock response.

1.6.2.6 *Tubastrea cocchineae*

Hayes and King (1995) studied the induction of the 70 kDa family of heat shock proteins in tissues of orange cup coral, *Tubastrea cocchineae*. A constitutive HSP70 was identified in the nonsymbiotic coral species, *T. cocchineae*. Experimental tissues fractionated by PAGE indicated that the initial induction of HSP70 occurred rapidly, within one hour of transfer to water of elevated temperature. Thereafter, the level of HSP70 decreases within 12-24 h to approximately the constitutive level.

1.6.2.7 *Astrangia danae*

Hayes and King (1995) also studied the induction of the 70 kDa family of heat shock proteins in tissues of symbiotic coral *Astrangia danae*. A constitutive HSP70 was identified in the coral lacking symbiotic algae, *A. danae*. Experimental tissues fractionated by PAGE indicated that the initial induction of HSP70 occurs rapidly, within one hour of transfer to water of elevated temperature. Thereafter, the level of HSP70 decreases within 12-24 h to approximately the constitutive level.

1.6.2.8 *Corynactis californica*

Rossi and Snyder (2001) studied the role of constitutive or inducible heat shock protein of the HSP70 family in intra- and interspecific competition for space in sessile pacific cnidarian *Corynactis californica*. *C. californica*, a subtidal corallimorpharian, expressed HSP70 in the absence of apparent physical stress. HSP concentrations were similar in the body and tentacles of *C. californica*. When different *C. californica* clones interacted, HSP70 expression in the outside and inside polyps was similar (1.5 versus 1.8 ng HSP70/microg P) and was fairly constant in the corallimorpharian in the different interspecific encounters. Rossi and Snyder (2001) suggested that HSP70 expression might be involved in the recovery of tissues damaged by the allelochemical, cytotoxic, or corrosive substances produced by different enemies. *C. californica* clones appeared prepared for defense, as evidenced by the high constant expression of HSP70 in the polyps. Rossi and Snyder (2001) proposed that stress proteins could be used to quantify space competition or aggression among sessile marine invertebrates.

1.6.3 Sea fans

1.6.3.1 *Leptogorgia virgulata*

Kingsley *et al.* (2003) studied the response of the temperate shallow-water gorgonian, *Leptogorgia virgulata*, to temperature stress. Proteins were pulse labeled with (35) S-methionine/cysteine for 1 h to 2 h at 22 °C (control), or 38 °C, or for 4 h at 12.5 °C. Heat shock induced synthesis of unique proteins of

112, 89, and 74 kDa, with 102, 98 and 56 kDa proteins present in the control as well. Cold shock from 22 °C -12.5 °C induced the synthesis of a 25 kDa protein, with a 44 kDa protein present in the control as well. Control samples expressed unique proteins of 38 and 33 kDa. Assay with antibodies to heat shock proteins (HSPs) revealed HSP60 to be the major protein in *L. virgulata*. Although HSP47, HSP60, and HSP104 were present in all samples, the expression of HSP60 was enhanced in heat stressed colonies, while HSP47 and HSP104 expression were greatest in cold shocked samples. Inducible HSP70 was expressed in cold shocked, heat shocked, and field samples. Constitutively expressed HSP70 was absent from all samples. The expression of HSP90 was limited to heat shocked colonies. Kingsley *et al.* (2003) reported the expression of both HSP70 and HSP104 suggested that the organism might also develop a stress tolerance response.

1.6.4 Jelly fish

1.6.4.1 *Aurelia*

Black and Bloom (1984) identified heat shock proteins (HSP) in *Aurelia* by one-dimensional SDS-PAGE of sizes 93, 83, 70, 68, 45 and 39 kDa the most rapidly labeled being was HSP70 in all developmental stages. Labeled HSP in the polyp were found mostly in the epidermis; gastrodermal nuclei were also labeled. The minimum temperature for induction of the proteins was about the same (27 to 28 °C), regardless of whether polyps had been cultured at 15 or 24 °C. Adults and planulae taken from natural water at 28 °C did not show

accumulation of HSP70. Induction of strobilation by raising polyps from 15 to 25 °C was not associated with appreciable labeling of HSPs. Polyps transferred to higher or lower salinity observed to have decreased protein synthesis and cessation of synthesis of stress proteins.

1.7 Research hypotheses

Interest in the toxicological aspects of environmental pollutants and associated environmental and oxidative stress at molecular level has grown in recent years. The major reasons for studying environmental stress and oxidative stress (pro-oxidant and other radical processes) at molecular level are to understand the action of toxic substances in causing stress related diseases, the molecular basis of stress response, and determining specific criteria which can be used for diagnosis and treatment of diseases (Halliwell and Gutteridge, 1999). Similar considerations may apply to aquatic organisms. Elucidating the action of toxic substances is of most relevant, particularly in the context of environmental management. It has become apparent that aquatic organisms respond to environmental and oxidative stress. Research in fish has demonstrated that mammalian and piscine systems exhibit similar toxicological and adaptive responses to oxidative stress. This suggests that aquatic models including, in addition to traditional mammalian and piscine models, may be useful for further understanding the mechanisms underlying the environmental and oxidative stress response (Kelly *et al.*, 1998; Malins and Ostrander, 1991).

Specifically, knowledge of normal and contaminant-related pro-oxidant and antioxidant processes in aquatic animals is needed for (a) the assessment of the quality of the aquatic system; (b) the identification of chemicals with pro-oxidant activity; (c) the design of assays for monitoring of pro-oxidant contaminants and contaminant mixtures in the environment; (d) the design of assays to detect pro-oxidant activity for use in toxicity testing of new compounds; (e) assessment of the quantitative importance of such pro-oxidants and pro-oxidant processes in contaminant-mediated diseases and other aspects of impaired animal fitness; and (f) the identification of interactive environmental and biological factors which may enhance contaminant-mediated free radical processes and damage; etc. (Steinert *et al.*, 1998; Livingstone, 1991; Gamble *et al.*, 1995; Hetherington *et al.*, 1996).

Alternative model organisms are being used to study environmental and oxidative stress to elucidate the mechanisms underlying cellular damage and response, and are providing scientific clues for human health issues surrounding environmental and oxidative stress. Hydra being a basal metazoan and a sister group to the bilateria (Holland, 1999) is expected to have the basic mechanism of environmental and oxidative stress response machinery and mechanism conserved (Kultz, 2005). It has been shown that *H. magnipapillata* has a heat shock response both at transcriptional and physiological levels, while *H. oligactis* has only a transcriptional response to heat and metal stress. In many other toxicological studies involving hydra there were apparent lack of correlation in

toxicological responses and contaminant levels due to lack of molecular data. Hence the apparent lack of correlation in toxicological responses and contaminant levels warrants probing the assay end points at the molecular level. This necessitates the study of the molecular machinery of stress response of hydra in order to better characterize the toxicological responses. Results of these studies may help in identifying stress response genes that can be proposed as biomarkers of environmental stress and toxicity and characterizing the cellular and molecular basis of stress response in a basal metazoan.

To understand the molecular basis of toxicant effect and stress response, the studies described in this project focused on cloning and characterizing the genes coding heat shock protein 70, manganese superoxide dismutase (MnSOD), extracellular copper zinc superoxide dismutase (EC-CuZnSOD), phospholipid hydroperoxide glutathione hydroperoxidase (PHGPx) and catalase from hydra *H. vulgaris*. The expression of *H. vulgaris* HSP70, EC-CuZnSOD, Mn-SOD, PHGPx and catalase mRNA was assayed with respect to different metal stress (= environmental contaminants) (i.e., copper, zinc, cadmium, chromium, arsenic and selenium), thermal stress (heat), oxidative stress (H₂O₂, paraquat) and non-oxidative stress (starvation). The detection of stress messages in hydra can constitute an early warning marker for the presence of potentially deleterious agents in water, and in general will act as a potential sentinel animal species. In addition, minimal time and cost, high efficiency, and ease of the assay will permit it to be run multiple times in a variety of formats

(Johnson *et al.*, 1982; Lum *et al.*, 2003). Because *H. vulgaris* are sensitive to a variety of compounds, the bioassay used here could be applied as a prescreening tool in determining the relative toxicity of many toxicants, and new compounds that are to be screened for toxicity. The overwhelming majority of existing substances and most of the new ones appearing in commerce annually can be evaluated for their potential health hazards.

Corresponding nucleotide and protein sequences from model organisms were retrieved from public databases (including the *H. magnipapillata* EST database) and were analyzed along with hydra stress response proteins characterized in the current study to find the similarities and differences they manifest at primary sequence levels. Structural models of the proteins/enzymes were produced and are presented in the context of what we know about them from other organisms: the conservation of key residues, catalytic core, ligand pockets, domain topology; etc. Finally relevant phylogenetic analysis was conducted to determine the phylogenetic position of hydra stress proteins and their evolutionary relevance and function.

1.8 Research objectives

Therefore to advance our knowledge of the mechanisms of stress response in hydra, the specific objectives of this research were fourfold:

1. To clone *H. vulgaris* HSP70 gene and characterize its expression with respect to thermal, starvation, metal and oxidative stress

2. To clone *H. vulgaris* Mn-superoxide dismutase and extracellular Cu-Zn superoxide dismutase gene and characterize their expression with respect to thermal, metal and oxidative stress
3. To clone *H. vulgaris* phospholipid hydroperoxide glutathione peroxidase and heme containing monofunctional catalase genes and characterize their expression with respect to thermal, starvation, metal and oxidative stress
4. To conduct relevant bioinformatics analyses to develop structural models and phylogenetic tress for the above mentioned hydra proteins

CHAPTER II
MOLECULAR CLONING AND CHARACTERIZATION OF A HEAT SHOCK
PROTEIN 70 FROM *HYDRA VULGARIS*

Organisms from both flora and fauna respond to environmental stress (Macario *et al.*, 1999; Sun *et al.*, 2002), such as exposure to heat, heavy metal ions and xenobiotics, by the immediate synthesis of several heat shock proteins (HSPs) and often the cessation of synthesis of most other proteins (Lindquist, 1986). A 70 KDa heat shock protein is the major HSP in all organisms, because of its implication in protein chaperoning (Jolly and Morimoto, 2000; Feder and Hofmann, 1999; Gething and Sambrook, 1992) and acquired tolerance processes (Basu *et al.*, 2002, Lindquist and Craig, 1988; Clegg *et al.*, 1998). DNA sequence analysis of genes encoding HSP70 from a variety of organisms has shown them to be highly conserved in evolution (Kultz, 2005; Lowe *et al.*, 1983; Ingolia and Craig, 1982a; Ingolia *et al.*, 1982b; Craig, 1985) and contain both heat-inducible and constitutive genes (HSC), both of which encode stress proteins under normal conditions (Hightower, 1993; Wood *et al.*, 1998). HSP70 gene from diverse organisms can be activated by heat shock in cells (Feder and Hofmann, 1999; Lindquist, 1986) and understandably the induction mechanism itself also seems to be conserved. Also, heat shock transcription factors from organisms as diverse as *Drosophila* and yeast have also been shown to be remarkably similar (Wiederrecht *et al.*, 1987).

Heat shock proteins have been proposed as a possible tool for monitoring environmental toxicants (Kammenga *et al.*, 2000; Dunlap and Matsumura, 1997; Sanders and Martin, 1993; Kohelr *et al.*, 1992). Induction of HSPs indicates exposure to cellular stress and adverse cellular effects, thus serving as biomarkers of these effects. The highly conserved HSP70 proteins are expressed under proteotoxic conditions also (Krone *et al.*, 2005). Induction of HSP70 in earthworms (Nadeau *et al.*, 2001) represented a good wide-spectrum biomarker of exposure but also a biomarker of effect since known toxicants altered gene expression in tissues of these animals, as contrasted with a simple accumulation of HSP.

Quite a few studies have been done on stress proteins in aquatic organisms and results are highly variable (Sanders and Martin, 1993). Few complete or partial sequences of HSP70 genes and cDNA of aquatic organisms available in the GenBank are that of *Crassostrea gigas* (Gourdon *et al.*, 2000; Boutet *et al.*, 2003b), *Crassostrea virginica* (Rathinam *et al.*, 2000), *Mytilus edulis* (Luedeking and Koehler, 2004), *Ostrea edulis* (Boutet *et al.*, 2003a), *Carassius auratus* (Kondo and Watabe, 2004), *Stylophora pistillata* (Tom *et al.*, 1999), *H. magnipapillata* (Gellner *et al.*, 1992) and *H. oligactis* (Gellner *et al.*, 1992); etc.

Hydra, a fresh water aquatic organism, is also used as an ideal environmental toxicological model to study the acute and chronic toxicity effects of several environmental toxicants because of its simplified structure and its high

regenerative capacity (Lum *et al.*, 2003). As diploblasts, all of the cells of hydrae are in close proximity to the aqueous medium and the immediate environment. This characteristic enables hydra to be very sensitive and susceptible to minute amounts of environmental toxicants (Lum *et al.*, 2003). The changes in external gross morphology, anatomy, and physiology are useful as markers of toxicity or toxicity end points in the hydra bioassays. It may be postulated that the detection of HSP70 message in hydra can constitute an early-warning marker for the presence of potentially deleterious agents in water, and thus may in general act as a potential sentinel animal species. In addition, minimal time and cost and ease of culturing and running hydra bioassay in multiple times in a variety of formats (Johnson *et al.*, 1982; Lum *et al.*, 2003) make it a model organism for detecting HSP70 message in toxicological assays. Because *H. vulgaris* are sensitive to a variety of compounds, the detection of HSP70 message could be applied as a prescreening tool in determining the relative toxicity of many toxicants, and new compounds that are to be screened for toxicity. The overwhelming majority of existing substances and most of the new ones appearing in commerce annually can be evaluated for their potential health hazards.

In the present study, a gene encoding HSP70 from fresh water hydra *H. vulgaris* is described. The expression of hydra HSP70 (HvHSP70) mRNA is assayed with respect to both environmental contaminant challenge (i.e., arsenic, cadmium, selenium, zinc and copper) and stress (both oxidative and non-

oxidative). In addition, the phylogenetic position of HvHSP70 is characterized and a suitable homology based structural model of HvHSP70 is also presented to assist in understanding the structural and functional evolutionary significance of the protein.

2.1 Materials and methods

2.1.1 Hydra culture

Hydra vulgaris (formerly known as *Hydra attenuata*) were originally obtained from E. Marshall Johnson, Jefferson Medical College (Philadelphia, PA, USA). Adult *H. vulgaris* were maintained in shallow dishes at 18 °C in a medium containing 1 mM CaCl₂·2H₂O, 0.012 mM EDTA, and 0.458 mM TES (N-tris[hydroxymethyl]-methyl-2-amino-ethanesulfonic acid, sodium salt) buffer (pH 7.0). Hydrae were fed with brine shrimp (*Artemia nauplii*) hatched in a solution of 1 % sodium chloride and treated with iodine (40 µg/ml). Hydrae were maintained free from bacterial and fungal contamination and were not fed for 24 h before initiating the experiments. Deionized water was used throughout this study (Mayura *et al.*, 1991).

2.1.2 RNA isolation and clean up

Total RNA was extracted from hydrae by application of 2 ml of TRIzol[®] reagent (Invitrogen, USA) to approximately 20 mg of fresh tissue using the manufacturer's protocol. The RNA was quantified by ultraviolet (UV) absorbance at 260 nm. Integrity of the total RNA was confirmed by 1 % formaldehyde agarose gel electrophoresis. The RNA isolated was cleaned up from

contaminating DNA using RNeasy Mini Kit (Invitrogen, USA) following the manufacturer's procedures.

2.1.3 Oligonucleotides

All oligonucleotides were procured from IDT Inc. (IA, USA). AP₂ primer (5'-GATCAGGACGTTTCGTTTGAGd(T)₁₇-3') was used for 5'-RACE (Rapid Amplification of cDNA Ends) experiments. The oligo(dT) bifunctional primer N (Not I-d(T)₁₈: 5'-AACTGGAAGAATTCGCGGCCGCAGGAAd(T)₁₈-3') was supplied in a cDNA preparation kit (Amersham Biosciences, USA) and was used for 3'-RACE experiments.

HSP70 protein sequences from diverse organisms (Figure 5) including cnidaria/hydrae (Figure 6) obtained from the NCBI protein database (<http://www.ncbi.nlm.nih.gov/entrez/query.fcgi?db=Protein>) were aligned using program ClustalW and degenerate oligonucleotides DF and DR (Table 4) were designed corresponding to the conserved amino acids ADAYLGK and AGDTHLG, respectively. Other primers (*H. vulgaris* gene specific) used in the experiments are shown in Table 4.

2.1.4 Cloning and identification of a partial fragment of *H. vulgaris* HSP70 cDNA

All polymerase chain reaction (RT-PCR and RACE-PCR) experiments were performed using *Taq* DNA polymerase (Invitrogen, USA) and a thermal cycler (MJ Research, USA).

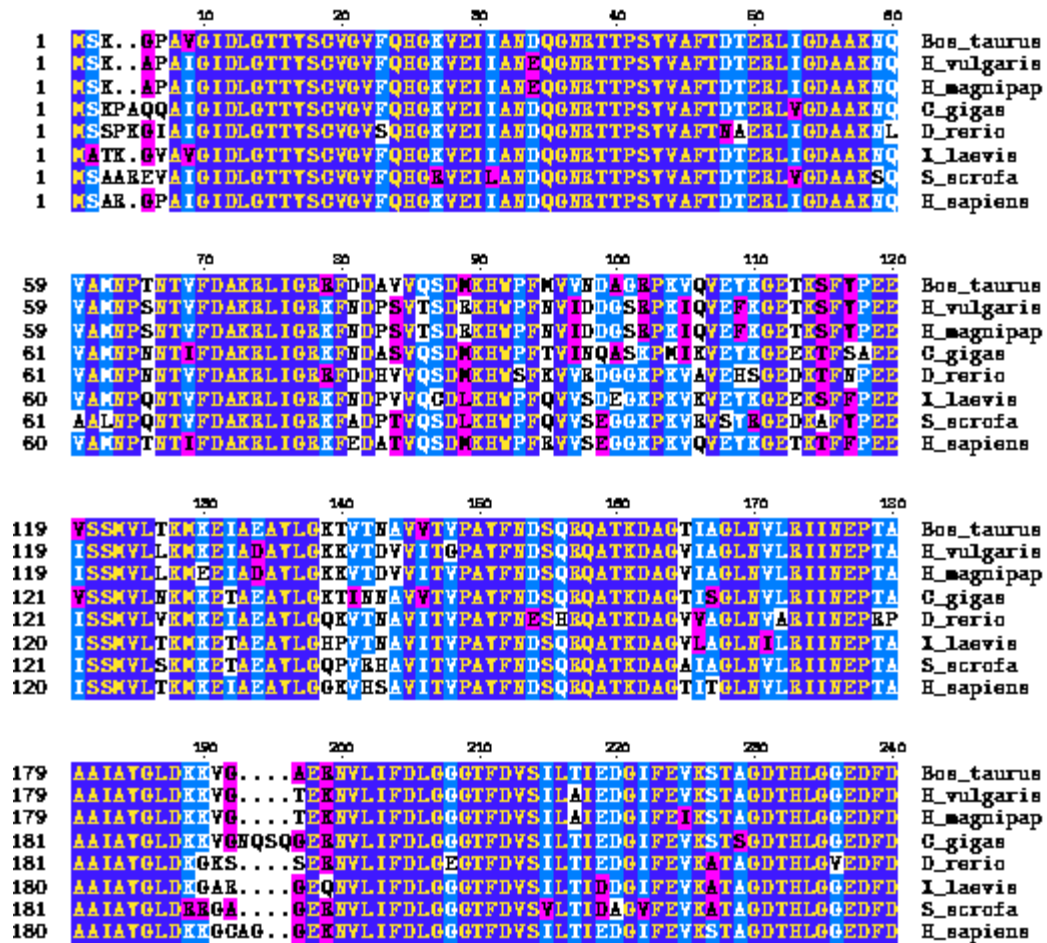


Figure 5. Multiple sequence alignment of HSP70 proteins using the program ClustalW. Accession numbers of the proteins as extracted using the Entrez web service (<http://www.ncbi.nlm.nih.gov/Entrez/protein.html>) are: gi|50347095 (*Bos Taurus*), *Hydra vulgaris* (from this study), gi|159268 (*Hydra magnipapillata*), gi|4838561 (*Crassostrea gigas*), gi|34784832 (*Danio rerio*), gi|64796 (*Xenopus laevis*) and gi|32879973 (*Homo sapiens*). The properties of amino acids are identified different shadings.

	260	270	280	290	300	
235	NRVNHFI	AEFRKKHKD	ISENKR	AVRRL	TACERAKRTLSSSTQASIEIDSL	YEGIDFY Bos_taurus
235	NRLVNHFI	AEFRKKHKD	ISSNKR	ALRRL	TACERAKRTLSASTQASVEIDSL	FDGIDFY H_vulgaris
235	NRLVNHFI	AEFRKKHKD	ISSNKR	ALRRL	TACERAKRTLSASTQASVEIDSL	FDGIDFY H_magnipap
241	NRVNHFI	QAEFRKKHKD	ISENKR	AVRRL	TACERAKRTLSSSSQASIEIDSL	YEGIDFY G_gigas
237	NRTVNHFI	AEFRKKHKD	ISQNK	ALRRL	TACERAKRTLSSSSQASIEIDSL	YEGIDFY D_rerio
236	NRVNHFI	VEEFRKKHKD	IQGNKR	ALRRL	TACDRAKRTLSSSSQASIEIDSL	FEGIDFY I_laevis
237	NRLVNHFI	MEEFRKKHKD	LSRNKR	ALRRL	TACERAKRTLSSSTQATLEIDSL	FEGVDFY S_scrofa
238	NRVSHLAE	AEFRKKHKD	IGPNKR	AVRRL	STACERAKRTLSSSTQASIEIDSL	YEGVDFY H_sapiens

	310	320	330	340	350	360	
295	TSITRARFEEL	NADLFEGTLD	PVEKALRDA	KLDK	SQIEDIVLVGGSTRIPKIQ Bos_taurus	
295	TSITRARFEEL	CIDLFEGTLD	GVADAI	RGKXSSGQNF	SKSDIE	EVVLVGGSTRIPKIVQ H_vulgaris	
295	TSITRARFEEL	CIDLFEGTLD	GVADAI	RGKXSSGQNF	SKSDIE	EVVLVGGSTRIPKIVQ H_magnipap	
301	TSITRARFEEL	NADLFEGTLD	PVEKALRDA	KLDK	SAQIEDIVLVGGSTRIPKIQ G_gigas	
297	TSITRARFEEL	CSDLFEGTLD	PVEKALRDA	KMDK	SAQIEDIVLVGGSTRIPKIQ D_rerio	
296	TAITRARFEEL	CSDLFEGTLD	PVEKALRDA	KLDK	SQIEDIVLVGGSTRIPKIVQ I_laevis	
297	TSITRARFEEL	CSDLFEGTLD	PVEKALRDA	KLDK	SAQIEDIVLVGGSTRIPKIQ S_scrofa	
298	TSITRARFEEL	NADLFEGTLD	PVEKALRDA	KLDK	GQIQIEDIVLVGGSTRIPKIQ H_sapiens	

	370	380	390	400	410	420	
348	KLLQDFF	FGKELNKS	INPDEAVATGA	AAVQAA	ILSGDKSE	EVQDLLLLDVTPLSLGIETAG Bos_taurus	
355	SLLQEFF	FGKELNKS	INPDEAVATGA	AAVQAA	ILAGDKE	HAQVDLLLLDVAPLSLGIETAG H_vulgaris	
355	SLLQEFF	FGKELNKS	INPDEAVATGA	AAVQAA	ILAGDKE	HAQVDLLLLDVAPLSLGIETAG H_magnipap	
354	KLLQDFF	FGKELNKS	INPDEAVATGA	AAVQAA	ILSGDKSE	EVQDLLLLDVTPLSLGIETAG G_gigas	
350	KLLQDFF	FGKELNKS	INPDEAVATGA	AAVQAA	ILMGDTSG	GVQDMLLLDVAPLSLGIETAG D_rerio	
349	KLLQDFF	FGKELNKS	INPDEAVATGA	AAVQAA	ILMGDKSE	EVQDLLLLDVAPLSLGLIETAG I_laevis	
350	KLLQDFF	FGKELNKS	INPDEAVATGA	AAVQAA	ILMGDKSE	EVQDLLLLDVAPLSLGLIETAG S_scrofa	
351	KLLQDFF	FGKELNKS	INPDEAVATGA	AAVQAA	ILIGDKSE	EVQDLLLLDVTPLSLGIETAG H_sapiens	

	430	440	450	460	470	480	
408	GVMTV	LIRKNTT	IPKQTQ	TFTTYS	DNQPGVLIQV	TEGERAMTKDNLLGKFELTGIPPA Bos_taurus	
415	GVFTPL	LIRKNTT	VPKTSQ	VFTTYS	ANQPGVLIQV	TEGERSMPAPNLLGKFELTGIPPA H_vulgaris	
415	GVFTPL	LIRKNTT	VPKTSQ	VFTTYS	DNQPGVLIQV	TEGERSMTAENLLGKFELTGIPPA H_magnipap	
414	GVMTL	LIRKNTT	IPKQTQ	TFTTYS	DNQPGVLIQV	TEGERAMTKDNLLGKFELTGIPPA G_gigas	
410	GVMTL	LIRKNTT	IPKQTQ	TFTTYS	DNQPGVLIQV	TEGEGAMTKDNLLGKFELTGIPPA D_rerio	
409	GVMTV	LIRKNTT	IPKQTQ	SFTTYS	DNQPGVLIQV	TEGERAMTKDNLLGKFELTGIPPA I_laevis	
410	GVMTL	LIRKNTT	IPKQTQ	TFTTYS	DNQPGVLIQV	TEGERAMTEENLLGKFELTGIPPA S_scrofa	
411	GVMTPL	LIRKNTT	IPKQTQ	TFTTYS	DNQSSVLYQV	TEGERAMTKDNLLGKFELTGIPPA H_sapiens	

Figure 5 (Continued).

	490	500	510	520	530	540	
468	PRGVPQIEVTFDIDANGILVSAVDKSTCKENK	ITITNDKGRLSKEDIERMVQEAKEYKA	Bos_taurus				
475	PRGVPQIEVTFDIDANGILVSAVDKSTCKENK	IPITNDKGRLSKEDIERMVQEAKEYKA	H_vulgaris				
475	PRGVPQIEVTFDIDANGILVSAVDKSTCKENK	ITITNDKGRLSKEDIERMVQEAKEYKA	H_magnipap				
474	PRGVPQIEVTFDIDANGILVSAVDKSTCKENK	ITITNDKGRLSKEDIERMVQEAKEYNQ	G_gigas				
470	PRGVPQIEVTFDIDANGILVSAVDKSTCKENK	ITITNDKGRLSKEDIERMVQEAKEYKA	D_rerio				
469	PRGVPQIEVTFDIDANGILVSAVDKSTCKENK	ITITNDKGRLSKEDIERMVQEAKEYKA	I_laevis				
470	PRGVPQIEVTFDIDANGILSVTATDSTCKENK	ITITNDKGRLSKEDIERMVQEAKEYKA	S_scrofa				
471	PRGVPQIEVTFDIDANGILVTAADKSTCKENK	ITITNDKGRLSKEDIERMVQEAKEYKA	H_sapiens				
	550	560	570	580	590	600	
528	EDELQREDEVSSKNSLESVAFMKATVEDEKLQAKI	EDDQXILDKCEFIINVLDEKQTA	Bos_taurus				
535	DDDLQREDEVQAKNSLESVCTMKQTVDEKFKGKISEEDKTI	IKKCEETVEVYDEKQTA	H_vulgaris				
535	DDDLQREDEVQAKNSLESVCTMKQTVDEKFKGKISEEDKTI	IKKCEETVEVYDEKQTA	H_magnipap				
534	EDELQREDEVQAKNSLESVAFMKATVEDEKLQAKI	EDDQXILDKCEFIINVLDEKQTA	G_gigas				
530	DDDLQREDEVQAKNSLESVCTMKQTVDEKFKGKISEEDKTI	IKKCEETVEVYDEKQTA	D_rerio				
529	DDDLQREDEVQAKNSLESVAFMKATVEDEKLQAKI	EDDQXILDKCEFIINVLDEKQTA	I_laevis				
530	EDELQREDEVQAKNSLESVCTMKQTVDEKFKGKISEEDKTI	IKKCEETVEVYDEKQTA	S_scrofa				
531	EDELQREDEVQAKNSLESVCTMKQTVDEKFKGKISEEDKTI	IKKCEETVEVYDEKQTA	H_sapiens				
	610	620	630	640	650	660	
588	EKEEFYEHQKELEKVGHPITKLTCSAGGMPGG	MPGGMP...GGPCC...GAPPSGAS	Bos_taurus				
595	EKEEFYEHQKELEKVGHPITKLTCSAGGMPGG	MPGGMP...GGPCC...GSK...ASS	H_vulgaris				
595	EKEEFYEHQKELEKVGHPITKLTCSAGGMPGG	MPGGMP...GGPCC...GSK...ASS	H_magnipap				
594	EKEEFYEHQKELEKVGHPITKLTCSAGGMPGG	MPGGMP...GGPCC...GAP...GGSG	G_gigas				
590	EKEEFYEHQKELEKVGHPITKLTCSAGGMPGG	MPGGMP...GGPCC...GAP...GGSG	D_rerio				
589	EKEEFYEHQKELEKVGHPITKLTCSAGGMPGG	MPGGMP...GGPCC...GAP...GGSG	I_laevis				
590	EKEEFYEHQKELEKVGHPITKLTCSAGGMPGG	MPGGMP...GGPCC...GAP...GGSG	S_scrofa				
591	EKEEFYEHQKELEKVGHPITKLTCSAGGMPGG	MPGGMP...GGPCC...GAP...GGSG	H_sapiens				
642	SOPTIEEVD	Bos_taurus					
642	GOPTIEEVD	H_vulgaris					
646	GOPTIEEVD	H_magnipap					
651	GOPTIEEVD	G_gigas					
635	GOPTIEEVD	D_rerio					
639	SOPTIEEVD	I_laevis					
635	TOPVIEEVD	S_scrofa					
631	GOPTIEEVD	H_sapiens					





 non conserved
 similar
 conserved
 all match

Figure 5 (Continued).

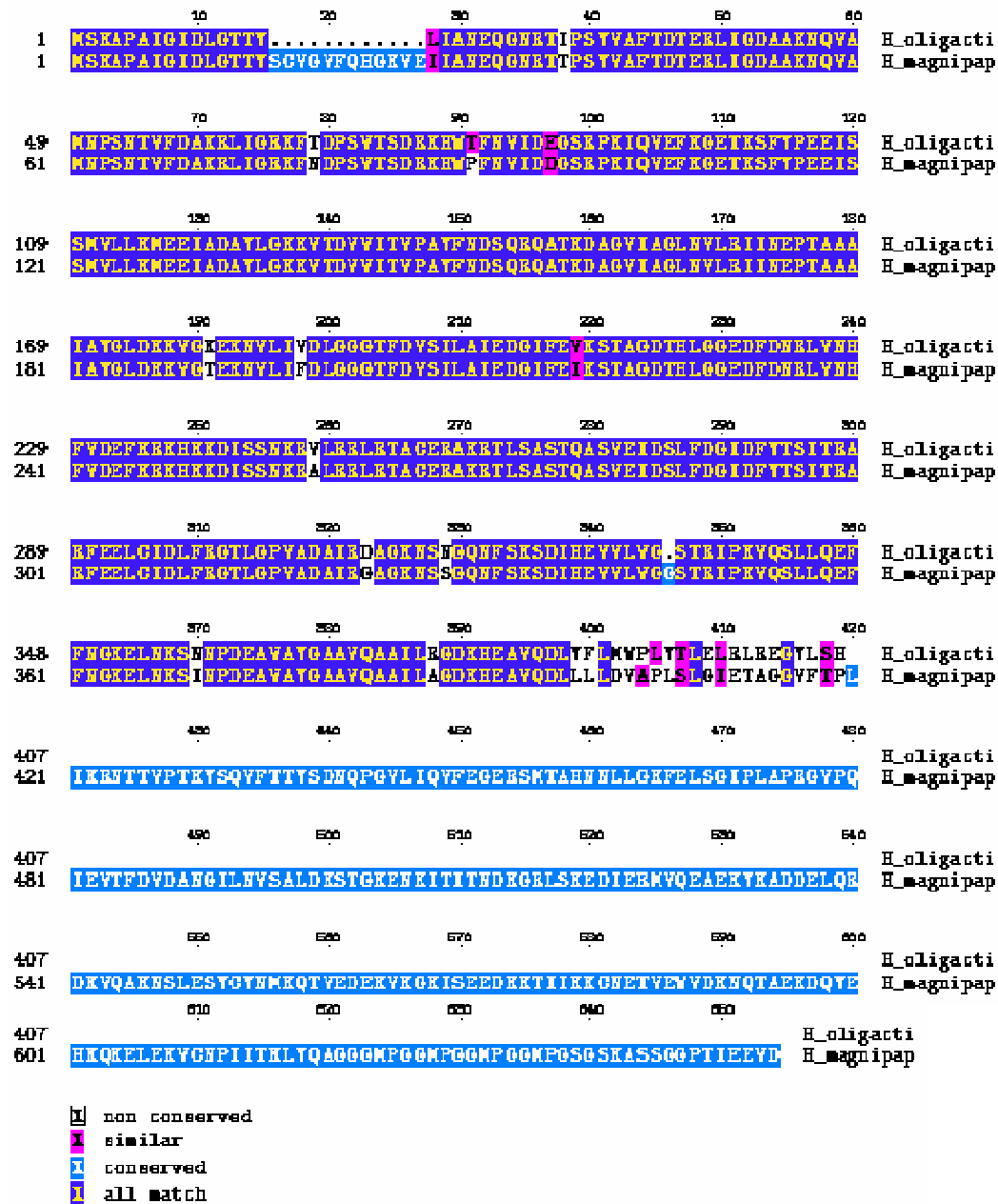


Figure 6. HSP70 protein sequence comparison of the *H. magnipapillata* to that of *H. oligactis*. The accession numbers of the proteins are gi|159268 and gi|1711306 respectively. The properties of different amino acids are identified by different shadings as identified by the legend.

TABLE 4

Oligonucleotide Used in the Cloning of HvHSP70 Gene

Oligonucleotide	Sequence
DF	5'-WGCRGATGCKTATCTKGGTA-3'
DR	5'-RCCAAGATGWGTGTCACCYG-3'
F1	5'-AGCGGATGCGTATCTTGGTA-3'
F2	5'-GGGAGTTATTGCTGGGTTGA-3'
N	5'-AACTGGAAGAATTCGCGGCCGCAGGAAd(T) ₁₈ -3'
AP ₂	5'-GATCAGGACGTTTCGTTTGAGd(T) ₁₇
R1	5'-TCTATAGTTGGTCCACCGGAA-3'
R2	5'-GGTCCACCGGAAGTAGCTTT-3'
R3	5'-AAAGGTGCGACATCAAGAAG-3'
R4	5'-TGAAGGGTTCATAGCAACTTGA-3'
F3	5'-GCTTGCTAATTTTCTATGAATTC-3'
R5	5'-TGTGTCTGGTAAATGCAACGT-3'
F4	5'-TTCAACCCGAGTAAATTGATGA-3'
R6	5'-TGAAGGGTTCATAGCAACTTGA-3'
F5	5'-ACGTTGCATTTACCGACACA-3'
R7	5'-TCCCGCATCTTTAGTTGCTT-3'
F6	5'-ATAGCGGATGCGTATCTTGG-3'
R8	5'-AAAGGTGCGACATCAAGAAG-3'
F7	5'-AGCAGCTATTTTGGCTGGTG-3'
R9	5'-GGTCCACCGGAAGTAGCTTT-3'
F8	5'-GAAAGGATGGTGCAAGAAGC-3'
F9	5'-AGCGGATGCGTATCTTGGTA-3'
R10	5'-CAGGTGACACACATCTTGGTGGT-3'
AF	5'-AAGCTCTTCCCTCGAAGAATC-3'
AR	5'-CCAAAATAGATCCTCCGATCC-3'

Mix base definitions: W=A, T; R=A, G; K=G, T; Y=C, T

RNA (5 µg) was reverse-transcribed to cDNA at 37 °C for 60 min using the oligo(dT) bifunctional primer and the AMV RT supplied in the cDNA synthesis kit (Amersham Biosciences, USA). The first-strand cDNA was amplified using the primers DF and DR (Table 4). The PCR was performed for 30 cycles, consisting of 94 °C for 30 s, 50 °C for 30 s and 72 °C for 1 min and a final extension at 72 °C for 10 min. The resultant PCR products (Figure 7) was subcloned into the pCR[®]II-TOPO[®] vector using a TA cloning kit (Invitrogen, USA) according to the manufacturer's instructions. Multiple independent clones were sequenced using automated methods (DNA Technologies Lab, Department of Veterinary Pathobiology, Texas A&M University) on an ABI PRISM[™] 310 Genetic Analyzer (PE Biosystems, USA) using a Big-Dye sequencing kit (PE Biosystems) and M13 primers. The identity of the clones was evaluated by matching the sequences to the nucleotide/protein sequences available at the GenBank (<http://www.ncbi.nlm.nih.gov/>). The cloned sequences constituted residues 1090 to 1387 in the HvHSP70 sequence (Figure 8).

2.1.5 3'-RACE of the HvHSP70 cDNA

First-strand cDNA prepared above was amplified using the oligo(dT) bifunctional primer N and a gene-specific primer F1 (Table 4) (complementary to nt 1090 to 1109) for 30 cycles of 94 °C for 30 s, 55 °C for 30 s and 72 °C for 3 min. The PCR-products were diluted 100 times and a second round of PCR was done using a gene specific primer F2 (complementary to nt 1183 to 1202) for 30 cycles of 94 °C for 30 s, 55 °C for 30 s and 72 °C for 3 min.

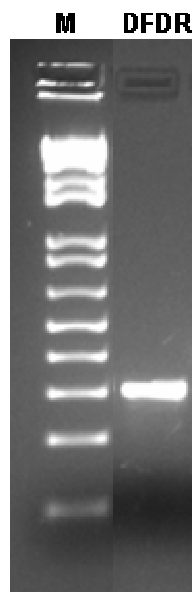


Figure 7. Image of electrophoretic gel for degenerate PCR products of HvHSP70 gene. The PCR products were produced using primer DF and DR. M = 1 kb plus DNA ladder.

```

1      gcttgctaatttttctatgaattctataataattcaactcgagtaaattgatgatattgta 60
61      aatggtaaatcgagaacattacgaatttaccgtctgattctttaaaaaactagaactat 120
121     ctagaaaattttgaaattaggaatactaaaaaaattttacagttaacatatttttagtagtt 180
181     tatagcataaaattatttttttaacttaaaacgtataaaaagtattacttttttaggcta 240
241     ttagaaaaatattaaatttttttttactctattcaactttttgacaaacatttagttata 300
301     agctgcaccccccgtttatgaatacaataaatcagtataaaacgataaacttgtatatgat 360
361     gataaacaaacttttaagtcggttagccgtcaaagaaaagagagagaaagaaaggagcaga 420
1      taaattatttttaaatacaaaaatgtctaaagcgccagctattggaattgatcttggcac 480
14 T Y S C V G V F Q H G K V E I I A N E Q
481     aacttactcttgtgtcggagttttccaacacggaagtgaaataattgctaacgagca 540
34 G N R T T P S Y V A F T D T E R L I G D
541     agggaatcgcaccactccaagttacgttgcatttaccgacacagaaagattaattggaga 600
54 A A K N Q V A M N P S N T V F D
601     tgcagcaaaaaatcaagttgctatgaacccttcaaacacagtgtttgGTAAGCGTTAAAA 660
661     TAGTTATTCATTTATAAACTTTTTTTTTTAATTAGAAATTTTAGATTGATTGTCAAGTAA 720
70      A K R L I G R K F
721     AATAATAACCAATAACGTAAAAATTTTGTAGatgcgaaacgattgattggtagaaaatt 780
79 N D P S V T S D R K H W P F N V
781     taacgatccatcggtcacttcagatagaaaacattggccatttaatgtAAGCTGTTGTTT 840
841     TCTAAATCAAGAGAAATCTAAACAATAACTTTGCTAGATTTTATTACTAATAAACTA 900
901     TATCTGTTAGTTTTCTTTAATTTGAAATATTTTACATACTTATTACGAAATCTGAATTG 960
95      I D D G S R P K I Q V E F
961     CGTTTTGGTTTACTTACAGGttatagatgatggatccaggccaaagattcaagttgagtt 1020
108 K G E T K S F Y P E E I S S M V L L K M
1021     taaaggagaaacgaaatcattctacccagaggagatatcctccatggtgctgctaaagat 1080
128 K E I A D A Y L G K K V T D V V I T G P
1081     gaaggaaatagcggatgcgtatcttggtaaaaaagtcacagatggtgtcataactggacc 1140
148 A Y F N D S Q R Q A T K D A G V I A G L
1141     tgcttacttttaatgattctcaacgtcaagcaactaaagatgcgggagttattgctgggtt 1200
168 N V L R I I N E P T A A A I A Y G L D K
1201     gaatgttttgcgaattatcaatgaaccgactgcagctgcgattgcttatggtctcgataa 1260
188 K V G T E K N V L I F D L G G G T F D V
1261     aaaagttggaacggagaaaaatgtgcttatctttgatttgggtggtggaacttttgatgt 1320
208 S I L A I E D G I F E V K S T A G D T H
1321     ttctattcttgcgatagaagatggtatatttgaagtaaaatcaactgcaggtgacacaca 1380

```

Figure 8. Nucleotide and deduced amino acid sequence of *H. vulgaris* HSP70. The three introns identified by genomic PCR and sequencing are in italicized capital letters. The underlined bold face nucleotides in the 5'-non-translated region mark the putative heat shock elements (HSE). The putative CAAT and TATA boxes are shown in bold face. The transcription-start site identified by 5'-RACE is italicized. The stop codon is identified with an asterisk. The nucleotide and amino acid sequences are numbered from the 5'-end of the cDNA sequence, and from the N-terminal start codon methionine, respectively.

```

228 L G G E D F D N R L V N H F V D E F K R
1381 tcttggtggtgaagatttcgataatcgtcttgtcaaccattttggtgatgaatttaaaag 1440
248 K H K K D I S S N K R A L R R L R T A C
1441 aaaacataagaaagatatttcttccaacaaaagagctctgcgtcgcttacgaacagcatg 1500
268 E R A K R T L S A S T Q A S V E I D S L
1501 cgagaggggctaagagaacactttcagccagttactcaagcaagtgttgaaattgattcttt 1560
288 F D G I D F Y T S I T R A R F E E L C I
1561 gtttgatggaattgatttttacacgtcaatcacacgcgcacgttttgaagagttatgcat 1620
308 D L F R G T L G P V A D A I R D A G K N
1621 tgatttggttagaggtaccctaggtcctgttgcggtgctattagagatgctggaaaaaa 1680
328 S S G Q N F S K S D I H E V V L V G G S
1681 cagtagcgggtcaaaatttctcaaagctdgacatccacgaagttgttttggttggtgctc 1740
348 T R I P K V Q S L L Q E F F N G K E L N
1741 aactcgtattccaaaagtgcaggctctacttcaggaattttttaatggtaaggagcttaa 1800
368 K S I N P D E A V A Y G A A V Q A A I L
1801 caaatcaattaatccggatgaagctggtgcttatgggtgccgctgttcaagcagctatttt 1860
388 A G D K H E A V Q D L L L L D V A P L S
1861 ggctggtgataaacatgaagcagttcaagatctattacttcttgatgtcgcacctttatc 1920
408 L G I E T A G G V F T P L I K R N T T V
1921 acttggaaattgagacagctggtggagtatttactccattaattaaaagaaacactactgt 1980
428 P T K Y S Q V F T T Y S A N Q P G V L I
1981 tccaactaaatattcccggtgttcacgacgtattcagccaatcaacctggagttttaat 2040
448 Q V F E G E R S M P A P N N L L G K F E
2041 ccaagtttttgagggagaaagaagtatgccagccccaataacctcctgggcaagtttga 2100
468 L T G I P P A P R G V P Q I E V T F D V
2101 actcacgggaattccccctgctccaagaggtgttcctcaaactcgaggtaacttttgatgt 2160
488 D A N G I L N V S A L D K S T G K E N K
2161 tgatgcaaatggaattctaataatgtttctgcactagacaaaagtactggaaaagaaaaata 2220
508 I P I T N D K G R L S K E D I E R M V Q
2221 aattcccataactaatgataaaggctcgtcttttctaagaagatattgaaaggatggtgca 2280
528 E A K A D D E L Q R D K V Q A K N
2281 agaagctgaaaagtacaaagccgatgacgaacttcagcgagataaagttcaagcaagaa 2340
548 S L E S Y C Y N M K Q T V E D E K V K G
2341 ctctttggaaagctactgttataatatgaaacaaactgttgaggatgaaaaagttaaagg 2400
568 K I S E E D K K T I I K K C N E T V E W
2401 aaaaattagcgaagaagataaaaagaccattattaaaaaatgcaatgaaacggtagaatg 2460
588 V D K N Q
2461 ggttgataaaaatcagGTGGGCCGTTTGTCTTAAATTTTTTAAATTTTTCTAATTTTT 2520

2521 ACATGCATTTTAAGTATCAACTCTTTAAATTTAAGGAAATAGATATATTTCTTTCTATA 2580
593 T A E K D E Y E
2581 TGCGTCTTAGTATGTTATATGTTTTAATCGTTATAGactgccgaaaaagatgagtatgag 2640
601H K Q K E L E K V C N P I I T K L Y Q A
2641 cataaacaaaaagaacttgaaaaagtgtgcaaccctattattacgaagctttatcaagct 2700
621G G G M P G G M P G G M P G S G S K A S
2701 ggtggtggttatgccaggtggttatgccaggtggttatgccagggagtggtcttaaagctagt 2760
641S G G P T I E E V D *
2761 tccggtggaccaactatagaagaagtagattaaatgtattttattaaattcaactatttgt 2820

2821 atttattgtagattttatttttacatgtgtattataaatgtaataggaaatataaattatg 2880

2881 caatcaaaaaaaaaaaaaaaaaaaaaa 2907

```

Figure 8 (Continued).

The PCR products (Figure 9) were subcloned and sequenced as described above. The identity of the clones was evaluated by matching the sequences to the nucleotide/protein sequences available at the GenBank (<http://www.ncbi.nlm.nih.gov/>).

2.1.6 5'-RACE of the HvHSP70 cDNA

The template cDNA was synthesized using a gene specific primer R1 (Table 4) (complementary to nt 2759-2780) and Superscript II enzyme (Invitrogen, USA), followed by dA tailing of the cDNA using dATP and terminal transferase (Invitrogen, USA) using standard procedures (Sambrook *et al.*, 1989). The first strand cDNA was amplified using the anchor primer AP₂ (5'-GATCAGGACGTTCGTTTGAGd(T)₁₇-3') and the gene-specific primer R1, and the first-round PCR products were amplified using primer AP₂ and another gene-specific primer R2 (Table 4) (complementary to nt 2752-2771). Each PCR was performed with an initial amplification of 95 °C for 5 min, 48 °C for 5 min and 72 °C for 5 min followed by 20 cycles of 95 °C for 40 s, 48 °C for 1 min and 72 °C for 3 min with a final extension of 10 min at 72 °C. The PCR products (Figure 10A) were subcloned and sequenced as described above. The identity of the clones was confirmed by matching the sequences to the nucleotide/protein sequences available at the GenBank (<http://www.ncbi.nlm.nih.gov/>).

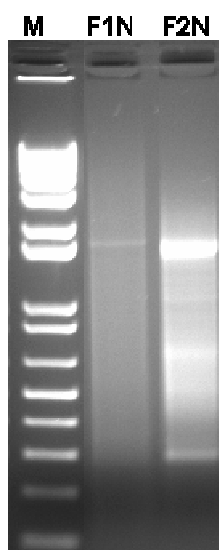


Figure 9. Image of electrophoretic gel for 3'-RACE PCR products of HvHSP70 gene. The first round of PCR products were produced using primer F1 and N. The second round of PCR products were produced using primer F2 and N. M = 1 kb plus DNA ladder.

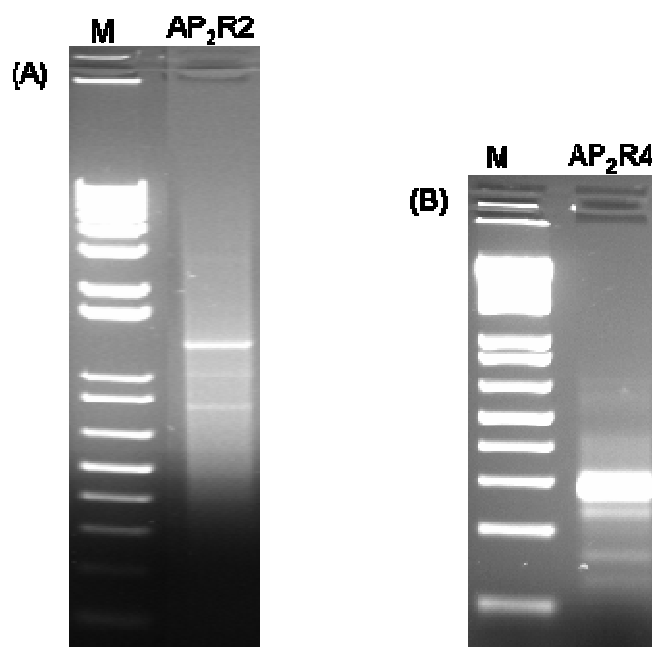


Figure 10. Images of electrophoretic gels for 5'-RACE PCR products of HvHSP70 gene. (A) The PCR products were produced using primer AP₂ and R2. (B) The PCR products were produced using with primer AP₂ and R4. M = 1 kb plus DNA ladder.

The 5'-RACE experiment was performed once again to clone the full-length cDNA. The template cDNA was synthesized using gene specific primer R3 (Table 4) (complementary to nt 1898-1917), as stated above and the template cDNA was amplified using the anchor primer AP₂ (Table 4) and the gene-specific primer R3. The first-round PCR products were amplified using the PCR anchor primer AP₂ and another gene-specific primer R4 (Table 5) (complementary to nt 613-634). PCR conditions were as above. The PCR products (Figure 10B) were subcloned and sequenced as described above. The identity of the clones was confirmed as previously described.

2.1.7 Cloning the 5' non-coding region

The nucleotide sequences cloned above were highly identical to the *H. magnipapillata* HSP70.1 sequence (gi|159267). Assuming that *H. vulgaris* will have similar promoter sequence, the 5'-flanking sequence of HvHSP70 gene was amplified using a primer F3 complementary to nt 1-23 (that was designed based on the *H. magnipapillata* HSP70 sequence, gi|159267; nt 7-29) and R5 (complementary to nt 564-583). The amplified products (Figure 11) were subcloned and sequenced using M13 primers.

2.1.8 Determination of the exon/intron structure of the HvHSP70 gene

The genomic DNA of hydra was extracted using DNeasy Tissue Kit (QIAGEN, USA) according to the manufacturer's instructions and the HSP70 gene was amplified using the genomic PCR with the *Taq* DNA polymerase

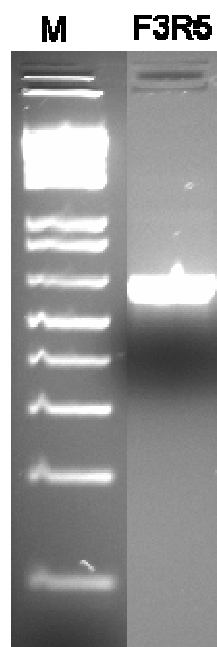


Figure 11. Image of electrophoretic gel for PCR products of 5' flanking sequence of HvHSP70 gene. The PCR products were obtained with primer combination F3 and R5. M = 1 kb plus DNA ladder.

(Invitrogen, USA). The genomic PCRs were performed using following overlapping primer combinations: primer F4 (complementary to nt 32-53) and a primer R6 (complementary to nt 613-634); primer F5 (complementary to nt 564-583) and primer R7 (complementary to nt 1167-1186); primer F6 (complementary to nt 1088-1109) and primer R8 (complementary to nt 1898-1917); primer F7 (complementary to nt 1849-1868) and a primer R9 (complementary to nt 2752-2771); and primer F8 (complementary to nt 2267-2286) and primer R9 complementary to nt 2752-2771 .

All the above reaction mixtures (50 μ l) contained 200 ng of genomic DNA template, 10 pmol of each oligonucleotide primer, a 10 mM concentration of each dNTP, and 2.5 U of *Taq* DNA polymerase (Invitrogen, USA). PCR amplification preceded by a 5 min denaturation step at 94 $^{\circ}$ C proceeded through 30 cycles of denaturation (94 $^{\circ}$ C, 1 min), annealing (55 $^{\circ}$ C, 1 min), and polymerization (72 $^{\circ}$ C, 3 min) and a 10 min elongation step at 72 $^{\circ}$ C. The amplified products (Figure 12) were subcloned to a pCR[®]II-TOPO[®] vector using a TA cloning kit (Invitrogen, USA) according to the manufacturer's instructions and sequenced as described above. The identity of the clones was confirmed as stated above.

2.1.9 Heat treatment

Hydrae were incubated at 18 (control temperature), 30 and 37 (maximum induction temperature) $^{\circ}$ C for both 1 h and 6 h in 5 ml hydra media.

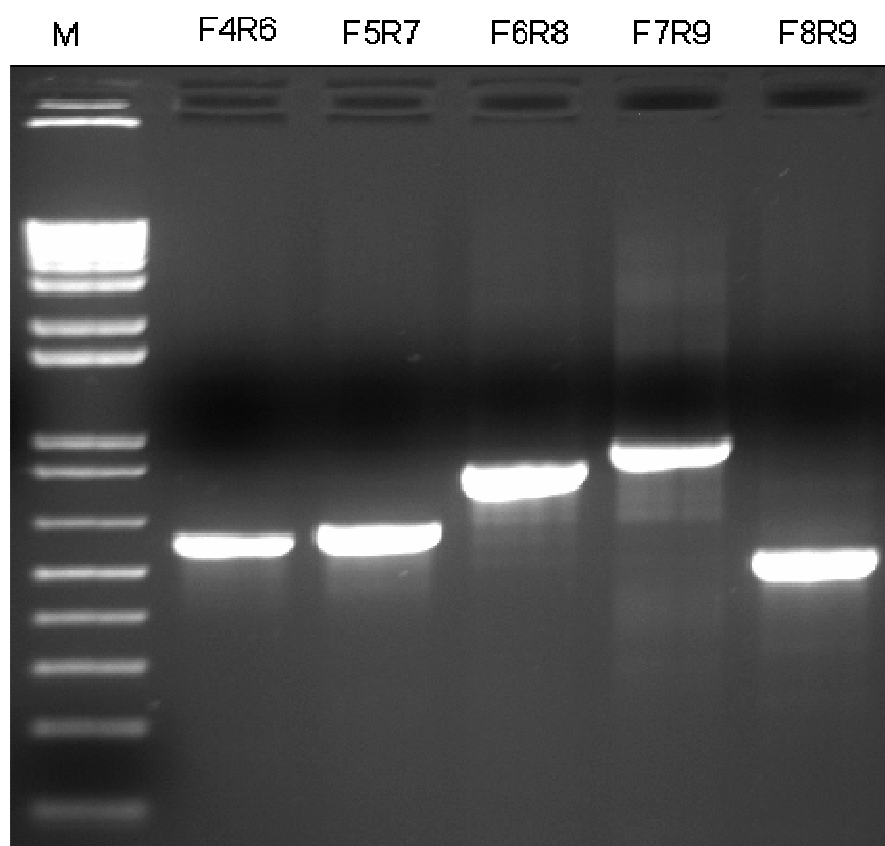


Figure 12. Image of electrophoretic gel for genomic PCR products of HvHSP70 gene. The PCR products were obtained with primer combination of F4 and R6; F5 and R7; F6 and R8; F7 and R9; and F8 and R9. M = 1 kb plus DNA ladder.

2.1.10 Metal treatment

Approximately 500 hydrae were incubated at 100 ppm of $\text{CuSO}_4 \cdot 5\text{H}_2\text{O}$, ZnCl_2 , $\text{CdCl}_2 \cdot 2.5\text{H}_2\text{O}$, $\text{K}_2\text{Cr}_2\text{O}_7$, As_2O_3 , Na_2HAsO_4 and Na_2SeO_3 for 1 h and 6 h in 5 ml hydra media. Hence, the concentration (active ingredients) of Cu (II), Zn (II), Cd (II), Cr (VI), As (III), As (V), and Se (IV) were calculated to be 0.4 mM (= 25.4 ppm), 0.73 mM (= 47.9 ppm), 0.43 mM (= 49.2 ppm), 0.33 mM (= 17.6 ppm), 0.506 mM (= 37.8 ppm), 0.302 mM (= 24.0), and 0.57 mM (= 45.6 ppm) respectively.

2.1.11 Oxidative stress treatment

Approximately 500 hydrae were incubated at 300 ppm (= 9.79 mM) H_2O_2 , 30 ppm (= 0.979 mM) of H_2O_2 , 100 ppm (= 0.38 mM) of paraquat and 100 ppm (= 1.538 mM) sodium azide in 5 ml hydra media for 1 or 6 h.

2.1.12 Starvation treatment

For starvation experiments, hydrae were maintained without feeding for 5 days.

In all cases, treatments were carried out in 14 ml polypropylene round-bottom tubes (Becton-Dickinson, NJ, USA) containing 5 ml hydra media. At the end of the treatment, hydrae were collected by centrifugation at 7,500 Xg for 5 min. The supernatants were discarded. Then hydrae were washed once in 5 ml of 0.05 M PBS for 5 min @ 7,500 Xg. The supernatants were discarded as before and the animals were homogenized immediately in 2 ml of TRIzol[®] (Invitrogen, USA).

2.1. 13 Expression analysis of HvHSP70 mRNA in hydrae

Total RNA was extracted from TRIzol[®] (Invitrogen, USA) treated whole hydrae and cleaned as before using RNeasy Mini Kit (Invitrogen, USA) following the manufacturer's instruction. For RT-PCR, 5 µg of total cleaned RNA was reverse transcribed using 500 ng of oligo(dT)₁₂₋₁₈ primer (Invitrogen, USA) and 200 units of the Superscript II enzyme (Invitrogen, USA) for 50 min at 42 °C. The reaction was inactivated by heating the mixture at 70 °C for 15 min. PCR assays were designed to normalize HvHSP70 gene expression levels to actin transcription rate. Two µl of first strand cDNA (from 25 µl of reverse transcription mix) was diluted 100 times prior to PCR amplification. PCR was carried out in 50 µl total volume of 1 × PCR buffer (20 mM Tris-HCl, pH 8.4, 50 mM KCl), 2 mM MgCl₂, 0.1 mM each of dNTPs, 10 pmol each of primers, and 0.5 U *Taq* DNA polymerase (Invitrogen, USA) using 2 µl of (1:100) diluted RT-product. Actin mRNA was amplified using the AF and AR primers and the HvHSP70 was amplified using the F9 (complementary to 1090-1109) and R10 (complementary to 1368 - 1390) primers. Cycling profile after initial denaturation at 94 °C for 4 min was 30 cycles of amplification as follows: denaturation at 94 °C for 30 s, annealing at 55 °C for 30 s, and extension at 72 °C for 45 s. These number of PCR cycles ensured quantification within the exponential phase of amplification. Equal amounts of RT-PCR reactions (9.5 µl) were loaded on standardized 2 % agarose gels containing 0.1 µg/ml ethidium bromide. The gel images were digitalized by a gel documentation system (Kodak Laboratories, USA).

2.1.14 General bioinformatic analyses

Conceptual translation of the full-length cDNA was performed using the program SIXFRAME (<http://biologyworkbench.ucsd.edu>). Homology to other HvHSP70 gene and proteins were identified with the Blast program with default settings (<http://www.ncbi.nlm.nih.gov/BLAST>). The identification of HvHSP70 domains were performed by use of the SMART program (<http://smart.embl-heidelberg.de/>) using default pattern definitions. Prosite (<http://us.expasy.org/prosite/>) identification of glycosylation, phosphorylation, myristilation and amidation sites was performed by use of the ExPASy program using default settings. The isoelectric point (pI) and the molecular weight (M_w) of HvHSP70 were calculated using the ExPASy program (http://us.expasy.org/tools/pi_tool.html). Several HSP70 protein sequences retrieved from the National Center for Biotechnology Information (NCBI) Entrez Web service (<http://www.ncbi.nlm.nih.gov/Entrez/>) were aligned to each other using the web program T-coffe (http://igs-server.cnrs-mrs.fr/Tcoffee/tcoffee_cgi/index.cgi), ClustalW (<http://www.ch.embnet.org/software/ClustalW.html>), or the ClustalW program embedded in program Mega 3.1 (<http://www.megasoftware.net/>) (Figure 5).

2.1.15 Phylogenetics

For phylogenetic analysis sequences were aligned using the ClustalW program embedded in the program Mega 3.1 (<http://www.megasoftware.net/>). The aligned sequences were converted into the “PhylipIPhylip44” format

(Felsenstein, 1993) using the Readseq program (<http://iubio.bio.indiana.edu/cgi-bin/readseq.cgi>) and saved as a text file. The text file in the interleaved format was uploaded to the PHYML Online (<http://atgc.lirmm.fr/phyml/online.html>) web interface (Guindon and Gascuel, 2003). Following parameters were chosen for the construction of the tree: substitution model - JTT; number of bootstrap data sets - 500, proportion of invariable sites - 0 and fixed; number of substitution rate categories - 1; starting tree(s) - BIONJ; optimize topology - yes; optimize branch lengths and rate parameters -yes. Nonparametric bootstrap (Felsenstein, 1985) was applied to assess the reliability of internal branches for (large) datasets. The tree generated in the NEWICK format was displayed using the Drawtree program (<http://www.phylodiversity.net/~rick/drawtree/>).

The of heat shock protein 70 sequences (with their accession numbers) used for phylogenetic analysis are: *Beroe ovata* (AF026512), *Asbestopluma hypogea* (AF026513), *Petrosia ficiformis* (AF026514), *Rhabdocalyptus dawsoni* (AF026515), *Funiculina quadrangularis* (AF026516), *Eunicella cavolini* (AF026518), *Petrobiona massiliana* (AF026520), *Bruggia malavi* (M68933), *Ceratitis capitata* (U20256), *Drosophila melanogaster* (J01103), *Echinococcus granulosus* (U26448), *Mesocestoides corti* (U70213), *Geodia cydonium* (X94985), *Saccharomyces cerevisiae* (Z35836), *Pichia angusta* (Z29379), *Arabidopsis thaliana* (X77199), *Lycopersicon esculentum* (L41253), *Oxytricha nova* (U37280), HSC70-prov P *Xenopus laevis* (gi|27371247), HS70 P 8 *Bos taurus* (gi|27805925), HS70P *Mus musculus* (gi|1661134), *Ambystoma*

mexicanum (gi|18031682), *Pimephales promelas* (gi|43439894), HSC70 *Gallus gallus* (gi|45384370), HSP70 *Gallus gallus* (gi|37590083), *Artemia franciscana* (gi|16611913), Hsp70 *P Danio rerio* (gi|34784832), *Cotesia rubecula* (gi|25527326), HSC 70.II *P Xenopus laevis* (gi|1326171), HSP70 *Canis familiaris* (gi|32813265), *Locusta migratoria* (gi|37993866), HSP 70 *Bos taurus* (gi|50347095), *Oncorhynchus mykiss* (gi|17129570), *Rhabdosargus sarba* (gi|40888897), HSP70 *Gallus gallus* (gi|55742654), HSP70.2 – mouse (gi|109946), HSCP *Bombyx mori* (gi|20563125), HSC70 *Carassius auratus* (gi|29467493), *Crassostrea gigas* (gi|4838561), HS70P 1A *Rattus norvegicus* (gi|14010867), *Crassostrea ariakensis* (gi|31322197), HSP70 *Mus musculus* (gi|3986772), HSP70 *Rattus norvegicus* (gi|396270), HSP70 *Mus musculus* (gi|3986773), *Sus scrofa* (gi|1978), *Schizosaccharomyces pombe* (gi|3581889), *Crassostrea virginica* (gi|7688162), *Vigna radiate* (gi|45331281), *Hydra magnipapillata* (gi|159268) and *Arabidopsis thaliana* (gi|9294373).

2.1.16 Threading

Five threading methods used to find suitable structure template(s) for the HvHSP70 were as follows: TOPITS (<http://dodo.cpmc.columbia.edu/predictprotein/>); HMM (<http://www.cse.ucsc.edu/research/compbio/HMM-apps/HMM-applications.html>); 3D-JIGSAW (<http://www.bmm.icnet.uk/~3djigsaw/>); 3D-PSSM (<http://www.sbg.bio.ic.ac.uk/~3dpssm/>); and HFR (<http://www.cs.bgu.ac.il/~bioinbgu/>). TOPITS (Rost, 1995) and 3D-PSSM (Kelley *et al.*, 2000) are methods based on matching the predicted secondary structure

and solvent accessibility or solvation potentials of the query sequence with those of the proteins of known structures. HFR (Fischer, 2000) is a hybrid method that combines results from five threading programs to search the most consistent fold prediction among them. HMM (Karplus *et al.*, 1998) uses a hidden Markov model (HMM) engine to compare the query sequence with sequences of known protein structures to derive a possible structure class for the query one. The 3D-JIGSAW (Bates *et al.*, 2001) Web server builds 3D models for proteins based on homologs of known structures. Through the threading experiments on the Web sites, several templates for the query sequence were found. These templates were further screened using the SWISS-MODEL Protein Modeling Server (Guex and Peitsch, 1997) on the Web. Protein 3HSC (3HSC.pdb) (Flaherty *et al.*, 1990) was selected as the structure template for the query sequence HvHSP70.

2.1.17 Molecular modeling

Using the alignment in Figure 13, a 3D model of the HvHSP70 protein was built based on the coordinates of 3HSC (3HSC.pdb). The template and target assembly (Figure 13) was submitted to the 3D-JIGSAW web server and a model was retrieved (Figure 14).

2.1.18 Analysis of the model

The overall stereo-chemical quality of the model was assessed using the program PROCHECK (<http://biotech.ebi.ac.uk:8400/cgi-bin/sendquery>) (Laskowski *et al.*, 1994). A secondary structure (Figure 15) and

```

SCORE=100
*
  BAD AVG GOOD
*
HvHSP70 : 100
3HSC    : 100

HvHSP70      1 KAPAICIDLGTTYS CVGVFQHGRVEIIANEQQGRRTTSPSYVAFTCTERLIGD 51
3HSC         1 KQPAVGIDLGTTYS CVGVFQHGRVEIIANDQQGRRTTSPSYVAFTCTERLIGD 51

Cons         1 *.....*.....*.....*.....*.....*.....*.....*.....*.....*..... 51

HvHSP70      52 AAKNQVAHNPSTNTVFDAXRLIGRKFNDSVTSORKHWPFPNVIDCGSRPKIQ 102
3HSC         52 AAKNQVAHNPSTNTVFDAXRLIGRRTDDAVVQSDMKHWPFPNVVNCAGRPKVQ 102

Cons         52 *****.....*.....*.....*.....*.....*.....*.....*.....*.....*..... 102

HvHSP70     103 VEPKGETKSPYDPEEISSMVLTKMKIADAYLCKKVTDVVTGDPAYFNDSQR 153
3HSC        103 VEPKGETKSPYDPEVSSMVLTKMKIADAYLCKTWTNAVVTVPAYFNDSQR 153

Cons        103 *.....*.....*.....*.....*.....*.....*.....*.....*.....*..... 153

HvHSP70     154 QATEDAGVIAGLNVLRINEPTAAAIAYGLDKKVGTEKNVLIFCLGCGCTFD 204
3HSC        154 QATEDAGTIAGLNVLRINEPTAAAIAYGLDKKVGAEENVLIFCLGCGCTFD 204

Cons        154 *****.....*.....*.....*.....*.....*.....*.....*.....*.....*..... 204

HvHSP70     205 VSILAIEDGIFEVKSTAGDTHLGGEDFQNLVNHVVDSPKREHMKDISSE 255
3HSC        205 VSILTIEDGIFEVKSTAGDTHLGGEDFQNLVNHVVFIAEFKREHMKDISSE 255

Cons        205 *****.....*.....*.....*.....*.....*.....*.....*.....*.....*..... 255

HvHSP70     256 BALRRLRTACERAKRTLSSSTQASVEIDSLFQCIDFYTSITRPFEEICID 306
3HSC        256 RAVRRLRTACERAKRTLSSSTQASIEIDSLVECIDFYTSITRPFEEINAD 306

Cons        256 *.....*.....*.....*.....*.....*.....*.....*.....*.....*..... 306

HvHSP70     307 LFRGTLPVADAIRDA GKNSSQG NTSKSDIHEVVLVGGSTRIPNVQSILQE 357
3HSC        307 LFRGTLPVAKALRDA ----- KLDKSDIHOIVLVGGSTRIPNIIQKILQE 350

Cons        307 *****.....*.....*.....*.....*.....*.....*.....*.....*.....*..... 357

HvHSP70     358 FFNCKELNKSINPDEAVAYCAAVQAAILAGDR 369
3HSC        351 FFNCKELNKSINPDEAVAYCAAVQAAILSGDR 362

Cons        358 *****.....*.....*.....*.....*.....*.....*.....*.....*.....*..... 369

```

Figure 13. Target (HvHSP70) and template (3HSC) assembly used for generation of HvHSP70 model. The alignment was performed using the program T-coffee (<http://igs-server.cnrs-mrs.fr/Tcoffee/tcoffee.cgi/index.cgi>). The red shading highlights that the two protein sequences are highly homologous. The score of the alignment is 100.



Figure 14. A 3D model of the N-terminal fragment of the HvHSP70. The three-dimensional structure of the HvHSP70 N-terminal fragment was modeled on the published crystal structure of *B. taurus* HSC70 (Flaherty *et al.*, 1990). The figure displayed was drawn using the program Chimera (<http://www.cgl.ucsf.edu/chimera/>).

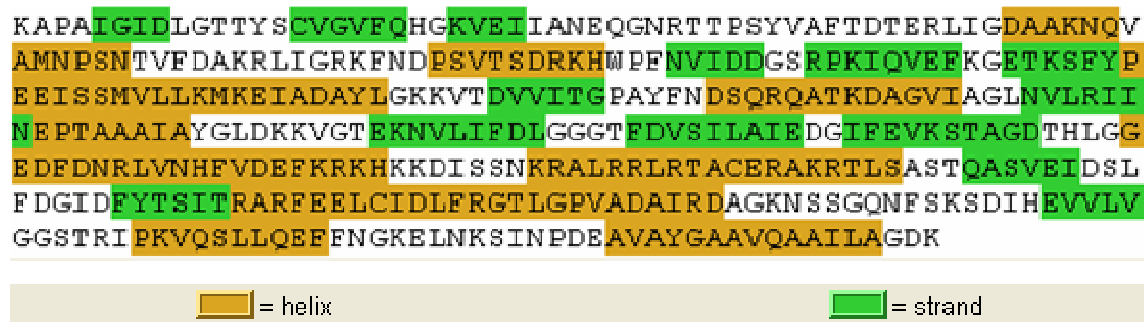


Figure 15. Secondary structural elements of the HvHSP70 model. The green shaded amino acids make up the β -strands and the orange shaded elements make up the helices of HvHSP70. Structural elements are highlighted using the program Chimera (<http://www.cgl.ucsf.edu/chimera/>).

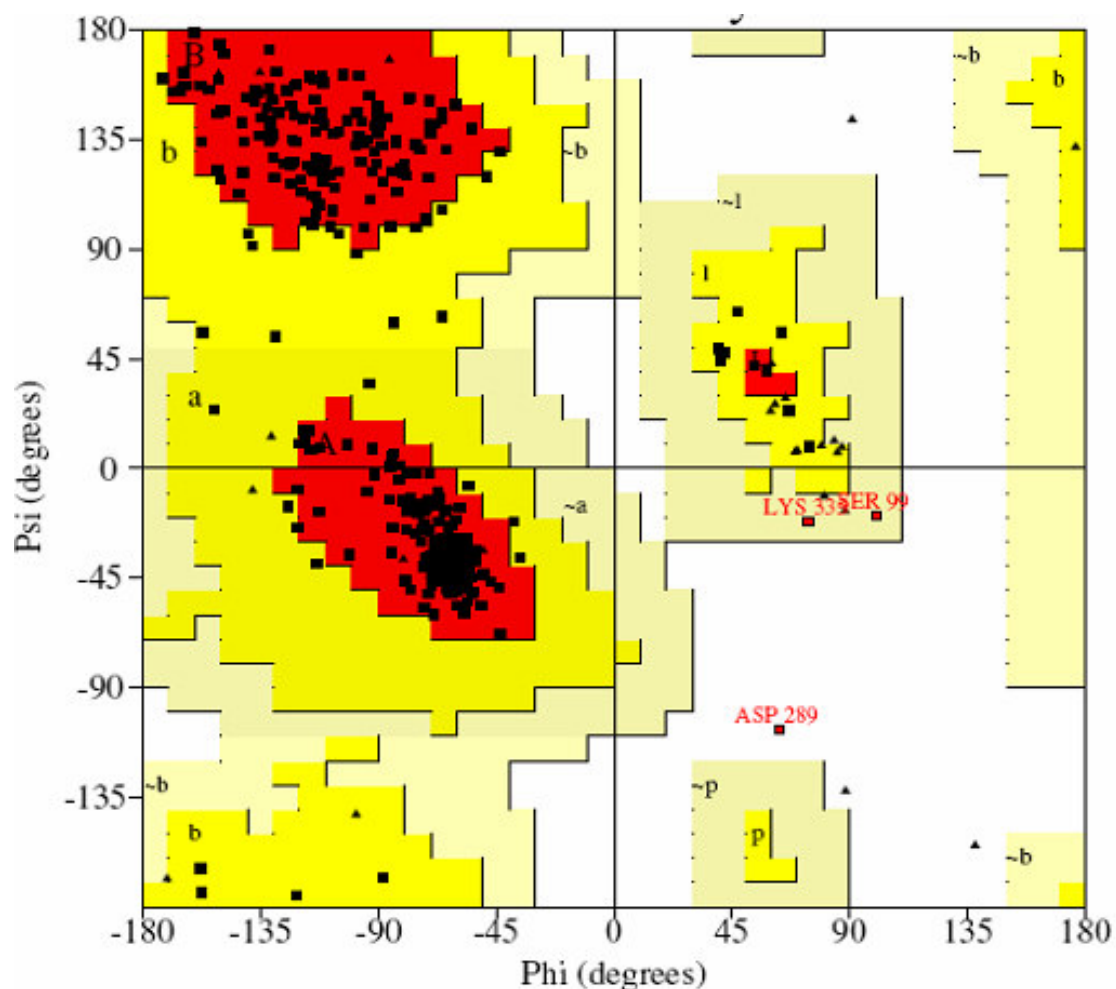


Figure 16. Ramachandran plot of model HvHSP70. The Asp 289 is the only non-glycine residue found outside the most favored and additionally allowed regions. The Ramachandran plot of the model was generated using the program Procheck.

Ramachandran plot (Figure 16) of the model was also drawn. The structural quality of the model was also verified using program Verify-3D (http://nihserver.mbi.ucla.edu/Verify_3D/). It measures the compatibility of a protein model with its sequence, the values being calculated using 3D profile (Bowie *et al.*, 1991).

2.2 Results

2.2.1 Cloning and analysis of HSP70 gene

Comparative analysis of amino acid sequences of HSP70 from several species showed that stretches of amino acids are highly conserved among HSP70s (Figure 5). This multiple sequence alignment (Figure 5) along with the sequence alignment between two known hydrae HSP70 sequence alignment (Figure 6) led to the identification two stretches of conserved amino acids ADAYGK and AGDTHLG. A pair of degenerate primers (DF and DR) was designed corresponding to these two conserved stretches of amino acids (Table 4) and were used in RT - PCR experiments to amplify a segment of HvHSP70 cDNA. An amplified cDNA product of ~300 bp (Figure 7) was subcloned and sequenced. Initial sequence analysis indicated that the presence of an open reading frame encoding a polypeptide with a high degree of similarity to HSP70 of many organisms and an almost match to the *H. magnipapillata* HSP70.1.

The full-length cDNA sequence encoding the putative HSP70 was cloned employing the 5'-/3'-RACE methods using gene specific primers from the above cloned segment (Table 4). 5'-RACE was performed twice in order to clone the

full-length 5'-end of the cDNA. The nucleotide and the predicted amino acid sequence of the HvHSP70 gene obtained by combined analysis of the cDNA and genomic PCR are shown in Figure 8. The putative transcription initiation site found by 5'- RACE is located at nucleotide position 386 (Figure 4). The initiation site of translation was placed at nt 443 (Figure 8), inferred by conceptual translation of the sequence in all three reading frames and alignment with the known sequences of HSP70 and cognate proteins available in the GenBank database.

The HvHSP70 cDNA (Figure 8) is shown to contain a 1950 base pair (bp) open reading frame (ORF) and an in-frame TAA stop codon at the 3'-end of the coding region. The ORF is flanked by a 57 bp 5'-untranslated region and a 92 bp 3'-untranslated region followed by the putative poly(A) tail. As shown in Figure 8, the deduced protein is composed of 650 amino acid residues and the amino acid composition of the polypeptide is given in Table 5. The molecular weight (M_w) of HvHSP70 is determined to be 710,037 Da with an average isoelectric point (pI) of the protein being 5.56.

The deduced amino acid sequence of the HvHSP70 gene exhibited the three characteristic motifs of the HSP70 family: IDLGTTYIS (residues 9 to 16), DLGGGTFD (residues 199 to 206) and EEVD (residues 647 to 650). A notable feature in the protein is the presence of three consecutive repeats of the tetrapeptide motif GGMP at its C-terminal region (residues 622 to 633). This putative HSP70 displayed high sequence similarity with members of the HSP70

TABLE 5**Amino Acid Composition of the HvHSP70 Polypeptide**

Amino acid	Number of residues	Percent
Ala	50	7.69
Cys	6	0.92
Asp	45	6.92
Glu	48	7.38
Phe	26	4.00
Gly	55	8.46
His	8	1.23
Ile	44	6.77
Lys	57	8.77
Leu	44	6.77
Met	10	1.54
Asn	32	4.92
Pro	28	4.31
Gln	23	3.54
Arg	27	4.15
Ser	41	6.31
Thr	41	6.31
Val	48	7.38
Trp	2	0.31
Tyr	15	2.31
Total	650	100.0

family (Figure 6; Table 6).

Identification of GGMP repeats, cytosolic HSP70-specific motif EEVD at the C-terminus of the sequence and sequence homology with members of the HSP70 family (Table 6) suggested that the putative HSP70 of the *H. vulgaris* possessed the essential properties of an HSP70 family. Consequently, it is concluded that the HSP reported here is a cytosolic 70 kDa HSP and might be inducible like other inducible HSP70s.

2.2.2 Exon/intron structure of the HvHSP70 gene

Most HSP70 genes have introns in their open reading frames (ORFs) and several of them have been shown to have conserved introns at corresponding positions among various species. Thus the exon/intron structure of the HSP70 gene was determined by genomic PCR. The HSP70 gene is interrupted by three introns (shown in capital letters): intron 1 (nt 648-752) being 105 bp, intron 2 (829-980) being 137 bp and intron 3 (2477- 2616) being 140 bp in length (Figure 8). Consequently the HvHSP70 gene has four exons. The length each exon is 205, 60, 1604 and 283 bp, respectively.

2.2.3 The 5' non-coding region

The sequence of the HvHSP70 gene given in Figure 8 was analyzed to locate potential consensus elements in the promoter region. From nt 1 to 422, several A- and T-rich stretches were observed. The sequences immediately upstream of the translation start site revealed the presence of putative heat shock elements (HSEs). The HSEs found are: (I) 5'-TTCTATGAATTCT-3'; and

TABLE 6

**Similarities among *H. vulgaris* HSP70 and 70 kDa Heat Shock Proteins
from Other Organisms^a**

Protein	% similarity to HvHSP70
<i>Hydra magnipapillata</i> HSP 70.1	98
<i>Numida meleagris</i> HSP70	91
<i>Homo sapiens</i> HSP70	91
<i>Mus musculus</i> HSP	91
<i>Pan troglodytes</i> HSP70	91
<i>Danio rerio</i> HSP70	87
<i>Xenopus laevis</i> HSP70	88
<i>Carassius auratus gibelio</i> HSC70	91
<i>Gallus gallus</i> HSP80	90
<i>Artemia franciscana</i> HSP70	89
<i>Mytilus galloprovincialis</i> HSP70	90
<i>Bos taurus</i> HSP70.2	89
<i>Bos taurus</i> HSP70.1	89
<i>Gallus gallus</i> HSP70	89
<i>Crassostrea gigas</i> HSP70	84
<i>Caenorhabditis elegans</i> HS70A	88
<i>Rattus norvegicus</i> HSP70	88
<i>Triticum aestivum</i> HSP 70	84
<i>Arabidopsis thaliana</i> HSP70	85
<i>Dictyostelium discoideum</i> HSC70.2	85

^aComparisons of amino acid sequences were made with the algorithm of NCBI BLAST.

(II) 5'-CGAGAACATTACGAATTTACCGTCTGATTC-3' corresponds to the classical ...nTTC..nGAAn motif; and HSEs (III) 5'-CTAGAACTATCTAGAAAATTTTGAAATTAGGAA-3'; and (IV) 5'-CCGTTTATGAA-3' corresponded to the classical nGAAn motif. Putative CAAT and TATA boxes at nucleotide 325 and 353 were discernible (Figure 8).

2.2.4 Sequence conservation in HSP70 proteins

A comparison of the nucleotide sequence of the *H. vulgaris* HSP70 gene with that of the HSP70 genes of other eukaryotic organisms showed a relatively low degree of overall homology (data not shown), but the derived amino acid sequence showed striking homologies with large stretches of virtual identity across the various taxonomic groupings (Figure 5). As shown in Figure 5, the sequence alignment of HvHSP70 with all these HSP70 could be extended both N- and C-terminally to encompass the entire HSP70 fold. The comparison of the derived amino acid sequence of the HSP70 polypeptide of *H. vulgaris* with the HSP70 sequences available in the GenBank revealed strongly conserved regions in the N-terminal half while homology became relatively weak on progressing towards the C-terminus (Figure 5). At the sequence level amino acid residues are mostly conserved (Table 6) among all sequences and a few residues represent the major differences among all the HSP70s. *H. vulgaris* HSP70 is similar to most of the HSP70 proteins described (Table 6). For example, *H. vulgaris* HSP70 is 98 and 88 % similar to the *H. magnipapillata* and *X. laevis* HSP70, respectively (Table 6).

2.2.5 Phylogenetic analysis

All the heat shock 70 protein sequences retrieved from the GenBank were aligned across their entire lengths and subjected to PHYML analysis. PHYML (Guindon and Gascuel, 2003) is a traditional heuristic maximum likelihood program which seeks to find the optimal topology in respect to the likelihood value and capable of optimizing model parameters (Stamatakis *et al.*, 2005). It currently represents the most efficient genetic algorithm for phylogenetic analysis and is very fast and outperforms other recent approaches including MrBayes and MetaPIGA (Lemmon and Milinkovitch, 2002). PHYML analysis of heat shock 70 sequences across flora and fauna resulted in displaying a distinct lineage for hydra HSP70s as compared to others (Figure 17). As expected the HSP70 from *H. vulgaris* and *H. magnipapillata* are grouped together.

2.2.6 The structural model of HvHSP70

By threading analysis it was found that the bovine heat shock cognate protein 70 (PDB code: 3HSC.pdb) (Flaherty *et al.*, 1990) is the best template for homologous modeling of the target protein HvHSP70. They share a quite high degree of homology at the ATPase domain of 3HSC (Figure 13).

The structure of the HvHSP70 ATPase fragment modeled after the structure of 3HSC is shown in Figure 14 and the corresponding secondary structural elements are shown in Figure 15. The comparative stereo-chemical analysis of the ϕ - ψ plots (Ramachandran diagram) of the model (HvHSP70) and

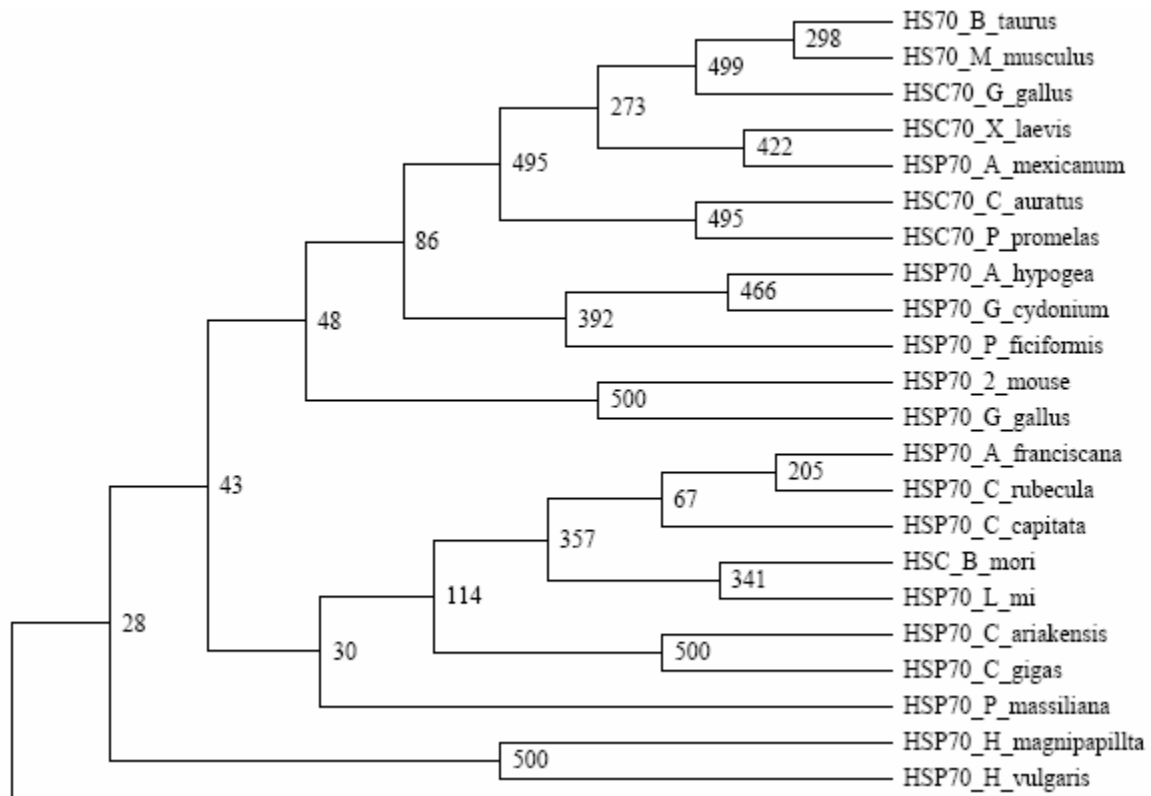


Figure 17. Phylogenetic alignment of the amino acid sequences of the HSP70s from different organisms. The tree was constructed by the maximum likelihood method using the program PHYML (Guindon and Gascuel, 2003). Bootstrap confidence values for the sequence groupings are indicated in the tree ($n = 500$). The hydra HSP70s forms a distinct lineage as compared to other HSP70s.

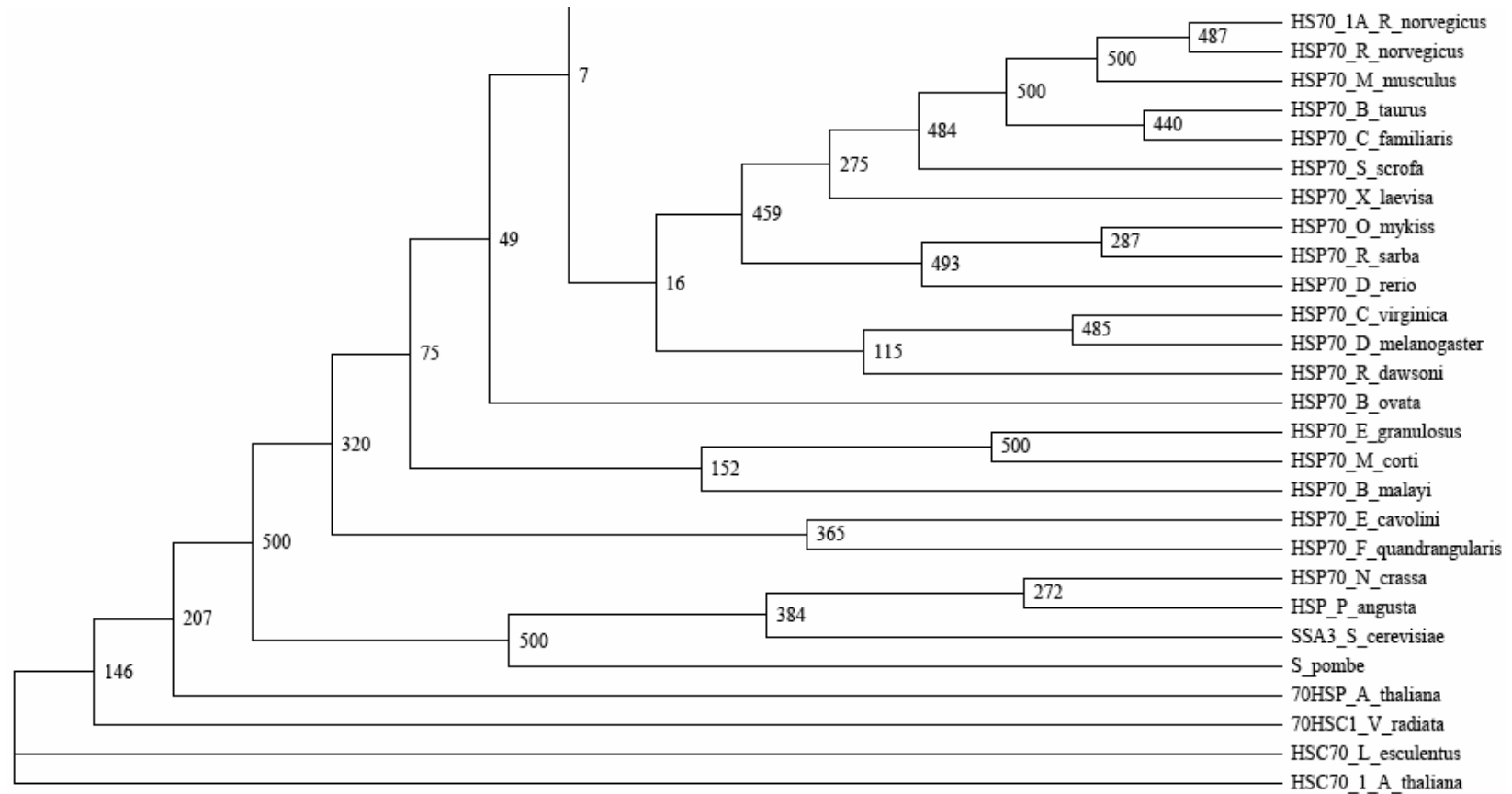


Figure 17 (Continued). Phylogenetic alignment of the amino acid sequences of the HSP70s from different organisms.

structure template (3HSC) is shown in Table 7. The analysis for crystallographic structure of the model (HvHSP70) present 88.6 % of residues in the most favorable, 10.5 % of residues in additional allowed regions, 0.6 % of the residues in generously allowed regions, and 0.3 % of the residues in disallowed regions, which strongly indicates that the molecular model presented here has a good overall stereo-chemical quality. A Verify-3D run on the model also showed a good stereo-chemical quality of the model (data not shown).

The HvHSP70 model essentially displayed similar tertiary structural features to that of bovine heat shock cognate protein. It comprised of two lobes, one the right and one on the left in the view shown, with a deep cleft in between them. In the view shown in Figure 14, each lobe partition into an upper and lower domain, the lower domains consist of five (right lobe) and four-strand β -sheets (left lobe) flanked by helices; whereas the two upper domains are composed of four (right lobe) and two β -strands (left lobe) flanked by also helices.

The overall similarity in structure of the HvHSP70 model to that of 3HSC suggested that the N-terminal segment of the HvHSP70 protein might as well function as a kinase. Additionally it had the similar nucleotide (ATP) binding domains of the actin, hexokinase and glycerol kinase indicating HvHSP70 as a member of a family of phosphotransferases and utilizes the same structural motif to bind ATP and possess an ATPase activity. The lower two domains might have functional imperatives in the ATPase activity, this region of the protein

TABLE 7

**Comparison of the Ramachandran Plot Statistics between Template 3HSC
and the Model HvHSP70**

Structure	Region of the Ramachandran plot (%)			
	Most favorable	Additional allowed	Generously allowed	Disallowed
3HSC	90.6	9.1	0.0	0.3
HvHSP70	88.6	10.5	0.6	0.3

might interact directly with the nucleotide ATP. The 4 acidic residues that either bind divalent Mg^{2+} (Asp-10 and Asp-199) or have been suggested as candidate proton acceptors (Glu-175 and Asp-206) for the ATPase activity are absolutely conserved in HvHSP70.

2.2.7 HvHSP70 mRNA expression analysis

H. vulgaris was exposed to a variety of toxicants (some of them known inducers) and stressors and to examine the level of HSP70 transcripts in *H. vulgaris* before and after stressor exposure, the expression patterns of the HvHSP70 mRNA were investigated in whole organisms by reverse transcriptase-polymerase chain reaction (RT-PCR) (Figure 18 and Figure 19). It was found that HvHSP70 mRNA was induced by heat shock both at 30 (1 and 6 h exposure) (Figure 18, lanes 2-3) and 37 (1 h exposure) (Figure 18, lane 4) °C, the intensity of expression was highest at 30 °C when hydrae were exposed to heat shock for 1 h. Exposure of animals to 37 °C for 6 h (Figure 18, lane 5) almost completely inhibited the expression of the HSP70 mRNA. Although induction of HSP70 mRNA was detectable over a broad temperature range (22-37 °C) (the data for 22 °C is not shown), the level of synthesis depended on the stress temperature, with the highest level at 30 °C temperature. In the non-oxidative (starvation) stress the expression of HSP70 mRNA wasn't affected in 5 d starved hydrae at 18 °C (Fig 14, lane 6). However, when the 5 d starved animals were exposed to heat shock, a heat shock response was provoked (Figure 18, lane 7) by increasing mRNA synthesis. In

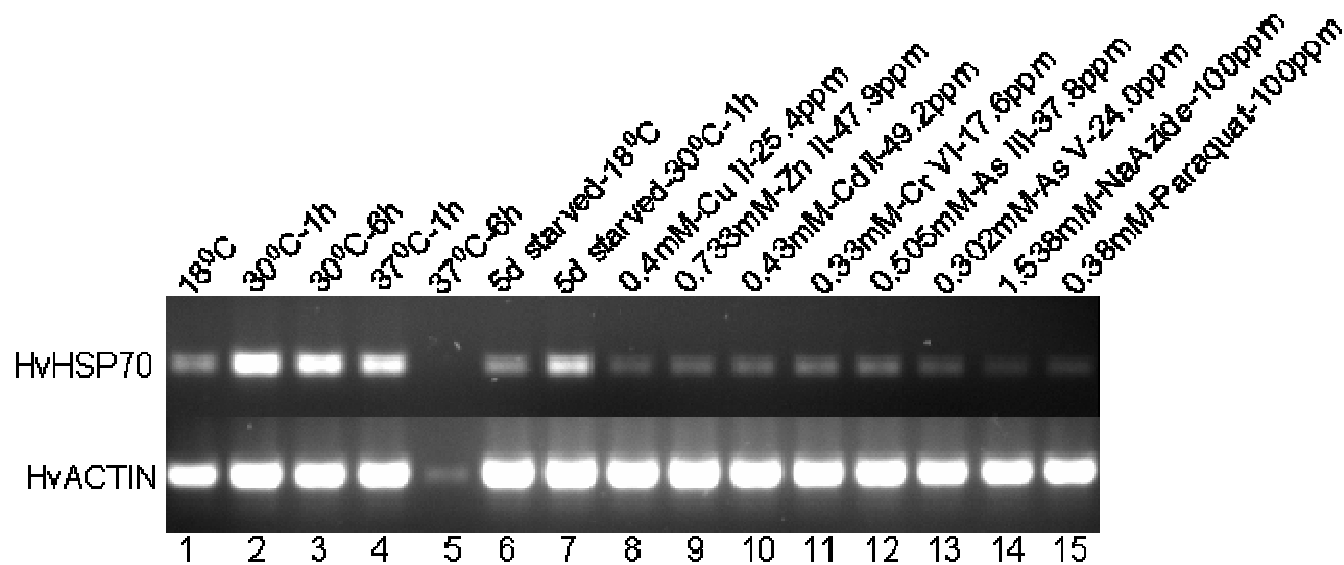


Figure 18. Expression analysis of HSP70 mRNA from *H. vulgaris* exposed to thermal, starvation, metal and oxidative stress. The figure above represent the expression of HvHSP70 under different stress conditions as described in the material and methods section: Thermal stress for 1 and 6 h (lanes 2-5), starvation stress (lane 6-7), metal stress for 6 h (lanes 8-13), and oxidative stress for 6 h (lanes 14-15). The expression HvHSP70 mRNA is compared to that of actin.

contrast to HSP70, transcription of actin DNA was almost constant before and after heat shock except at the 6 h exposure of 37 °C where the transcription of actin has been drastically reduced.

Oxidative stress (exposure to paraquat and H₂O₂ for either 1 or 6 h at the tested concentrations) did not affect the expression of HSP70 mRNA (Figure 18, lanes 14-15; Figure 19, lanes 9-12). When animals were exposed to metal stress none of the metals tested had an effect on HSP70 mRNA expression both at 1 and 6 h treatment except that zinc at the tested dose under 1 h treatment (Figure 19, lane 3) induced HSP70 mRNA expression.

2.3 Discussion

The objective of the study was to clone and characterize the of HSP70 gene in *H vulgaris*. To confirm that the cDNA and PCR cloning products are indeed from the same gene, the full-length ORF and gene was cloned by PCR and sequenced (data not shown). Comparison of the predicted amino acid sequence of the cloned hydra gene with sequences of the members of the HSP70 family revealed that the product of the isolated gene is homologous to the HSP70 family of stress proteins (Figure 5, Table 6). Consistent with the prediction that the protein product has a molecular mass of 70 kDa, the hydra protein is designated as HvHSP70.

The HvHSP70 amino acid sequence exhibited the three characteristic motifs of the HSP70 family: IDLGTTYS, DLGGGTFD and EEVD. The C-terminal region had three repeats of a tetrapeptide motif, GGMP which might be

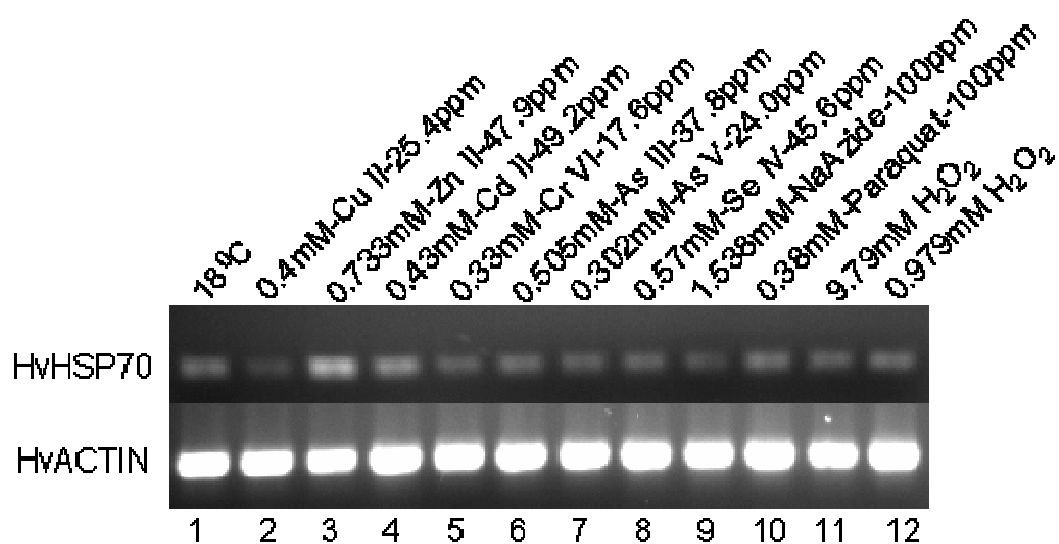


Figure 19. Expression analysis of HSP70 mRNA from *H. vulgaris* exposed to metal and oxidative stress for 1 h. The figure above represents the expression of HvHSP70 mRNA under different stress conditions as described in the material and methods section: Metal stress for 1 h (lanes 2-8), and oxidative stress for 1 h (lanes 9-12). The expression HvHSP70 mRNA is compared to that of actin.

important in binding for a distinct set of chaperone cofactors (Demand *et al.*, 1998). Similar sequences have been observed in HSP70 proteins from other organisms such as *C. gigas* (Boutet *et al.*, 2003b), *Rattus rattus* (O'Malley *et al.*, 1985) and *Homo sapiens* (Dworniczak and Mirault, 1987). Identification of GGMP repeats, as well as the presence of the cytosolic HSP70-specific motif EEVD at the C-terminus of the HvHSP70 sequence, strongly suggests that this protein is a cytosolic 70 kDa HSP (Demand *et al.*, 1998; Vayssier *et al.*, 1999). Gellner *et al.* (1992) also suggested that the presence of GGMP motif in nearly all known HSP70 and HSP60 proteins may favor structural flexibility and hydrophobic interaction, and also be an important site for the folding/unfolding function common to both classes of heat shock proteins.

5'-RACE was performed to locate the putative transcription initiation sites, by using synthetic adapter primer AP2: 5'-GATCAGGACGTTCTTTGAGd(T)₁₇-3'. The start site is located at position 386. The immediate upstream environment of the start codon (ATG) at nt 443 appeared to be consistent with a typical eukaryotic translational start site environment because of positions being occupied by purines. Therefore it is concluded that the 5' non-translated region is 57 bp long.

Heat-shock elements (HSE) with matching to the palindromic canonical sequence CNNGAANN TTCNNG (Amin *et al.*, 1996; Bienz, 1985) were found at nucleotide positions 12, 71, 101 and 311. HSE sequences are binding sites for the heat-shock transcription factors and are the only elements specifically

required for heat and/or stress regulation (Bienz and Pelham, 1987). Therefore, the presence of the GAA units in the HvHSP70 gene suggests that transcription of this gene is induced by heat shock.

The conceptual translation of the HSP70 cDNA sequence and a direct comparison with the amino acid sequences of other eukaryotes suggested the presence of introns within the coding sequence. The positions of the various introns were mapped by cloning and sequencing the genomic DNA. A comparison of the PCR products derived from mRNA and DNA templates showed differences in size consonant with the occurrence of three introns, intron (I) 105 nt, intron (II) 137 nt and intron (III) 140 nt. The first intron was situated close to the N terminus, interrupting codon 69 for D (Aspartate), followed by exon 2 of 76 nt; the second intron interrupted codon 94 for H (Histidine). Exons 3 and 4 are 1604 and 283 nt, respectively, in length. The third intron situated between codon 592 (Q: Glutamine) and 593 (T: Threonine) and was situated close to the C-terminus. These results are consistent with the findings that introns have been reported in stress-responsive HSP70 genes of other hydra species for which sequences have been published, namely, the *H. magnipapillata* and *H. oligactis* (Gellner *et al.*, 1992). The first intron site in HvHSP70 gene is identical to that of *H. magnipapillata* HSP70.1 gene. However, the second intron site in *H. vulgaris* HSP70 gene is not an intron site in *Hydra magnipapillata* HSP70.1 gene. *H. vulgaris* HSP70 is interrupted by a third intron not seen any other hydra HSP70 genes. Since heat shock disrupts pre-mRNA

splicing (Yost *et al.*, 1990; Hunt and Morimoto; 1985), the presence of introns in the heat inducible *H. vulgaris* HSP70 gene indicates that early in metazoan evolution, mechanisms must have been evolved to allow correct splicing of HSP70 pre-mRNA.

Comparative modeling uses experimentally determined protein structure(s) to predict conformation of other proteins with similar amino acid sequences and the models generated consist of coordinates for all non-hydrogen atoms in the modeled part of a protein. For modeling of HvHSP70 the restrained-based modeling (Sali and Blundell, 1993) approach was used. The N-terminal HvHSP70 segment (ATPase domain) model building was implemented in an automated approach using the interactive mode of the comparative modeling server 3D-JIGSAW. The model provided a detailed probable structural and functional framework for ATPase domain of HvHSP70 since the key residues that either bind divalent Mg^{2+} (D-10 and D-199) or have been suggested as candidate proton acceptors (E-175 and D-206) for the ATPase activity are absolutely conserved in HvHSP70.

Heat shock proteins have been proposed as a possible tool for monitoring environmental toxicants (Kohler *et al.*, 1992). HSPs indicate exposure to cellular stress and adverse cellular effects, thus serving as biomarkers of these effects. The highly conserved HSP70 proteins are expressed under proteotoxic conditions (Krone *et al.*, 2005). To test whether HvHSP70 behaved in a similar way, hydrae were exposed to a variety of toxicants (some of them known

inducers) and treatments and the HSP70 mRNA expression was studied by RT-PCR using actin gene as a control. Although induction of HSP70 mRNA was detectable over a broad temperature range (22 - 37 °C), the level of synthesis depended on the stress temperature and exposure duration, with the highest level of expression at the highest temperature 30 °C. Consistent with the view that heat shock proteins are involved in ecological variation in thermotolerance are observations that *H. vulgaris* accumulates higher HSP70 mRNA after heat shock. These results are consistent with the previous report that *H. magnipapillata* induces HSP70 at 30 °C and the expression goes down at 37 °C (Bosch *et al.*, 1988). Also Bosch *et al.* (1988) observed thermotolerance and heat shock proteins in *H. vulgaris*. The total lack of expression of HSP70 when exposed to 37 °C for 6 h may be due to that the biochemical machinery at the base of the heat shock response is compromised. In a comparable study involving *O. edulis*, it is reported that thermal stress caused the expression of a 69 kDa inducible isoform in gills of *O. edulis* but not in the digestive gland (Piano *et al.*, 2004). Transcription of HSP69 mRNA observed within 3 h of stress recovery of oyster exposure to 32 and 35 °C. However, HSP70 mRNA transcripts were not present in the gills of animals exposed to 38 °C after 3 h of post stress recovery, but they were detected after 24 h. The expression of a 69 kDa protein in *O. edulis* exposed to 38 °C was rather low or totally absent.

The findings that metals at the tested concentrations didn't affect the HvHSP70 mRNA expression (except the Zn exposure for 1 h) are consistent

with results of Ait-Aissa *et al.* (2003) in that in a 21-day exposure study involving sublethal water concentrations of the metals cadmium (Cd) (1.5 µg/L) and zinc (Zn) (150 µg /L), the liver biomarker heat shock proteins (HSP70 and HSP60) in juvenile rainbow trout (*Oncorhynchus mykiss*) weren't induced. Cd, and Zn to a lesser extent, induced an adaptive response in the liver shown by an increase in antioxidant defences (total glutathione GSH, superoxide dismutase, Trolox equivalent antioxidant capacity (TEAC), without any impairment of GSH redox status or induction of heat shock proteins. Similarly orthopteran insect *Tetrix tenuicornis* collected from the polluted area that showed 1.5, 4.03, 4.32 and 41.73 times higher concentrations of copper (Cu), zinc (Zn), lead (Pb) and cadmium (Cd), respectively than insects of the same species collected from unpolluted areas showed only small changes, and rather a decrease in the concentration of constitutive and inducible heat shock proteins HSP70 (Warchalowska-Sliwa *et al.*, 2005).

It is not surprising that HvHSP70 mRNA was not expressed following arsenic treatment though exposure to arsenicals either *in vitro* or *in vivo* in a variety of model systems has been shown to cause the induction of a number of the major stress protein families such as heat shock proteins (HSP) (Del Razo *et al.*, 2001). In most of the cases, the induction of stress proteins depends on the capacity of the arsenical to reach the target, its valence, and the type of exposure. HSP induction is also a rapid dose-dependent response (1-8 h) to the acute exposure to arsenite (Del Razo *et al.*, 2001).

Oxidative stress (exposure to paraquat and H_2O_2) at the tested concentrations didn't affect the expression of HSP70 at either 1 or 6 h treatment times. This may indicate that the dose of the stressors weren't sufficient enough to provoke a stress response or were high enough to cause cellular toxicity and subsequent compromise in HSP70 expression. In the non-oxidative (starved for 5 d) stress the expression of HSP70 mRNA wasn't affected. However, when the starved animals were exposed to heat shock a heat shock response was provoked. This may be due to the intrinsic heat shock response in *H. vulgaris* rather than a compounding effect of starvation on heat shock response.

In the context of known inducers metals and oxidative stressors not provoking a stress response at the tested concentration offers few possibilities. It may be due to that the doses tested couldn't provoke a response or the doses tested cause toxicity impairing the transcriptional ability of *H. vulgaris*. It may be also that *H. vulgaris* lacks a stress response or may be due to a similar mechanism as shown by Gellner *et al.* (1992) that the reduced transcript level in *H. oligactis* (as compared to *H. magnipapillata*) under heat shock is due to less stable mRNA but not due to reduced ability of transactivation of *H. oligactis* HSP70. It may be also that regulatory mechanisms other than mRNA stability may also be important in the context of *H. vulgaris*.

In the context of present findings and known stress response mechanism in *H. oligactis* and *H. magnipapillata*, *H. vulgaris* appear to offer new opportunities for the study of the stress response because it offers an experimental system in

which three species can be compared which have differential stress response and is adapted to different habitats. Also it would be intuitive to know how *H. vulgaris* heat shock response would fare in terms expression and mRNA stability in comparison to *H. magnipapillata* and *H. oligactis*.

CHAPTER III

MOLECULAR CLONING AND CHARACTERIZATION OF A MANGANESE SUPEROXIDE DISMUTASE FROM *HYDRA VULGARIS*

Reactive oxygen species (ROS) produced as by-products of aerobic metabolism or exposure to pro-oxidants become toxic or lethal when they damage nucleic acids, proteins and membrane lipids (Docampo and Moreno 1984). In order to resist these potentially damaging oxygen species, aerobic organisms have developed a protection system where the antioxidant enzymes superoxide dismutase (EC 1.15.1.1, abbreviated SOD), glutathione peroxidase and catalase play an essential role. SOD activity reduces the superoxide radical $O_2^{\cdot -}$ into hydrogen peroxide and molecular oxygen (Fridovich, 1975; Carlloz and Touati, 1986; Farr *et al.*, 1986). Eukaryotic SODs are classified into three groups: (1) manganese-containing SOD (MnSOD) synthesized in the cytosol and imported post-translationally into the mitochondrial matrix, (2) cytosolic copper/ zinc-containing SOD (CuZnSOD), and (3) extracellular SOD (EC-SOD) secreted by many types of cells (Weisiger and Fridovich, 1973; Marklund, 1982; Mantonavi and Dejana, 1989). MnSODs described in eukaryotes are homologous to iron-dependent bacterial SODs (FeSOD) (Fridovich 1975; Fridovich 1995; Mantonavi and Dejana, 1989).

Genes encoding MnSOD enzymes have been identified in many organisms (Ditlow *et al.*, 1982; Marres *et al.*, 1985; Wan *et al.*, 1994; Henkle-

Dührsen *et al.*, 1995; Jones *et al.*, 1995). Also a large number of bacterial FeSOD genes have been described (Campbell and Laudenbach, 1995; Lah *et al.*, 1995; Tsolis *et al.*, 1995). There are no report on cnidarian MnSOD, though CuZnSODs have been reported in cnidarian *Anemonia viridis* (Plantivaux *et al.*, 2004), antarctic soft coral *Alcyonium paessleri* (accession number: AAG10392) and an extracellular SOD from *H. vulgaris* (accession number: DQ286039) in literature.

In the present study, a gene encoding MnSOD from a fresh water hydra, *H. vulgaris*, is described. The expression of hydra MnSOD (HvMnSOD) mRNA is assayed with respect to both environmental contaminant challenge (i.e., arsenic, cadmium, selenium, zinc and copper) and stress (both oxidative and non-oxidative). In addition, the phylogenetic position of HvMnSOD is analyzed and a suitable homology based structural model of HvMnSOD is also presented to study the structural and functional evolutionary significance of the protein.

3.1 Materials and methods

3.1.1 Hydra culture

Adult *H. vulgaris* were maintained in shallow dishes at 18 °C in a medium containing 1 mM CaCl₂.2H₂O, 0.012 mM EDTA, and 0.458 mM TES (N-tris[hydroxymethyl]-methyl-2-amino-ethanesulfonic acid, sodium salt) buffer (pH 7.0). Daily, hydrae were fed with brine shrimp (*Artemia nauplii*) hatched in a solution of 1 % sodium chloride treated with iodine (40 µg/ml). Hydrae were maintained free from bacterial and fungal contamination and were not fed for 24

h before initiating the experiments. Deionized water was used throughout this portion of the study (Mayura *et al.*, 1991).

3.1.2 RNA isolation and clean up

Total RNA was extracted from hydra by application of 2 ml of TRIzol[®] reagent (Invitrogen, USA) to approximately 20 mg of fresh tissue, according to manufacturer's instructions. The RNA was quantified by ultraviolet absorbance at 260 nm. Integrity of the total RNA was confirmed by 1 % formaldehyde agarose gel electrophoresis. The RNA isolated was cleaned up from contaminating DNA using RNeasy Mini Kit (Invitrogen, USA) following the manufacturer's instruction.

3.1.3 Oligonucleotides

All oligonucleotides were procured from Integrated DNA Technology Inc. (IA, USA). AP₂ primer (5'-GATCAGGACGTTTCGTTTGAGd(T)₁₇-3') was used for 5'-RACE (Rapid Amplification of cDNA Ends) experiments. The oligo(dT) bifunctional primer N (Not I-d(T)₁₈: 5'-AACTGGAAGAATTCGCGGCCGCAGGAA d(T)₁₈-3') was supplied in a cDNA preparation kit (Amersham Biosciences, USA) and was used for 3'-RACE experiments.

MnSOD protein sequences from diverse organisms retrieved from the NCBI protein (<http://www.ncbi.nlm.nih.gov/entrez/query.fcgi?db=Protein>) database were aligned using ClustalW (Figure 20) resulted in identifying the conserved region in MnSODs and oligonucleotides DF and DR were designed

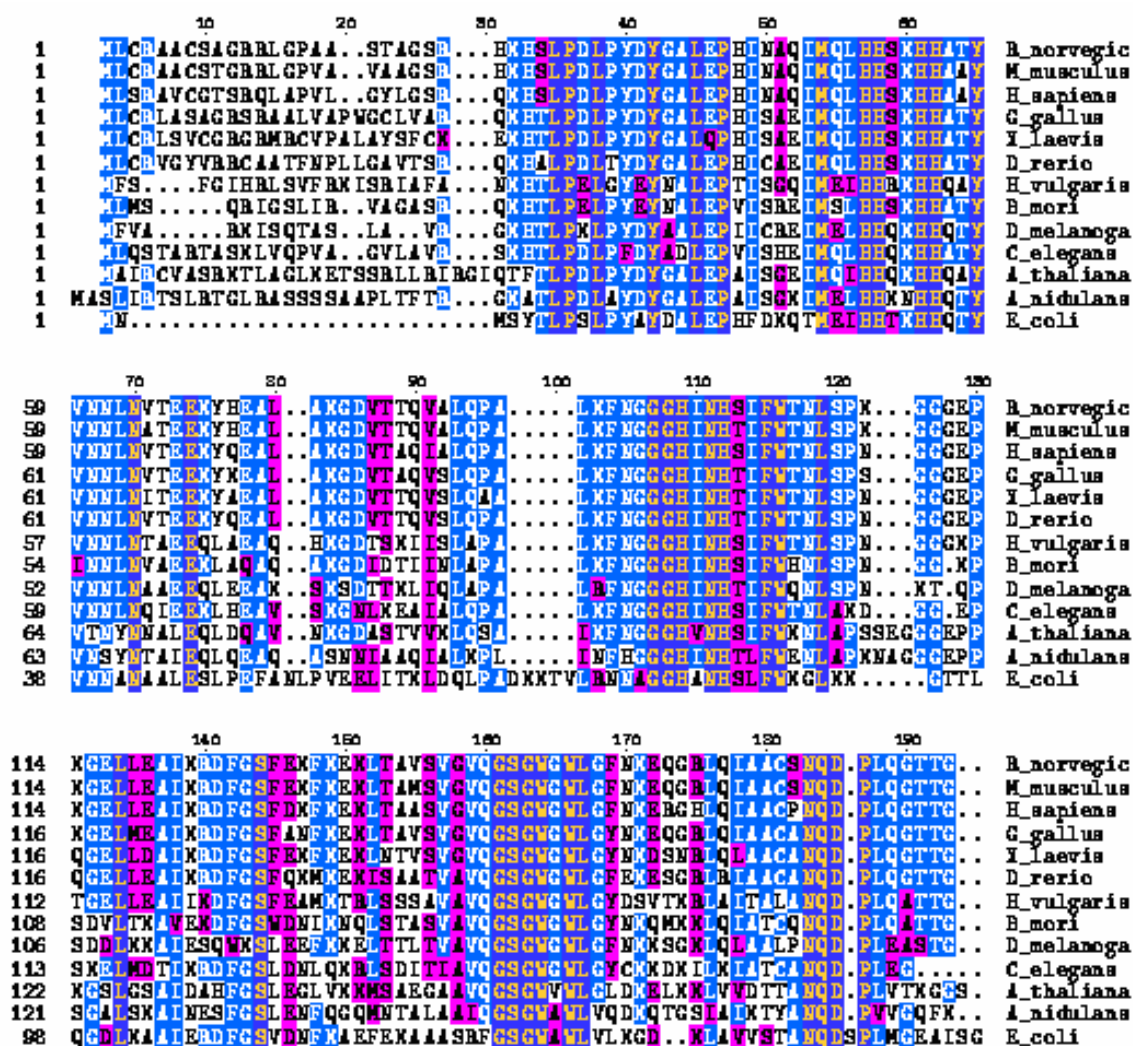


Figure 20. Multiple sequence alignment of MnSOD proteins performed using the program ClustalW. Accession numbers from the proteins as extracted using the Entrez web service (<http://www.ncbi.nlm.nih.gov/Entrez/protein.html>) are: gi|7302882 (*Drosophila melanogaster*), gi|6016702 (*Arabidopsis thaliana*), gi|30582773 (*Homo sapiens*), gi|53450 (*Mus musculus*), gi|57273 (*Rattus norvegicus*), gi|34305125 (*Xenopus laevis*), *Hydra vulgaris* (current study), gi|3875775 (*Caenorhabditis elegans*), gi|58429979 (*Bombyx mori*), gi|45383702 (*Gallus gallus*), gi|55962254 (*Danio rerio*), gi|7677029 (*Emericella nidulans*) and gi|42972 (*Escherichia coli*). The properties of amino acids are identified by different shadings as given in the legend.

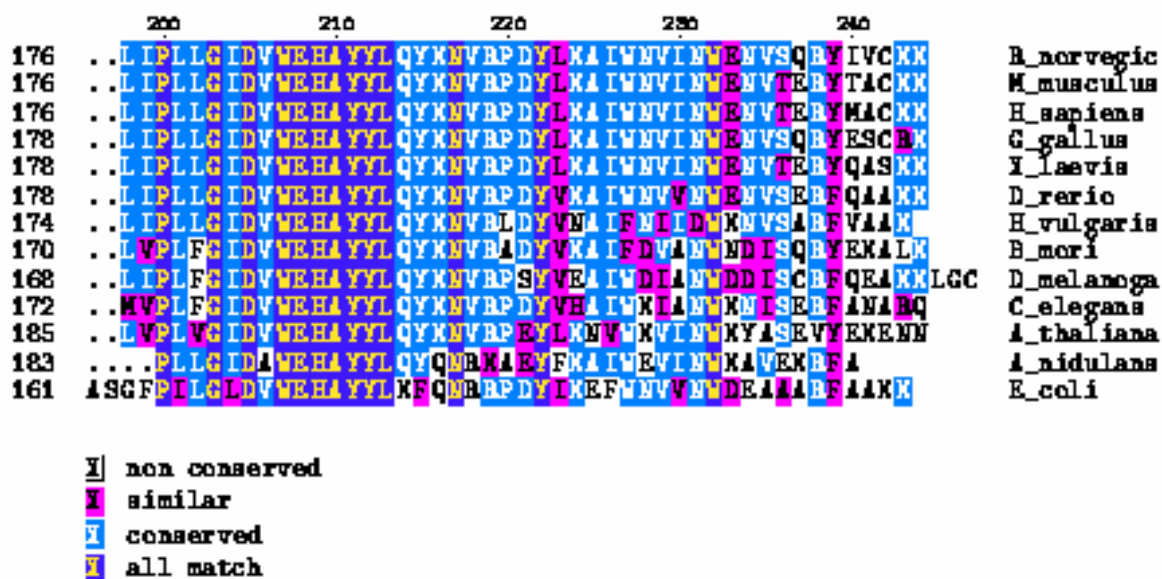


Figure 20 (Continued).

TABLE 8**Oligonucleotides Used in the Cloning of HvMnSOD cDNA**

Oligonucleotide	Sequence
DF	5'-TTCAATGGWGGWGGRCAYATYA-3'
DR	5'-TAGTAMGCRTGCTCCCAMAC-3'
F	5'-TTCAATGGAGGTGGGCACATCA-3'
R	5'-TAGTACGCATGCTCCCAAAC-3'
R2	5'-TTCATTGCCTCAAAAGACCC-3'
R3	5'-ATGGAATGATTGATGTGCCC-3'
N	5'-AACTGGAAGAATTGCGGGCCGCAGGAAd(T) ₁₈ -3'
AP ₂	5'-GATCAGGACGTTTCGTTTGAGd(T) ₁₇ -3'
AF	5'-AAGCTCTTCCCTCGAAGAATC-3'
AR	5'-CCAAAATAGATCCTCCGATCC-3'

Mix base definitions: W=A, T; R=A, G; Y=C, T; M=A, C

corresponding to the amino acids FNGGGHIN and VWEHAYY (Table 8). Other primers (*H. vulgaris* gene specific) used in the experiments are also shown in Table 8.

3.1.4 Cloning and identification of a partial fragment of HvMnSOD cDNA

All polymerase chain reaction (RT-PCR and RACE-PCR) experiments were performed using *Taq* DNA polymerase (Invitrogen, USA) and a thermal cycler (MJ Research, USA).

RNA (5 µg) was reverse-transcribed to cDNA at 37 °C for 60 min using the oligo(dT) bifunctional primer and the AMV RT supplied in the cDNA synthesis kit (Amersham Biosciences, USA). The first-strand cDNA was amplified using the primers DF and DR (Table 8). The PCR was performed for 30 cycles, consisting of 94 °C for 30 s, 50 °C for 30 s and 72 °C for 1 min and a final extension at 72 °C for 10 min. The resultant PCR products (Figure 21A) was subcloned into the pCR®II-TOPO® vector using a TA cloning kit (Invitrogen, USA) according to the manufacturer's instructions. Multiple independent clones were sequenced using automated methods (DNA Technologies Lab, Department of Veterinary Pathobiology, Texas A&M University) on an ABI PRISM™ 310 Genetic Analyzer (PE Biosystems, USA) using a Big-Dye sequencing kit (PE Biosystems) and M13 primers. The identity of the clones was evaluated by matching the sequences to the nucleotide/protein sequences available at the GenBank (<http://www.ncbi.nlm.nih.gov/>). The cloned sequence constituted residues 322 to 623 in the nucleotide sequence shown in Figure 22.

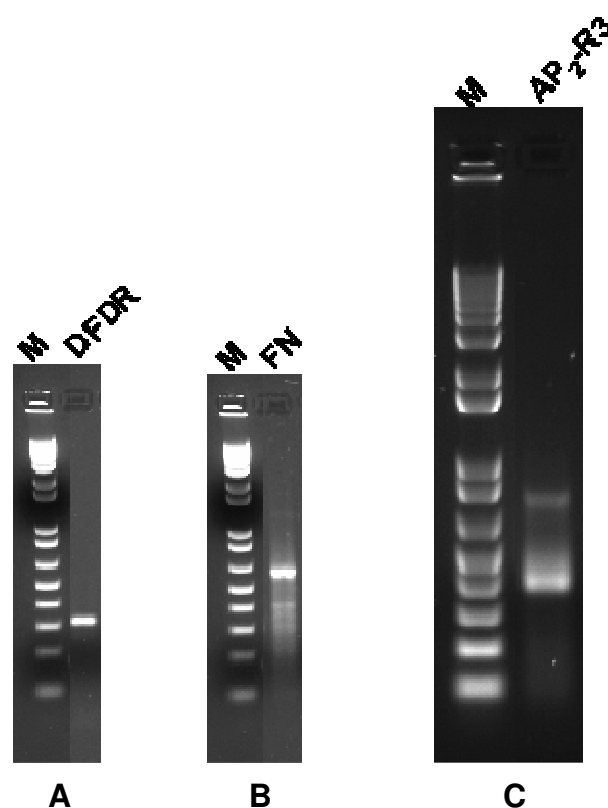


Figure 21. Images of electrophoretic gels for PCR products of HvMnSOD gene. (A) The PCR products were produced using primer DF and DR. (B) The 3'-RACE PCR products were produced using with primer F and N (= Not *I*-d(T)₁₈). (C) The 5'-RACE PCR products were produced using with primer AP₂ and R3. M = 1 kb plus DNA ladder.

```

1   ctttctacggaaaaaacacatactgaaacttttttagtccctgtgtaataagctagcaca 60
   1 M F S F G I H R L S V F R K I S R I A F
61  atgttttcttttgaatccaccgcctttcagtttttcgaaaaatatcgagaatagcattt 120
   21 A N K H T L P E L G Y E Y N A L E P T I
121 gctaataagcacactcttccagaattgggtatgaatataatgcattggaaccaacaatc 180
   41 S G Q I M E I H H R K H H Q A Y V N N L
181 agcgggtcaaattatggaaatacatcatcgcaaacaccaccaagcttatgtaaataactta 240
   61 N T A E E Q L A E A Q H K G D T S K I I
241 aatacagcagaagaacagttagctgaagctcagcataaaggagatacgtcaaagattatt 300
   81 S L A P A L K F N G G G H I N H S I F W
301 tcttttagctcctgcgttaaaattcaatggaggtgggcacatcaatcattccatttttgg 360
  101 T N L S P N G G G K P T G E L L E A I I
361 actaatctttcgccaaacggtggaggaaaaccaacaggtgaactattagaagccataata 420
  121 K D F G S F E A M K T R L S S S A V A V
421 aaagactttgggtcttttgaggcaatgaaaacacggttatcgtcttcagctgttgcaagt 480
  141 Q G S G W G W L G Y D S V T K R L A I T
481 caaggttcaggttgggttgggtgggatgattctgtcactaaaagacttgcaattaca 540
  161 A L A N Q D P L Q A T T G L I P L L G I
541 gcttttagctaatcaagatcctttgcaagctactactgggttaataccggttactcggtatt 600
  181 D V W E H A Y Y L Q Y K N V R L D Y V N
601 gatgtttgggagcatgcgtactacttgcaagtataagaatgttcgtcttgattatgtcaac 660
  201 A I F N I I D W K N V S A R F V A A K *
661 gcaatatttaacatcattgattggaaaaatgtatccgcaagggttgcgcagctaaatga 720

721 aataagagcgatgtcatctggctgttatcatcttctgtaaagataatcttttaattgattt 780

781 tgtgttcaattgaataatataagaataatataagaagaaaaaagaactcgaattacaaa 840

841 aaaaaaaaaaaaaa 853

```

Figure 22. Nucleotide and deduced amino acid sequence of *H. vulgaris* manganese superoxide dismutase. The nucleotide and amino acid sequences are numbered from the 5'-end of the 853 bp cDNA sequence, and from the N-terminal start codon methionine, respectively. The first residue of the presumed matured protein asparagine (N) is shown bold face. Amino acid residues corresponding to the metal-binding ligands are bold face and underlined. The asterisk denotes the translation stop signal.

3.1.5 3'-RACE of the HvMnSOD cDNA

First-strand cDNA prepared above was amplified using the oligo(dT) bifunctional primer and a gene-specific primer F (Table 8) (complementary to nucleotide (nt) 322 to 343, Figure 22) for 35 cycles of 94 °C for 30 s, 55 °C for 30 s and 72 °C for 3 min. The PCR products (Figure 21B) were subcloned and sequenced as described above. The identity of the clones was evaluated by matching the sequences to the nucleotide/protein sequences available at the GenBank (<http://www.ncbi.nlm.nih.gov/>).

3.1.6 5'-RACE of the HvMnSOD cDNA

The template cDNA was synthesized using a primer R2 (Table 8) (complementary to nt 430 to 449) and Superscript II (Invitrogen, USA), followed by dA tailing of the cDNA using dATP and terminal transferase (Invitrogen, USA) using standard procedures (Sambrook *et al.*, 1989). The first strand cDNA was amplified using an oligo(dT) anchor primer AP₂ (5'-GATCAGGACGTTTCGTTTGAGd(T)₁₇-3') and the gene-specific primer R2, and the first-round PCR products were reamplified using the PCR anchor primer AP₂ and another gene-specific primer R3 (Table 8) (complementary to nt 334 to 353). Each PCR was performed with an initial amplification of 95 °C for 5 min, 48 °C for 5 min and 72 °C for 5 min followed by 20 cycles of 95 °C for 40 s, 48 °C for 1 min and 72 °C for 3 min with a final extension of 10 min at 72 °C. The PCR products (Figure 21C) were subcloned and sequenced as described above. The identity of the clones was confirmed by matching the sequences to

the nucleotide/protein sequences available at the GenBank (<http://www.ncbi.nlm.nih.gov/>).

3.1.7 Heat treatment

Hydrae were incubated at 18 (control temperature), 30 and 37 (maximum induction temperature) °C for 1 h and 6 h in 5 ml hydra media.

3.1.8 Metal treatment

Approximately 500 hydrae were incubated with 100 ppm of $\text{CuSO}_4 \cdot 5\text{H}_2\text{O}$, ZnCl_2 , $\text{CdCl}_2 \cdot 2.5\text{H}_2\text{O}$, $\text{K}_2\text{Cr}_2\text{O}_7$, As_2O_3 , Na_2HAsO_4 and Na_2SeO_3 for 1 h and 6 h in 5 ml hydra media. Hence the concentration of Cu (II), Zn (II), Cd (II), Cr (VI), As (III), As (V), and Se (IV) (active ingredients) were 0.4 mM (= 25.4 ppm), 0.73 mM (= 47.9 ppm), 0.43 mM (= 49.2 ppm), 0.33 mM (= 17.6 ppm), 0.506 mM (= 37.8 ppm), 0.302 mM (= 24.0), and 0.57 mM (= 45.6 ppm) respectively.

3.1.9 Oxidative stress treatment

Approximately 500 hydrae were incubated in 300 ppm (= 9.79 mM) H_2O_2 , 30 ppm (= 0.979 mM) of H_2O_2 , 100 ppm (= 0.38mM) of paraquat and 100 ppm (= 1.538 mm) sodium azide in 5 ml hydra media for 1 or 6 h.

In all cases, treatments were carried out in 14 ml polypropylene round-bottom tubes (Becton-Dickinson, NJ, USA) containing 5 ml hydra media. At the end of the treatment, hydrae were collected by centrifugation at 7,500 Xg for 5 min. The supernatants were discarded. Then hydrae were washed once in 5 ml of 0.05 M PBS for 5 min @ 7,500 Xg. The supernatants were discarded as before and the animals were homogenized immediately in 3 ml of TRIzol[®].

3.1.10 Expression analysis of HvMnSOD mRNA in hydrae

Total RNA was extracted from TRIzol[®] (Invitrogen, USA) treated whole hydrae and cleaned as before using RNeasy Mini Kit (Invitrogen, CA, USA) following procedures previously described. For RT-PCR, 5 µg of total cleaned RNA was reverse transcribed using 500 ng of oligo(dT)₁₂₋₁₈ primer (Invitrogen, USA) and 200 units of the Superscript II enzyme (Invitrogen, USA) for 50 min at 42 °C. The reaction was inactivated by heating the mixture at 70 °C for 15 min. PCR assays were designed to normalize HvMnSOD mRNA expression levels to actin transcription rate. Two µl of first strand cDNA (from 25 µl of reverse transcription mix) was diluted 100 times prior to PCR amplification. PCR was carried out in 50 µl total volume of 1 × PCR buffer (20 mM Tris-HCl, pH 8.4, 50 mM KCl), 2 mM MgCl₂, 0.1 mM each of dNTPs, 10 pmol each of primers, and 0.5 U *Taq* DNA polymerase (Invitrogen, USA) using 2 µl of (1:100) diluted RT-product. Actin mRNA was amplified using the AF and AR primers and the MnSOD mRNA was amplified using the F and R primers. Cycling profile after initial denaturation at 94 °C for 4 min was 30 cycles of amplification as follows: denaturation at 94 °C for 30 s, annealing at 55 °C for 30 s, and extension at 72 °C for 45 s. These number of PCR cycles ensured quantification within the exponential phase of amplification. Equal amounts (9.5 µl) of RT-PCR reactions were loaded on standardized 2 % agarose gels containing 0.1 µg/ml ethidium bromide. The gel images were digitalized by a gel documentation system (Kodak Laboratories, USA).

3.1.11 General bioinformatic analyses

Conceptual translation of the full-length cDNA was performed using the program SIXFRAME (<http://biologyworkbench.ucsd.edu>). Homology to other MnSOD gene and proteins were identified by using the Blast program with default settings (<http://www.ncbi.nlm.nih.gov/BLAST>). The identification of HvMnSOD domains were performed by use of the SMART program (<http://smart.embl-heidelberg.de/>) using default pattern definitions. Prosite (<http://us.expasy.org/prosite/>) identification of glycosylation, phosphorylation, myristilation and amidation sites was performed by use of the ExPASy program using default settings. The isoelectric point (pI) and the molecular weight (M_w) of the HvMnSOD were calculated using the ExPasy (http://us.expasy.org/tools/pi_tool.html) program. The prediction of the presence and location of signal peptide cleavage sites in amino acid sequence of HvMnSOD was done using the program SignalP 3.0 (<http://www.cbs.dtu.dk/services/SignalP/>). The secondary structure analysis of the HvMnSOD transit peptide was done using the program GOR4 (http://npsa-pbil.ibcp.fr/cgi-bin/npsa_automat.pl?page=npsa_gor4.html) (Garnier *et al.*, 1996). An axial projection of the transit peptide residues on a helical wheel was done using the web server (<http://bioinf.man.ac.uk/~gibson/HelixDraw/helixdraw.html>). Several MnSOD domain-containing sequences retrieved from the National Center for Biotechnology Information (NCBI) Entrez Web service

(<http://www.ncbi.nlm.nih.gov/Entrez/>) were aligned to each other using the web program T-coffee (http://igs-server.cnrs-mrs.fr/Tcoffee/tcoffee_cgi/index.cgi), ClustalW (<http://www.ch.embnet.org/software/ClustalW.html>), or the ClustalW program embedded in Mega (<http://www.megasoftware.net/>).

3.1.12 Phylogenetic analysis

For phylogenetic analysis sequences were aligned using the ClustalW program embedded in the program Mega 3.1 (<http://www.megasoftware.net/>). The aligned sequences were converted into the “PhylipIPhylip44” format (Felsenstein, 1993) using the Readseq program (<http://iubio.bio.indiana.edu/cgi-bin/readseq.cgi>) and saved as a text file. The text file in the interleaved format was uploaded to the PHYML Online (<http://atgc.lirmm.fr/phyml/online.html>) web interface (Guindon and Gascuel, 2003). Following parameters were chosen for the construction of the tree: substitution model - JTT; number of bootstrap data sets - 500, proportion of invariable sites - 0 and fixed; number of substitution rate categories - 1; starting tree(s) - BIONJ; optimize topology - yes; optimize branch lengths and rate parameters -yes. Nonparametric bootstrap (Felsenstein, 1985) was applied to assess the reliability of internal branches for (large) datasets. The tree generated in the NEWICK format was displayed using the Drawtree program (<http://www.phylodiversity.net/~rick/drawtree/>) (Figure 23).

The accession numbers of protein sequences used for phylogenetic analysis are: gi|23503540 (*Callithrix jacchus*), gi|30582773 (*Homo sapiens*), gi|23503536 (*Macaca mulatta*), gi|58865326 (*Macaca nemestrina*), gi|53450

(*Mus musculus*), gi|57273 (*Rattus norvegicus*), gi|59858341 (*Bos taurus*), gi|57031787 (*Canis familiaris*), gi|12230617 (*Equus caballus*), gi|45383702 (*Gallus gallus*), gi|29373127 (*Melopsittacus undulatus*), gi|49670623 (*Xenopus tropicalis*), gi|34305125 (*Xenopus laevis*), gi|55962254 (*Danio rerio*), gi|56785773 (*Epinephelus coioides*), gi|68161098 (*Ictalurus punctatus*), gi|46243653 (*Biomphalaria glabrata*), *Hydra vulgaris* (current study), gi|8347758 (*Callinectes sapidus*), gi|51534181 (*Lepeophtheirus salmonis*), gi|39595775 (*Caenorhabditis briggsae*), gi|3875775 (*Caenorhabditis elegans*), gi|562770 (*Onchocerca volvulus*), gi|58429979 (*Bombyx mori*), gi|7302882 (*Drosophila melanogaster*), gi|8347760 (*Callinectes sapidus*-2), gi|57813149 (*Cryptococcus neoformans* var. *grubii*), gi|32418882 (*Neurospora crassa*), gi|66824921 (*Dictyostelium discoideum*), gi|20902 (*Pisum sativum*), and gi|6016702 (*Arabidopsis thaliana*).

3.1.13 Threading

Five web-available threading methods used to find the structure templates for the HvMnSOD domain were as follows: TOPITS (<http://dodo.cpmc.columbia.edu/predictprotein/>); HMM (<http://www.cse.ucsc.edu/research/compbio/HMM-apps/HMM-applications.html>); 3D-JIGSAW (<http://www.bmm.icnet.uk/~3djigsaw/>); 3D-PSSM (<http://www.sbg.bio.ic.ac.uk/~3dpssm/>); and HFR (<http://www.cs.bgu.ac.il/~bioinbgu/>). TOPITS (Rost, 1995) and 3D-PSSM (Kelley *et al.*, 2000) are methods based on matching the predicted secondary structure and solvent accessibility or solvation

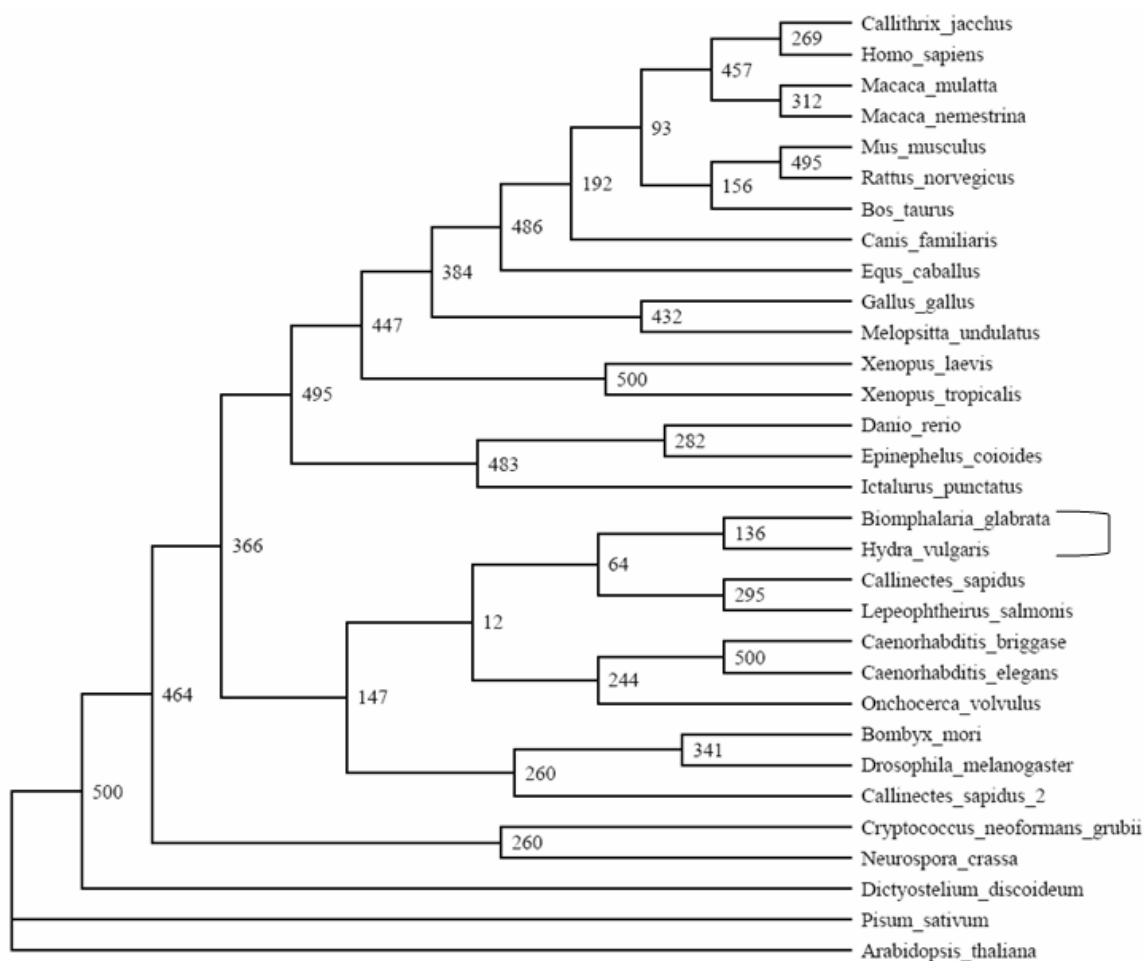


Figure 23. Phylogenetic alignment of the amino acid sequences of the MnSODs from different organisms. The tree was constructed by the maximum likelihood method using the program PHYML (Guindon and Gascuel, 2003). Bootstrap confidence values for the sequence groupings are indicated in the tree ($n = 500$). The hydra MnSOD is grouped with mollusk and crustaceans.

potentials of the query sequence with those of the proteins of known structures. HFR (Fischer, 2000) is a hybrid method that combines results from five threading programs to search the most consistent fold prediction among them. HMM (Karplus *et al.*, 1998) uses a hidden Markov model (HMM) engine to compare the query sequence with sequences of known protein structures to derive a possible structure class for the query one. The 3D-JIGSAW (Bates *et al.*, 2001) Web server builds 3D models for proteins based on homologs of known structures. Through the threading experiments on the Web sites, several templates for the query sequence were found. These templates were further screened using the SWISS-MODEL Protein Modeling Server (Guex and Peitsch, 1997) on the Web. Protein 1LUV (Hearn *et al.*, 2003) was selected as the structure template for the query sequence HvMnSOD.

3.1.14 Molecular modeling

Using the alignment in Figure 24, a 3D model of the HvMnSOD protein was built based on the coordinates of 1LUV: A (1LUV.pdb). The template and target assembly (Figure 24) was submitted to the 3D-JIGSAW web server and a model was retrieved (Figure 25).

3.1.15 Analysis of the model

The overall stereo-chemical quality of the final model was assessed by the program PROCHECK (<http://biotech.ebi.ac.uk:8400/cgi-bin/sendquery>) (Laskowski *et al.*, 1994). A secondary structure (Figure 26) and Ramachandran plot (Figure 27) of the model was also drawn. The structural quality of the model

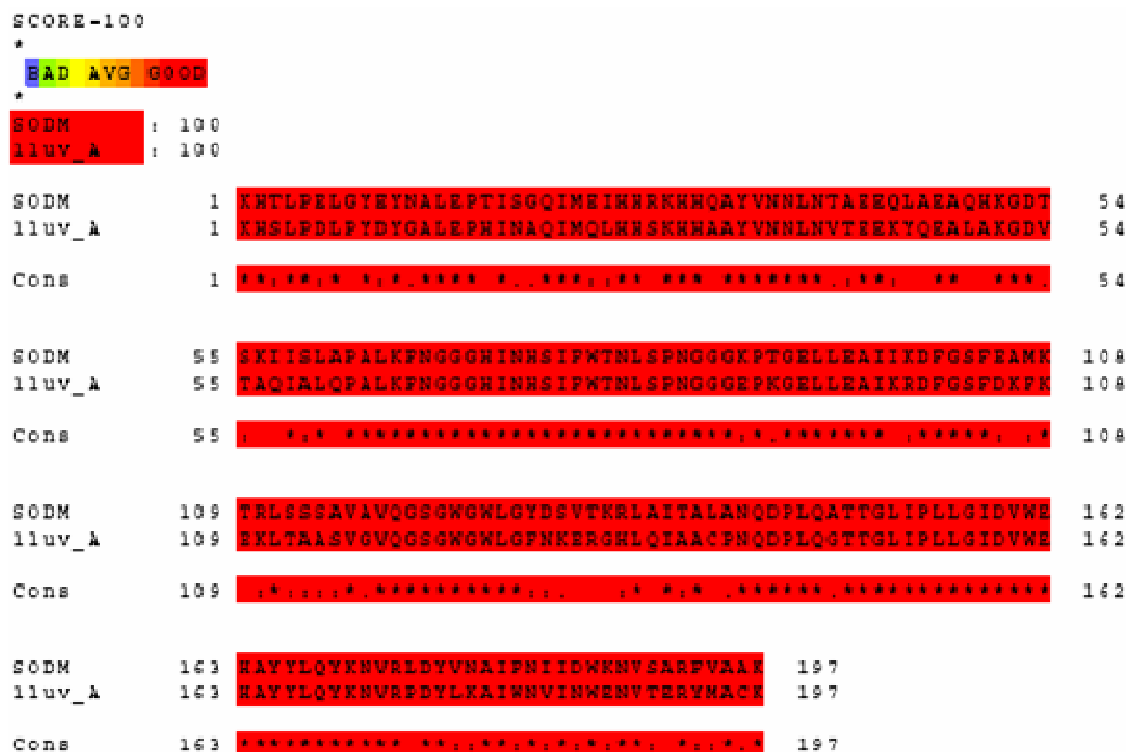


Figure 24. Target and template assembly used for generation of *H. vulgaris* MnSOD model. The alignment was performed using the program T-coffee (<http://igs-server.cnrs-mrs.fr/Tcoffee/tcoffee.cgi/index.cgi>). The red shading highlights that the two protein sequences are highly homologous. The score of the alignment is 100.

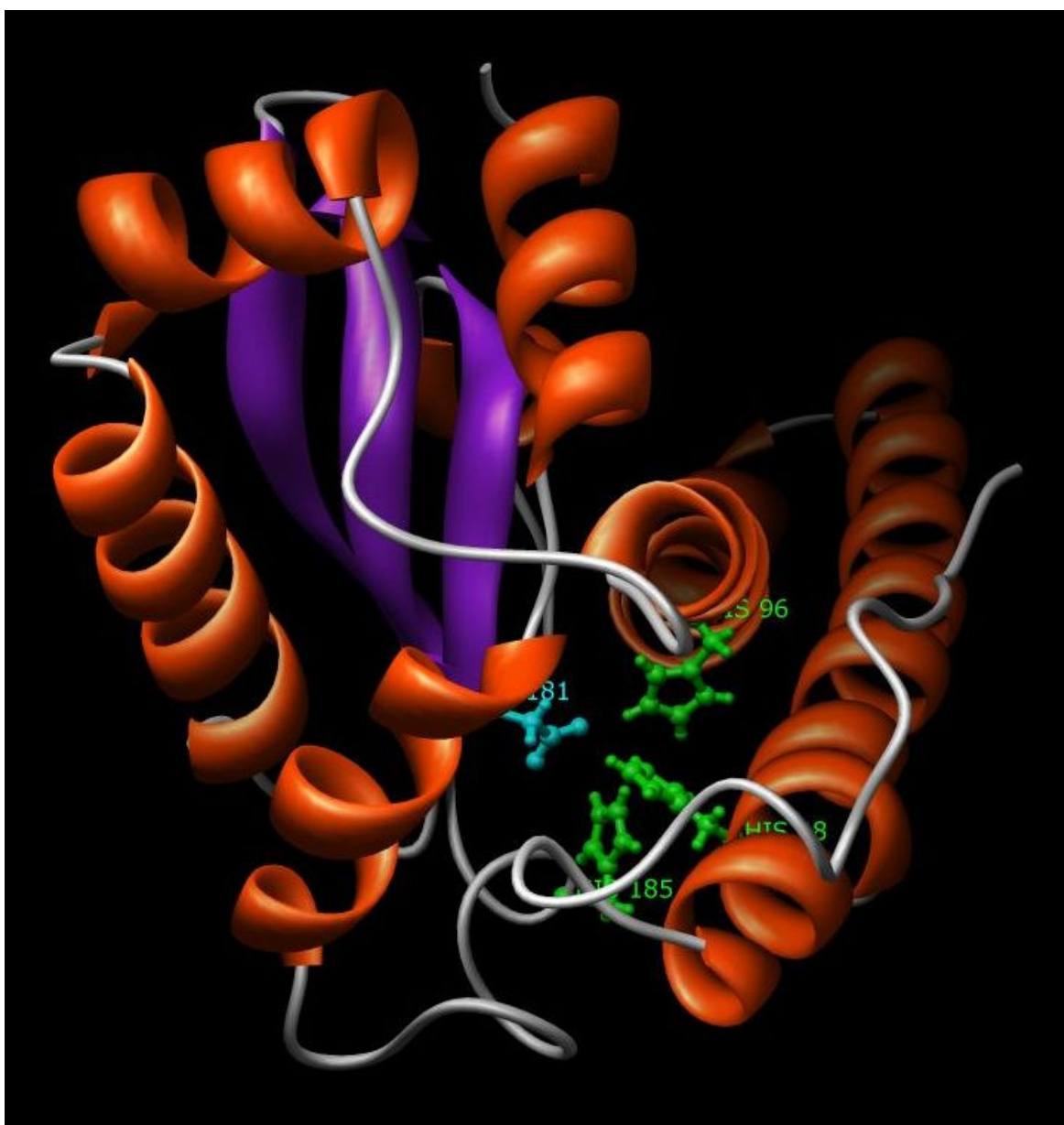


Figure 25. A 3D model of the *H. vulgaris* MnSOD. HvMnSOD was modeled on the published crystal structure of human manganese superoxide dismutase (Hearn *et al.*, 2003). The ligands of the metal manganese are His 48, His 96, His 185 (green colored residues) and Asp 181 (cyan colored residue).

KHTLPGLGYEYNALPTISGQIMEIHHRKHHQAYVNNLNTAEEQLAEAQHKGDTSKIISLAPALKE
 NGGCHINHSIFWTNLS PNGGKPTGELLEAIKDFGSFEAMKTRLSSSAVAVQGS GMGLGYDSVT
 KRLAITALANQDPLQATTGLIPLLGIDVMEHAYYLQYKNVRLDYVNAIENI IDWKNVSAREVA AK

 = helix
 = strand

Figure 26. Secondary structural elements of the HvMnSOD model. The green shaded amino acids make up the β -strands and the orange shaded elements make up the helices of HvMnSOD. Structural elements are highlighted using the program Chimera (<http://www.cgl.ucsf.edu/chimera/>).

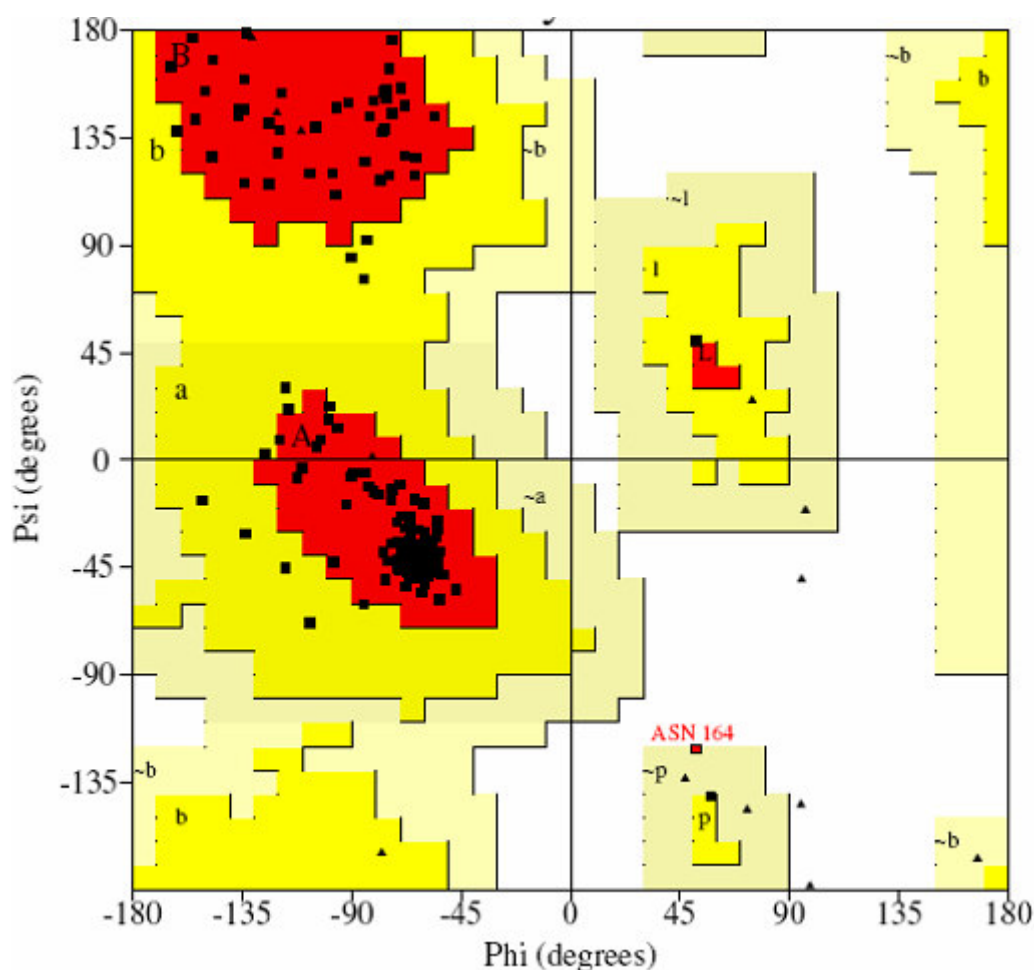


Figure 27. Ramachandran plot of model HvMnSOD. No residue has been found in the disallowed regions. The Ramachandran plot of the model was generated using the program Procheck.

was also verified using the program Verify-3D (http://nihserver.mbi.ucla.edu/Verify_3D/) that measures the compatibility of a protein model with its sequence where the values are calculated using 3D profile (Bowie *et al.*, 1991).

3.2 Results

3.2.1 Cloning and analysis of HvMnSOD cDNA

Comparative analysis of amino acid sequences of MnSODs from several species revealed that stretches of amino acids are highly conserved among them and multiple sequence alignment (Figure 20) led to the identification two stretches of conserved amino acids: FNGGGHIN and VWEHAYY. A pair of degenerate primers (DF and DR) was designed corresponding these two conserved stretches of amino acids (Table 8) and were used in RT - PCR experiments to amplify a segment of HvMnSOD. An amplified cDNA product of little more than 300 base pair (bp) was subcloned and sequenced (Figure 21A). Initial sequence analysis of the cloned fragment indicated the presence of an open reading frame encoding a polypeptide with a high degree of similarity to MnSOD of many organisms.

The full-length cDNA sequence encoding the putative HvMnSOD was cloned employing the 5'-/3'-RACE method using gene specific primers from the above cloned segment (Table 8). The putative transcription initiation site found by 5'-RACE is located at nucleotide (nt) position 1 (Figure 22). The nucleotide and the predicted amino acid sequence of the HvMnSOD cDNA are shown in

Figure 22. The initiation site of translation was placed at nt 61, inferred by conceptual translation of the sequence in all three reading frames and alignment with the known sequences of MnSOD proteins available in the GenBank database. The putative HvMnSOD cDNA (Figure 22) is shown to contain a 657 bp open reading frame (ORF) and an in-frame TGA stop codon at the 3'-end of the coding region. The ORF is flanked by a 117 bp 3'-untranslated region followed by the putative poly(A) tail. Three polyadenylation consensus sequence (5'-AATAA-3') is located between the stop codon and the poly(A) tail. The cDNA sequence also contained a splice leader (nt 7 to 52) in the 5'-untranslated region and belonged to the splice leader B (SL-B) category.

As shown in Figure 22, the deduced protein is composed of 219 amino acid residues and the amino acid composition of the polypeptide is given in Table 9. The theoretical isoelectric point (pI) and molecular weight (M_w) of the protein sequence is calculated to be 9.02 and 24348.75 Da, respectively.

The predicted amino acid sequence of the HvMnSOD gene exhibited the characteristic motifs of the MnSOD family. Four residues known to be involved in metal binding in Fe or Mn SODs are found in the HvMnSOD amino acid sequence (H-48, H-96, D-181 and H-185) (Figure 25). The consensus sequence DXWEH observed in MnSODs is located between the above mentioned D-181 and H-185 and is DVWEH in HvMnSOD. Also the sequence LPEL, resembling the peptide LPDL conserved at the N-terminal region in most of eukaryotic MnSODs, is present in HvMnSOD. A single potential N-

TABLE 9**Amino Acid Composition of the HvMnSOD Polypeptide**

Amino acid	Number of residues	Percent
Ala	22	10.05
Cys	0	0.00
Asp	7	3.20
Glu	11	5.02
Phe	10	4.57
Gly	18	8.22
His	10	4.57
Ile	18	8.22
Lys	13	5.94
Leu	21	9.59
Met	3	1.37
Asn	14	6.39
Pro	7	3.20
Gln	8	3.65
Arg	8	3.65
Ser	15	6.85
Thr	11	5.02
Val	10	4.57
Trp	5	2.28
Tyr	8	3.65
Total	219	100

glycosylation site (NXS/T) is also found at H-96 (NHS) in HvMnSOD (Figure 22). A putative mitochondrial transit peptide consisting of residues 1-21 (MFSFGIHRLSVFRKISRIAFA) is also identified by program Signal 3.

Analysis of residues 1-21 of the HvMnSOD mitochondrial transit peptide showed that residues 9-15 (LSVFRKI) likely to form an α -helix. An axial projection of amino acid residues 9-15 on a helical wheel showed that the helix forms an amphiphilic structure. Hydrophobic residues (L-9, V-11, F-12, I-15) are clustered on one side of the helix, and a polar residue (ser-10) along with two positively charged (R-13, K-14) residues are found on the opposite side of the helix.

This putative MnSOD displayed high sequence similarity with members of the MnSOD family (Figure 20; Table 10). So, identification of DVWEH and LPEL motif, mitochondria transit peptide, conserved metal binding residues and homology to other MnSOD proteins strongly suggested that this protein is a MnSOD. Overall, these results suggested that the putative HvMnSOD of the *H. vulgaris* possessed the essential properties of MnSOD family.

3.2.2 Sequence conservation in MnSOD proteins

The HvMnSOD deduced amino acid sequence was aligned by the ClustalW method with several Mn- and Fe- SODs (data not shown). The absolutely conserved residues in all these sequences are H-48, Y-56, H-96, D-181, W-183, E-184, H-185 and Y-188 (numbering is based on HvMnSOD amino acid sequence). An alignment of HvMnSOD with 13 representative MnSODs is

TABLE 10

**Similarities among *H. vulgaris* MnSOD and Mn-/Fe-SOD Proteins from
Other Organisms^a**

Protein	% similarity to HvMnSOD
<i>Danio rerio</i> MnSOD	80
<i>Callinectes sapidus</i> MnSOD	82
<i>Bos taurus</i> MnSOD	80
<i>Xenopus tropicalis</i> MnSOD	77
<i>Macaca mulatta</i> MnSOD	82
<i>Xenopus laevis</i> MnSOD	82
<i>Mus musculus</i> MnSOD	78
<i>Homo sapiens</i> MnSOD	81
<i>Rattus norvegicus</i> MnSOD	80
<i>Bombyx mori</i> MnSOD	80
<i>Gallus gallus</i> MnSOD	80
<i>Oryctolagus cuniculus</i> MnSOD	80
<i>Biomphalaria glabrata</i> MnSOD	82
<i>Equus caballus</i> MnSOD	81
<i>Cavia porcellus</i> MnSOD	82
<i>Caenorhabditis elegans</i> MnSOD	78
<i>Drosophila melanogaster</i> MnSOD	76
<i>Callinectes sapidus</i> cytosolic MnSOD	76
<i>Ictalurus punctatus</i> MnSOD	80
<i>Dictyostelium discoideum</i> MnSOD	73
<i>Arabidopsis thaliana</i> MnSOD	69
<i>Cinnamomum camphora</i> Fe-SOD	68
<i>Tetrahymena pyriformis</i> Fe-SOD	67
<i>Mycobacterium tuberculosis</i> MnSOD	67
<i>Propionibacterium shermanii</i> SOD [Mn/Fe]	70

^aComparisons of amino acid sequences were made with the algorithm of NCBI BLAST

shown in Figure 20. The 219 amino acid protein deduced from the cDNA sequence when compared to the proteins of GenBank database using the program BLAST gave significant scores with MnSODs (*Danio rerio*, *Callinectes sapidus*, *Bos taurus*, *Xenopus laevis*, *Mus musculus*, *Homo sapiens*, *Rattus norvegicus*, *Biomphalaria glabrata*, *D. melanogaster*, *C. elegans*, etc.) and FeSODs (*Cinnamomum camphora*, *Tetrahymena pyriformis*, *Mycobacterium tuberculosis*, *Propionibacterium shermanii*, etc.) (Table 10).

3.2.3 Phylogenetic analysis

In order to further characterize the putative protein sequence, the protein sequence was compared to several published MnSOD sequences from various organisms using the program PHYML (Guindon and Gascuel, 2003). PHYML, a traditional maximum likelihood program which seeks to find the optimal topology in respect to the likelihood value and capable of optimizing model parameters (Stamatakis *et al.*, 2005), currently represents the most efficient genetic algorithm for phylogenetic analysis and is very fast and outperforms other recent approaches including MrBayes and MetaPIGA (Lemmon and Milinkovitch, 2002). Phylogenetic analysis (Figure 23) showed that HvMnSOD is grouped with crustaceans (*Biomphalaria*) and mollusks (*Callinectes* and *Lepeophtheirus*), the closest relationship being with the crustaceans (*Biomphalaria*).

3.2.4 The structural model of HvMnSOD

By threading analysis it was found that the human manganese superoxide dismutase (PDB code: 1LUV.pdb) (Hearn *et al.*, 2003) is the best

template for homologous modeling of the HvMnSOD (target protein). It shared a high degree homology across its entire length (Figure 24) with HvMnSOD.

The model retrieved from the 3D-JIGSAW server is shown in Figure 25. The comparative stereo-chemical analysis of the ϕ - ψ plots (Ramachandran diagram) of the model (HvMnSOD) and structure template (1LUV: A) is shown in Table 11. The analysis for crystallographic structure of the model (HvMnSOD) present 90.6 % of residues in the most favorable, 8.8 % of residues in additional allowed regions, 0.6 % of the residues in generously allowed regions, and 0.0 % of the residues in disallowed regions, which strongly indicated that the molecular models presented here has a good overall stereo-chemical quality. A Verify-3D run on the model also showed a good stereo-chemical quality of the model (data not shown).

The HvMnSOD model (Figure 25) displayed active sites having conserved metal-binding residues (H-48, H-96, D-181, and H-185) and active-site structures, including shells of aromatic residues (Y-31, Y-33, Y-56, F-88, F-99, W-100, W-145, W-147, W-183, Y-187, Y-188, Y-191, Y-198, F-203) that surrounded the active-site metal and its ligands. N-terminal domain is a long alpha antiparallel hairpin and the C-terminal domain is a mixed alpha/beta fold (Figure 25).

3.2.5 HvMnSOD mRNA expression analysis

Exposure of hydrae to temperatures of both 30 and 37 °C for 1 h (Figure 28, lane 2 and 4) increased the MnSOD mRNA expression although 6 h

TABLE 11

**Comparison of the Ramachandran Plot Statistics between the Model
HvMnSOD and the Template 1LUV: A**

Structure	Region of the Ramachandran plot (%)			
	Most favorable	Additional allowed	Generously allowed	Disallowed
HvMnSOD	90.6	8.8	0.6	0.0
1LUV:A	91.0	8.1	0.9	0.0

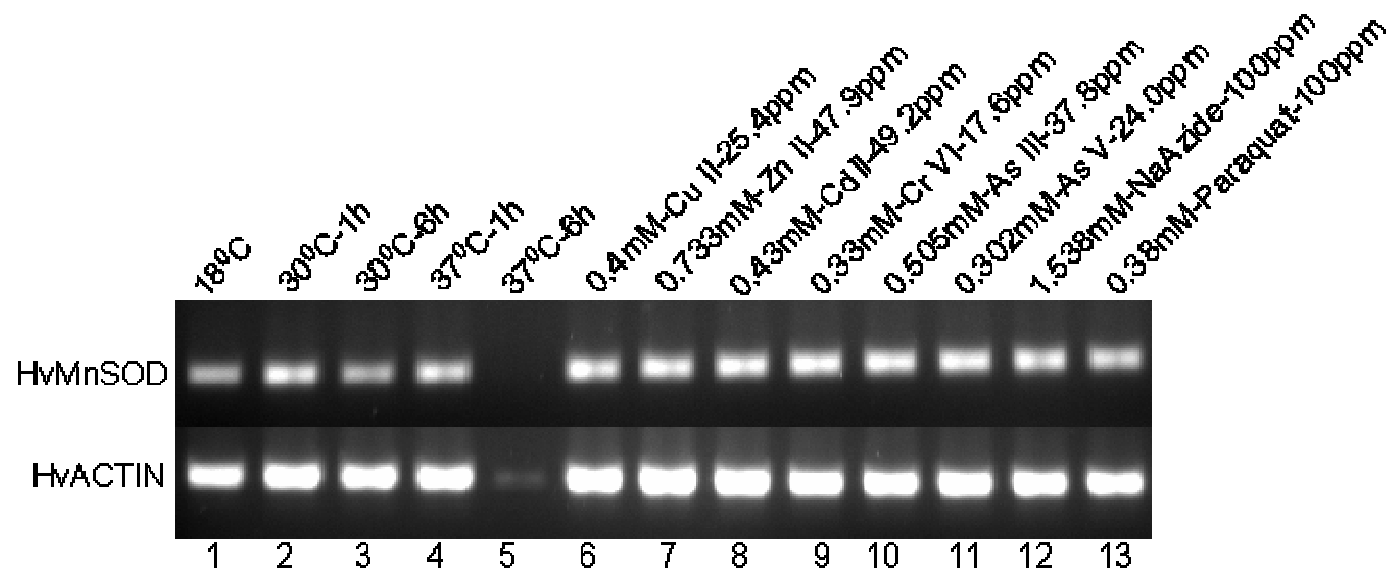


Figure 28. Expression analysis of MnSOD mRNA from *H. vulgaris* exposed to thermal, metal and oxidative stress. The figure represents the expression of HvMnSOD mRNA under different stress conditions as described in the material and methods section: (A) Thermal stress (lanes 2-5); (B) Metal stress for 6 h (lanes 6-11), (C) Oxidative stress for 6 h (lanes 12-13). The expression HvMnSOD mRNA is compared to that of actin.

exposure to 30 °C didn't result in increased MnSOD mRNA expression (Figure 28, lane 3). However, HvMnSOD mRNA expression was drastically reduced when animals were exposed to 37 °C for 6 h (Figure 28, lane 5). Hydrae exposed to H₂O₂ and paraquat for both 1- and 6-h (Figure 28, lane 13; Figure 29, lanes 10-12), increased the expression of HvMnSOD mRNA. Also exposure to 1.538 mM sodium azide for 6 h enhanced the expression of HvMnSOD mRNA (Figure 28, lane 12).

The expression HvMnSOD mRNA was increased when hydrae were exposed to metals at the tested concentrations for 6 h (Figure 28, lanes 6-11) and similar observations were noted after 1 h exposure to Zn (II), As (III), As (V) and Se (IV) (Figure 29). Exposure to Cu (II), Cd (II), and Cr (VI) at the tested concentrations for 1 h seemed not to affect the HvMnSOD mRNA expression (Figure 29)

3.3 Discussion

The objective of the study was to clone and characterize the MnSOD gene in *H vulgaris*. Here, heterologously designed degenerate primers combined with 5'-/3'-RACE experiments were used to clone a full-length ORF of HvMnSOD. To confirm that the cDNA and PCR cloning products are indeed from the same gene, the full-length ORF was cloned by PCR and sequenced (data not shown).

Superoxide dismutases (SODs) are the first line of defense against toxic intracellular radicals produced during normal cellular metabolism or under

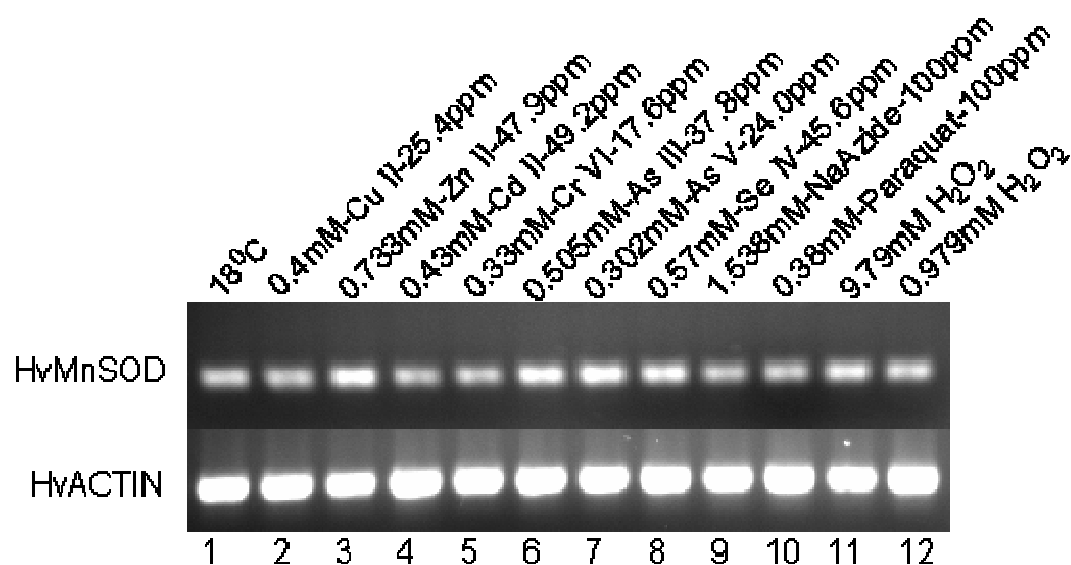


Figure 29. Expression analysis of MnSOD mRNA from *H. vulgaris* exposed to metal and oxidative stress for 1 h. The figure above represents the expression of HvMnSOD mRNA under different stress conditions as described in the material and methods section: (A) Metal stress for 1 h (lanes 2-8) and (B) Oxidative stress for 1 h (lanes 9-12). The expression HvMnSOD mRNA is compared to that of actin.

oxidative stress (Fridovich, 1975). MnSODs located in the mitochondrial matrix scavenge superoxide anions and, typically, active as homotetramers (Hearn *et al.*, 2003). The finding of a putative mitochondrial transit peptide in HvMnSOD entails its localization to mitochondria and similar role.

Crystallographic studies with human MnSOD and *E. coli* FeSOD have shown that metal-binding sites of these two enzymes are located at three histidine residues and one aspartate residue (Carlioz *et al.*, 1988; Borgstahl *et al.*, 1992). The corresponding residues in *H. vulgaris* MnSOD are identified as H-48, H-96, D-181 and H-185 (Figure 25). These residues, as well as the sequence DXWEH including D-181 and H-185, are conserved in all MnSODs so far described (Figure 20). Also potential N-glycosylation site, NXS/T, located at H-96 in HvMnSOD is also conserved in all other eukaryotic species except *S. cerevisiae* (Ditlow *et al.*, 1982).

Most of the eukaryotic MnSODs include a putative mitochondrial transit peptide. However, bacterium *E. coli* (Takeda and Avila, 1986), fungus *A. fumigatus* (Crameri *et al.*, 1996) and *G. microsporum* (Pan *et al.*, 1997) and chlorophycean *Chlamydomonas reinhardtii* (Kitayama *et al.*, 1995) MnSOD reportedly lacked a transit peptide (Figure 20). Although mitochondrial transit peptides from MnSODs are not very similar, targeting sequences are generally rich in positively charged and hydroxylated amino acids and lack acidic amino acids (Roise *et al.*, 1988; Hartl and Neupert, 1990). The hydra MnSOD transit peptide contained 2 ala , 4 phe, 3 ile, 1 leu, 1 met, 1 val (all hydrophobic

residues); 1 his, 1 lys, , 3 arg (all basic residues); and 1 gly, 3 ser (all polar residues). It lacked acidic residues. It also possessed the amphiphilic structural characteristics typical of mitochondrial-targeting sequences where residues 9-15 (LSVFRKI) are likely to form an α helix; hydrophobic residues (L-9, V-11, F-12, I-15) one face of the helix and a polar residue (ser-10) along with two positively charged (arg-13, lys-14) residues on the other face of the helix. In the absence of MnSOD information from similar cnidarian species, the grouping of HvMnSOD with mollusks and crustaceans would be expected as shown in this study.

Messenger RNAs have been identified that can receive either splice leader A or B (SL-A or -B), although the impact of the two different SLs on the function of the mRNA is not known (Stover and Steele, 2001). To date, SL addition has been identified in four metazoan phyla (Nematoda, Platyhelminthes, Chordata and Cnidaria) and in one unicellular eukaryotic phylum (Sarcomastigophora). No evidence of SL addition has been detected in any intensively studied plants, fungi, insects, echinoderms, or vertebrates (Stover and Steele, 2001). So the presence of SL-B addition in the HvMnSOD is another addition to the repertoire of mRNAs that receive splice leaders in cnidaria and raises interesting questions regarding the evolution of this process.

Many studies have identified the enzymatic activities and expression of MnSOD protein upon exposure to stressors and metals. MnSODs are inducible enzymes and its expression is regulated by many agents, including tumor necrosis factor, interleukin-1, interleukin-6, lipopolysaccharide, phorbol esters

and inhibitors of protein synthesis (Wong and Goeddel, 1988; Visner *et al.*, 1990; Fujii and Taniguchi, 1991; Fujii *et al.*, 1994). Most of the studies conducted on MnSODs are in mammalian systems. Few studies conducted on other organisms are available; and results observed in the current study are comparable to them if a direct relation between transcriptional activity and enzymatic activity is assumed which is often the case unless other regulatory mechanisms such as reduced mRNA stability, translational feed back inhibition, etc. exist and are important.

Lee and Gu (2003) used a recombinant bioluminescent *Escherichia coli* strain, (sodA::luxCDABE), containing the promoter for the manganese superoxide dismutase (sodA) gene fused to the *Vibrio fischeri* luxCDABE operon, and characterized with regard to redox-cycling agents, such as paraquat and chromium. Both strongly induced a sodA - regulated response in dose-dependent manners, resulting in an increase of the bioluminescence. Similarly, Rohrdanz and Kahl (1998) studied the effect of hydrogen peroxide (H_2O_2) on the expression of different antioxidant enzymes in primary rat hepatocytes and showed that MnSOD mRNA levels were induced after exposure to H_2O_2 . Similar observations are made in the current study that paraquat, H_2O_2 and chromium induced the expression of HvMnSOD mRNA. As expected, hydra responded to oxidative stress by inducing MnSOD mRNA. Similar mechanisms and response that protects organisms from deleterious effects of reactive oxygen species (ROS) formed due to exposure to oxidants or as a natural consequence of

metabolism are well conserved in prokaryotes and eukaryotes (Angelova *et al.*, 2005). Metals are also known to influence the oxidative status of organisms, and antioxidant enzymes have been often proposed as biomarkers of effect (Geret *et al.*, 2002).

Thus HvMnSOD mRNA is highly inducible under stress and exposure to toxicants; and the deduced protein sequence has similar topological features and domains of higher model organisms. These features of HvMnSOD combined with the ease of conducting hydra bioassay offer an opportunity to use *H. vulgaris* as a model system to study the pro-oxidant properties of chemicals and environmental toxicants.

CHAPTER IV
MOLECULAR CLONING AND CHARACTERIZATION OF AN
EXTRACELLULAR COPPER ZINC SUPEROXIDE DISMUTASE FROM
HYDRA VULGARIS

Superoxide dismutases (SOD) (EC 1.15.1.1) disproportionate superoxide and therefore, are master regulator of free radical balance and reactive oxygen species in cells (Winterbourn, 1994). There are three types of SOD identified in eukaryotic cells and they differ by the metallic ion present at the active site: copper and zinc (CuZnSOD), manganese (MnSOD), or iron (FeSOD) (Halliwell and Gutteridge, 1999). These metalloenzymes dismutate the superoxide anion into oxygen and hydrogen peroxide ($2\text{O}_2^{\cdot-} + 2\text{H}^+ \rightarrow \text{H}_2\text{O}_2 + \text{O}_2$) thus preventing the superoxide anion from initiating a radical chain reaction which again results in the generation of reactive oxygen species (ROS) (Plantivaux *et al.*, 2004). ROS may damage nucleic acids, proteins, and membrane lipids.

Though these enzymes catalyze the same reaction, CuZnSODs are structurally distinct from MnSODs and FeSODs, which share a high degree of amino acid sequence and structural homologies (Halliwell and Gutteridge, 1999; Stallings *et al.*, 1984). Two CuZnSODs encoded by two different genes are found in eukaryotes: intracellular CuZnSODs and extracellular CuZnSODs (EC-CuZnSODs). Intracellular CuZnSODs are generally found in the cytosol and in

chloroplasts of plants. Alternatively, EC-SODs can be anchored to the plasma membrane or circulate in the extracellular fluids (Stallings *et al.*, 1984; Fattman *et al.*, 2003). The two forms of CuZnSOD also share high sequence similarity. MnSOD is present in mitochondria; whereas, FeSOD is present within the chloroplasts of some plants (Bannister *et al.*, 1987).

Genes encoding extracellular CuZnSODs have been cloned from several organisms. EC-CuZnSOD catalyzes the dismutation of superoxide radical in extracellular fluids (plasma, lymph, and synovial fluid) in humans. It is a secretory, tetrameric glycoprotein containing copper and zinc, with a high affinity to certain glycosaminoglycans, such as heparin and heparan sulfate (He *et al.*, 2002). It has been suggested that EC-CuZnSOD may play a role in reducing the superoxide-induced injuries of the tissues (i.e., aorta restenosis in rabbits and murine collagen-induced arthritis) and also prevent telomere damage in human fibroblast resulting from oxidative stress (Fattman *et al.*, 2003; Laukkanen *et al.*, 2002; Iyama *et al.*, 2001; Serra *et al.*, 2003). The level of EC-CuZnSOD expression is profoundly influenced by cytokines involved in the inflammatory response in human skin fibroblasts (Marklund, 1992). Human EC-SOD (SOD3) constitutes up to 70 % of the total SOD activity in arteries (Oury *et al.*, 1996; Stralin *et al.*, 1995).

Also an EC-CuZnSOD gene sequence is available for cnidaria sea anemone (*Anemonia viridis*) (Plantivaux *et al.*, 2004). Many studies indicated their presence and importance along with the other forms of SODs in several

cnidarians (Plantivaux *et al.*, 2004; Dykens and Shick, 1982; Dykens and Shick, 1984; Shick, 1991; Hawkrigde *et al.*, 2000; Downs *et al.*, 2002; Brown *et al.*, 2002; Richier *et al.*, 2003). For example, the symbiotic corals and sea anemones revealed a very efficient defense system against reactive oxygen species (ROS) (Dykens and Shick, 1982; Dykens and Shick, 1984).

In this research, the molecular analysis of an extracellular CuZnSOD in cnidarian, *H. vulgaris*, is described. The expression of hydra EC-CuZnSOD (HvEC-CuZnSOD) mRNA is assayed with respect to different environmental contaminant challenge (i.e., arsenic, cadmium, senium, zinc and copper) and stressors (both oxidative and non-oxidative). The phylogenetic position of HvEC-CuZnSOD is also studied. Furthermore, a suitable homology based structural model of HvEC-CuZnSOD is also presented to assist in understanding the structural and functional evolutionary significance of the protein. The molecular analysis of hydra EC-CuZnSOD is the first reported for a diploblastic hydrozoan organism and represents an important step in the evolutionary study of this enzyme.

4.1 Materials and methods

4.1.1 Hydra culture

Adult *H. vulgaris* were maintained in shallow dishes at 18 °C in a medium containing 1 mM CaCl₂.2H₂O, 0.012 mM EDTA, and 0.458 mM TES (N-tris[hydroxymethyl]-methyl-2-amino-ethanesulfonic acid, sodium salt) buffer (pH 7.0). Daily, hydrae were fed with brine shrimp (*Artemia nauplii*) hatched in a

solution of 1 % sodium chloride treated with iodine (40 µg/ml). Hydrae were maintained free from bacterial and fungal contamination and were not fed for 24 h before initiating the experiments. Deionized water was used throughout this portion of the study (Mayura *et al.*, 1991).

4.1.2 RNA isolation and clean up

Total RNA was extracted from hydra by application of 2 mL of TRIzol[®] reagent (Invitrogen, USA) to approximately 20 mg of fresh tissue, using the manufacturer's instructions. The RNA was quantified by ultraviolet absorbance at 260 nm. Integrity of the total RNA was confirmed by 1 % formaldehyde agarose gel electrophoresis. The RNA isolated was cleaned up from contaminating DNA using RNeasy Mini Kit (Invitrogen, USA) following the manufacturer's instruction.

4.1.3 Identification of a partial fragment of *H. magnipapillata* CuZnSOD cDNA

The GenBank (<http://www.ncbi.nlm.nih.gov/entrez/query.fcgi?db=nucleotide>) was searched for the cnidaria/hydra CuZnSOD. An expressed sequence tag (EST) was found from the hydra *H. magnipapillata* under the accession number gi|57833081 coding for a CuZnSOD that is similar to the N-terminal end of *Caenorhabditis elegans* superoxide dismutase (Cu-Zn) (P34697). The CuZnSOD coded by the *H. magnipapillata* EST had similar conserved amino acid residues as identified by multiple sequence alignment of several CuZnSODs (Figure 30). Hence, a pair

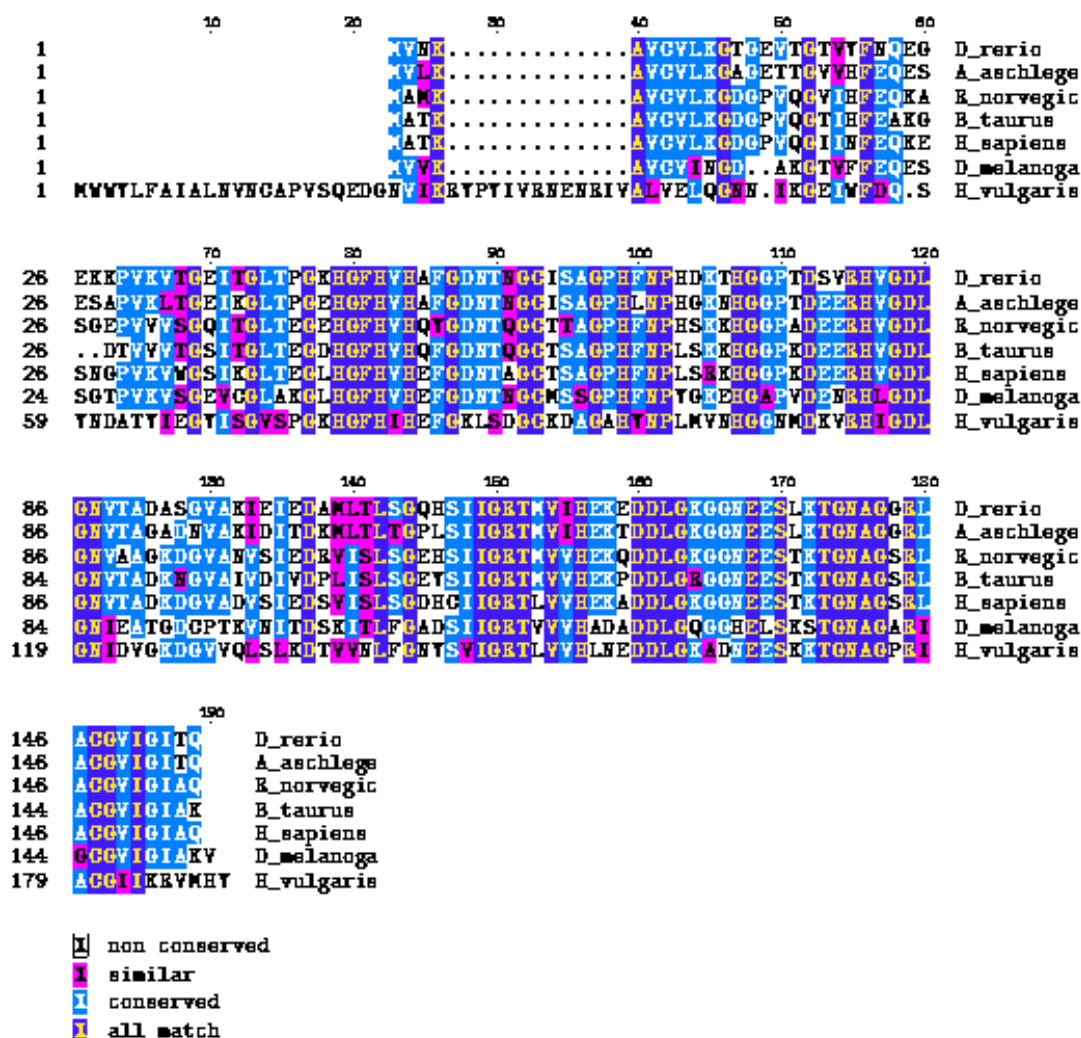


Figure 30. Multiple sequence alignment of CuZnSOD proteins performed using the program ClustalW. Accession numbers from the proteins as extracted using the Entrez web service (<http://www.ncbi.nlm.nih.gov/Entrez/protein.html>) are: *Hydra vulgaris* (current study), *Danio rerio* (Y12236), *Acanthopagrus schlegelii* (AJ000249), *Rattus norvegicus* (Y00404), *Bos taurus* (M81129), *Homo sapiens* (X02317) and *Drosophila melanogaster* (Y00367). The properties of different amino acids are identified by shading as given in the legend.

TABLE 12**Oligonucleotides Used in the Cloning of HvEC-CuZnSOD cDNA**

Oligonucleotide	Sequence
F	5'-CATGGTTTTCATATCCA-3'
R	5'-TGCTTTCCCCAAATCATC-3'
AP ₂	5'-GATCAGGACGTTTCGTTTGAGd(T) ₁₇ -3'
N	5'-AACTGGAAGAATTTCGCGGCCGCAGGAAd(T) ₁₈ -3'
R1	5'-TTGCACCACTCCATCTTTACC-3'
R2	5'-CGTTATCTGCTTTCCCCAAA-3'
AF	5'-AAGCTCTTCCCTCGAAGAATC-3'
AR	5'-CCAAAATAGATCCTCCGATCC-3'

of primes F and R (Table 12) was designed from the EST sequence that corresponded to the conserved amino acid residues (HGFHIH and DDLGKA) to clone a fragment of CuZnSOD from *H. vulgaris*.

4.1.4 Oligonucleotides

All oligonucleotide were procured from IDT Inc. (IA, USA). AP₂ primer (5'-GATCAGGACGTTTCGTTTGAGd(T)₁₇-3') was used for 5'-RACE (Rapid Amplification of cDNA Ends) experiments. The oligo(dT) bifunctional primer N (Not I-d(T)₁₈: 5'-AACTGGAAGAATTCGCGGCCGCAGGAAT₁₈-3') was supplied in a cDNA preparation kit (Amersham Biosciences, USA) and was used for 3'-RACE experiments. Other primers and *H. vulgaris* gene specific primers used in the experiments are given in the Table 12.

4.1.5 Cloning and identification of a partial fragment of *H. vulgaris* CuZnSOD cDNA

All polymerase chain reaction (RT-PCR and RACE-PCR) experiments were performed using *Taq* DNA polymerase (Invitrogen, USA) and a thermal cycler (MJ Research, USA).

RNA (5 µg) was reverse-transcribed to cDNA at 37 °C for 60 min using the oligo(dT) bifunctional primer and the AMV RT supplied in the cDNA synthesis kit (Amersham Biosciences, USA). The first-strand cDNA was amplified using the primers F and R (Table 12). The PCR was performed for 30 cycles, consisting of 94 °C for 30 s, 50 °C for 30 s and 72 °C for 1 min and a final extension at 72 °C for 10 min. The resultant PCR products (Figure 31A) were

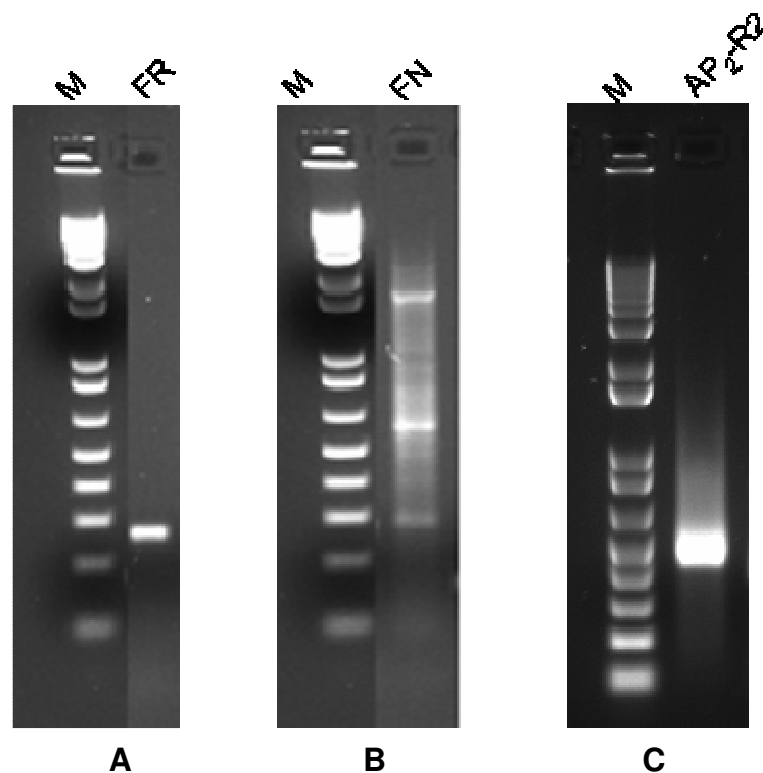


Figure 31. Images of electrophoretic gels for PCR products of HvEC-CuZnSOD gene. (A) The PCR products were produced using primer F and R. (B) The 3'-RACE PCR products were produced using with primer F and N (= NotI-d(T)₁₈). (C) The 5'-RACE PCR products were produced using with primer AP₂ and R₂. M = 1 kb plus DNA ladder.

subcloned into the pCR[®]II-TOPO[®] vector using a TA cloning kit (Invitrogen, USA) according to the manufacturer's instructions. Multiple independent clones were sequenced using automated methods (DNA Technologies Lab, Department of Veterinary Pathobiology, Texas A&M University) on an ABI PRISM[™] 310 Genetic Analyzer (PE Biosystems, USA) using a Big-Dye sequencing kit (PE Biosystems) and M13 primers. The identity of the clones was evaluated by matching the sequences to the nucleotide/protein sequences available at the GenBank. The cloned sequence constituted residues 368 to 628 in the nucleotide sequence shown in Figure 32.

4.1.6 3'-RACE of the HvCuZnSOD cDNA

First-strand cDNA prepared above was amplified using the oligo(dT) bifunctional primer and a gene-specific primer F (Table 12) (complementary to nucleotide (nt) 368 to 384, Figure 32) for 35 cycles of 94 °C for 30 s, 55 °C for 30 s and 72 °C for 3 min. The products (Figure 31B) were subcloned and sequenced as described above. The identity of the clones was evaluated by matching the sequences to the nucleotide/protein sequences available at the GenBank (<http://www.ncbi.nlm.nih.gov/>). The cloned sequence constituted residues 234 to 432 in the nucleotide sequence shown in Figure 32.

4.1.7 5'-RACE of the HvCuZnSOD cDNA

The template cDNA was synthesized using a primer R1 (Table 12) (complementary to nucleotide (nt) 509-529) and Superscript II (Invitrogen, USA), followed by dA tailing of the cDNA using dATP and terminal transferase

```

1      ccctttatcttggtttctttctcttcacatctgccctttcttttttttttcttctaacaat 60
61      aactttacagtgaccacagtaaaaagatagttaaaatatttttaaaaaattttaagttgg 120
      1      M W W Y L F A I A L N V N C
121      caaaagaaaaagttaaccatgtggtggtacttatttgcaattgcattgaatgtaaactg 180
      15 A P V S Q E D G N V I K R Y P Y I V R N
181      cgctcccgatatcccaagaagatggaaatgttataaaacgatatccttacatagtaagaaa 240
      35 E N R I V A L V E L Q G N N I K G E I W
241      cgaaaaccgaatagttgcacttggtgaattgcagggttaataacatcaaaggcgaaatatg 300
      55 F D Q S Y N D A T Y I E G Y I S G V S P
301      gtttgatcaatcttataatgatgcaacatatatagaaggctacatctcaggagtctcacc 360
      75 G K H G F H I H E F G K L S D G C K D A
361      tggtaagcacggttttcatatccatgaatttggtaaactatcagatggctgcaaagatgc 420
      95 G A H Y N P L M V N H G G N M D K V R H
421      aggtgcgactataatcctttaatggttaatcatggtgggaatatggataaggttcgaca 480
      115 I G D L G N I D V G K D G V V Q L S L K
481      cataggagatttgggtaatatagatgttggttaaagatggagtgggtgcaactttctttaa 540
      135 D T V V N L F G N Y S V I G R T L V V H
541      agatacagttgtaaacttatttggcaattatagcgttaattggaagaacttttagttgtca 600
      155 L N E D D L G K A D N E E S K K T G N A
601      ccttaatgaagatgatttggggaaagcagataacgaagaaagcaaaaaaacaggaaatgc 660
      175 G P R I A C G I I K R V M H Y *
661      agggccaagaattgcatgtggaataatcaaagagtaatgcactattgatctttcttagt 720
721      gaatcactgtcataatcttaaaaaattttcttcagaacttcgcagttgtaaacgttcatt 780
781      gaaattagaaacatttagaagttaaactgtggttatgaatttctcttcatttttaaaaga 840
841      tttctatttttaaaagatttttgtaaaaaatgtgtttttgatttttaaaatacatttctgt 900
901      ttattgaaaaaaaaaaaaaaaaaaaaa 927

```

Figure 32. Nucleotide and deduced amino acid sequence of *H. vulgaris* extracellular CuZnSOD. The deduced amino acid sequence is shown in single-letter code above the nucleotide sequence. The nucleotide and amino acid sequences are numbered from the 5'-end of the 927 bp cDNA sequence, and from the N-terminal start codon methionine, respectively. The first residue of the presumed matured protein glutamine (Q) is shown bold face. Amino acid residues corresponding to the metal-binding ligands are underlined. The asterisk denotes the translation stop signal.

(Invitrogen, USA) using standard procedures (Sambrook *et al.*, 1989). The first strand cDNA was amplified using an oligo(dT) anchor primer AP2 (5'-GATCAGGACGTTTCGTTTGAGd(T)₁₇-3') and the gene-specific primer R1, and the first-round PCR products were amplified using the PCR anchor primer AP₂ and another gene-specific primer R2 (Table 12) (complementary to nt 616 to 635). Each PCR was performed with an initial amplification of 95 °C for 5 min, 48 °C for 5 min and 72 °C for 5 min followed by 20 cycles of 95 °C for 40 s, 48 °C for 1 min and 72 °C for 3 min with a final extension of 10 min at 72 °C. The PCR products (Figure 31C) were subcloned and sequenced as described above. The identity of the clones was confirmed by matching the sequences to the nucleotide/protein sequences available at the GenBank (<http://www.ncbi.nlm.nih.gov/>).

4.1.8 Heat treatment

Animals were incubated at 18 (control temperature), 30 and 37 (maximum induction temperature) °C for 1 h and 6 h in 5 ml hydra media.

4.1.9 Metal treatment

Nearly 500 hydrae were incubated at 100 ppm of CuSO₄.5H₂O, ZnCl₂, CdCl₂.2.5H₂O, K₂Cr₂O₇, As₂O₃, Na₂HAsO₄ and Na₂SeO₃ for 1 h and 6 h in 5 ml hydra media. Hence the concentration of Cu (II), Zn (II), Cd (II), Cr (VI), As (III), As (V), and Se (IV) (active ingredients) were 0.4 mM (= 25.4 ppm), 0.73 mM (= 47.9 ppm), 0.43 mM (= 49.2 ppm), 0.33 mM (= 17.6 ppm), 0.506 mM (= 37.8 ppm), 0.302 mM (= 24.0), and 0.57 mM (= 45.6 ppm) respectively.

4.1.10 Oxidative stress treatment

Nearly 500 hydrae were incubated at 300 ppm (= 9.79 mM) and 30 ppm (= 0.979 mM) of H₂O₂, 100 ppm (= 0.38mM) paraquat and 100 ppm sodium azide (= 1.538 mM) in 5 ml hydra media.

4.1.11 Starvation treatment

For starvation experiment hydrae were unfed for 5 days.

In all cases, treatments were carried out in 14 ml polypropylene round-bottom tubes (Becton-Dickinson, NJ, USA) containing 5 ml hydra media. At the end of the treatment, hydrae were collected by centrifugation at 7,500 Xg for 5 min. The supernatants were discarded. Then hydrae were washed once in 5 ml of 0.05 M PBS for 5 min @ 7,500 Xg. The supernatants were discarded as before and the animals were homogenized immediately in 3 ml of TRIzol[®].

4.1.12 Expression analysis of HvCuZnSOD mRNA in hydra

Total RNA was extracted from TRIzol[®] (Invitrogen, USA) treated whole hydrae and cleaned as before using RNeasy Mini Kit (Invitrogen, USA) following the procedure described there in. For RT-PCR, 5 µg of total cleaned RNA was reverse transcribed using 500 ng of oligo(dT)₁₂₋₁₈ primer (Invitrogen, USA) and 200 units of the Superscript II enzyme (Invitrogen, USA) for 50 min at 42 °C. The reaction was inactivated by heating the mixture at 70 °C for 15 min. PCR assays were designed to normalize HvCuZnSOD gene expression levels to actin transcription rate. Two µl of first strand cDNA (from 25 µl of reverse transcription mix) was diluted 100 times prior to PCR amplification. PCR was carried out in

50 μ l total volume of 1 \times PCR buffer (20 mM Tris-HCl, pH 8.4, 50 mM KCl), 2 mM $MgCl_2$, 0.1 mM each of dNTPs, 10 pmol each of primers, and 0.5 U *Taq* DNA polymerase (Invitrogen, USA) using 2 μ l of (1:100) diluted RT-product. Actin mRNA was amplified using the AF and AR primers (Table 12) and the HvEC-CuZnSOD mRNA was amplified using the F and R primers. Cycling profile after initial denaturation at 94 $^{\circ}C$ for 4 min was 30 cycles of amplification as follows: denaturation at 94 $^{\circ}C$ for 30 s, annealing at 55 $^{\circ}C$ for 30 s, and extension at 72 $^{\circ}C$ for 45 s. These number of PCR cycles ensured quantification within the exponential phase of amplification. Equal amounts of RT-PCR reactions (9.5 μ l) were loaded on standardized 2 % agarose gels containing 0.1 μ g/ml ethidium bromide. The gel images were digitalized by a gel documentation system (Kodak Laboratories, USA).

4.1.13 General bioinformatic analyses

Conceptual translation of the full-length cDNA was performed using the program SIXFRAME (<http://biologyworkbench.ucsd.edu>). Homology to other CuZnSOD genes and proteins were identified by using the Blast program with default settings (<http://www.ncbi.nlm.nih.gov/BLAST>). The identification of HvEC-CuZnSOD domains were performed by use of the SMART program (<http://smart.embl-heidelberg.de/>) using default pattern definitions. Prosite (<http://us.expasy.org/prosite/>) identification of glycosylation, phosphorylation, myristilation and amidation sites was performed by use of the ExPASy program using default settings. The isoelectric point (pI) and the molecular weight (M_w) of

the deduced protein were calculated using the ExPasy (http://us.expasy.org/tools/pi_tool.html) program. The prediction of the presence and location of signal peptide cleavage sites in amino acid sequences was done using the program SignalP 3.0 (<http://www.cbs.dtu.dk/services/SignalP/>). Several CuZnSOD domain-containing sequences retrieved from the National Center for Biotechnology Information (NCBI) Entrez Web service (<http://www.ncbi.nlm.nih.gov/Entrez/>) were aligned to each other using the web program T-coffee (http://igs-server.cnrs-mrs.fr/Tcoffee/tcoffee_cgi/index.cgi), ClustalW (<http://www.ch.embnet.org/software/ClustalW.html>), or the ClustalW program embedded in Mega (<http://www.megasoftware.net/>) (Figure 33).

4.1.14 Phylogenetic analysis

For phylogenetic analysis, sequences were aligned using the ClustalW program embedded in the program Mega 3.1 (<http://www.megasoftware.net/>) and manually corrected for any obvious misalignments. The aligned sequences were converted into the “Phylip|Phylip44” format (Felsenstein, 1993) using the Readseq program (<http://iubio.bio.indiana.edu/cgi-bin/readseq.cgi>) and saved as a text file. The text file in the interleaved format was uploaded to the PHYML Online (<http://atgc.lirmm.fr/phyml/online.html>) web interface (Guindon and Gascuel, 2003). Following parameters were chosen for the construction of the tree: substitution model - JTT; number of bootstrap data sets - 500, proportion of invariable sites - 0 and fixed; number of substitution rate categories - 1; starting tree(s) - BIONJ; optimize topology - yes; optimize branch lengths and rate

parameters -yes. Nonparametric bootstrap (Felsenstein, 1985) was applied to assess the reliability of internal branches for (large) datasets. The tree generated in the NEWICK format was displayed using the Drawtree program (Figure 32).

The protein sequences (with their accession numbers) for intracellular CuZnSOD are: *Aplysia californica* (gi|21239418), *Lymnaea stagnalis* (gi|41387218), *Biomphalaria glabrata* (gi|41020714), *Acanthopagrus schlegelii* (AJ000249), *Danio rerio* (Y12236), *Pagrus major* (AF329278), *Bos taurus* (M81129), *Canis familiaris* (AF346417), *Macaca mulatta* (gi|23503520), *Equus caballus* (AB001692), *Homo sapiens* (X02317), *Oryctolagus cuniculus* (L12405), *Rattus norvegicus* (Y00404) and for the extracellular form of CuZnSOD are: *Callinectes sapidus* (AF264031), *Dirofilaria immitis* (U14994), *Homo sapiens* (J02947), *Mus musculus* (NM011435), *Onchocerca volvulus* (L13778), *Oryctolagus cuniculus* (Z67878), *Pacifastacus leniusculus* (AF122900), and *Rattus norvegicus* (X94371). The sequence from *Hydra vulgaris* (current study) was also included.

4.1.15 Threading

The five Web-available threading methods were used to find the structure templates for the HvCuZnSOD domain were as follows: TOPITS (<http://dodo.cpmc.columbia.edu/predictprotein/>); HMM (<http://www.cse.ucsc.edu/research/compbio/HMM-apps/HMM-applications.html>); 3D-JIGSAW (<http://www.bmm.icnet.uk/~3djigsaw/>); 3D-PSSM (<http://www.sbg.bio.ic.ac.uk/~3dpssm/>); and HFR

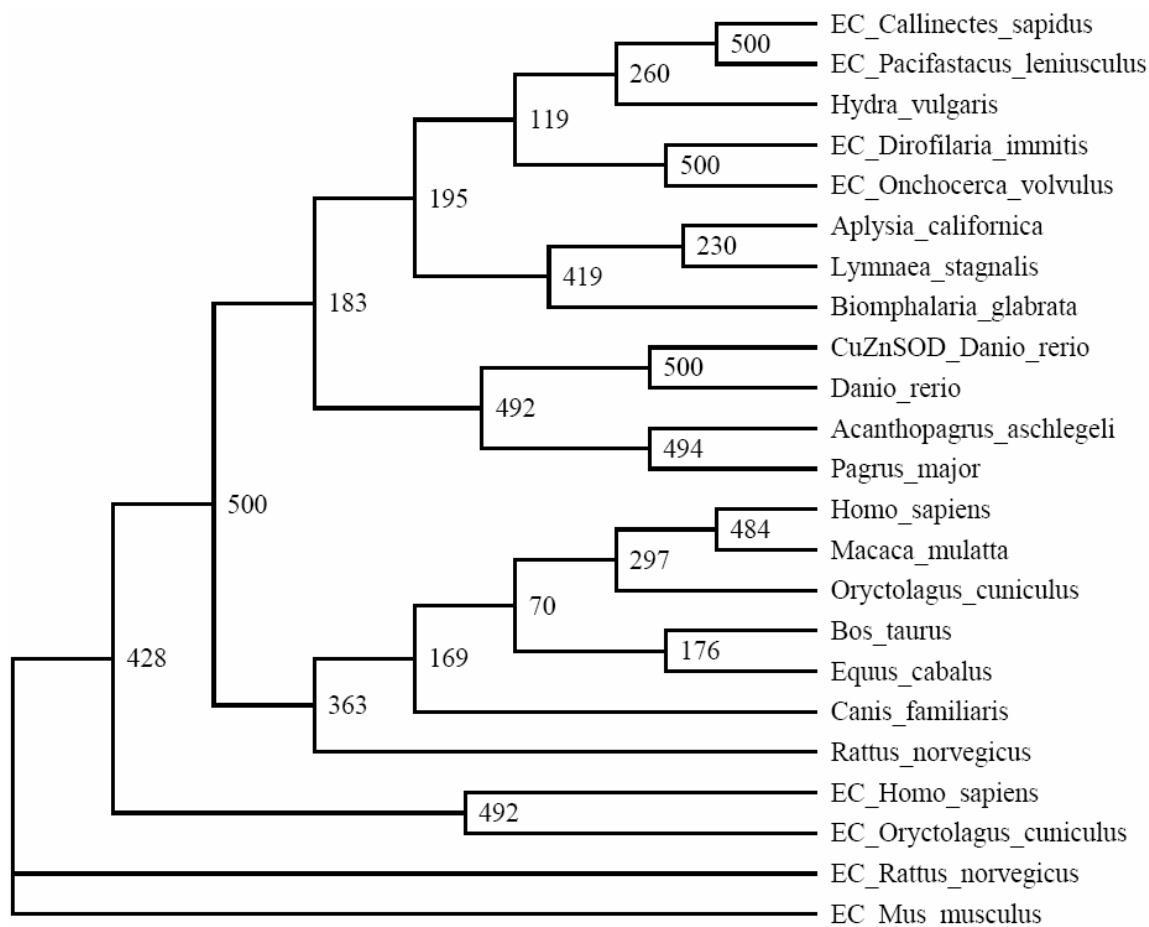


Figure 33. Phylogenetic alignment of the amino acid sequences of the CuZnSODs from different organisms. The tree was constructed by the maximum likelihood method using the program PHYML (Guindon and Gascuel, 2003). Bootstrap confidence values for the sequence groupings are indicated in the tree ($n = 500$). The *H. vulgaris* EC-CuZnSOD is grouped with crustacean EC-CuZnSODs and hence an indication that it is an EC-CuZnSOD.

(<http://www.cs.bgu.ac.il/~bioinbg/>). TOPITS (Rost, 1995) and 3D-PSSM (Kelley *et al.*, 2000) are methods based on matching the predicted secondary structure and solvent accessibility or solvation potentials of the query sequence with those of the proteins of known structures. HFR (Fischer, 2000) is a hybrid method that combines results from five threading programs to search the most consistent fold prediction among them. HMM (Karplus *et al.*, 1998) uses a hidden Markov model (HMM) engine to compare the query sequence with sequences of known protein structures to derive a possible structure class for the query one. The 3D-JIGSAW (Bates *et al.*, 2001) Web server builds 3D models for proteins based on homologs of known structures. Through the threading experiments on the Web sites, several templates for the query sequence were found. These templates were further screened using the SWISS-MODEL Protein Modeling Server (Guex and Peitsch, 1997) on the Web. Protein 1N18 (Cardoso *et al.*, 2002) was selected as the structure template for the query sequence HvEC-CuZnSOD.

4.1.16 Molecular modeling

Using the alignment in Figure 34, a 3D model of the Hv-CuZnSOD protein was built based on the coordinates of 1N18 (1N18.pdb). The template and target assembly (Figure 34) was submitted to the 3D-JIGSAW web server and a model was retrieved (Figure 35).

4.1.17 Analysis of the models

The overall stereo-chemical quality of the final model was assessed by the program PROCHECK (<http://biotech.ebi.ac.uk:8400/cgi-bin/sendquery>)

SCORE=99

*


*

Hydra	:	99	
Human	:	99	
Hydra	1	NDATYIEGYISGVSPGKHGPHIHEFGKLSDGCKDAGAHYNPLMVNHGGNMDKVR	54
Human	1	NGPVKVWGSIKGLTEGLHGFHVHEFGDNTAGCTSAGPHFNPLSRKHGGPKDEER	54
Cons	1	*. . . : * *. * : : * ***** : ***** . : *. . . *. * : ***** : ***** * : *	54
Hydra	55	HIGDLGNIDVGKDGVVQLSLKDTVVNLFNGNYSVIGRTLTVVHLNEDDLGKADNEE	108
Human	55	HVGDLGNVTADKDGVDVSIEDSVISLSGDHSIIIGRTLTVVHEKADDLGKGGNEE	108
Cons	55	* : ***** : . . . ***** : : * : : * : : * * : : * : : ***** : ***** : *****	108
Hydra	109	SKKTGNAGPRIACGI IK	125
Human	109	STKTGNAGSRLACGVIG	125
Cons	109	*. . . ***** . * : ***** *	125

Figure 34. Target and template assembly used for generation of *H. vulgaris* EC-CuZnSOD model. The alignment was performed using the program T-coffee (<http://igs-server.cnrs-mrs.fr/Tcoffee/tcoffee.cgi/index.cgi>). The red shading highlights that the two protein sequences are highly homologous. The score of the alignment is 99.

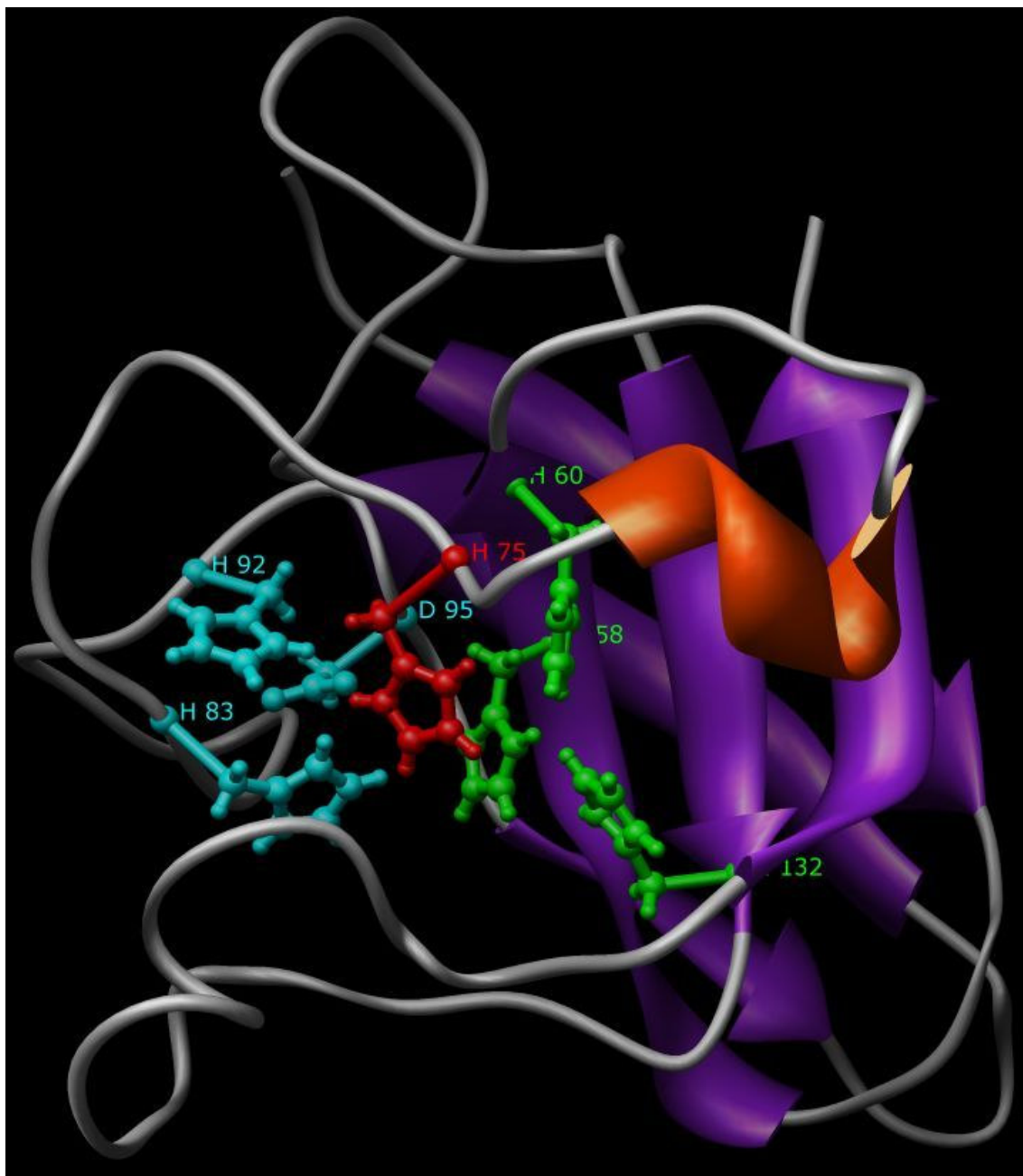


Figure 35. A 3D model of the *H. vulgaris* EC-CuZnSOD. HvEC-CuZnSOD was modeled on the published crystal structure of human CuZnSOD (Cardoso *et al.*, 2002). The ligands of the metal copper are His 58, His 60, His 132 (green colored residues) and His 75 (red colored residue); that of zinc are His 83, His 92, Asp 95 (cyan colored residue) and His 75 (red colored residue). The conserved β -barrel fold typical of CuZnSOD is also seen.

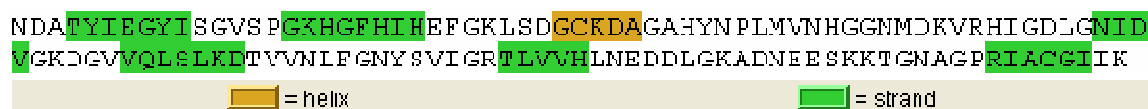


Figure 36. Secondary structural elements of the HvEC-CuZnSOD model. The green shaded amino acids make up the β -strands and the orange shaded elements make up the helices of HvEC-CuZnSOD. Structural elements are highlighted using the program Chimera (<http://www.cgl.ucsf.edu/chimera/>).

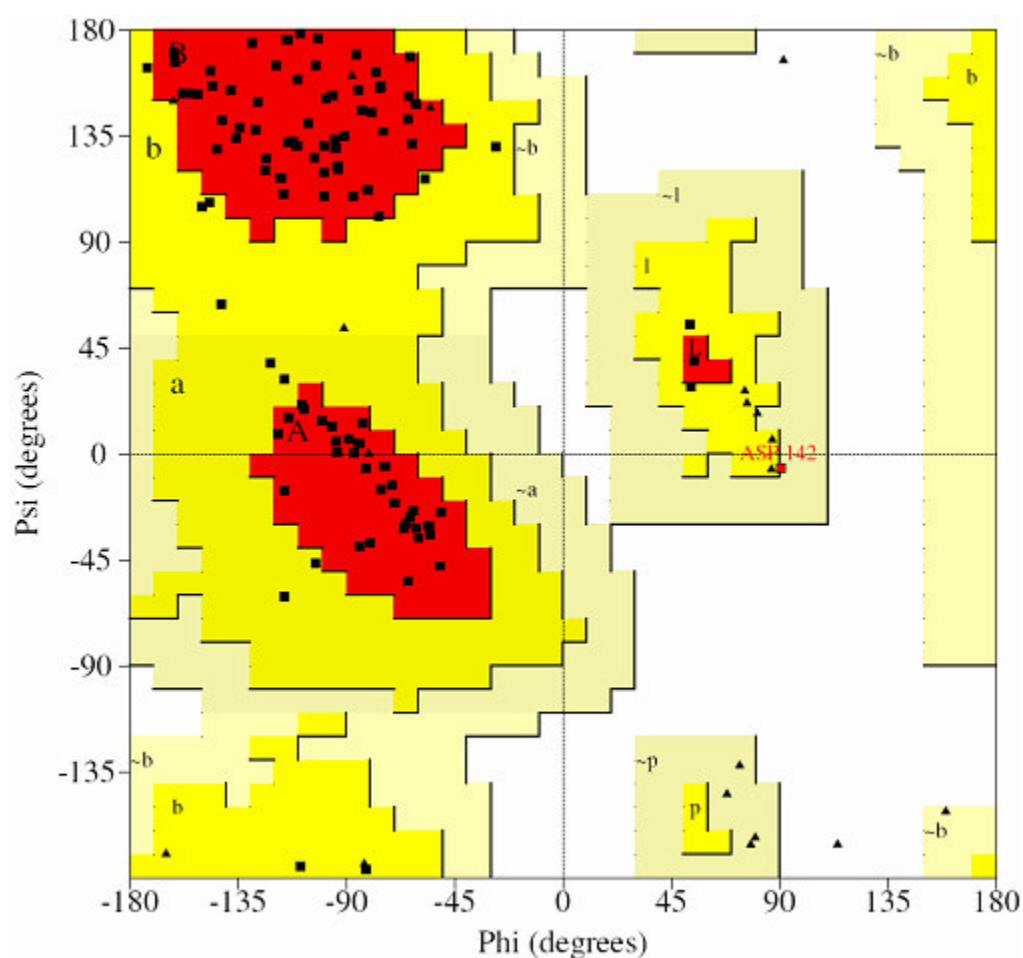


Figure 37. Ramachandran plot of model HvEC-CuZnSOD. No residue was found outside the most favored and additionally allowed regions. The Ramachandran plot of the model was generated using the program Procheck.

(Laskowski *et al.*, 1994). A secondary structure (Figure 36) and Ramachandran plot (Figure 37) of the model was also drawn. The structural quality of the model was also verified using the program Verify-3D (http://nihserver.mbi.ucla.edu/Verify_3D/) that measures the compatibility of a protein model with its sequence where the values are calculated using 3D profile (Bowie *et al.*, 1991).

4.2 Results

4.2.1 Cloning and analysis of HvEC-CuZnSOD cDNA

Prior to cloning of the Hv-CuZnSOD, a number of CuZnSODs from diverse organisms were aligned. Comparative analysis of amino acid sequences of CuZnSODs from several species showed that stretches of amino acids are highly conserved among CuZnSODs (Figure 30). Also, prior observations suggest that the conserved proteins between *H. magnipapillata* and *H. vulgaris* share high sequence similarity both at the protein and nucleotide sequence levels. Therefore, a pair of primers (F and R) was designed that corresponded to the stretches of conserved amino acids (HGFHIH and DDLGKA) among several CuZnSODs (also the same conserved residues are identified in an EST encoding CuZnSOD from *H. magnipapillata*). Primers F and R were used in RT - PCR experiments to amplify a segment of Hv-CuZnSOD (Figure 31A) and the amplified cDNA product of nearly 300 base pair (bp) was subcloned and sequenced. Initial sequence analysis indicated that the presence of an open

reading frame encoding a polypeptide with a high degree of similarity to CuZnSOD of many organisms.

The full-length cDNA sequence encoding the putative Hv-CuZnSOD was cloned using the 5'-/3'-RACE method using gene specific primers designed from the above cloned segment (Table 12). The putative transcription initiation site found by 5'-RACE is located at nucleotide (nt) position 1 (Figure 32). The initiation site of translation was placed at nt 141, inferred by conceptual translation of the sequence in all three reading frames and alignment with the known sequences of CuZnSOD proteins available in the GenBank database. The putative Hv-CuZnSOD cDNA (Figure 32) is shown to contain a 567 bp open reading frame (ORF) and an in-frame TGA stop codon at the 3'-end of the coding region. The ORF is flanked by a 218 bp 3'-untranslated region followed by the putative poly(A) tail. No polyadenylation consensus sequence (5'-AATAA-3') was observed between the stop codon and the poly(A) tail.

The predicted amino acid sequence of the Hv-CuZnSOD cDNA is shown in Figure 32. The deduced protein is composed of 189 amino acid residues and the amino acid composition of the polypeptide is given in Table 13. An N-glycosylation site is predicted on residue 143 (NYSV). The theoretical isoelectric point (pI) and molecular weight (M_w) for the protein sequence is calculated to be 6.22 and 20959.73 Da, respectively.

The predicted HvEC-CuZnSOD amino acid sequence exhibited the characteristic copper zinc superoxide dismutase signature GNAGpRiACgil

TABLE 13**Amino Acid Composition of the HvEC-CuZnSOD Polypeptide**

Amino acid	Number of residues	Percent
Ala	10	5.29
Cys	3	1.59
Asp	13	6.88
Glu	9	4.76
Phe	5	2.65
Gly	22	11.64
His	8	4.23
Ile	15	7.94
Lys	12	6.35
Leu	13	6.88
Met	4	2.12
Asn	17	8.99
Pro	5	2.65
Gln	4	2.12
Arg	7	3.70
Ser	8	4.23
Thr	4	2.12
Val	18	9.52
Trp	3	1.59
Tyr	9	4.76
Total	189	100

(residues 172 – 183) of the CuZnSOD family. Seven residues known to be involved in metal binding in CuZnSODs are also found in the Hv-CuZnSOD amino acid sequence. The residues required for coordinating copper are identified as: H-80, -82, -97, and -154 and for zinc are H-97, -114, -105 and D-117 with H-97 being the common residue for coordination. The same residues are identified as H-58, -60, -75, and 132 for catalytic copper and H-75, -83, -92 and D-95 for ligand zinc in Figure 35. Also the residues responsible for oligomerization of CuZnSODs are identified by multiple sequence alignment as G-71, V-72, H-77, C-91, R-113, G-119, I-178 and C-180. The arginine residue likely involved in the positioning of the substrate (superoxide) occurs at position 177. The two cysteines believed to be form a disulfide bond are: C-91 and C-180. Hv-CuZnSOD identified so far has a putative signal peptide as analyzed by program Signal 3 and SMART analysis. Analysis of residues showed that residues 1-19 of the hydra CuZnSOD might form a signal peptide.

Identification of copper zinc superoxide dismutase signature GNAGpRiACgil (residues 172 – 183), signal peptide and the presence of the conserved metal binding residues strongly suggested that this protein is an extracellular CuZnSOD. Overall, these results suggested that the putative Hv-CuZnSOD of the *H. vulgaris* identified possessed the essential properties of an EC-CuZnSOD and can be classified accordingly.

4.2.2 Sequence conservation in EC-CuZnSOD protein

The HvEC-CuZnSOD deduced amino acid sequence was aligned by the ClustalW method with several EC-CuZnSOD and CuZn-SODs (data not shown). The absolutely conserved residues in all these sequences are (numbering based on *H. vulgaris* amino acid sequence) : G-71, H-80, H-82, C-91, H-97, N-99, P-100, H-105, H-114, G-116, D-117, N-120, L-140, G-148, V-152, H-154, D-158, D-159, L-160, G-161, S-168, G-172, A-174, G-175, R-177 and C-190. An alignment of HvEC-CuZnSOD with 6 representative CuZn-SODs is shown in Figure 30. The 189 amino acid protein deduced from the cDNA sequence gave significant scores with CuZn-SODs when compared to the protein of GenBank database using the BLAST program. Significant scores with intracellular CuZn-SODs were of *Biomphalaria glabrata*, *Lymnaea stagnalis*, *Caretta caretta*, *Cavia porcellus*, *Macaca mulatta*, *Canis familiaris*, *Mus musculus*, *Equus caballus*, etc.; whereas extracellular CuZnSODs were of *Acanthocheilonema viteae*, *Brugia pahangi*, *Lasius niger*, *Onchocerca volvulus*, etc.) (Table 14).

4.2.3 Phylogenetic analysis

In order to further characterize the putative protein sequence, the protein sequence was compared to several published CuZnSODs sequences from various organisms using the program PHYML (Guindon and Gascuel, 2003). PHYML, a traditional maximum likelihood program seeks to find the optimal topology in respect to the likelihood value and capable of optimizing model parameters (Stamatakis *et al.*, 2005), currently represents the most efficient

TABLE 14

**Similarities among *H. vulgaris* EC-CuZnSOD and (EC)-CuZnSOD Proteins
from Other Organisms^a**

Protein	% similarity to HvEC-CuZnSOD
<i>Biomphalaria glabrata</i> Cu/Zn SOD	71
<i>Lymnaea stagnalis</i> Cu/Zn SOD	72
<i>Caretta caretta</i> Cu/Zn SOD	74
<i>Cavia porcellus</i> Cu-Zn SOD	71
<i>Macaca mulatta</i> Cu-Zn SOD	73
<i>Canis familiaris</i>	71
<i>Mus musculus</i> SOD1	71
<i>Rattus norvegicus</i> Cu/Zn SOD	72
<i>Equus caballus</i> Cu/Zn SOD	69
<i>Sus scrofa</i> SOD1	68
<i>Homo sapiens</i> SOD1	69
<i>Oryctolagus cuniculus</i> Cu/Zn SOD	68
<i>Danio rerio</i> Cu/Zn SOD	67
<i>Anemonia viridis</i> Cu/Zn SOD	70
<i>Acanthocheilonema viteae</i> EC-SOD	61
<i>Saccharomyces cerevisiae</i> Cu/Zn SOD	68
<i>Crassostrea gigas</i> Cu/Zn SOD	67
<i>Brugia pahangi</i> EC-SOD	64
<i>Lasius niger</i> EC-SOD	64
<i>Onchocerca volvulus</i> EC-SOD	65

^aComparisons of amino acid sequences were made with the algorithm of NCBI BLAST

genetic algorithm for phylogenetic analysis and outperforms other recent approaches including MrBayes and MetaPIGA (Lemmon and Milinkovitch, 2002). Phylogenetic analysis showed that HvEC-CuZnSOD is grouped with extracellular CuZnSOD of mollusks (*Callinectes* and *Pacifastacus*) and nematodes (*Dirofilaria* and *Onchocerca*), the closest relationship being with the mollusks (Figure 33).

4.2.4 The structural model of HvEC-CuZnSOD

By threading analysis it was determined that the human copper zinc superoxide dismutase (PDB code: 1N18.pdb) (Cardoso *et al.*, 2002) is the best template for homologous modeling of the HvEC-CuZnSOD (target protein). As shown in Figure 34, these share a high degree of homology across their entire lengths.

The model retrieved from the 3D-JIGSAW server is shown in Figure 35. The comparative stereo-chemical analysis of the ϕ - ψ plots (Ramachandran diagram) of the model (HvEC-CuZnSOD) and structure template (1N18: A) is shown in Table 15. The analysis for crystallographic structure of the model (HvEC-CuZnSOD) present 86.1 % of residues in the most favorable, 12.9 % of residues in additional allowed regions, 1.0 % of the residues in generously allowed regions, and 0.0 % of the residues in disallowed regions, which strongly indicated that the molecular model presented here has a good overall stereo-chemical quality. A Verify-3D run on the model also showed a good stereo-chemical quality of the model (data not shown).

TABLE 15

**Comparison of the Ramachandran Plot Statistics between the Model
HvEC-CuZnSOD and the Template 1N18**

Structure	Region of the Ramachandran plot (%)			
	Most favorable	Additional allowed	Generously allowed	Disallowed
HvEC-CuZnSOD	86.0	12.9	1.0	0.0
1N18	88.8	11.2	0.0	0.0

The model generated (Figure 35) displayed a six-stranded beta sandwich (conserved β -barrel fold). The HvEC-CuZnSOD model displayed active sites having conserved metal-binding residues: H-58, H-60, H-132 (green colored residues) and H-75 for copper; and H-83, H-92, D-95 (cyan colored residue) and H-75 (red colored residue) zinc. The model also revealed structural near-identity and clear evolutionary conservation of the active-site and β -barrel fold of the hydra enzyme with the much-studied eukaryotic (E-class) intracellular CuZnSODs.

4.2.5 HvEC-CuZnSOD mRNA expression analysis

The expression patterns of the HvEC-CuZnSOD mRNA were investigated in whole organisms by reverse transcriptase-polymerase chain reaction (RT-PCR) (Figure 38, Figure 39). For reverse RT-PCR gene-specific primers were used. The results obtained demonstrate that there is considerable variation in the levels of HvEC-CuZnSOD mRNA expression in different experimental treatments. Thermal stress for 1 h at 30 and 37 °C enhanced the expression of HvEC-CuZnSOD mRNA as compared to 18 °C, the expression being highest in 30 °C; whereas, thermal stress for 6 h at 30 and 37 °C drastically reduced the expression of HvEC-CuZnSOD mRNA as compared to control at 18 °C, the lowest being at 37 °C (Figure 38, lanes 3-5). Starvation seemed to enhance the expression of HvEC-CuZnSOD mRNA both at 18 °C and 30 °C as compared to the control (Figure 38, lanes 6-7). 1 h exposure of hydrae to Zn and Cd induced the expression of HvEC-CuZnSOD mRNA where as all other treatments

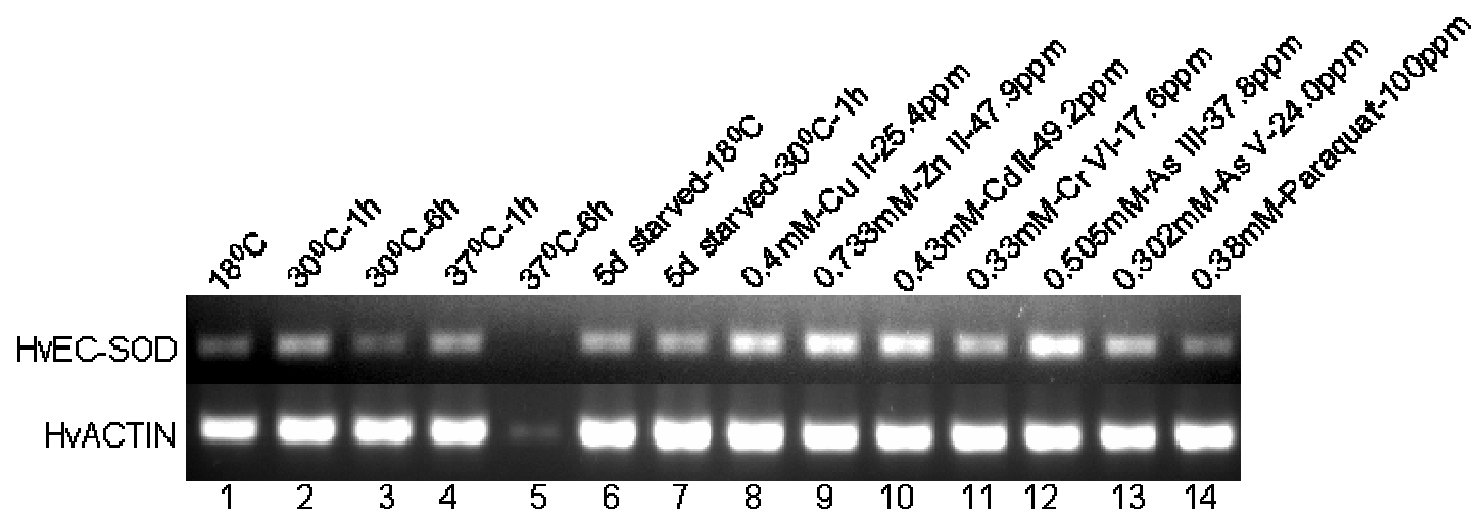


Figure 38. Expression analysis of EC-CuZnSOD mRNA from *H. vulgaris* exposed to thermal, starvation, metal and oxidative stress. The figure above represent the expression of HvEC-CuZnSOD mRNA under different stress conditions: (A) Thermal stress (lanes 2-5); (B) Starvation stress (lanes 6-7); (C) Metal stress for 6 h (lanes 8-13); and (D) Oxidative stress for 6 h (lane 14). The expression HvEC-CuZnSOD is compared to that of actin.

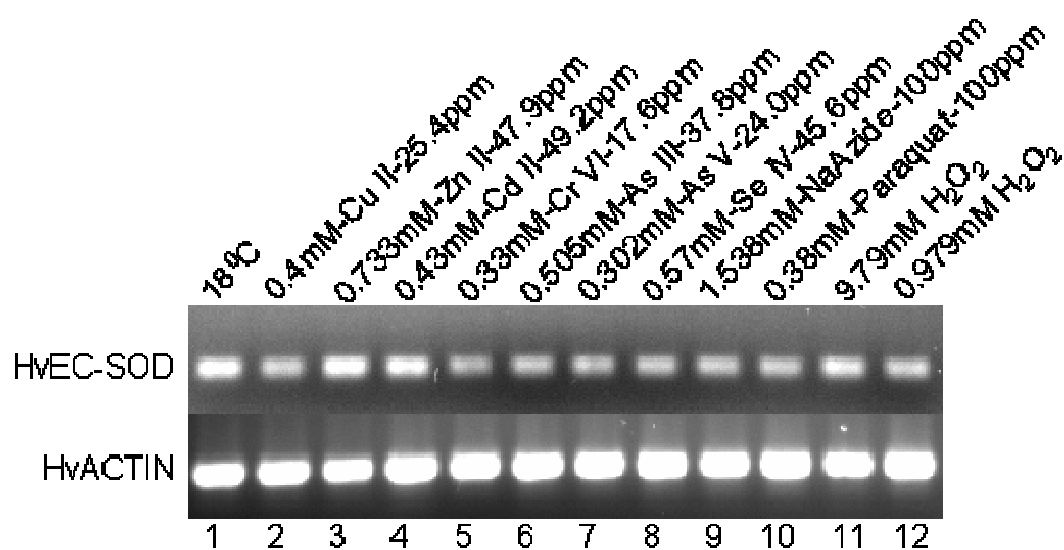


Figure 39. Expression analysis of EC-CuZnSOD mRNA from *H. vulgaris* under metal and oxidative stress for 1 h. The figures above represent the expression of HvEC-CuZnSOD under different stress conditions as described in the material and methods section: (A) Metal stress for 1 h (lanes 2-8); and (B) Oxidative stress for 1 h (lanes 1-12). The expression HvEC-CuZnSOD is compared to that of actin.

suppressed the expression of HvEC-CuZnSOD mRNA with the exception of 9.79 mM H₂O₂ treatment didn't alter the expression of HvEC-CuZnSOD mRNA. When hydrae were exposed to toxicants for 6 h (Figure 38); Cd, Cr and paraquat induced the expression of HvEC-CuZnSOD mRNA; whereas, all other treatments weren't able to perturb the expression of HvEC-CuZnSOD mRNA at the treated concentrations.

4.3 Discussion

Many gene-cloning strategies and gene surveys often provide partial sequence data. To exploit the information from these partial sequences numerous PCR-based approaches have been developed to clone full-length open reading frames (Sambrook *et al.*, 1989). These approaches can be successful using small quantities of cDNA or genomic DNA as starting material and avoid the need to go through the complex and tedious process of constructing and screening gene libraries. Here one of these approaches, called RACE (Rapid Amplification of cDNA Ends), was used to successfully clone a full-length open reading frame (ORF) of EC-CuZnCSOD from *H. vulgaris* utilizing EST information from *H. magnipapillata*. Moreover, to confirm that the cDNA and PCR cloning products are indeed from the same gene, the full-length ORF was cloned by PCR and sequenced (data not shown).

Only four CuZnSOD proteins with similar domain organization are known in cnidaria. They belong to anthozoa *Anemonia viridis* (Actiniaria) and *Alcyonium paessleri* (Alcyonacea). The sequence reported here is the first among

hydrozoans and is an extracellular CuZnSOD. The presence of copper zinc superoxide dismutase signature GNAGpRiACgil (residues 172 – 183), signal peptide and the conserved metal binding residues strongly suggested that the CuZnSOD protein reported here is an extracellular CuZnSOD. The predicted molecular mass of the HvEC-CuZnSOD monomer (about 20.9 kDa) is similar to the molecular mass of two EC-SODs from *Caenorhabditis elegans* (18.1 and 23.3 kDa) (Fujii *et al.*, 1998) and several other EC-SODs. Consequently, these data strongly suggested an extracellular localization for the HvEC-CuZnSOD. This extracellular enzyme could be released into the coelenteric cavity and/or be trapped within the mucus produced by hydra. A similar role has been suggested for EC-SOD in *A. viridis* (Plantivaux *et al.*, 2004). It could also be bound to the cell surface as found in the crustacean *Pacifastacus leniusculus* (Johansson *et al.*, 1999) or associated with the collagen present in the mesoglea, reducing its oxidative fragmentation, as demonstrated for human EC-SODs (Petersen *et al.*, 2004).

Phylogenetic analysis also showed that the hydra EC-CuZnSOD grouped with the EC-CuZnSODs from other organisms. Furthermore, HvEC-CuZnSOD did cluster with crustacean extracellular SODs with high bootstrap values in our phylogenetic analysis. Until now, EC-SODs have been identified only in platyhelminths (Hong *et al.*, 1992), nematodes (Fujii *et al.*, 1998), arthropods (Brouwer *et al.*, 2003; Johansson *et al.*, 1999) and mammals (Petersen *et al.*, 2004). Therefore HvEC-CuZnSOD would be the first EC-SOD described in

hydra (hydrozoans), an organism lacking a circulatory system or a coelom. The presence of a putative glycosylation site is another characteristic of an EC-SOD (Halliwell and Gutteridge, 1999), has also been found in HvEC-CuZnSOD sequence.

The structural model of *H. vulgaris* EC-CuZnSOD revealed structural near-identity and clear evolutionary conservation of the active-site and β -barrel fold of the hydra enzyme with the eukaryotic (E-class) intracellular CuZnSODs, exemplified in bovine, yeast, human and frog (Tainer *et al.*, 1982; Ogihara *et al.*, 1996; Parge *et al.*, 1992; Carugo *et al.*, 1994). HvEC-CuZnSOD has metal binding residues in the same sequence and structural order. The catalytic mechanism of CuZnSOD, established by numerous structural and spectroscopic studies (Getzoff *et al.*, 1983; Tainer *et al.*, 1982; Murphy *et al.*, 1997; Hart *et al.*, 1999) requires the successive reduction of tetrahedral Cu (II) to trigonal planar Cu (I) by superoxide, forming molecular oxygen, followed by re-oxidation of Cu (I) to Cu (II) by a second superoxide and $2H^+$, forming hydrogen peroxide. This transition involves the breaking and reforming of a bond from the solvent-accessible copper to the bridging histidine residue (H 75), which is also a ligand for the buried active-site zinc. The bridging histidine residue (H 75) and five additional histidine residues and one aspartate residue complete the structurally conserved active-site of hydra enzyme HvEC-CuZnSOD (Figure 35).

While few studies conducted on other organisms are available, the results observed in the current study are comparable to reported findings if a direct

relation between transcriptional activity and enzymatic activity and also similar regulatory mechanism for EC-CuZnSOD and CuZnSOD is assumed. This may not be often the case as other regulatory mechanisms such as reduced mRNA stability; translational feed back inhibition, etc. exist and are important. As observed in this study, Morales *et al.* (2004) observed in fish (*Dentex dentex*) liver that prolonged starvation (for 5 weeks) increased superoxide dismutase (SOD) activity and concluded that prolonged starvation leads to a pro-oxidant situation and oxidative stress. Downs *et al.* (2001) demonstrated that CuZnSOD activity was 2.3 times greater when the tropical coral *Montastraea faveolata* was heat-stressed than in controls. Similarly, Brown *et al.* (2002) showed a higher increase in CuZnSOD activity after a thermal stress on another tropical coral, *Goniastrea aspera*. Induction of CuZnSOD has also been observed in other invertebrates. For example, an inducible isoform of CuZnSOD from the blue mussel, *Mytilus edulis*, has been shown to be overexpressed in mussels collected in polluted sites or exposed to copper (Manduzio *et al.*, 2003). The total lack of expression of EC-CuZnSOD when exposed to 37 °C for 6 h may be due to that the biochemical machinery at the base of the oxidative stress response is compromised.

Atsushi *et al.* (2002) analyzed the expression of CuZnSOD and EC-CuZnSOD genes in 0.5 mM H₂O₂-treated *D. discoideum* cells by RT-PCR. The expression levels of CuZnSOD and EC-CuZnSOD increased (three- fold) following the treatment. Results showed that the gene for CuZnSOD

was induced by H_2O_2 exposure but not by UV irradiation, whereas gene for EC-CuZnSOD was induced both by H_2O_2 exposure and UV irradiation. Similarly, Stralin and Marklund (1994) exposed two fibroblast lines to a wide concentration range of oxidizing agents for periods of up to 4 days in order to determine the effect of oxidative stress on expression of extracellular superoxide dismutase and other SODs (EC-SOD). These agents included xanthine oxidase plus hypoxanthine, paraquat, pyrogallol, alpha-naphthoflavone, hydroquinone, catechol, Fe^{2+} ions, Cu^{2+} ions, buthionine sulfoximine, diethylmaleate, t-butyl hydroperoxide, cumene hydroperoxide, selenite, citiolone and high oxygen partial pressure (Stralin and Marklund, 1994). Under no condition was there any evidence of EC-SOD induction. Instead, the agents uniformly, dose-dependently and continuously reduced EC-SOD expression. Stralin and Marklund (1994) indicated that the effect may have been due to toxicity. Increased expression of EC-CuZnSOD in *Hydra vulgaris* under certain treatments like Zn, Cd, Cr, etc. suggests that one function of the HvEC-CuZnSOD is to shield the hydra against exogenous superoxide.

Expression of CuZnSODs is induced during environmental stress. Several regulation sites are known to induce the transcription of intracellular CuZnSODs. Indeed, metal responsive element (MRE), xenobiotic responsive element (XRE), hydrogen peroxide responsive element (HRE), and high stress element (HSE) have been found upstream the rat and human CuZnSOD genes (Chang *et al.*, 2002). AP1 and NF κ B are activated by ROS and are involved in

the upregulation of CuZnSODs (Zelko *et al.*, 2002; Legrand-Poels *et al.*, 1998). Among lower eukaryotes, Plantivaux *et al.* (2004) showed in *Anemonia viridis* that genomic flanking sequences of EC-CuZnSOD and intracellular CuZnSOD genes showed potential binding sites for transcription factors AP2 and NF κ B, suggesting that AvCuZnSOD expression would be submitted to transcriptional regulation. *Cis* elements like xenobiotic response element (XRE), metal response element (MRE) and heat shock element (HSE) were not present in their flanking regions. Also human and sea anemone intracellular CuZnSOD and EC-CuZnSOD share a homology in AA levels, though their regulatory elements are different. Both are regulated by different intrinsic factors and at different tissues in humans and anemones. Based on this evidence, further study is warranted to determine how hydra regulates its EC-CuZnSOD expression with respect to tissue specificity, regulatory elements, and both intrinsic and extrinsic stimuli. Further research should also focus on whether a CuZnSOD exist in hydra and how it would compare with its EC-form.

CHAPTER V

MOLECULAR CLONING AND CHARACTERIZATION OF A PHOSPHOLIPID HYDROPEROXIDE GLUTATHIONE PEROXIDASE FROM *HYDRA VULGARIS*

Glutathione peroxidase family consists of five isozymes. These include: (i) cellular glutathione peroxidase GSHPx-1 (Rotruck *et al.*, 1973), (ii) phospholipid hydroperoxide glutathione peroxidase PHGPx (Maiorino *et al.*, 1991), (iii) plasma glutathione peroxidase GSHPx-P (Maddipati *et al.*, 1987), (iv) gastrointestinal glutathione peroxidase, GSHPx-GI (Chu *et al.*, 1993), and (v) epididymal glutathione peroxidase GSHPx-5 (Ghyselinck and Dufaure, 1990). Among these isozymes, phospholipid hydroperoxide glutathione peroxidase (PHGPx), a selenium-dependent glutathione peroxidase (Bock *et al.*, 1991), is unique in its substrate specificity because it can interact with lipophilic substrates, including the peroxidized phospholipids and cholesterol, and reduce these hydroperoxides to hydroxide compounds (Ursini *et al.*, 1985, Thomas *et al.*, 1990). PHGPxs can be cytosolic and mitochondrial (Halliwell and Gutteridge, 1999)

Overexpression of PHGPx in a guinea pig cell line has been shown to protect cells from injury induced by lipid hydroperoxides such as dilinoleoyl phosphatidylcholine hydroperoxide and linoleic acid hydroperoxide (Yagi *et al.*, 1996). Also, mitochondrial PHGPx plays a critical role as an anti-apoptotic agent in mitochondrial death pathways (Nomura *et al.*, 1999) and may play a primary role in protecting cells from KCN-induced oxidative stress (Arai *et al.*, 1999).

Moreover, a high-level expression of PHGPx mRNA and its 12-lipoxygenase-inhibitory activity has been observed in cancer cells and endothelial cells (Huang *et al.*, 1999a; Chen *et al.*, 1997; Chen *et al.*, 2000).

Several PHGPx genes have been cloned and detected in tissues of different organisms. However, peroxidase like activity was only observed in ectodermal foot mucous cells (Hoffmeister-Ullerich *et al.*, 2002) and in lithium treated hydra (Jantzen *et al.*, 1998). Peroxidase activity is not specifically attributed to any gene products, though hydroperoxides are observed to play the role of second messengers in peroxidase activity of hydra.

In this work, the presence of a PHGPx gene was identified and isolated from *H. vulgaris* and the effects of metal and stressors exposure on its expression are studied. In addition, the phylogenetic position of hydra PHGPx (HvPHGPx) is analyzed and a suitable homology based structural model of HvPHGPx is presented to study the structural and functional evolutionary significance of the protein.

5.1 Materials and methods

5.1.1 Hydra culture

Adult *H. vulgaris* were maintained in shallow dishes at 18 °C in a medium containing 1 mM CaCl₂·2H₂O, 0.012 mM EDTA, and 0.458 mM TES (N-tris[hydroxymethyl]-methyl-2-amino-ethanesulfonic acid, sodium salt) buffer (pH 7.0). Daily, hydrae were fed with brine shrimp (*Artemia nauplii*) hatched in a solution of 1% sodium chloride treated with iodine (40 µg/ml). Hydrae were

maintained free from bacterial and fungal contamination and were not fed for 24 h before initiating the experiments. Deionized water was used throughout this portion of the study (Mayura *et al.*, 1991).

5.1.2 RNA isolation and clean up

Total RNA was extracted from hydra by application of 2 ml of TRIzol[®] reagent (Invitrogen, USA) to approximately 20 mg of fresh tissue, using the manufacturer's instructions. The RNA was quantified by ultraviolet absorbance at 260 nm. Integrity of the total RNA was confirmed by 1 % formaldehyde agarose gel electrophoresis. The RNA isolated was cleaned up from contaminating DNA using RNeasy Mini Kit (Invitrogen, USA) following the manufacturer's instruction.

5.1.3 Identification of a partial fragment of *H. magnipapillata* PHGPx cDNA

The GenBank (<http://www.ncbi.nlm.nih.gov/entrez/query.fcgi?db=nucleotide>) was searched for the cnidaria/hydra PHGPx. An expressed sequence tag (EST) was found from the hydra *H. magnipapillata* under the accession number gi|58483808 coding for a PHGPx similar to the N-terminal end of *Danio rerio* phospholipid hydroperoxide glutathione peroxidase B. The PHGPx coded by the *H. magnipapillata* EST sequence had similar conserved amino acid residues as identified by multiple sequence alignment of several PHGPxs (Figure 40). Hence a pair of primers F1 and R (Table 16) was designed from the EST

TABLE 16**Oligonucleotides Used in the Cloning of HvPHGPx Gene**

Oligonucleotide	Sequence
F	5'-ATGGCTGCATCAGACCCTAC-3'
F1	5'-TTTCCTTGTAATCAGTTTG-3'
R	5'-CTTTGAAAAATTCCATTTG-3'
R1	5'-TCATGCTTGACCGTTCATTG-3'
R2	5'-GAGGCGCCCACTATGACTTA-3'
AF	5'-AAGCTCTTCCCTCGAAGAATC-3'
AR	5'-CCAAAATAGATCCTCCGATCC-3'
N	5'-AACTGGAAGAATTCGCGGCCGCAGGAAd(T) ₁₈ -3'
AP ₂	5'-GATCAGGACGTTTCGTTTGAGd(T) ₁₇ -3'

sequence that corresponded to conserved amino acid residues FPCNQFG and KWNFSK to clone a fragment of phospholipid hydroperoxide glutathione peroxidase from *H. vulgaris*.

5.1.4 Oligonucleotides

All oligonucleotides were procured from IDT Inc. (IA, USA). AP₂ primer (5'-GATCAGGACGTTCGTTTGAGd(T)₁₇-3') was used for 5'-RACE (Rapid Amplification of cDNA Ends) experiments. The oligo(dT) bifunctional primer N (Not I-d(T)₁₈: 5'-AACTGGAAGAATTCGCGGCCGCAGGAAd(T)₁₈-3') was supplied in a cDNA preparation kit (Amersham Biosciences, USA) and was used for 3'-RACE experiments. *H. vulgaris* gene specific used in the experiments are also given in Table 16.

5.1.5 Cloning and identification of a partial fragment of *H. vulgaris* PHGPx cDNA

All polymerase chain reaction (RT-PCR and RACE-PCR) experiments were performed using *Taq* DNA polymerase (Invitrogen, USA) and a thermal cycler (MJ Research, USA).

RNA (5 µg) was reverse-transcribed to cDNA at 37 °C for 60 min using the oligo(dT) bifunctional primer N and the AMV RT supplied in the cDNA synthesis kit (Amersham Biosciences, USA). The first-strand cDNA was amplified using the primers F1 and R (Table 16). The PCR was performed for 30 cycles, consisting of 94 °C for 30 s, 50 °C for 30 s and 72 °C for 1 min and a final extension at 72 °C for 10 min. The resultant PCR products (Figure 41A) was

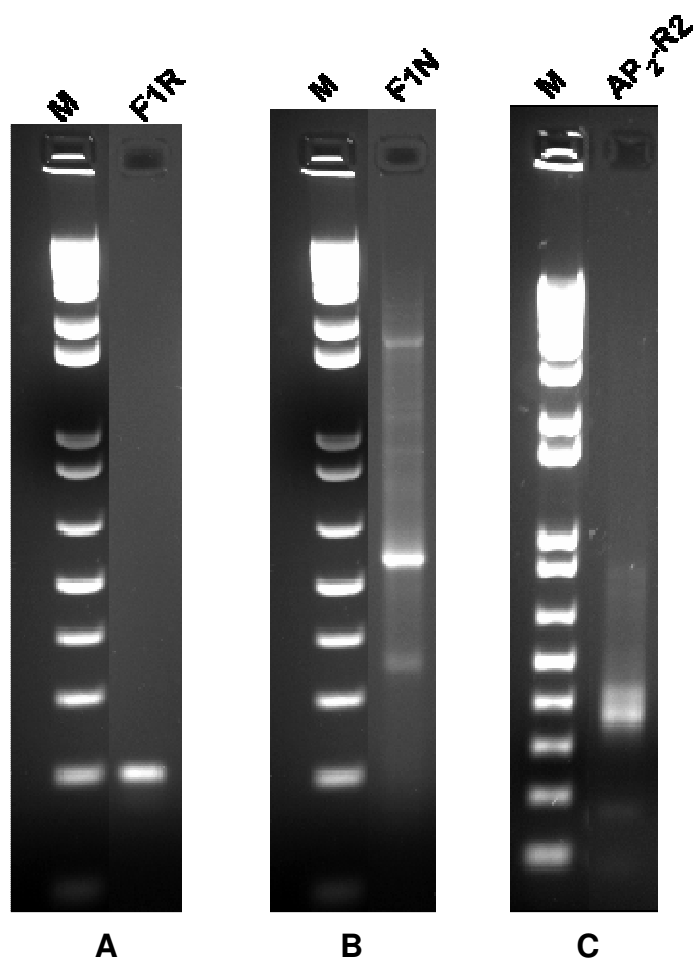


Figure 41. Images of electrophoretic gels for PCR products of HvPHGPx gene. (A) The PCR products were produced using primer F1 and R. (B) The 3'-RACE PCR products were produced using with primer F1 and N (=Not *I*-d(T)₁₈). (C) The 5'-RACE PCR products were produced using with primer AP₂ and R2. M = 1 kb plus DNA ladder.

subcloned into the pCR®II-TOPO® vector using a TA cloning kit (Invitrogen, CA, USA). Multiple independent clones were sequenced using automated methods (DNA Technologies Lab, Department of Veterinary Pathobiology, Texas A&M University) on an ABI PRISM™ 310 Genetic Analyzer (PE Biosystems, USA) using a Big-Dye sequencing kit (PE Biosystems) and M13 primers. The identity of the clones was evaluated by matching the sequences to the nucleotide/protein sequences available at the GenBank. The cloned sequence constituted residues 234 to 432 in the nucleotide sequence shown in Figure 42A.

5.1.6 3'-RACE of the HvPHGPx cDNA

First-strand cDNA prepared above was amplified using the oligo(dT) bifunctional primer N and a gene-specific primer F1 (Table 16) (complementary to nucleotide (nt) 283 to 301, Figure 42) for 35 cycles of 94 °C for 30 s, 55 °C for 30 s and 72 °C for 3 min. The PCR products (Figure 5.2B) were subcloned and sequenced as described above. The identity of the clones was evaluated by matching the sequences to the nucleotide/protein sequences available at the GenBank (<http://www.ncbi.nlm.nih.gov/>).

5.1.7 5'-RACE of the HvPHGPx cDNA

The template cDNA was synthesized using a primer R1 (Table 40) (complementary to nucleotide (nt) 556 to 675, Figure 42A) and Superscript II (Invitrogen, USA), followed by dA tailing of the cDNA using dATP and terminal transferase (Invitrogen, USA) using standard procedures (Sambrook *et al.*, 1989). The first strand cDNA was amplified using an oligo(dT) anchor primer

```

1      M A A S D P T K A S S I
1  gatcatataaaatttagcgtaataatggctgcatcagaccctacaaaagcttcttctata 60
13 F E F Q A K S I D G E D I S L S K Y K G
61 tttgaatttcaagcaaaaagtatatagatgggtgaagatatcagtccttcaaaatataaagg 120
33 F V T L I V N V A S K U G L T E L N Y A
121 tttgttacacttattgttaacgtggccagcaagtggaggtttaactgaactcaactatgct 180
53 Q L A D L H T K Y A E K G L R I L A F P
181 cagcttgctgatctgcacaccaagtatgctgagaaaggctcttcgaattcttgcttttcct 240
73 C N Q F G N Q E P G T D L E I K E F A L
241 tgtaatcagtttggttaaccaagagcctggtagacagatttagaaataaaagagtttgctta 300
93 A R G A H Y D L F S K I D V N G D K A D
301 gcgcgaggcgcccactatgacttattcagtaaaattgatgttaatggagataaggcagat 360
113 P L Y K Y L K S K Q K G I F G N K I K W
361 cctctgtataaatatattgaaatcaaagcagaaaggatatttttggtaataaaatcaaagg 420
133 N F S K F I C D K N G I P V K R Y A P T
421 aatttttcaaagtttattgtgataaaaacggtatccctgttaaaagatacgctcctaca 480
153 T E P L S L V P D I E K Y L C Q *
481 acagaacctttgtcattgggtccagatatcgaaaagtatttatgccaataacattttgtg 540
541 aaagacagataagaacaatctattgctttaatttttctctttattgtctttttatctata 600
601 aaaaaactttttataataatttttccatttttcttatgattgtttgtctgtaactcaatg 660
661 aacggtcaagcatgatgatgtttttatattgtgcagatgtaaaaaaatggattgtggaa 720
721 ataatttttatgattcttt 739

```

(A)

```

1  CCAAGTAGTTCACCTTGGTCAAATAGGTTACTTTACGCTTTAACTTTTCTTAAATATTTA 60
61  GTTTTAATGGTTAAGTTTTATTTATCAATATTTAGCTTTTATTAAAATTCTAAAAATTCT 120
121 GTTTTATTTTTGAAAAGGTGATGTATTTAATTATTCCTTATTGTAAAATAACTATTATTT 180
181 TT 182

```

(B-i)

```

1  GTTTTCGTTCTCACTCTTTCTTTCTTAACTGACGGATAAACATTAAGAAACAAACTTCTA 60
61  TTTTCTTAATAA 72

```

(B-ii)

```

1  ATTTGCACTCTTTTCGATTTTACTTTATTTAGCGGATTTTTAAAATCGTGATTTTTAAAAA 60
61  AGAAATAGTAAAAATTCAACCGTTTTTACCTTAAAAAAAAAAAAAAAAAAAAAAAAAAAA 120
121 AAAAAA 126

```

(C-i)

```

1  AAAAAAAAAAAAAAAAAAAAAAAAAAAAAAAAAAAAAAAAAAAAAAAAAAAAAA 45

```

(C-ii)

Figure 42. Nucleotide and deduced amino acid sequence of *H. vulgaris* PHGPx cDNA. (A) The deduced amino acid sequence is shown in single-letter code above the nucleotide sequence. The nucleotide and amino acid sequences are numbered from the 5'-end of the 739 bp cDNA sequence, and from the N-terminal start codon methionine, respectively. The selenocysteine residue is shown as U in bold face. The polyadenylation signal is underlined. The asterisk denotes the translation stop signal. (B-i and B-ii) The two alternative 5'-end of the PHGPx cDNA. (C-i and C-ii) The two alternative 3'-end of the PHGPx cDNA.

AP₂ (5'-GATCAGGACGTTCGTTTGAG-d(T)₁₇-3') and the gene-specific primer R1, and the first-round PCR products were reamplified using the PCR anchor primer AP₂ and another gene-specific primer R2 (Table 16) (complementary to nt 255 to 275, Figure 42A). Each PCR was performed with an initial amplification of 95 °C for 5 min, 48 °C for 5 min and 72 °C for 5 min followed by 20 cycles of 95 °C for 40 s, 48 °C for 1 min and 72 °C for 3 min with a final extension of 10 min at 72 °C. The PCR products (Figure 41C) were subcloned and sequenced as described above. The identity of the clones was confirmed by matching the sequences to the nucleotide/protein sequences available at the GenBank (<http://www.ncbi.nlm.nih.gov/>).

5.1.8 Determination of the exon/intron structure of the HvPHGPx gene

The genomic DNA of hydra was extracted using DNeasy Tissue Kit (QIAGEN, USA) according to the manufacturer's instructions and the PHGPx gene was amplified using the genomic PCR with the *Taq* DNA polymerase (Invitrogen). The genomic PCRs were performed using following primer combinations: primer F complementary to nt 25-44 (Figure 42A) and a primer R1 complementary to nt 613-634 (Figure 42A).

All the above reaction mixtures (50 µl) contained 200 ng of genomic DNA template, 10 pmol of each oligonucleotide primer, a 10 mM concentration of each dNTP, and 2.5 U of *Taq* DNA polymerase (Invitrogen, USA). PCR amplification preceded by a 5 min denaturation step at 94 °C proceeded through 30 cycles of denaturation (94 °C, 1 min), annealing (55 °C, 1 min), and

polymerization (72 °C, 3 min) and a 10 min elongation step at 72 °C. The amplified products were subcloned to a pCR®II-TOPO® vector using a TA cloning kit (Invitrogen, CA, USA) according to the manufacturer's instructions and sequenced as described above. The identity of the clones was confirmed as stated above.

5.1.9 Heat treatment

Animals were incubated at 18 (control temperature), 30 and 37 (maximum induction temperature) °C for 1 h and 6 h in 5 ml hydra media. Also 5 day starved animals were exposed to 30 °C in 5 ml hydra media.

5.1.10 Metal treatment

Nearly 500 Hydrae were incubated at 100 ppm of CuSO₄.5H₂O, ZnCl₂, CdCl₂.2.5H₂O, K₂Cr₂O₇, As₂O₃, Na₂HAsO₄ and Na₂SeO₃ for 1 h and 6-h in 5 ml hydra media. Hence the concentration of Cu (II), Zn (II), Cd (II), Cr (VI), As (III), As (V), and Se (IV) (active ingredients) were 0.4 mM (= 25.4 ppm), 0.73 mM (= 47.9 ppm), 0.43 mM (= 49.2 ppm), 0.33 mM (=17.6 ppm), 0.506 mM (= 37.8 ppm), 0.302 mM (= 24.0), and 0.57 mM (= 45.6 ppm), respectively.

5.1.11 Oxidative stress treatment

Nearly 500 hydrae were incubated at 300 ppm (=9.79 mM) and 30 ppm (= 0.979 mM) of H₂O₂ and 100 ppm (= 0.38mM) of paraquat in 5 ml hydra media. Also hydrae were exposed to 100 ppm sodium azide (= 1.538 mM) in 5 ml hydra media.

In all cases, treatments were carried out in 14 ml polypropylene round-bottom tubes (Becton-Dickinson, NJ, USA) containing 5 ml hydra media. At the end of the treatment, hydrae were collected by centrifugation at 7,500 Xg for 5 min. The supernatants were discarded. Then hydrae were washed once in 5 ml of 0.05 M PBS for 5 min @ 7,500 Xg. The supernatants were discarded as before and the animals were homogenized immediately in 3 ml of TRIzol[®].

5.1.12 Expression analysis of HvPHGPx mRNA in hydrae

Total RNA was extracted from TRIzol[®] (Invitrogen, USA) treated whole hydrae and cleaned as before using RNeasy Mini Kit (Invitrogen, USA) following the procedure described there in. For RT-PCR, 5 µg of total cleaned RNA was reverse transcribed using 500 ng of oligo(dT)₁₂₋₁₈ primer (Invitrogen, USA) and 200 units of the Superscript II enzyme (Invitrogen, USA) for 50 min at 42 °C. The reaction was inactivated by heating the mixture at 70 °C for 15 min. PCR assays were designed to normalize HvPHGPx gene expression levels to actin transcription rate. Two µl of first strand cDNA (from 25 µl of reverse transcription mix) was diluted 100 times prior to PCR amplification. PCR was carried out in 50 µl total volume of 1 × PCR buffer (20 mM Tris-HCl, pH 8.4, 50 mM KCl), 2 mM MgCl₂, 0.1 mM each of dNTPs, 10 pmol each of primers, and 0.5 U *Taq* DNA polymerase (Invitrogen, USA) using 2 µl of (1:100) diluted RT-product. Actin mRNA was amplified using the AF and AR primers and the PHGPx mRNA was amplified using the F1 and R primers. Cycling profile after initial denaturation at 94 °C for 4 min was 30 cycles of amplification as follows:

denaturation at 94 °C for 30 s, annealing at 55 °C for 30 s, and extension at 72°C for 45 s. These number of PCR cycles ensured quantification within the exponential phase of amplification. Equal amounts of RT-PCR reactions (9.5 µl) were loaded on standardized 2 % agarose gels containing 0.1 µg/ml ethidium bromide. The gel images were digitalized by a gel documentation system (Kodak Laboratories, USA).

5.1.13 General bioinformatic analyses

Conceptual translation of the full-length cDNA was performed using the program SIXFRAME (<http://biologyworkbench.ucsd.edu>). Homology to other PHGPx gene and proteins were identified by using the Blast program with default settings (<http://www.ncbi.nlm.nih.gov/BLAST>). The identification of HvPHGPx domains were performed by use of the SMART program (<http://smart.embl-heidelberg.de/>) using default pattern definitions. Prosite (<http://us.expasy.org/prosite/>) identification of glycosylation, phosphorylation, myristilation and amidation sites was performed by use of the ExPASy program using default settings. The isoelectric point (pI) and the molecular weight (M_w) of the HvPHGPx protein were calculated using the ExPasy (http://us.expasy.org/tools/pi_tool.html) program. Several glutathione peroxidase (GPx) domain-containing sequences retrieved from the National Center for Biotechnology Information (NCBI) Entrez Web service (<http://www.ncbi.nlm.nih.gov/Entrez/>) were aligned to each other using the web program T-coffe (http://igs-server.cnrs-mrs.fr/Tcoffee/tcoffee_cgi/index.cgi),

ClustalW (<http://www.ch.embnet.org/software/ClustalW.html>), or the ClustalW program embedded in Mega (<http://www.megasoftware.net/>).

5.1.14 Phylogenetics

For phylogenetic analysis sequences were aligned using the ClustalW program embedded in the program Mega 3.1 (<http://www.megasoftware.net/>). The aligned sequences were converted into the “Phylip|Phylip44” format (Felsenstein, 1993) using the Readseq program (<http://iubio.bio.indiana.edu/cgi-bin/readseq.cgi>) and saved as a text file. The text file in the interleaved format was uploaded to the PHYML Online (<http://atgc.lirmm.fr/phyml/online.html>) web interface (Guindon and Gascuel, 2003). Following parameters were chosen for the construction of the tree: substitution model - JTT; number of bootstrap data sets - 500, proportion of invariable sites - 0 and fixed; number of substitution rate categories - 1; starting tree(s) - BIONJ; optimize topology - yes; optimize branch lengths and rate parameters -yes. Nonparametric bootstrap (Felsenstein, 1985) was applied to assess the reliability of internal branches for (large) datasets. The tree generated in the NEWICK format was displayed using the Drawtree program (<http://www.phylodiversity.net/~rick/drawtree/>) (Figure 43)

The accession numbers of protein sequences used for phylogenetic analysis are: gi|48374968 (GPx *Sorghum bicolor*), gi|484374 (PHGPx *Sus scrofa*), gi|21617919 (PHGPx *Arabidopsis thaliana*), gi|71003492 (GPx *Bombyx mori*), gi|48374955 (GPx *Zea mays*), gi|44663004 (PHGPx *Setaria*

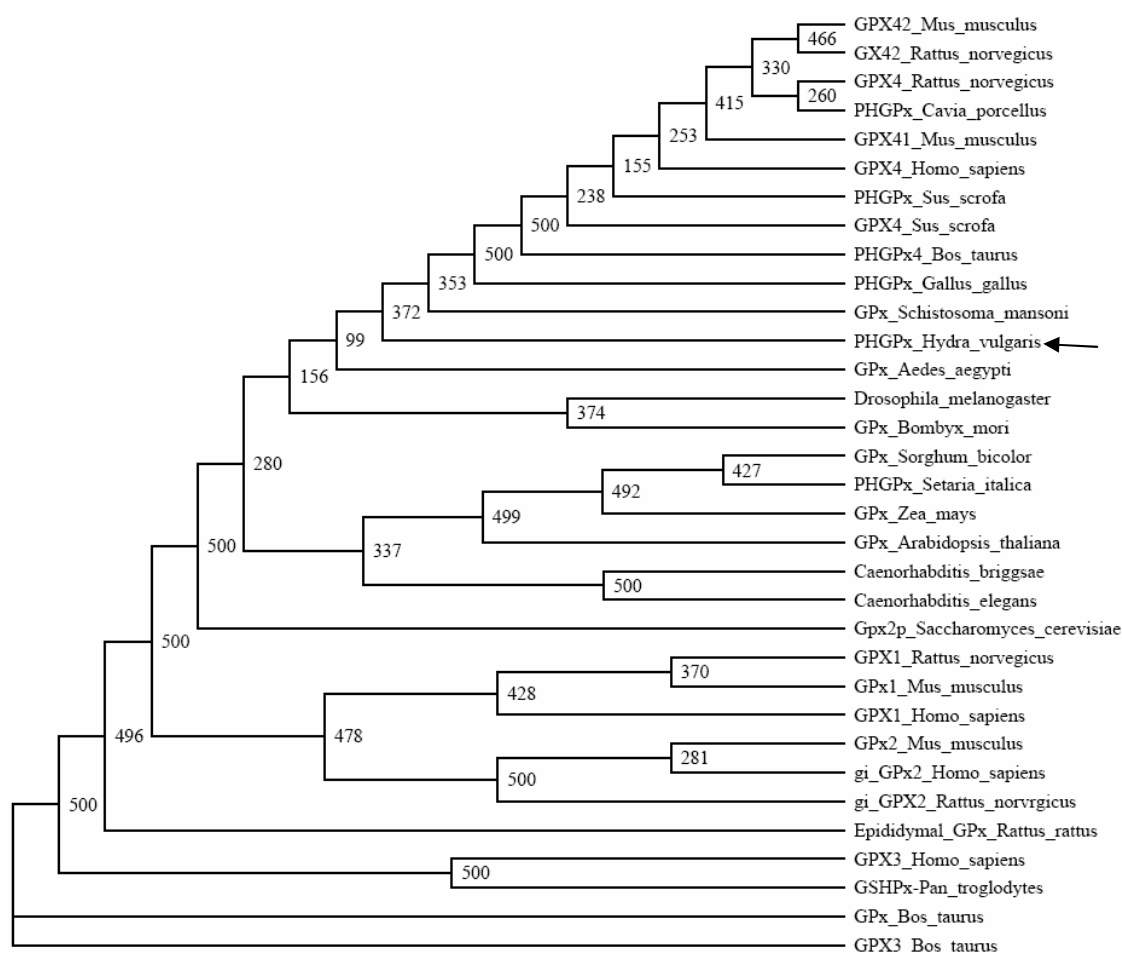


Figure 43. Phylogenetic alignment of the amino acid sequences of the glutathione peroxidases from different organisms. The tree was constructed by the maximum likelihood method using the program PHYML (Guindon and Gascuel, 2003). Bootstrap confidence values for the sequence groupings are indicated in the tree ($n = 500$). The *H. vulgaris* PHGPx (arrow marked) is grouped with other PHGPxs.

italica), gi|51316102 (PHGPx = GPx-4 *Bos taurus*), gi|32187521 (GPx-4 *Homo sapiens*), gi|45383680 (GPx-4 *Gallus gallus*), gi|47523868 (GPx-4 *Sus scrofa*), gi|31076717 (GPx42 *Mus musculus*), gi|13124257 (GPx41 *Mus musculus*), gi|27807491 (GPx-4 *Bos taurus*), gi|23092914 (*Drosophila melanogaster*), gi|31076659 (GX42_RAT), gi|2522259 (PHGPx *Mus musculus*), gi|15011854 (GPx 4 *Rattus norvegicus*), gi|7023973 (PHGPx *Cavia porcellus*), gi|39591382 (*Caenorhabditis briggsae*), gi|3878898 (*Caenorhabditis elegans*), gi|6319721 (GPx2p *Saccharomyces cerevisiae*), gi|47115524 (GPx2 Rat), gi|121672 (GPx3 Human), gi|121665 (GPx1 Human), gi|32967607 (GPx2 *Homo sapiens*), gi|27806593 (plasma-GPx3 *Bos taurus*).

5.1.15 Threading

Five web-available threading methods used to find the structure templates for the HvPHGPx domain were as follows: TOPITS (http://dodo.cpmc.columbia.edu/predict_protein/); HMM (<http://www.cse.ucsc.edu/research/compbio/HMM-apps/HMM-applications.html>); 3D-JIGSAW (<http://www.bmm.icnet.uk/~3djigsaw/>); 3D-PSSM (<http://www.sbg.bio.ic.ac.uk/~3dpssm/>); and HFR (<http://www.cs.bgu.ac.il/~bioinbgu/>). TOPITS (Rost, 1995) and 3D-PSSM (Kelley *et al.*, 2000) are methods based on matching the predicted secondary structure and solvent accessibility or solvation potentials of the query sequence with those of the proteins of known structures. HFR (Fischer, 2000) is a hybrid method that combines results from five threading programs to search the most consistent fold prediction among them. HMM

(Karplus *et al.*, 1998) uses a hidden Markov model (HMM) engine to compare the query sequence with sequences of known protein structures to derive a possible structure class for the query one. The 3D-JIGSAW (Bates *et al.*, 2001) Web server builds automatic 3D models for proteins based on homologs of known structures. Protein 1E2Y (1E2Y.pdb) (Alphey *et al.*, 2000) was automatically selected as the structure template for the query sequence HvPHGPx and a model was retrieved (Figure 44).

5.1.16 Analysis of the model

The overall stereo-chemical quality of the final model was assessed by the program PROCHECK (<http://biotech.ebi.ac.uk:8400/cgi-bin/sendquery>) (Laskowski *et al.*, 1994). A secondary structure (Figure 45) of the model was drawn. Ramachandran plot statistics of the model was also calculated (Table 17). The structural quality of the model was also verified using the program Verify-3D (http://nihserver.mbi.ucla.edu/Verify_3D/) that measures the compatibility of a protein model with its sequence where the values are calculated using 3D profile (Bowie *et al.*, 1991).

5.2 Results

5.2.1 Cloning and analysis of HvPHGPx cDNA

Prior to cloning of the HvPHGPx cDNA a number of PHGPxs from diverse organisms were aligned. Comparative analysis of amino acid sequences of PHGPxs from several species showed that stretches of amino acids are highly conserved among them (Figure 40). Also, it is noted that the conserved

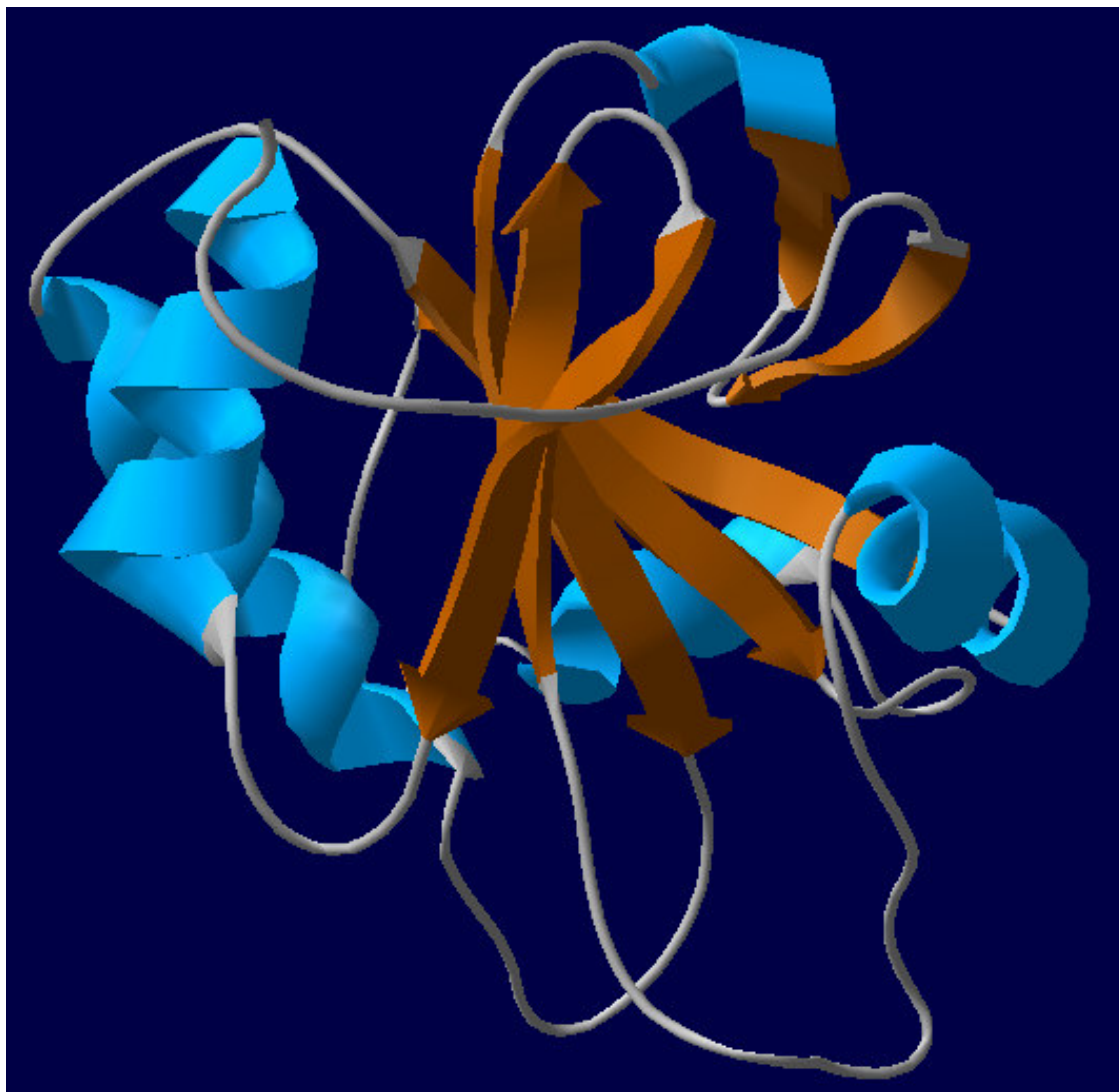


Figure 44. A 3D model of *H. vulgaris* PHGPx. HvPHGPx was modeled on the published crystal structure of parasitic trypanosomatid *Crithidia fasciculata* tryparedoxin peroxidase (TryP) (1E2Y.pdb) (Alphey *et al.*, 2000). The central β five-stranded structure together with two parallel α helices resembled the thioredoxin fold. The model was displayed using Swiss-Pdb Viewer.

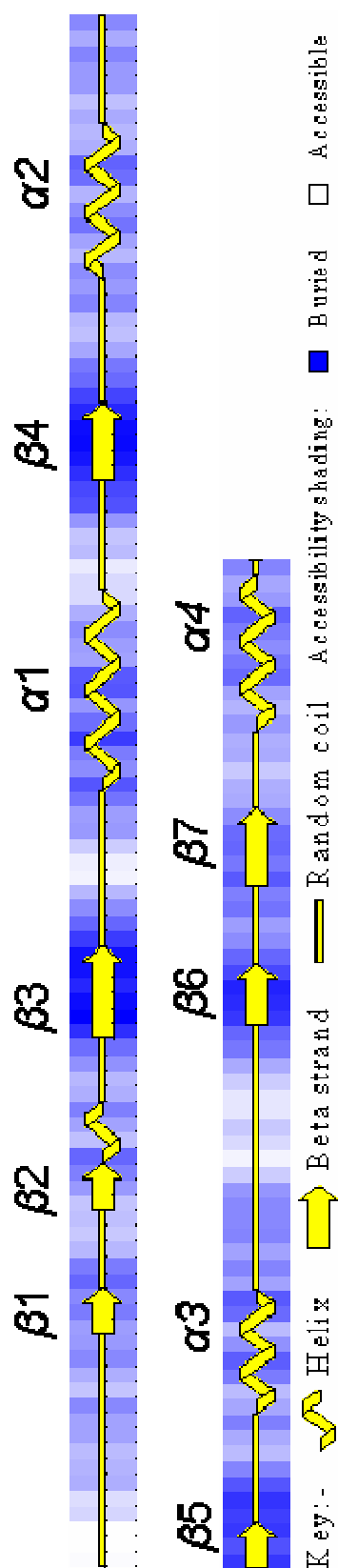


Figure 45. The secondary structural elements of the HvPHGPx model. The key to the linear representation of the structural elements is given below the drawing. Structural elements are highlighted using the program PROCHECK (<http://biotech.ebi.ac.uk:8400/cgi-bin/sendquery>).

TABLE 17**Ramachandran Plot Statistics of the 3D Model of HvPHGPx**

Structure	Region of the Ramachandran plot (%)			
	Most favorable	Additional allowed	Generously allowed	Disallowed
HvPHGPx	73.6	18.1	6.2	2.1

proteins between *H. magnipapillata* and *H. vulgaris* share high sequence similarities both at the protein and nucleotide sequence levels. Thus, a pair of primers (F1 and R), was designed that corresponded to the stretches of conserved amino acids sequences: FPCNQFG and KWNFSK (also conserved in the phospholipid hydroperoxide glutathione peroxidase encoded by an EST of *H. magnipapillata*). Primers F1 and R were used in RT - PCR experiments to amplify a segment of HvPHGPx (Figure 41A) and the amplified cDNA product of nearly 200 base pair (bp) was subcloned and sequenced. Initial sequence analysis indicated that the presence of an open reading frame encoding a polypeptide with a high degree of similarity to glutathione peroxidase (GPx) of many organisms.

The 3'- and 5'-end of the cDNA was cloned using 3'-RACE and 5'-RACE experiments respectively using gene specific primers (Table 16). 3'-RACE yielded two different sequences; one sequence (Figure 42C-i) was longer than the other (Figure 42C-ii) by 92 nucleotides before ending with a poly(A) tail. Similarly 5'-RACE yielded two different sequences that are completely different in their 5' non-translated regions (Figure 42B-i and 42B-ii). The nucleotide sequence that spanned from both 5'- and 3'-end and was common to both the 5'- and 3'-RACE products comprises of 739 nucleotides (Figure 42A). This nucleotide sequence harbored the open reading frame of 504 nucleotides that coded for a 168 amino acid polypeptide. This was inferred by conceptual translation of the sequence in all three reading frames and alignment with the

known sequences of PHGPx proteins available in the GenBank database. Two polyadenylation consensus sequence (5' AATAA 3') was observed in this nucleotide sequence are underlined (Figure 42A).

The deduced protein is composed of 168 amino acid residues and the amino acid composition of the polypeptide is given in Table 18. The theoretical iso-electric point (pI) and molecular weight (Mr) for the protein sequence is calculated to be 8.53 and 18746.51 Da, respectively. The predicted HvPHGPx amino acid sequence exhibited characteristic glutathione peroxidase signature residues LAFPCNQF (residues 69 – 76). HvPHGPx contained one selenocysteine residue (residue 44) identified as U in Figure 42A. Residues constituting the catalytic triad (U-44, Q-79, and W-132) are also conserved in HvPHGPx.

5.2.2 Exon/intron structure of the HvPHGPx Gene

The exon/intron structure of the HvPHGPx coding sequence was determined by genomic PCR as described in the materials and methods section. The HvPHGPx coding sequence was found not to be interrupted any introns.

5.2.3 Sequence conservation in PHGPx proteins

The HvPHGPx deduced amino acid sequence was aligned by the ClustalW method with several glutathione peroxidases (data not shown). The absolutely conserved residues in all these sequences are (numbering based on *H. vulgaris* amino acid sequence) : G-32, N-39, A-41, G-45, T-47, L-69, F-71, P-72, C-73, N-74, Q-75, F-76, V-106, N-107, G-108, W-132, N-133, F-134, K-

TABLE 18**Composition of the HvPHGPx Polypeptide**

Amino acid	Number of residues	Percent
Ala	14	8.33
Cys	4	2.38
Asp	11	6.55
Glu	9	5.36
Phe	10	5.95
Gly	11	6.55
His	1	0.60
Ile	12	7.14
Lys	20	11.90
Leu	17	10.12
Met	1	0.60
Asn	8	4.76
Pro	8	4.76
Gln	6	3.57
Arg	3	1.79
Ser	11	6.55
Thr	7	4.17
Val	6	3.57
Trp	1	0.60
Tyr	8	4.76
Total	219	100

136, F-137, G-143 and R-148. An alignment of HvPHGPx with 12 representative PHGPx is shown in Figure 40. The 168 amino acid protein deduced from the cDNA sequence when compared to the protein of GenBank databases using the program BLAST gave significant scores with *Homo sapiens* GPx-4, *Danio rerio* PHGPx-B, *Sus scrofa domestica* PHGPx (GPx-4), *Arabidopsis thaliana* PHGPx, *Bombyx mori* GPx, *Bos taurus* PHGPx (GPx-4), *Hordeum vulgare* GPx12Hv, *Gallus gallus* PHGPx, *Mus musculus* GPx-4, *Rattus norvegicus* GPx-4, *Cavia porcellus* PHGPx, *Schistosoma mansoni* GPx-2, *Caenorhabditis briggsae*, *Saccharomyces cerevisiae* GPx2, etc. (Table 19).

5.2.4 Phylogenetic analysis

In order to further characterize the putative protein sequence, the protein sequence was compared to several published glutathione peroxidase (GPx) sequences from various organisms using the program PHYML. PHYML (Guindon and Gascuel, 2003), a traditional maximum likelihood program seeks to find the optimal topology in respect to the likelihood value and is capable of optimizing model parameters (Stamatakis *et al.*, 2005). PHYML currently represents the most efficient genetic algorithm for phylogenetic analysis and is very fast and outperforms other recent approaches including MrBayes and MetaPIGA (Lemmon and Milinkovitch, 2002). Phylogenetic analysis showed that HvPHGPx is grouped with PHGPx of *M. musculus*, *R. norvegicus*, *C. porcellus*, *H. sapiens*, *S. scrofa*, *B. Taurus*, *G. gallus*, etc (Figure 43).

TABLE 19

Similarities among *H. vulgaris* PHGPx and GPx Proteins from Other Organisms^a

Protein	% similarity to HvPHGPx
<i>Homo sapiens</i> GPx-4	72
<i>Danio rerio</i> PHGPx-B	71
<i>Sus scrofa domestica</i> PHGPx	72
<i>Arabidopsis thaliana</i> PHGPx	71
<i>Bombyx mori</i> GPx	71
<i>Bos taurus</i> PHGPx	72
<i>Hordeum vulgare</i> GPx12Hv	71
<i>Gallus gallus</i> PHGPx	71
<i>Mus musculus</i> GPx-4	71
<i>Rattus norvegicus</i> GPx-4	71
<i>Cavia porcellus</i> PHGPx	70
<i>Schistosoma mansoni</i> GPx-2	65
<i>Caenorhabditis briggsae</i>	66
<i>Saccharomyces cerevisiae</i> GPx2	63

^aComparisons of amino acid sequences were made with the algorithm of NCBI BLAST

5.2.5 The structural model of HvPHGPx

By threading analysis it was found that the parasitic trypanosomatid *Crithidia fasciculata* tryparedoxin peroxidase 1E2Y (1E2Y.pdb) (Alphey *et al.*, 2000) is the best template for homologous modeling of the HvPHGPx (target protein). The model retrieved from the 3D-JIGSAW server is shown in Figure 44. The stereo-chemical analysis of the ϕ - ψ plots (Ramachandran diagram) of the model (HvPHGPx) is shown in Table 17. The analysis of the structure of the model (HvPHGPx) present 73.6 % of residues in the most favorable, 18.1 % of residues in additional allowed regions, 6.2 % of the residues in generously allowed regions, and 2.1 % of the residues (3 residues) in disallowed regions, which indicated that the molecular model presented here has a good overall stereo-chemical quality. A Verify-3D run on the model also showed an acceptable stereo-chemical quality of the model (data not shown).

The model (monomer) consisted of a single polypeptide chain of 165 amino acid residues and constructed around a seven-stranded twisted β -sheet with parallel and anti-parallel alignments (Figure 44). The sheet is surrounded by four α -helices of varying length. An extended structure at the N terminus leads into a β -hairpin (β 1 and β 2), followed by a section of α -helix then two $\beta\alpha\beta$ units (β 3- α 1- β 4- α 2- β 5) (Figure 45). The central β five-stranded structure together with two parallel α helices resembled the thioredoxin fold. The active site residues (C-44, Q-79 and W-132) of HvPHGPx model are located in flat depressions on the molecular surface. Hence the active site of HvPHGPx model also can be

assumed to be located on the molecular surface. The catalytically active selenocysteine was found at the N-terminal end of long α -helix and are surrounded by an accumulation of aromatic side-chains.

5.2.6 HvPHGPx mRNA expression analysis

To examine the level of PHGPx transcripts in *H. vulgaris* before and after stressor exposure, the expression patterns of the HvPHGPx mRNA were investigated in whole organisms by reverse transcriptase-polymerase chain reaction (RT-PCR) (Figure 46 and Figure 47). For RT-PCR experiments, gene-specific primers were used. The results obtained demonstrate that there is considerable variation in the levels of HvPHGPx mRNA expression following different experimental treatments, though transcription of actin DNA was almost constant before and after exposure to stressor. Thermal stress for 1 h at 30 and 37 °C (Figure 46, lane 2 and 4) enhanced the expression of HvPHGPx mRNA as compared to 18 °C (control) (Figure 46, lane 1). However, thermal stress for 6 h at 30 °C did not affect the expression of HvPHGPx mRNA as compared to control at 18 °C. In contrast, the expression of the HvPHGPx mRNA was drastically reduced when hydrae were exposed to thermal stress at 37 °C for 6h (Figure 46, lane 5). Hydrae starved for 5 days showed enhanced expression of PHGPx mRNA both at 18 °C and 30 °C as compared to the to the control maintained at 18 °C (unfed for 2 days). One hour exposure of hydrae to 1.538 mM sodium azide, 0.38 mM paraquat and 9.79 mM H₂O₂ (Figure 47, lanes 9, 10 and

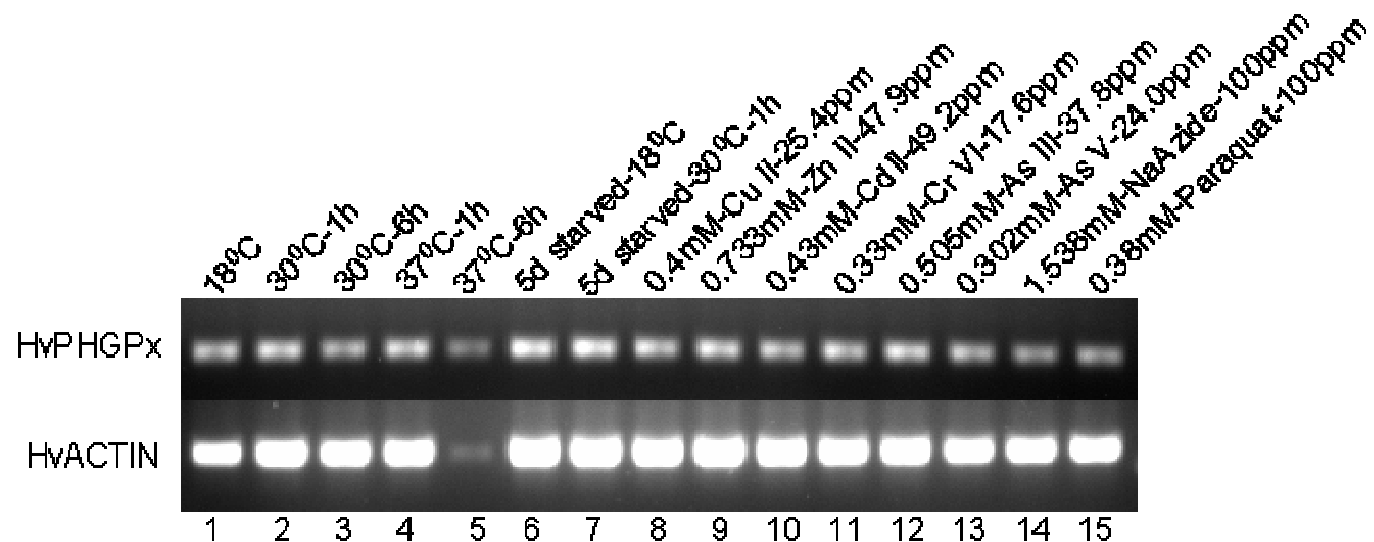


Figure 46. Expression analysis of PHGPx mRNA from *H. vulgaris* exposed to thermal, starvation, metal and oxidative stress. The figure above represents the expression of HvPHGPx mRNA under different stress conditions as described in the material and methods section: (A) Thermal stress (lanes 2-5); (B) Starvation stress (lanes 6-7); (D) Metal stress for 6 h (lanes 8-13); and (F) Oxidative stress for 6-h (lane14-15). The expression HvPHGPx mRNA is compared to that of actin.

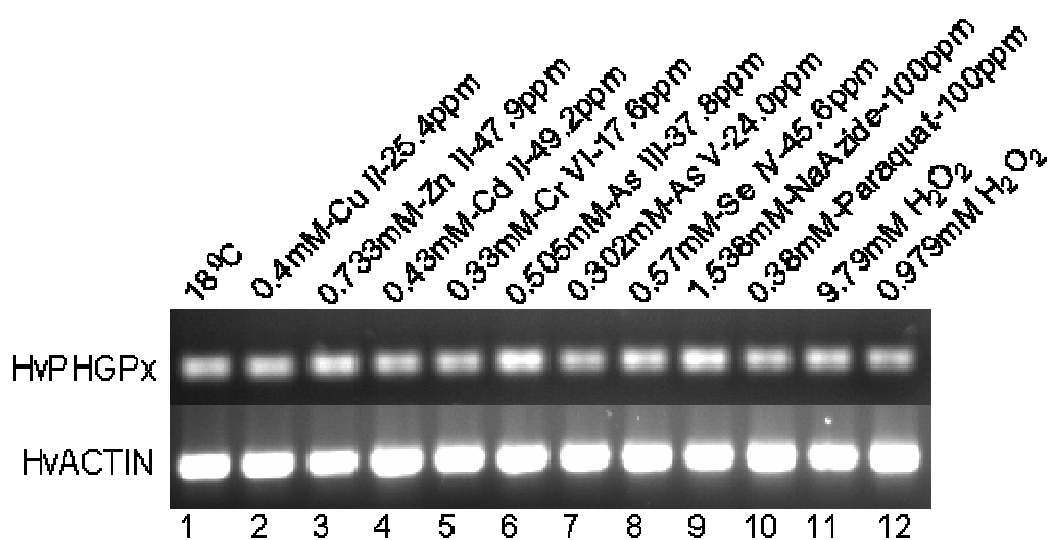


Figure 47. Expression analysis of PHGPx mRNA from *H. vulgaris* under metal and oxidative stress for 1 h. The figures above represent the expression of PHGPx mRNA under different stress conditions as described in the material and methods section: (A) Metal stress for 1 h (lanes 2-8); and (B) Oxidative stress for 1 h (lanes 9-12). The expression HvPHGPx mRNA is compared to that of actin.

enhanced the expression of HvPHGPx mRNA at the treated concentrations as compared to the control whereas 1 h exposure of hydrae to 0.979 mM H₂O₂ (Figure 47, lane 12) did not affect the expression of PHGPx mRNA as compared to control. When hydrae were exposed to metal toxicants for 1 h, all the metals tested except Cu (II) and As (V) induced the expression of HvPHGPx mRNA at the treated concentrations as compared to control (Figure 47). Following 6 h exposure of hydrae to metals at the tested concentrations, the expression of HvPHGPx mRNA was not noticeably affected in comparison to the control (Figure 46).

5.3 Discussion

The objective of the study was to clone and characterize the PHGPx gene from *H. vulgaris*. Here 5'-/3'-RACE was used successfully clone full-length ORFs (open reading frame) of PHGPx from *H. vulgaris* utilizing EST information from *H. magnipapillata*. To confirm that the cDNA and PCR cloning products are indeed from the same gene, the full-length ORF and gene was cloned by PCR and sequenced (data not shown).

The *H. vulgaris* PHGPx contained an amino acid selenocysteine that is encoded by the opal terminator codon UGA. Phospholipid hydroperoxide glutathione peroxidase (PHGPx) is the second selenoenzyme discovered (Ursini *et al.*, 1985) and glutathione peroxidase (GPx) is the first protein known in higher organisms to contain selenocysteine (Sukenaga *et al.*, 1987). This unusual amino acid occurs at the active site of GPx. Bacterial formate dehydrogenase

also contains selenocysteine (Zinoni *et al.*, 1986). Phylogenetic analysis showed that the HvPHGPx grouped with other phospholipid hydroperoxide glutathione peroxidases. Structurally, in the HvPHGPx model one of the helices runs antiparallel to the neighbouring β -strands giving rise to a $\beta\alpha\beta$ substructure, an architecture that has been found in several other proteins e.g. flavodoxin, thioredoxin, rhodanese and dehydrogenases (Alphey *et al.*, 2000).

Identification of glutathione peroxidase signature residues LAFPCNQF (residues 69 - 76), the presence of the conserved selenocysteine residue (residue 44), phylogenetic grouping with several PHGPxs and typical thioredoxin fold in the currently described protein strongly suggested that this protein is phospholipid glutathione peroxidase.

The coding sequence of HvPHGPx gene lacked intron. The absence of intron in stress-induced genes could also compensate for the stress-induced inhibition of RNA-splicing. This characteristic enables preferential expression of these proteins during periods of stress, with the nuclear export signal probably being provided by the mRNA secondary or tertiary structure (Boutet *et al.*, 2003; Huang *et al.*, 1999b).

In normal polyps and regenerates, a peroxidase activity is located in the ectodermal foot mucous cells only (Hoffmeister-Ullerich., 2002). Long-term treatment of *H. vulgaris* with 1 mM LiCl resulted in the appearance of a peroxidase-like activity at several sites of the body, including the prospective head region in regenerates. Also Jantzen *et al.* (1998) reported that strain-

specific effects of lithium on patterning are mediated by hydroperoxides. Overproduction of lipid hydroperoxides is manifested in oxidative stress. So it is concluded that the lithium induced appearance of a peroxidase-like activity could be an indicator of an oxidative stress situation.

Similarly metal induced oxidative stress, due to production of reactive oxygen species including lipid hydroperoxides (Valko *et al.*, 2005; Galaris and Evangelou, 2002) might have lead to induction of PHGPx in hydra as was observed in this study (i.e., exposure of hydra to zinc(II), arsenic (III) and selenium (IV) induced PHGPx mRNA expression).

The effects of varying selenium levels on the activity of PHGPx have been studied in several isolated cell systems *in vitro* (Maiorino *et al.*, 1991; Geiger *et al.*, 1991; Lin *et al.*, 1992). *In vivo* effects of selenium depletion and long-term repletion on PHGPx activity in various mouse organs have been described (Weitzel *et al.*, 1990). Selenium deficiency caused little change in mRNA levels for phGSH-Px in rat liver. Activity of PHGPx has been shown to decrease significantly in rat liver in response to selenium deficiency, but not in testis. In rats fed with Se-deficient diet, phospholipid hydroperoxide glutathione peroxidase mRNA levels were little affected by selenium deficiency in the liver, whereas classical GPx mRNA levels were decreased by 90 % in the same samples (Sunde *et al.*, 1990). In contrast, this study showed increase in the expression of PHGPx mRNA in hydrae after 1-h exposure to Se (0.57 mM).

de Haan *et al.* (1998) demonstrated that paraquat transcriptionally upregulates glutathione peroxidase (GSHPx-1) in normal cells, and GSHPx-1 *-/-* mice is highly sensitive to the oxidant paraquat. The effects of paraquat were dose-related and thus demonstrated a role for GSHPx-1 in protection against oxidative stress. Cortical neurons from GSHPx-1 *-/-* mice are more susceptible to peroxide; 30% of neurons from GPx1-deficient mice were killed when exposed to 65 μ M peroxide, whereas the wildtype controls were unaffected. de Haan *et al.* (1998) proposed that their data established function for GSHPx-1 in protection against some oxidative stressors and in protection of neurons against peroxide. Although tissue specific experiments were not conducted in this study, there is ample evidence that PHGPx mRNA is induced in whole hydra due to paraquat and hydrogen peroxide. Higher concentration of H₂O₂ (9.79 mM) induced PHGPx mRNA transcription as compared to lower concentration of H₂O₂ (0.979 mM) during 1 h exposure of hydra to H₂O₂ thus providing an indirect evidence that HvPHGPx is involved in oxidative stress.

Thus, the evaluation of PHGPx mRNA levels could be considered as a potential biomarker of toxicity associated with contaminant and stressor exposure in aquatic organisms. Also, data presented here contributed to better understanding of the significance of PHGPx from structural, phylogenetic and functional point of view.

CHAPTER VI
MOLECULAR CLONING AND CHARACTERIZATION OF A CATALASE
FROM *HYDRA VULGARIS*

Oxidative stress and the occurrence of reactive oxygen species/intermediates (ROS/ROI) are common to aerobically living organisms and might be deleterious for living cells (Halliwell and Gutteridge, 1989; Moradas-Ferreira *et al.*, 1996). Reactive oxygen species are generated during normal cell metabolism or by abiotic processes comprise superoxide, hydroxyl radicals, hydrogen peroxide, and singlet oxygen. Superoxide gets degraded by superoxide dismutase to hydrogen peroxide. Hydroxyl radicals are highly reactive and have a limited radius of action. Hydrogen peroxide easily penetrates cellular structures (cell walls, plasma membranes, etc.) and forms adducts with sugars and amino acids that are transported by numerous dedicated permeases (Schubert and Wilmer, 1991). Hence, hydrogen peroxide can inflict damage anywhere in a cell or tissue through oxidation of proteins (sulfhydryl groups) and single strand breakage in nucleic acids (Richter and Loewen, 1982; Imlay *et al.*, 1988).

Enzymes that reduce hydrogen peroxide or use it as a reductant are generally termed hydroperoxidases (HP) or catalases. Catalatic hydroperoxidases (CHPs), also known as catalases, primarily dismutate hydrogen peroxide to water and dioxygen by two-electron transfer redox

reactions. CHPs are ubiquitous enzymes found in both prokaryotes and eukaryotes involved in the protection of cells from the toxic effects of peroxides. CHPs are considerable diverse. Generally, these proteins are placed into four main groups: (1) the "classic" heme-containing monofunctional catalases for which hydrogen peroxide is both electron donor and acceptor, (2) the heme-containing bifunctional catalatic peroxidases (CPXs) in which the catalatic activity is much higher than the peroxidatic activity, (3) the nonheme-containing catalases (Allgood and Perry, 1986), and (4) a miscellaneous group containing proteins with minor catalatic but no peroxidatic activities (Nadler *et al.*, 1986; Jones and Wilson, 1978). Most CHPs exist as tetramers of 60-65KD subunits (Nadler *et al.*, 1986).

More than 300 CHPs sequences are now available, divided among monofunctional catalases (> 225), bifunctional catalase-peroxidases (> 50) and manganese-containing catalases (> 25) (Chelikani *et al.*, 2004). Frequently, organisms use different isozymes, which are expressed simultaneously or under developmental-stage- and environment-specific conditions (Schnellhorn, 1994; Zou *et al.*, 1999).

In the present study, a cDNA encoding the c-terminal end of a monofunctional catalase from a fresh water hydra, *H. vulgaris*, is described. The expression of hydra monofunctional catalase (HvCatalase) mRNA is assayed with respect to both environmental contaminant challenge (i.e., arsenic, cadmium, zinc and copper) and stress (both oxidative and non-oxidative). In

addition, the phylogenetic position of hydra catalase is analyzed to study the evolutionary significance of the protein.

6.1 Materials and methods

6.1.1 Hydra culture

Adult *H. vulgaris* were maintained in shallow dishes at 18 °C in a medium containing 1 mM $\text{CaCl}_2 \cdot 2\text{H}_2\text{O}$, 0.012 mM EDTA, and 0.458 mM TES (N-tris[hydroxymethyl]-methyl-2-amino-ethanesulfonic acid, sodium salt) buffer (pH 7.0). Daily, hydrae were fed with brine shrimp (*Artemia nauplii*) hatched in a solution of 1 % sodium chloride treated with iodine (40 µg/ml). Hydrae were maintained free from bacterial and fungal contamination and were not fed for 24 h before initiating the experiments. Deionized water was used throughout this portion of the study (Mayura *et al.*, 1991).

6.1.2 RNA isolation and clean up

Total RNA was extracted from hydra by application of 2 ml of TRIzol[®] reagent (Invitrogen, USA) to approximately 20 mg of fresh tissue, using the manufacturer's instructions. The RNA was quantified by ultraviolet absorbance at 260 nm. Integrity of the total RNA was confirmed by 1 % formaldehyde agarose gel electrophoresis. The RNA isolated was cleaned up from contaminating DNA using RNeasy Mini Kit (Invitrogen, USA) following the manufacturer's instruction.

6.1.3 Identification of a partial fragment of *H. magnipapillata* Catalase cDNA

The GenBank (<http://www.ncbi.nlm.nih.gov/entrez/query.fcgi?db=nucleotide>) was searched for the cnidaria/hydra catalase. An expressed sequence tag (EST) was found from the hydra, *H. magnipapillata*, under the accession number gi|60408694. The expressed sequence tag coded for a catalase similar to the N-terminal end of *Sus scrofa* catalase. This EST sequence was used to design primers F and R (Table 20) to clone a fragment of catalase from *H. vulgaris*.

6.1.4 Oligonucleotides

All oligonucleotides were procured from IDT Inc. (IA, USA). The oligo(dT) bifunctional primer N (Not I-d(T)₁₈: 5'-AACTGGAAGAATTCGCGGCCGCAGGAAT₁₈-3') was supplied in a cDNA preparation kit (Amersham Biosciences, USA) and was used in 3'-RACE experiments. *H. vulgaris* gene specific primers used in the experiments are also given in Table 20.

6.1.5 Cloning and identification of a partial fragment of *H. vulgaris* Catalase cDNA

All polymerase chain reaction (RT-PCR and RACE-PCR) experiments were performed using *Taq* DNA polymerase (Invitrogen, USA) and a thermal cycler (MJ Research, USA).

RNA (5 µg) was reverse transcribed to cDNA at 37 °C for 60 min using the oligo(dT) bifunctional primer and the AMV RT supplied in the cDNA

TABLE 20

Oligonucleotides Used in Cloning of the Partial Sequence of HvCatalase	
Oligonucleotide	Sequence
F	5'-ATGGTGTTGGATCGTAATCCTG-3'
F1	5'-CGGGTGTTGAGACATCTCCT-3'
R	5'-CTTGAGGGCCATTAAAGCTG-3'
N	5'-AACTGGAAGAATTCGCGGCCGCAGGAAd(T) ₁₈ -3'
AF	5'-AAGCTCTTCCCTCGAAGAATC-3'
AR	5'-CCAAAATAGATCCTCCGATCC-3'

synthesis kit (Amersham Biosciences, USA). The first-strand cDNA was amplified using the primers F and R (Table 20). The PCR was performed for 30 cycles, consisting of 94 °C for 30 s, 50 °C for 30 s and 72 °C for 1 min and a final extension at 72 °C for 10 min. The resultant PCR products (Figure 48A) was subcloned into the pCR®II-TOPO® vector using a TA cloning kit (Invitrogen, USA.) according to the manufacturer's instructions. Multiple independent clones were sequenced using automated methods (DNA Technologies Lab, Department of Veterinary Pathobiology, Texas A&M University) on an ABI PRISM™ 310 Genetic Analyzer (PE Biosystems, USA) using a Big-Dye sequencing kit (PE Biosystems) and M13 primers. The identity of the clones was evaluated by matching the sequences to the nucleotide/protein sequences available at the GenBank (<http://www.ncbi.nlm.nih.gov/>). The cloned sequence constituted residues 1 to 289 in the nucleotide sequence shown in Figure 49.

6.1.6 3'-RACE of the HvCatalase cDNA

First-strand cDNA prepared above was amplified using the oligo(dT) bifunctional primer N and a gene-specific primer F (Table 48) (complementary to nucleotide (nt) 1 to 22, Figure 49) for 35 cycles of 94 °C for 30 s, 55 °C for 30 s and 72 °C for 3 min. The first-round PCR products were reamplified using the primer F1 (Table 20) (complementary to nucleotide (nt) 77 to 96, Figure 49) and oligo(dT) bifunctional primer N. The PCR products (Figure 48B) were subcloned and sequenced as described above. The identity of the clones was evaluated by matching the sequences to the nucleotide/protein sequences of GenBank.

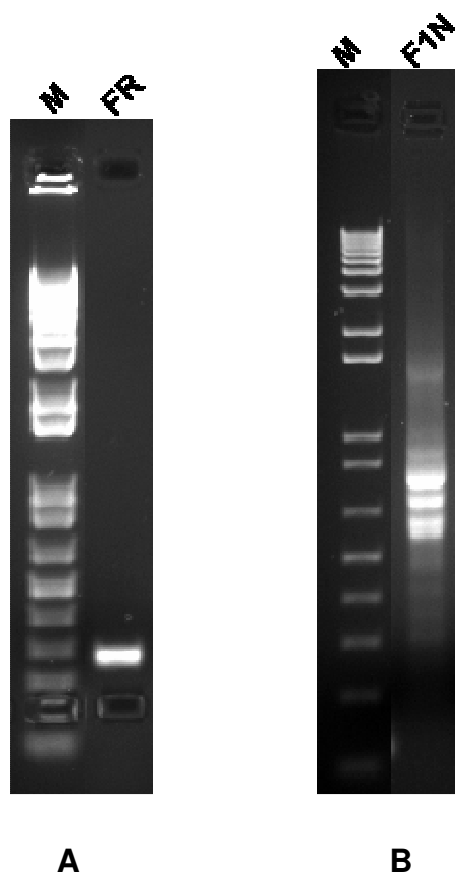


Figure 48. Images of electrophoretic gels for PCR products of HvCatalase gene. (A) The PCR products were produced using primer F and R. (B) The 3'-RACE PCR products were produced using with primer F1 and N (= Not *I*-d(T)₁₈). M = 1 kb plus DNA ladder.

```

1 M V L D R N P E N Y F A D V E Q A A F S
1 atgggtgttgatcgtaatcctgaaaattatcttgctgatgttgaaacaggctgctttttct 60
21 P A H M P P G V E T S P D K M L Q G R L
61 cctgcacatatgccaccgggtgttgagacatctcctgataaaatgttacagggcagatta 120
41 F S Y G D T H R H R L G C N Y Q Q L P V
121 ttttcctatgggtgatacacatcgccatcgattaggatgcaattatcaacagttgcctgta 180
61 N C P L K G Q H N Y Q R D G P Q A F N N
181 aattgtccattaaaagggtcagcataactaccagagagatggacctcaagcatttaataat 240
81 Q G S A P N Y F P N S F N G P Q E Q R Q
241 caaggtagtgctccaaactacttccctaacagctttaatggccctcaagaacaaagacag 300
101 F S N H V D S Y N G E C R R Y Q S G D E
301 tttagcaatcatgttgatagttacaatggggagtgtagaagatatcaatcaggtgatgaa 360
121 D N F S Q P K L F W E N V L D D K E K S
361 gataacttctctcagccaaaattgttttgggaaaatgtgttgatgataaagaaaaaatca 420
141 D L I S N I A G H L K N A Q E F I R K R
421 gatctaatatctaataattgctgggcacttaaaaaatgctcaagaatttattcgcaagaga 480
161 V I K N F S D V H Q D F G R R L N E A I
481 gttataaagaatttttctgatgtccatcaggattttggacgtcgattaaatgaagcgata 540
181 D E L V K G T T S A K A N L *
541 gatgagcttgtaaagggaacaacttcggcaaaagcaaatttgtgaacgacttttttttagt 600

601 tactactaaatgattgtcactgttgaagttttcttgttggtttatcttttcttatttttt 660

661 aaatttagagattttatcttcatacgtttgaaaaaatatttactgtgtaatgtaacacgca 720

721 cgcacacaaagttttaaacgtactcagtggtgtgtgagttttaaacgtacacctgtgttgt 780

781 gtgtacatcggaattacatttttaataaaaagtgtgatgtaaaaaaaaaagaataaaaaa 840

841 attctgccggccgtatatcttcaagtttaggccgaattcttgca 883

```

Figure 49. Partial nucleotide and deduced amino acid sequence of *H. vulgaris* monofunctional catalase. The deduced amino acid sequence is shown in single-letter code above the nucleotide sequence. The nucleotide and amino acid sequences are numbered from the 5'-end of the 883 bp cDNA sequence, and from the C-terminal codon methionine, respectively. The asterisk denotes the translation stop signal.

6.1.7 Heat treatment

Hydrae were incubated at 18 (control temperature), 30 and 37 (maximum induction temperature) °C for 1 h and 6 h in 5 ml hydra media. Also 5 day starved animals were exposed to 30 °C in 5 ml hydra media.

6.1.8 Metal treatment

Nearly 500 hydrae were incubated at 100 ppm of $\text{CuSO}_4 \cdot 5\text{H}_2\text{O}$, ZnCl_2 , $\text{CdCl}_2 \cdot 2.5\text{H}_2\text{O}$, $\text{K}_2\text{Cr}_2\text{O}_7$, As_2O_3 , Na_2HAsO_4 and Na_2SeO_3 for 1 h and 6 h in 5 ml hydra media. Hence the concentration of Cu (II), Zn (II), Cd (II), Cr (VI), As (III), As (V), and Se (IV) (active ingredients) were 0.4 mM (= 25.4 ppm), 0.73 mM (= 47.9 ppm), 0.43 mM (= 49.2 ppm), 0.33 mM (= 17.6 ppm), 0.506 mM (= 37.8 ppm), 0.302 mM (= 24.0), and 0.57 mM (= 45.6 ppm) respectively.

6.1.9 Oxidative stress treatment

Nearly 500 hydrae were incubated at 300 ppm (= 9.79 mM) and 30 ppm (= 0.979 mM) of H_2O_2 and 100 ppm (= 0.38mM) of paraquat in 5 ml hydra media for 1 or 6 h. Also hydrae were exposed to 100 ppm (= 1.538 mM) sodium azide in 5 ml hydra media for 1 or 6 h.

In all cases, treatments were carried out in 14 ml polypropylene round-bottom tubes (Becton-Dickinson, NJ, USA) containing 5 ml hydra media. At the end of the treatment, hydrae were collected by centrifugation at 7,500 Xg for 5 min. The supernatants were discarded. Then hydrae were washed once in 5 ml of 0.05 M PBS for 5 min @ 7,500 Xg. The supernatants were discarded as before and the animals were homogenized immediately in 3 ml of Trizol®.

6.1.10 Expression analysis of HvCatalase mRNA in hydrae

Total RNA was extracted from TRIzol[®] (Invitrogen, USA) treated whole hydrae and cleaned as before using RNeasy Mini Kit (Invitrogen, USA) following the procedure described there in. For RT-PCR, 5 µg of total cleaned RNA was reverse transcribed using 500 ng of oligo(dT)₁₂₋₁₈ primer (Invitrogen, USA) and 200 units of the Superscript II enzyme (Invitrogen, USA) for 50 min at 42 °C. The reaction was inactivated by heating the mixture at 70 °C for 15 min. PCR assays were designed to normalize HvCatalase gene expression levels to actin transcription rate. Two µl of first strand cDNA (from 25 µl of reverse transcription mix) was diluted 100 times prior to PCR amplification. PCR was carried out in 50 µl total volume of 1 × PCR buffer (20 mM Tris-HCl, pH 8.4, 50 mM KCl), 2 mM MgCl₂, 0.1 mM each of dNTPs, 10 pmol each of primers, and 0.5 U *Taq* DNA polymerase (Invitrogen) using 2 µl of (1:100) diluted RT-product. Actin mRNA was amplified using the AF and AR primers and the HvCatalase was amplified using the F and R primers. Cycling profile after initial denaturation at 94 °C for 4 min was 30 cycles of amplification as follows: denaturation at 94 °C for 30 seconds, annealing at 55 °C for 30 seconds, and extension at 72 °C for 45 seconds. These number of PCR cycles ensured quantification within the exponential phase of amplification. Equal amounts of RT-PCR reactions were loaded on standardized 2 % agarose gels containing 0.1 µg/ml ethidium bromide. The gel images were digitalized by a documentation system (Kodak Laboratories).

6.1.11 General bioinformatic analyses

Conceptual translation of the full-length cDNA was performed using the program SIXFRAME (<http://biologyworkbench.ucsd.edu>). Homology to other catalase genes and proteins were identified by using the Blast program with default settings (<http://www.ncbi.nlm.nih.gov/BLAST>). The identification of HvCatalase domains were performed by use of the SMART program (<http://smart.embl-heidelberg.de/>) using default pattern definitions. Prosite (<http://us.expasy.org/prosite/>) identification of glycosylation, phosphorylation, myristilation and amidation sites was performed by use of the ExPASy program using default settings. Several catalase sequences were retrieved from the National Center for Biotechnology Information (NCBI) Entrez Web service (<http://www.ncbi.nlm.nih.gov/Entrez/>) were aligned to each other using the web program T-coffee (http://igs-server.cnrs-mrs.fr/Tcoffee/tcoffee_cgi/index.cgi), ClustalW (<http://www.ch.embnet.org/software/ClustalW.html>) (Figure 50), or the ClustalW program embedded in Mega (<http://www.megasoftware.net/>).

6.1.12 Phylogenetics

For phylogenetic analysis sequences were aligned using the ClustalW program embedded in the program Mega 3.1 (<http://www.megasoftware.net/>). The aligned sequences were used for bootstrap test of phylogeny using maximum likelihood neighbor joining method with following parameters: substitution model - JTT; bootstrap -1000 replicates, seed = 2442, gaps/missing data – complete deletion, pattern among lineages – same and rate among sites

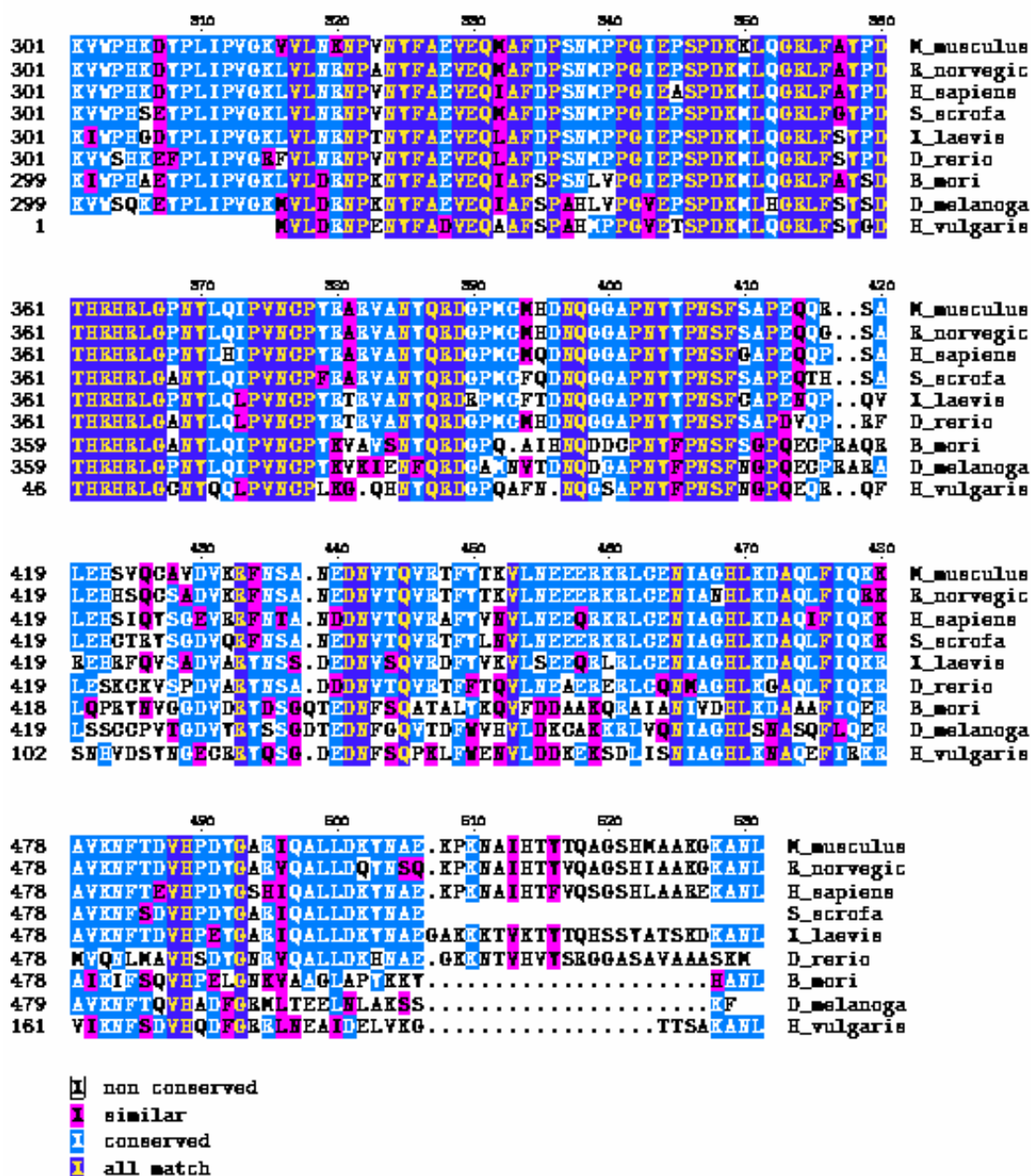


Figure 50. Multiple sequence alignment of catalase proteins using the program ClustalW. Accession numbers from the proteins as extracted using the Entrez web service (<http://www.ncbi.nlm.nih.gov/Entrez/protein.html>) are: gi|6753272 (*Mus musculus*), gi|6978607 (*Rattus norvegicus*), gi|5102626 (*Homo sapiens*), gi|50979303 (*Sus scrofa*), gi|32822922 (*Xenopus laevis*), gi|30185757 (*Danio rerio*), gi|51571867 (*Bombax mori*), gi|7690 (*Drosophila melanogaster*) (gi|50347095), and current study (*Hydra vulgaris*).

- uniform. The consensus bootstrap tree generated is displayed in Figure 51.

The accession numbers of protein sequences used for phylogenetic analysis are: gi|12666585 (*Methanobrevibacter arboriphilus*), gi|5713198 (*Xanthomonas campestris* pv. *phaseoli*), gi|416753(CATA_ECOLI), gi|30580356 (CAT2_NEUCR: *Neurospora crassa*), gi|32700075 (CATA_MYCBO: *Mycobacterium tuberculosis*), gi|29427888 (CATA_SALTI: *Salmonella enterica* serovar *typhi*), gi|20141210 (CATA_SALTY: *Salmonella typhimurium* LT2), gi|13626145 (CATA_CAUCR: *Caulobacter crescentus*), gi|12643777 (CATA_MYCSM: *Mycobacterium smegmatis*), gi|9972799 (CATA_YERPE: *Yersinia pestis*), gi|9972797 (CATA_LEGPN: *Legionella pneumophila*), gi|9972792 (CATB_STRCO: *Streptomyces coelicolor*), gi|9972752 (CATB_STRRE: *Streptomyces reticuli*), gi|9972746 (CATA_HALSA: *Halobacterium salinarum*), gi|9972736 (CATA_HALMA: *Haloarcula marismortui*), gi|9972733 (CATA_ARCFU: *Archaeoglobus fulgidus*), gi|9972730 (CATA_MYCFO), gi|6226842 (CATA_MYCTU: *Mycobacterium tuberculosis*), gi|1345687 (CATA_BACST: *Geobacillus stearothermophilus*), gi|584884 (CATA_RHOCA: *Rhodobacter capsulatus*), gi|35213340 (CATA_GLOVI: *Gloeobacter violaceus* PCC 7421), gi|29372835 (*Thermus thermophilus* HB27), gi|56965177 (*Bacillus clausii* KSM-K16), gi|56421571 (*Geobacillus kaustophilus* HTA426), gi|47564251 (*Bacillus cereus* G9241), gi|1752756 (*Lactobacillus plantarum*), gi|21321250 (*Pyrobaculum calidifontis*), and gi|19910933 (*Thermoleophilum album*).

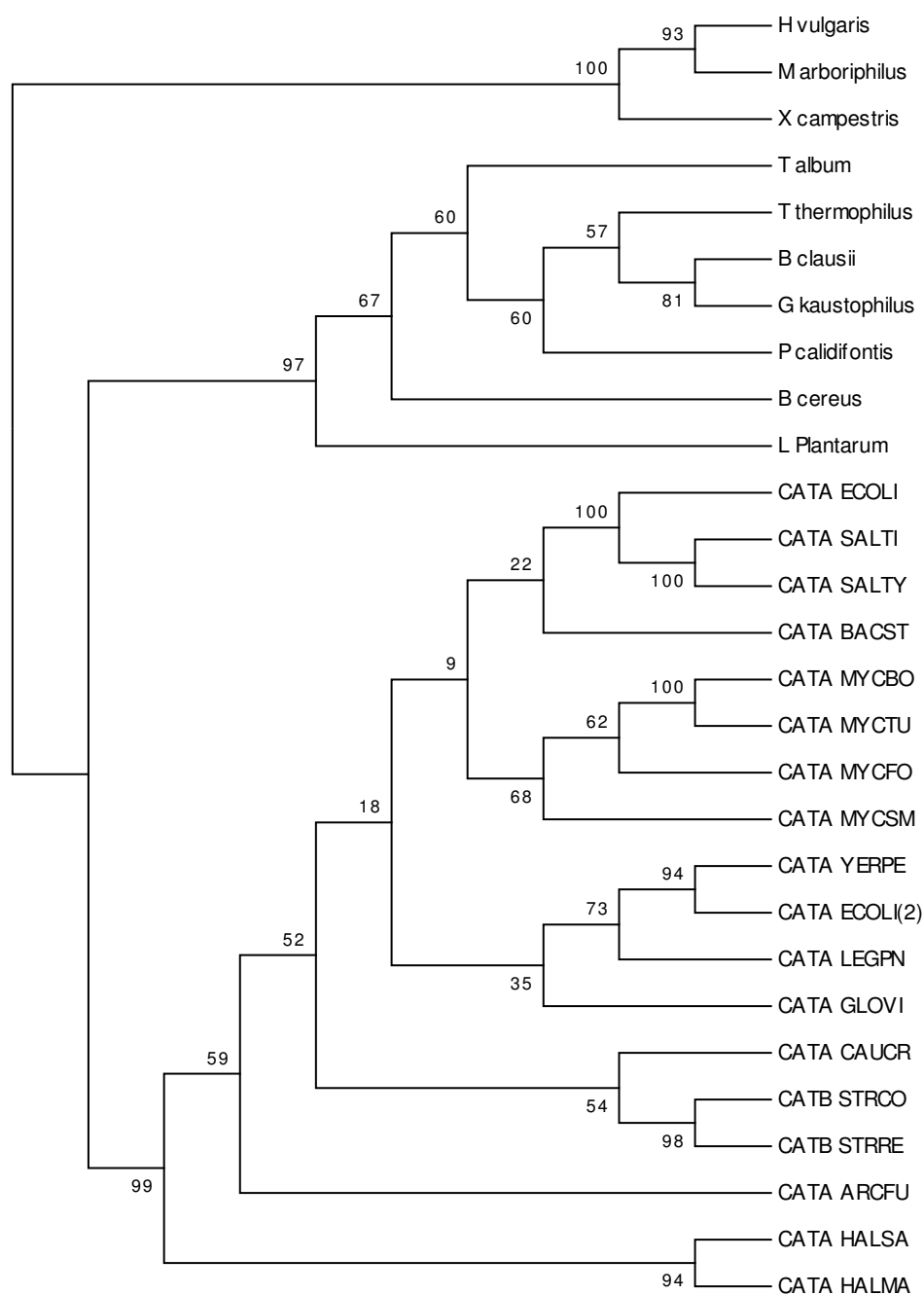


Figure 51. Phylogenetic alignment of the amino acid sequences of the catalases from different organisms. The tree was constructed by the maximum likelihood neighbor-joining method using the program MEGA 3.1. Bootstrap confidence values for the sequence groupings are indicated in the tree ($n = 100$). The hydra catalase is grouped with monofunctional catalases.

6.2 Results

6.2.1 Cloning and analysis of HvCatalase cDNA

Prior to cloning of the Hv-Catalase cDNA, GenBank was searched for the cnidaria/hydra catalase and an expressed sequence tag (EST) was found from the hydra *H. magnipapillata* under the accession number similar to the 5'-end of *Sus scrofa* catalase. This cDNA sequence was used to clone a partial fragment of catalase from *H. vulgaris* based on the realization that the conserved proteins between *H. magnipapillata* and *H. vulgaris* share high sequence similarity both at the protein and nucleotide sequence levels. Primers F and R (Table 20) were used in RT - PCR experiments to amplify a segment of Hv-Catalase (Figure 48A) and the amplified cDNA product of nearly 300 base pair (bp) was subcloned and sequenced. Initial sequence analysis indicated the presence of an open reading frame (ORF) encoding a polypeptide with a high degree of similarity to catalases of many organisms.

The 3'-end of the cDNA was cloned using 3'-RACE experiment as illustrated in the material and methods section using gene specific primers (Table 20). Though 3'-RACE yielded multiple PCR bands (Figure 48B), only clones belonging to one PCR band yielded an ORF encoding a polypeptide with a high degree of similarity to catalases of many organisms before ending up with a poly(A) tail. As shown in Figure 49, the the deduced protein is composed of 194 amino acid residues. The predicted HvCatalase amino acid sequence exhibited the characteristic catalase signature RLFSYgDTH (residues 39-47).

The C-terminal end also contained important residues that interact with heme group are: M-35, G-38, R-39, Y-43, T-46, H-47 and R-50.

6.2.2 Sequence conservation in Catalase proteins

The C-terminal end of the putative HvCatalase amino acid sequence was aligned by the ClustalW method with several catalases (data not shown). The absolutely conserved residues in the C-terminal end in all these sequences are (numbering based on *H. vulgaris* amino acid sequence) : V-2, L-3, N-6, P-7, N-9, Y-10, F-11, A-12, V-14, E-15, Q-16, A-18, F-19, P-21, P-26, G-27, E-29, S-31, P-32, D-33, K-34, L-36, G-38, R-39, L-40, F-41, T-43, D-45, T-46, H-47, R-48, H-49, R-50, L-51, G-52, N-54, Y-55, P-59, V-60, N-61, C-62, P-63, N-69, Q-71, E-72, D-73, N-80, Q-81, P-85, N-86, Y-87, P-89, N-90, S-91, F-92, P-95, R-114, D-121, N-122, Q-125, N-145, H-149, L-150, A-153, F-146, V-168, H-169 and G-173. An alignment of the C-terminal HvCatalase with 9 representative catalases is shown in Figure 50. The 194 amino acid protein deduced from the cDNA sequence when compared to the protein of GenBank databases using the program BLAST gave significant scores with catalase of *Sus scrofa domestica*, *Rana rugosa*, *Cavia porcellus*, *Haemonchus contortus*, *Canis familiaris*, *Litopenaeus vannamei*, *Homo sapiens*, *Drosophila melanogaster*, *Xenopus laevis*, *Mus musculus*, *Melopsittacus undulates*, *Rattus norvegicus*, *Danio rerio*, *Bombyx mori*, *Caenorhabditis elegans*, *Dictyostelium discoideum*, *Saccharomyces pombe*, etc. (Table 21).

TABLE 21

Similarities among *H. vulgaris* Catalase and Catalase Proteins from Other Organisms^a

Protein	% similarity to HvCatalase
<i>Sus scrofa</i> catalase	76
<i>Rana rugosa</i> catalase	72
<i>Cavia porcellus</i> catalase	75
<i>Haemonchus contortus</i> catalase	75
<i>Canis familiaris</i> catalase	75
<i>Litopenaeus vannamei</i> catalase	71
<i>Homo sapiens</i> catalase	75
<i>Drosophila melanogaster</i> catalase	72
<i>Xenopus laevis</i> catalase	73
<i>Mus musculus</i> catalase	75
<i>Melopsittacus undulatus</i> catalase	74
<i>Rattus norvegicus</i> catalase	74
<i>Danio rerio</i> catalase	71
<i>Bombyx mori</i> catalase	71
<i>Caenorhabditis elegans</i> catalase	68
<i>Dictyostelium discoideum</i> catalase	64
<i>Schizosaccharomyces pombe</i> catalase	61

^aComparisons of amino acid Sequences were made with the algorithm of NCBI BLAST

Also multiple sequence alignment identified NADPH binding residues as (numbering based on *H. vulgaris* amino acid sequence): G-27, S-31, D-32, M-34, L-35, Q-36, R-38, F-40, Y-42, D-44, R-47, R-49, G-51, N-53, P-58, V-59 and N-60.

6.2.3 Phylogenetic analysis

In order to further characterize the putative protein sequence, the protein sequence was compared to several published catalases sequences from various organisms using the maximum likelihood neighbor joining method embedded in program MEGA 3.1. Phylogenetic analysis showed that HvCatalase grouped with monofunctional catalases and hence is concluded as a classic heme-containing monofunctional catalase (Figure 51).

6.2.4 HvCatalase mRNA expression analysis

The expression patterns of the HvCatalase mRNA were investigated in whole organisms by reverse transcriptase-polymerase chain reaction (RT-PCR) (Figure 52 and Figure 53). For RT-PCR experiment gene-specific primers were used. Thermal stress for 1 h at 30 and 37 °C (Figure 52, lanes 2 and 4) enhanced the expression of HvCatalase mRNA as compared to 18 °C (control) (Figure 52, lane 1). However, thermal stress for 6 h at 30 °C (Figure 52, lane 3) reduced the expression of HvCatalase mRNA as compared to control at 18 °C. But the expression of the HvCatalase mRNA almost vanished when hydrae were

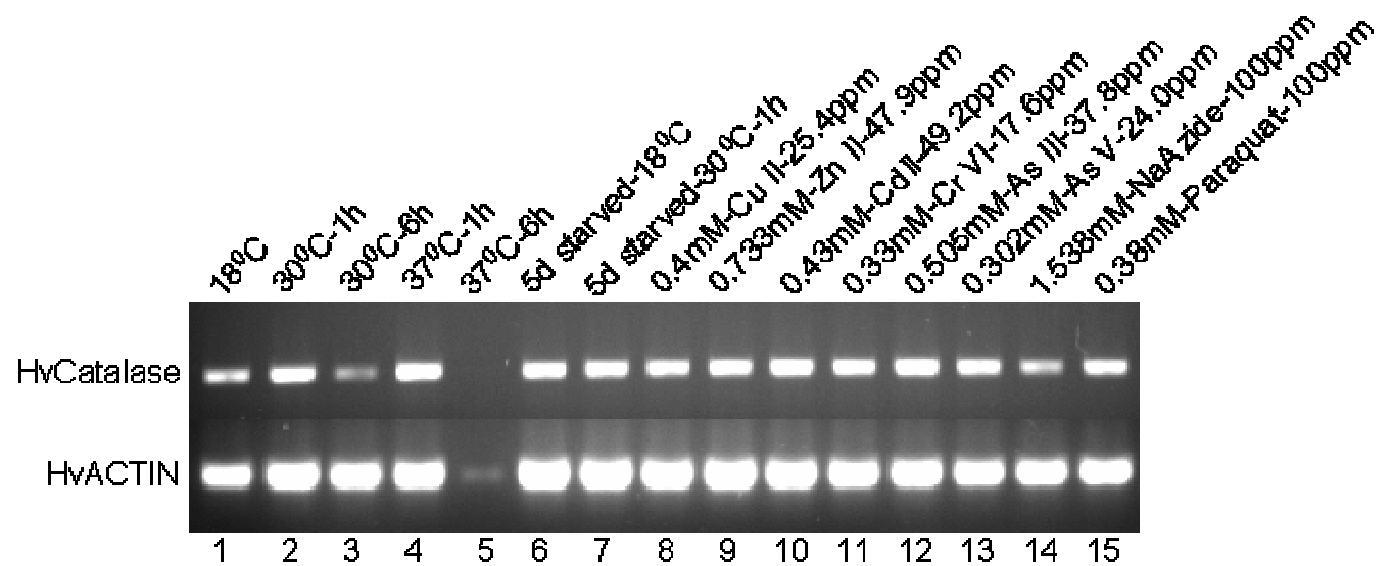


Figure 52. Expression analysis of catalase mRNA from *H. vulgaris* exposed to thermal, starvation, metal and oxidative stress. The figure represents the expression of HvCatalase mRNA under different stress conditions as described in the material and methods section: (A) Thermal stress (lanes 2-5); (B) Starvation stress (lanes 6-7); (C) Metal stress for 6 h (lanes 8-12); and (D) Oxidative stress for 6 h (lane 14-15). The expression HvCatalase mRNA is compared to that of actin.

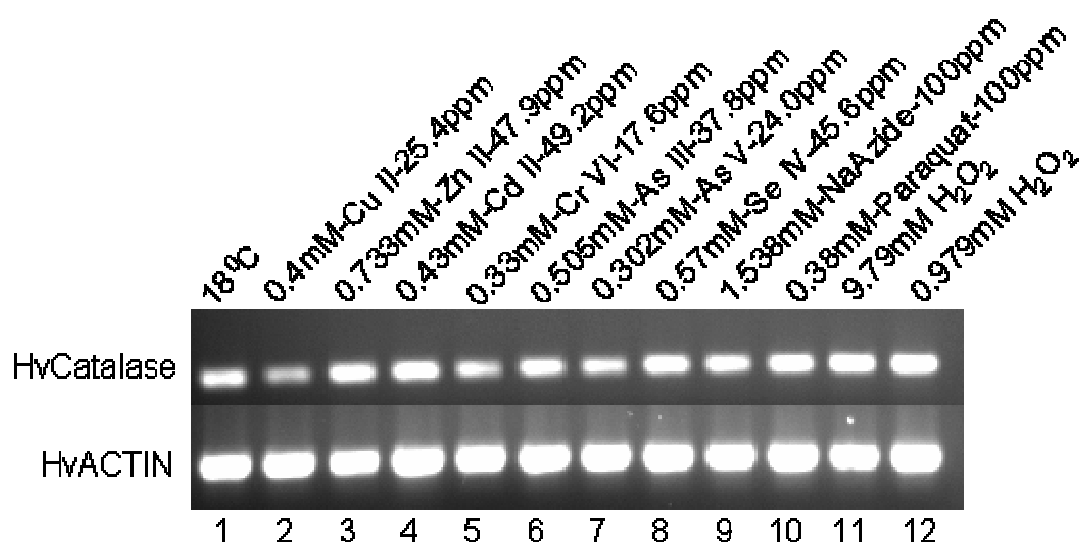


Figure 53. Expression analysis of catalase mRNA from *H. vulgaris* exposed to metal and oxidative stress for 1 h. The figure represents the expression of HvCatalase under different stress conditions as described in the material and methods section: (A) Metal stress for 1 h (lanes 2-8); and (B) Oxidative stress for 1 h (9-12). The expression HvCatalase mRNA is compared to that of actin.

exposed to thermal stress at 37 °C for 6 h (Figure 52, lane 5). Hydrae starved for 5 days showed enhanced expression of HvCatalase mRNA both at 18 °C and 30 °C (Figure 52, lanes 6-7) as compared to the control maintained at 18 °C (unfed for 2-days). Exposure of hydrae to sodium azide (1 h) (Figure 53, lane 9), paraquat (1 and 6 h) (Figure 53, lane 10 and Figure 52, lane 15) and H₂O₂ (1 h) (Figure 53, lanes 11-12) enhanced the expression of HvCatalase mRNA at the treated concentrations as compared to the control. When hydrae were exposed to metal toxicants for 1 h; all the metals tested except Cu (II), Cr (VI) and As (V) induced the expression of HvCatalase at the treated concentrations (Figure 53) as compared to control and when the exposure of hydrae to metals at the tested concentrations lasted for 6 h; the expression of HvCatalase was enhanced as compared to control (Figure 52).

6.3 Discussion

Here primers designed from an expressed sequence tag (EST) information available for *H. magnipapillata* catalase along with 3'-RACE method was used to successfully clone a 3'-end of a cDNA encoding the C-terminal end of a catalase from *H. vulgaris*. Identification of catalase signature RLFSYgDTH (residues 39-47), the presence of the conserved important residues interacting with heme group M-35, G-38, R-39, Y-43, T-46, H-47, R-50 and phylogenetic grouping with several monofunctional catalases strongly suggested that this protein is a monofunctional catalase.

Catalase gene is shown to be regulated by various stimuli. Rohrdanz and Kahl (1998) showed that primary rat hepatocytes exposed to H_2O_2 induced expression of catalase 2-fold. Guinea pig cell cultures harboring vector-borne expression of a cyanobacterial catalase-peroxidase (CPX) conferred significantly higher resistance to hydrogen peroxide and paraquat than the parental cells (Ishikawa *et al.*, 1998). Similar observation was made in current study in that exposure of hydrae to oxidant paraquat (0.38 mM) for 1 and 6 h enhanced the expression of catalase mRNA. Also exposure of hydrae 0.979 and 9.79 mM H_2O_2 for 1 h induced the expression of catalase mRNA. Because the primary role of catalase is to rid the cell of the strong oxidant H_2O_2 before it causes unwanted reactions or gives rise to even more reactive hydroxyl radical, the increase in catalase response to H_2O_2 at the transcriptional level is an easily understood protective response to an oxidative stress (Morgan *et al.*, 1986).

The observation that heat shock enhances catalase mRNA expression in hydra is consistent with the observation that yeast CTT1 transcription is induced by heat shock (Wieser *et al.*, 1991).

Algae *Scenedesmus* sp. exposed to elevated levels of heavy metals during short- (6 h) and long-term (7 d) exposure to Cu^{2+} and Zn^{2+} resulted in increased catalase activities only at 2.5 μM Cu^{2+} and 25 μM Zn^{2+} when oxidative stress was mild, but were inhibited at 10 μM Cu^{2+} under intense oxidative stress (Tripathy *et al.*, 2005). Li *et al.* (2005) similarly showed that copper and zinc stimulated the activities of catalase in the marine microalga *Pavlova viridis* when

algal cells were grown at different concentrations of copper and zinc. Results suggested that an activation of antioxidant enzyme catalase was enhanced to counteract the oxidative stress induced by the two metals. Similar observation is made in the current study that in order to overcome the oxidative stress induced by metal exposures, hydrae have enhanced the expression of catalase mRNA.

Thus the efficient catalase mRNA expression system in hydra could be a useful tool for testing involvement of H_2O_2 in toxicological responses and processes associated with reactive oxygen species like heavy metal exposure. Thus the evaluation of catalase expression levels could be considered as a potential biomarker of toxicity associated with contaminant exposure in hydra. Also, data presented here contributed to better understanding of the evolutionary significance of HvCatalase both at phylogenetic and functional level.

CHAPTER VII

SUMMARY AND CONCLUSIONS

Organisms are exposed to stress due to various situations and sources. Stress in organisms may be due to endogenous (internal to the animal) or exogenous (external to the animal) sources. The internal sources of stress are primarily due to metabolism, a big part of which is due to partially reduced oxygen species produced during electron transport chain TCA cycle in the mitochondria. The external sources of stress may be due to exposure to heat, heavy metal ions, xenobiotics, oxygen, etc. The stress due to oxygen, known as oxidative stress, may also originate from internal or external sources. Intracellular oxidative stressors are generated during electron transport associated with mitochondrial membranes. Microsomal and nuclear membranes containing cytochromes P-450 and b_5 , may produce superoxides and oxygen radicals also. In addition, several catalytic cytosolic enzymes contribute to the generation of superoxide and hydrogen peroxide. The superoxide radical, the first intermediate in the sequential univalent reduction of O_2 , leads to the formation of many other reactive species (ROS), including hydrogen peroxide. The iron-catalyzed reaction of superoxide with hydrogen peroxide produces the highly reactive hydroxyl radical. Hydroxyl radicals can oxidize practically any molecule contained in the cell (Halliwell and Gutteridge, 1990). Therefore, the oxygen that is essential for the survival of all aerobic organisms contribute to the

processes of aging, the promotion of cancer, and several pathological disorders in organisms and carries the risk of destroying the very life for which it serves as the source of useful energy (Keher, 1993; Yu, 1994).

Organisms from both flora and fauna respond to stress (Macario *et al.*, 1999; Sun *et al.*, 2002) by the immediate synthesis of several proteins and often the cessation of synthesis of most other proteins (Lindquist, 1986). This response to stress is known as cellular stress response (CSR). CSR helps organisms survive and overcome stress by the use of several proteins. The CSR proteome of cellular organisms consists of about 300 proteins including approximately 40 well known proteins important in redox regulation (Glutathione reductase, Thioredoxin, Superoxide dismutase, etc.); DNA damage sensing and repair (MutS/MSH, MutL/MLH, RecA/Rad51, etc.); molecular chaperoning (DnaK/HSP70, DnaJ/HSP40, GrpE, etc.); protein degradation (Lon protease/protease La, FtsH/proteasome regulatory subunit, etc.); fatty acid or lipid metabolism (Long chain fatty acid ABC transporter, Long chain fatty acid CoA ligase, Multifunctional beta oxidation protein, etc.); energy metabolism (Citrate synthase, Ribosomal RNA methyltransferase, Enolase, etc.); other functions (Inositol monophosphatase, Nucleotide diphosphate kinase, etc.). These are well conserved in cellular proteomes and are known to constitute the minimal stress proteome (MSP) of cellular organisms.

The 70 KDa heat shock protein is the major HSP in all organisms and is important in protein chaperoning (Jolly and Morimoto, 2000; Feder and

Hofmann, 1999; Gething and Sambrook, 1992) and acquired tolerance processes (Basu *et al.*, 2002, Lindquist and Craig, 1988 and Clegg *et al.*, 1998). The enzyme superoxide dismutase (SOD) (Brouwer *et al.*, 2003) constitutes the first line of defense against oxidative damage by catalyzing the disproportionation of superoxide to produce oxygen and hydrogen peroxide (Fridovich, 1995). Glutathione peroxidase and catalase remove hydrogen peroxide. Among glutathione peroxidases (GPx), phospholipid hydroperoxide glutathione peroxidase (PHGPx), a selenium-dependent glutathione peroxidase, is unique in the substrate specificity because it can interact with lipophilic substrates, including the peroxidized phospholipids and cholesterol, and reduce these hydroperoxide to hydroxide compounds (Ursini *et al.*, 1985, Thomas *et al.*, 1990). Catalases promote the disproportionation of hydrogen peroxide; contain heme or manganese or none of them as a prosthetic group (Nadler *et al.*, 1986). Nonenzymic antioxidants, such as the lipid-soluble vitamin α -tocopherol, the water-soluble vitamin ascorbate, and the intracellular tripeptide glutathione, are also essential in terminating chain reactions initiated in membrane lipids (Buettner, 1993) and in the removal of free radicals from the cytosol (Martensson and Meister, 1991; Reed, 1990).

In this work, five different stress response genes were cloned and characterized from a fresh water organism *H. vulgaris*. These include: (i) heat shock protein 70 (HvHSP70), (ii) manganese superoxide dismutase (HvMnSOD), (iii) extracellular copper zinc superoxide dismutase (HvEC-

CuZnSOD), (iv) phospholipid peroxidase glutathione peroxidase (HvPHGPx) and (v) monofunctional catalase. The modulation of these genes by different stressors including metals was studied along with the prediction of their structure and phylogenetic position. Data generated in the study support the observation that key stress response proteins are conserved in hydra.

A 70 KDa heat shock protein gene was cloned from *H. vulgaris* and is consistent with the observation that *H. vulgaris* possessed thermotolerance, acquired tolerance, and can live and survive in unstable habitats ascribed to heat shock protein induction (Bosch *et al.*, 1988). The *H. vulgaris* HSP70 exhibited the characteristic motifs of the HSP70 family: IDLGTTYS (residues 9 to 16), DLGGGTFD (residues 199 to 206) and EEVD (residues 647 to 650). A notable feature in the protein is the presence of three consecutive repeats of the tetrapeptide motif GGMP at its C-terminal region. Identification of GGMP repeats, as well as the presence of the cytosolic HSP70-specific motif EEVD at the C-terminus of the HSP70 sequence, strongly suggested that this protein is a cytosolic 70 kDa HSP. This HSP70 displayed high sequence similarity with members of the HSP70 family. Taken together, these results suggested that the HSP70 of the *H. vulgaris* possessed the essential properties of an HSP70 family. Consequently, it is concluded that the HSP70 characterized in this study is an inducible HSP like other inducible HSP70s.

As observed in other HSP70 genes the protein coding sequence is interrupted by three intron sequences. The 5' non-coding region of the HvHSP70

gene possessed the canonical heat shock elements and is consistent with the observation their presence in the 5' non-coding region of HSP70 genes in other species. A molecular model generated for the N-terminal fragment of the HvHSP70 displayed the heat shock protein fold which had similar nucleotide (ATP) binding domains of heat shock cognate protein 70, actin, hexokinase and glycerol kinase. This suggested that HvHSP70 is a member of a family of phosphotransferases and utilizes the same structural motif to bind ATP and possesses an ATPase activity. Phylogenetic analysis showed that the HvHSP70 forms a distinct lineage compared to other heat shock protein 70s.

The two different superoxide dismutases that were characterized from *H. vulgaris* in this study are: (i) an extracellular copper zinc superoxide dismutase (HvEC-CuZnSOD) and (ii) manganese superoxide dismutase (HvMnSOD). The predicted HvEC-CuZnSOD polypeptide consisting of 189 amino acids ($M_w = 20959.73$) exhibited the characteristic copper zinc superoxide dismutase signature GNAGpRiACgil (residues 172 - 183) of the CuZnSOD family. Seven residues known to be involved in metal binding in CuZnSODs are also found in the Hv-CuZnSOD amino acid sequence. The residues required for coordinating copper are identified as: H-80, -82, -97, and -154; and for zinc are: H-97, -114, -105 and D-117; H-97 being the common residue for coordination of both metals copper and zinc. Also the residues responsible for oligomerization of CuZnSODs are identified by multiple sequence alignment as: G-71, V-72, H-77, C-91, R-113, G-119, I-178 and C-180. The arginine residue likely involved in the

positioning of the substrate (superoxide) occurs at position 177. The two cysteines believed to be form a disulfide bond are: C-91 and C-180.

EC-CuZnSODs identified so far has a putative signal peptide. Analysis of residues in HvEC-CuZnSOD showed that residues 1-19 of the hydra EC-CuZnSOD might form a signal peptide. Hence these results suggested that the putative Hv-CuZnSOD of the *H. vulgaris* identified and reported here, possessed the essential properties of an EC-CuZnSOD and concluded as an EC-CuZnSOD. A molecular model generated for the HvEC-CuZnSOD displayed the CuZnSOD β -barrel fold and had similar metal binding residues in the same sequence and structural order. Phylogenetic analysis showed that the HvEC-CuZnSOD grouped together with extracellular CuZnSODs from several organisms.

The predicted *H. vulgaris* manganese superoxide dismutase (HvMnSOD) polypeptide consisting of 219 amino acids ($M_w = 24348.75$) exhibited the characteristic motifs of the MnSOD family. Four residues known to be involved in metal binding in Fe or Mn SODs are found in the HvMnSOD amino acid sequence (H-48, H-96, D-181 and H-185). The consensus sequence DXWEH observed in MnSODs is located between the above mentioned D-181 and H-185 and is seen here as DVWEH. Also the sequence LPEL, resembling the polypeptide LPDL conserved at the N-terminal region in most of eukaryotic MnSODs, is present in HvMnSOD. A single potential N-glycosylation site (NXS/T) is also found at His-96 (NHS) in HvMnSOD. HvMnSOD has a putative

mitochondrial transit peptide consisting of residues 1-21 (MFSFGIHRLSVFRKISRIFAFA). Analysis of residues 1-21 of the MnSOD transit peptide showed that residues 9-15 (LSVFRKI) are likely to form an α -helix. An axial projection of amino acid residues 9-15 on a helical wheel showed that the helix forms an amphiphilic structure. Hydrophobic residues (L-9, V-11, F-12, I-15) are clustered on one side of the helix, and a polar residue (S-10) along with two positively charged (R-13, K-14) residues are found on the opposite side of the helix. This putative MnSOD displayed high sequence similarity with members of the MnSOD family. A molecular model generated for the HvMnSOD displayed the N-terminal long alpha antiparallel hairpin and the C-terminal mixed alpha/beta fold characteristic of MnSODs. The active-site structures including similar shells of aromatic residues are conserved in HvMnSOD. Phylogenetic analysis showed that the HvMnSOD is clustered with mollusk and crustacean MnSODs.

H. vulgaris possessed a selenium-dependent phospholipid hydroperoxide glutathione peroxidase (HvPHGPx). This provides indirect (theoretical) evidence that hydra has also evolved a mechanism to manage cellular lipid hydroperoxides though specific experiments are needed to examine the exact nature of the PHGPx analyzed in the current study. The phospholipid hydroperoxide glutathione peroxidase (PHGPx) isolated from *H. vulgaris* encodes a polypeptide of 168 amino acids, including a TGA-encoded selenocysteine at residue 44, with a calculated M_w of 18746.51 Da. The

predicted HvPHGPx amino acid sequence exhibited the characteristic glutathione peroxidase signature LAFPCNQF (residues 69 - 76). Residues important for the reducing substrate glutathione (GSH) and catalysis of lipophilic substrates that constitute the catalytic triad (U-44, Q-79, and W-132) are conserved in HvPHGPx. A molecular model generated for the HvPHGPx displayed the thioredoxin fold. Phylogenetic analysis showed that the HvPHGPx grouped together with other PHGPxs from several organisms.

The finding that hydra possess heme containing monofunctional catalases is an evidence in theory that it has also evolved a mechanism to disproportionate toxic H_2O_2 from its cellular environment, though specific experiments are needed to examine the exact nature of the catalase analyzed in the current study . The 3'-end of the cDNA sequence encoding for catalase isolated from *H. vulgaris* encodes a polypeptide of 168 amino acids. The predicted HvCatalase amino acid sequence exhibited the characteristic catalase signature RLFSYgDTH (residues 39-47). The C-terminal residues interacting with heme group are identified as M-35, G-38, R-39, Y-43, T-46, H-47, and R-50. Phylogenetic analysis showed that the HvCatalase grouped together with monofunctional catalases and is concluded as a classic heme-containing monofunctional catalase.

Parameters of stress/oxidative stress (induction of stress genes) were higher in hydrae exposed to stressors and contaminants. As shown in the current study, HvHSP70 mRNA levels in heat-stressed (1- and 6-h @ 30 and 37

$^{\circ}\text{C}$) and zinc-exposed (1-h @ 0.733 mM) hydrae were higher than unexposed hydrae (control). Increased levels of HSP70 mRNA suggested that stress was greater in the cytoplasm. Hence the induction of HSP70 mRNA can be ascribed to HSP70's role as a molecular chaperone and protector of cytoplasmic toxicity in the event of stress. Similarly increased levels of HvEC-CuZnSOD mRNA as shown in the current study may suggest that stress was greater in the extracellular space due to starvation (starved 5-days @ 18°C and starved 5-days @ 18°C and exposed to 30°C for 1-h), heat stress (1-h @ 30 and 37°C), oxidative stress (6-h @ 0.38 mM of paraquat) and metal stress (6 h @ 0.43 mM Cd and 0.33 mM Cr) and increased levels of HvEC-CuZnSOD mRNA suggested HvEC-CuZnSOD's role in protecting the cellular environment right from outer space before the cellular cytosol is damaged due to stress. HvMnSOD mRNA is observed to be up-regulated by heat (1-h @ 37°C), sodium azide (1-h @ 1.538 mM), H_2O_2 (1-h @ 9.79 mM), paraquat (6-h @ 0.38 mM), Cu II (6-h @ 0.4 mM), Zn II (1- and 6-h @ 0.733 mM), Cd II (6-h @ 0.43 mM), Cr VI (6-h @ 0.33 mM), As III (1 and 6-h @ 0.505 mM), As V (1 and 6-h @ 0.302 mM) and Se IV (1-h @ 0.57 mM) and the increased levels of HvMnSOD mRNA may suggest HvMnSOD's role in protecting the mitochondrial environment from damage due to partially reduced oxygen species and subsequent stress. HvPHGPx mRNA is observed to be up-regulated by heat (1-h @ 30 and 37°C), starvation (starved 5-days @ 18°C and starved 5-days @ 18°C and exposed to 30°C for 1-h), sodium azide (1-h @ 1.538 mM), H_2O_2 (1-h @ 9.79 mM),

paraquat (1-h @ 0.38 mM), Zn II (1-h @ 0.733 mM), As III (1-h @ 0.505 mM), and Se IV (1-h @ 0.57 mM) and the increased levels of HvPHGPx mRNA may suggest HvPHGPx's role in protecting the cellular environment from damage due lipid hydroperoxides generated due to exposure to different stressors. HvCatalase mRNA is observed to be up-regulated by heat (1-h @ 30 and 37 °C), starvation (starved 5-days @ 18 °C and starved 5-days @ 18 °C and exposed to 30 °C for 1-h), sodium azide (1-h @ 1.538 mM), H₂O₂ (1-h @ 0.979 and 9.79 mM), paraquat (1 and 6-h @ 0.38 mM), Cu II (6-h @ 0.4 mM), Zn II (1 and 6-h @ 0.733 mM), Cd II (1 and 6-h @ 0.43 mM), Cr VI (6-h @ 0.33 mM), As III (1 and 6-h @ 0.505 mM), As V (6-h @ 0.505 mM) and SeIV (1 and 6-h @ 0.57 mM) and the increased levels of HvPHGPx mRNA may suggest catalase's role in protecting the cellular environment from hydrogen peroxide damage due to exposure to different stressors.

HSP70 gene was not observed to be induced by most of the treatments on hydrae except to that of heat, starvation, Zn (II) and Cd (II). The lack of induction of HSP70 mRNA may be ascribed to toxicity due to higher doses of the chemicals tested as it may deregulate the normal cellular metabolism and hence the mRNA synthesis and its stability. Consistent exposure of hydrae to metal toxicants for 1 and 6-h did not induce HSP70 mRNA except to that of Zn and Cd for 1-h. It was also observed that expression of HSP70 mRNA had come to its normal levels in Zn (II) and Cd (II) exposed hydrae during 6-h. Alternatively this may be ascribed to the feed back inhibition mechanism that normally regulates

the HSP70 expression in organisms involving the heat shock transcription factor (HSF).

In the event of oxidative stress, H_2O_2 did not induce EC-CuZnSOD mRNA at two different doses; however, paraquat induced EC-CuZnSOD mRNA only after 6-h of exposure though during 1-h exposure its expression was observed to be reduced. Therefore, the induction of EC-CuZnSOD mRNA by paraquat can be ascribed to duration of exposure, while in the case of oxidant H_2O_2 , the lack of change of expression of EC-CuZnSOD may be ascribed to dose and duration of exposure since the expression of EC-CuZnSOD was observed higher in the higher dose of H_2O_2 tested (9.79 mM). In the case of metal stress, only 1-h exposure to Zn and Cd did not change the expression of EC-CuZnSOD while others suppressed its expression. This suppression can be ascribed to cellular toxicity at higher doses which was observed in 6 h exposure studies (with the exception of Cd and Cr which induced EC-CuZnSOD mRNA expression). The induction of EC-CuZnSOD mRNA by Cd (II) may be related to the duration of exposure, while the induction of EC-CuZnSOD by Cr can't be described on the basis of current observation and needs further investigation.

These results indicated that the genes characterized in the current study are involved in the cellular stress response processes triggered by stress and contaminant exposure. Analysis of the results showed that starvation leads to the up-regulation of all the stress genes studied here. It may be concluded that starvation leads to a pro-oxidant situation that may play a role in up-regulation of

hydra stress genes, though other factors yet unknown may be involved in their regulation.

It is also observed that the same stressor at the same dose and duration of exposure transcriptionally regulate different genes differently. This may only reflect the differential sensitivity of different genes to different stressors. In a comparative qualitative assessment it was observed that MnSOD is only upregulated at higher temperature (37 °C) in comparison to EC-CuZnSOD (both 30 and 37 °C). Another observation was that copper is less involved in stress gene transcription whereas Zn is very much involved in their transcription as compared to other metals (Cd, Cr, As and Se). This may be ascribed to differential stress inducing ability Cu and Zn and to the limited experimental conditions.

In the absence of clear mechanistic study it is not possible to clearly explain the observed variations in gene expression (upregulation, downregulation and no regulation) seen in the current study. However, conclusions can be drawn on the basis certain hypotheses and observations made in other organisms and are described in detail in the discussion sections of each chapter and also above. The observed variation may be ascribed to dose and duration of exposure, deregulation of cellular metabolism, rate of mRNA synthesis and stability, etc.

As shown here, the presence of stress response in *H. vulgaris* can be correlated with a high level of resistance to environmental stress of the sort seen

in *H. vulgaris*. Also the presence of stress response can be attributable to its presence and survival in a wide range of habitats (Bosch *et al.*, 1988) like that of *H. magnipapillata* but not like *H. oligactis*. Such habitats would be characterized by fluctuating temperature, presence of heavy metal ions, etc. In other words, it may be stated that selection to retain a strong stress response is characteristic of *H. vulgaris* living in relatively unstable habitats (Bosch *et al.*, 1988). Hence *H. vulgaris*, like *H. magnipapillata*, can colonize more stressful environments with a wide range of stressors. The findings imply that the induction of stress response may be a consequence of adaptations of life in different habitats (Brennecke *et al.*, 1998) and has ecological advantage for *H. vulgaris*.

Owing to their responsiveness to diverse forms of stress, stress response genes have undergone widespread application in biomonitoring and environmental toxicology (Feder and Hofmann, 1999; de Pomerai, 1996; Sanders and Dyer, 1994; Ryan and Hightower, 1996) especially in aquatic organisms. In many cases, heat shock proteins (HSPs) are useful biomarkers because they are sensitive to induction by stress than traditional indices such as growth inhibition. For example, exposing freshwater sponges to pollutants extracted from river water elevates HSP70 levels, which further increase when thermal stress is also imposed (Mueller *et al.*, 1995). Additional examples of HSP expression in aquatic toxicology concern rotifers (Cochrane *et al.*, 1991), marine sponges (Krasko *et al.*, 1997), amphipods (Werner and Nagel, 1997), polychaetes (Ruffin *et al.*, 1994), mollusks (Steinert and Pickwell, 1988;

Veldhuizen *et al.*, 1991; Nascimento *et al.*, 1996; Sanders and Dyer, 1994), and fish (Ryan and Hightower, 1994; Dyer *et al.*, 1993; Vijayan *et al.*, 1997). Other applications purposefully deploy organisms in potentially polluted aquatic systems as biosensors (Van Dyk *et al.*, 1994, Veldhuizen *et al.*, 1991). Similarly the characterization of hydra HSP70, EC-CuZnSOD, MnSOD, PHGPx and catalase mRNA levels studied under different experimental conditions in this research may find application in biomonitoring and environmental toxicology.

Some aspects of stress response in organisms present problems and ambiguities for the use of stress proteins as biomarkers in environmental toxicology. Because so many different stresses induce stress genes, it may be difficult to attribute changes in stress gene expression to any particular environmental stress. Organisms in the field often undergo multiple stresses simultaneously, the interaction of which can yield significant stress gene and protein expression even when no single toxicant is at harmful levels. Conversely, stress genes induced by another stress can enhance tolerance of a toxicant whose presence is being monitored. Numerous laboratory studies have demonstrated the difficulty of teasing apart environmental factors and attributing stress gene induction to a single stressor. For example, freshwater sponges exhibit greater tolerance of pollutants following a sublethal heat stress (Mueller *et al.*, 1995). Among the vertebrates, diseased fish have elevated levels of HSPs in their tissues, and disease-related expression may interfere with the use of HSPs as a biomarker (Forsyth *et al.*, 1997). Thus, because numerous factors

can induce HSP expression and stress tolerance, the utility of HSPs as biomarkers of environmental toxicity has been described as limited (Feder and Hofmann, 1999). Similar problems might be encountered in assessing other stress genes as biomarkers of environmental toxicity.

In spite of the difficulty in attributing stress gene induction to a single stressor, the premise that hydra stress genes can respond to stressors and contaminants, can constitute a molecular biomarker system (MBS) to assess quality of an aquatic environment or pro-oxidant quality of chemicals. The repertoire of MBS parameters can be expanded to other genes and proteins and their responses to xenobiotics, pesticides, herbicides, heavy metals, etc. can be studied in hydra. Antibody or spectrophotometric assays could be developed to assay MBS parameters. Employing MBS to address ecological or environmental contamination questions would require the rigorous experimental designs and statistical methods as used by human medical diagnostic technology and analysis (Schaeffer *et al.*, 1988). These MBS techniques could be advanced to robotic high-throughput microarray, ELISA and spectrophotometric assays to meet large assay designs and sampling requirements.

In order to better understand the basis of stress response in *H. vulgaris*, as observed in this research, further study is warranted. Future studies should focus and address the following areas: (i) the number of stress response elements (STRE), metal binding elements (MBE) and other transcription factor binding sites in their 5' non-coding region and assay their role in stress gene

regulation; (ii) the stability of mRNA levels under different treatment conditions; (iii) protein synthesis levels under different conditions, (iv) enzyme activity under different treatment conditions; (v) time and dose dependent expression of stress gene mRNA and protein levels and their correlation with each other and treatments; (vi) tissue specificity of stress gene expression; (vii) existence of transcription factors that regulate the expression of stress genes such as heat shock factor (HSF) that activate HSP70, Cu trans-activator that control the expression of yeast Cu/Zn SOD, etc; (vi) the physiological levels of α -tocopherol, ascorbate, tripeptide glutathione; (vii) dose-equivalent studies to compare the stress generating ability of individual stressors; etc.

This research showed that hydra stress genes respond to a variety of stressors and contaminants and these results suggest that hydra may serve as a molecular biomarker system (MBS) to assess quality of an aquatic environment. The same suite of genes can be assayed in a laboratory set up to assess the stress and radical generating capacity of compounds and pharmaceuticals. In other words the hydrae can be used to assess the oxidant and pro-oxidant quality of several chemicals as was demonstrated in this work.

REFERENCES

- Ait-Aissa, S., Ausseil, O., Palluel, O., Vindimian, E., Garnier-Laplace, J., and Porcher, J. M. (2003). Biomarker responses in juvenile rainbow trout (*Oncorhynchus mykiss*) after single and combined exposure to low doses of cadmium, zinc, PCB77 and 17beta-oestradiol. *Biomarkers* **8**, 491-508.
- Ake, C. L., Wiles, M. C., Huebner, H. J., McDonald, T. J., Cosgriff, D., Richardson, M. B., Donnelly, K. C., and Phillips, T. D. (2003). Porous organoclay composite for the sorption of polycyclic aromatic hydrocarbons and pentachlorophenol from groundwater. *Chemosphere* **51**, 835-844.
- Allgood, G. S., and Perry, J. J. (1986). Characterization of a manganese containing catalase from the obligate thermophile *Thermoleophilum album*. *J. Bacteriol.* **168**, 563-567.
- Alphey, M. S., Bond, C. S., Tetaud, E., Fairlamb, A. H., and Hunter, W. N. (2000). The structure of reduced trypanothione peroxidase reveals a decamer and insight into reactivity of 2Cys-peroxiredoxins *J. Mol. Biol.* **300**, 903-916.
- Amin, V., Cumming, D. V., and Latchman, D. S. (1996). Over-expression of heat shock protein 70 protects neuronal cells against both thermal and ischaemic stress but with different efficiencies. *Neurosci. Lett.* **206**, 45-48.
- Anderson, P. A., and Spencer, A. N. (1989). The importance of cnidarian synapses for neurobiology. *J. Neurobiol.* **20**, 435-457.
- Angelova, M. B., Pashova, S. B., Spasova, B. K., Vassilev, S. V., and Slokoska, L.S. (2005). Oxidative stress response of filamentous fungi induced by hydrogen peroxide and paraquat. *Mycol. Res.* **109**, 150-158.
- Apel, K., and Hirt, H. (2004). Reactive oxygen species: Metabolism, oxidative stress, and signal transduction. *Annu. Rev. Plant. Biol.* **55**, 373-399.

- Arai, M., Imai, H., Koumura, T., Yoshida, M., Emoto, K., Umeda, M., Chiba, N., and Nakagawa, Y. (1999). Mitochondrial phospholipids hydroperoxide glutathione peroxidase plays a major role in preventing oxidative injury to cells. *J. Biol. Chem.* **274**, 4924-4933.
- Arkhipchuk, V. V., Goncharuk, V. V., Chernykh, V. P., Maloshtan, L. N., and Gritsenko, I. S. (2004). Use of a complex approach for assessment of metamizole sodium and acetylsalicylic acid toxicity, genotoxicity and cytotoxicity. *J. Appl. Toxicol.* **24**, 401-417.
- Artinger, M., Blitz, I., Inoue, K., Tran, U., and Cho, K. W. Y. (1997). Interaction of goosecoid and brachyury in *Xenopus* mesoderm patterning. *Mech. Dev.* **65**, 187-196.
- Asada, K. S., Kanematsu, S., and Ushida, K. (1977). Superoxide dismutases in photosynthetic organisms: Absence of cuprozinc enzyme in Eukaryotic algae. *Arch. Biochem. Biophys.* **179**, 243-256.
- Atsushi, T., Yuya, A., Ken-Ichi, K., and Hiroo, Y. (2002). Copper/zinc superoxide dismutases in *Dictyostelium discoideum*: Amino acid sequences and expression kinetics. *J. Biochem. Mol. Biol. Biophys.* **6**, 215-220.
- Ayala, F.J., and Rzhetsky, A. (1998). Origin of the metazoan phyla: Molecular clocks confirm paleontological estimates. *Proc. Natl. Acad. Sci. U. S. A.* **95**, 606-611.
- Bannister, J. V., Bannister, W. H., and Rotilio, G. (1987). Aspects of the structure, function, and applications of superoxide dismutase. *CRC Crit. Rev. Biochem.* **22**, 111-180.
- Basu, N., Todgham, A. E., Ackerman, P. A., Bibeau, M. R., Nakano, K., Schulte, P. M., and Iwama, G. K. (2002). Heat shock protein genes and their functional significance in fish. *Gene* **7**, 173-183.
- Bates, P. A., Kelley, L. A., MacCallum, R. M., and Sternber, M. J. E. (2001). Enhancement of protein modeling by human intervention in applying the

- automatic programs 3D-JIGSAW and 3D-PSSM. *Proteins Suppl.* **5**, 39-46.
- Beach, M. J., and Pascoe, D. (1998). The role of *Hydra vulgaris* (Pallas) in assessing the toxicity of freshwater pollutants. *Water Res.* **32**, 101-106.
- Bellis, S. L., Grosvenor, W., Kass-Simon, G., and Rhoads, D. E. (1991). Chemoreception in *Hydra vulgaris* (*attenuata*): Initial characterization of two distinct binding sites for L-glutamic acid. *Biochem. Biophys. Acta* **1061**, 89 -94.
- Bienz, M. (1985). Transient and developmental activation of heat-shock genes. *Trends Biochem. Sci.* **10**, 157-61.
- Bienz, M., and Pelham, H. R. B. (1987). Mechanisms of heat-shock gene activation in higher eukaryotes. *Adv. Genet.* **24**, 31-72.
- Black, R. E., and Bloom, L. (1984). Heat shock proteins in *Aurelia* (Cnidaria, Scyphozoa). *J. Exp. Zool.* **230**, 303-307.
- Blair, J. E., Ikeo, K., Gojobori, T., and Hedges, S. B. (2002). The evolutionary position of nematodes. *BMC Evol. Biol.* **2**, 7.
- Bock, A., Forchhammer, K., Heider, J., Leinfelder, W., Sawers, G., Veprek, B., and Zinoni, F. (1991). Selenocysteine: The 21st amino acid. *Mol. Microbiol.* **5**, 515-520.
- Bode, H. R. (1996). The interstitial cell lineage of hydra: A stem cell system that arose early in evolution. *J. Cell Sci.* **109**, 1155-1164.
- Bode, H. R., Dunne, J., Heimfeld, S., Huang, L., Javois, L., Koizumi, O., Westerfield, J., and Yaross, M. (1986). Transdifferentiation occurs continuously in adult hydra. *Curr. Top. Dev. Biol.* **20**, 257-280.

- Borgstahl, G. E. O., Parge, H. E., Hickey, M. J., Beyer, W. F., Hallewell, R. A., and Tainer, T. A. (1992). The structure of human mitochondrial manganese superoxide dismutase reveals a novel tetrameric interface of two 4-helix bundles. *Cell* **71**, 107- 118.
- Bosch, T. C. G., Krylow, S. M., Bode, H. R., and Steele, R. E. (1988). Thermotolerance and synthesis of heat shock proteins: These responses are present in *Hydra attenuata* but absent in *Hydra oligactis*. *Proc. Natl. Acad. Sci. U. S. A.* **85**, 7927-7931.
- Bosch, T. C. G. (1998). Hydra. In *Cellular and Molecular Basis of Regeneration: From Invertebrates to Humans* (P. Ferretti and J. Geraudie, Eds.), pp. 111-134. Wiley, New York.
- Bosch, T. C., and David, C. N. (1984). Growth regulation in Hydra: Relationship between epithelial cell cycle length and growth rate. *Dev. Biol.* **104**, 161-171.
- Bottger, A., Alexandrova, O., Cikala, M., Schade, M., Herold, M., and David, C. N. (2002). GFP expression in hydra: Lessons from the particle gun. *Dev. Genes Evol.* **212**, 302-305.
- Boutet, I., Tanguy, A., and Moraga, D. (2003a). Organization and nucleotide sequence of the European flat oyster *Ostrea edulis* heat shock cognate 70 (hsc70) and heat shock protein 70 (hsp70) genes. *Aquat. Toxicol.* **65**, 221-225.
- Boutet, I., Tanguy, A., Rousseau, S., Auffret, M., and Moraga, D. (2003b). Molecular identification and expression of heat shock cognate 70 (hsc70) and heat shock protein 70 (hsp70) genes in the Pacific oyster *Crassostrea gigas*. *Cell Stress Chaperones* **8**, 76-85.
- Bowie, J. U., Luthy, R., and Eisenberg, D. (1991). A method to identify protein sequences that fold into a known three-dimensional structure. *Science* **253**, 164-170.

- Brennecke, T., Gellner, K., and Bosch, T. C. (1998). The lack of a stress response in *Hydra oligactis* is due to reduced hsp70 mRNA stability. *Eur. J. Biochem.* **255**, 703-709.
- Broun, M., Sokol, S., and Bode, H. R. (1999). Cngsc, a homologue of goosecoid, participates in the patterning of the head, and is expressed in the organizer region of hydra. *Development* **126**, 5245-5254.
- Brouwer, M., Hoexum, B. T., Grater, W., and Brown-Peterson, N. (2003). Replacement of a cytosolic copper/zinc superoxide dismutase by a novel cytosolic manganese superoxide dismutase in crustaceans that use copper (haemocyanin) for oxygen transport. *Biochem. J.* **374**, 219-228.
- Brown, B. E., Downs, C. A., Dunne, R. P., and Gibb, S. W. (2002). Exploring the basis of thermotolerance in the reef coral *Goniastrea aspera*. *Mar. Ecol. Prog. Ser.* **242**, 119-129.
- Browne, E. N. (1909). The production of new hydrants in hydra by insertion of small grafts. *J. Exp. Zool.* **7**, 1-23.
- Buettner, G. R. (1993). The pecking order of free radicals and antioxidants: Lipid peroxidation, alpha-tocopherol, and ascorbate. *Arch. Biochem. Biophys.* **300**, 535-543.
- Burton, G. A. Jr., Greenberg, M. S., Rowland, C. D., Irvine, C. A., Lavoie, D. R., Brooker, J. A., Moore, L., Raymer, D. F., and McWilliam, R. A. (2005). *In situ* exposures using caged organisms: A multi-compartment approach to detect aquatic toxicity and bioaccumulation. *Environ. Pollut.* **134**, 133-144.
- Campbell, R. D. (1988). The nematocyte: An encapsulation of developmental processes. In *The Biology of Nematocysts* (D. A. Hessinger and H. M. Lenhoff, Eds.), pp. 115-121. Academic Press, San Diego.
- Campbell, R. D., and Marcum, B. A. (1980). Nematocyte migration in hydra: Evidence for contact guidance *in vivo*. *J. Cell Sci.* **41**, 33-51.

- Campbell, W. S., and Laudenbach, D. E. (1995). Characterization of four superoxide dismutase genes from a filamentous cyanobacterium. *J. Bacteriol.* **177**, 964-972.
- Capo, C., Stroppolo, M. E., Galtieri, A., Lania, A., Costanzo, S., Petruzzelli, R., Calabrese, L., Polticelli, F., and Desideri, A. (1997). Characterization of Cu, Zn superoxide dismutase from the bathophile fish, *Lampanyctus crodonilus*. *Comp. Biochem. Physiol.* **117B**, 404-407.
- Cardoso, R. M. F., Thayer, M. M., Didonato, M., Lo, T. P., Bruns, C. K., Getzoff, E. D., and Tainer, J. A. (2002). Insights into Lou Gehrig's disease from the structure and instability of the A4V mutant of Cu, Zn superoxide dismutase. *J. Mol. Biol.* **324**, 247-256.
- Carloz, A., Ludwig, M. L., Stallings, W. C., Fee, J. A., Steinman, H. M., and Touati, D. (1988). Iron superoxide dismutase: Nucleotide sequence of the gene from *Escherichia coli* K12 and correlations with crystal structures. *J. Biol. Chem.* **263**, 1555-1562.
- Carloz, A., and Touati, D. (1986). Isolation of superoxide dismutase mutants in *Escherichia coli*: Is superoxide dismutase necessary for aerobic life? *EMBO J.* **5**, 623-630.
- Carugo, K. D., Battistoni, A., Carri, M. T., Polticelli, F., Desideri, A., Rotilio, G., Coda, A., and Bolognesi, M. (1994). Crystal structure of the cyanide-inhibited *Xenopus laevis* Cu, Zn superoxide dismutase at 98 K. *FEBS Lett.* **349**, 93-98.
- Chang, M. S., Yoo, H. Y., and Rho, H. M. (2002). Transcriptional regulation and environmental induction of gene encoding copper- and zinc-containing superoxide dismutase. *Meth. Enzymol.* **349**, 293-305.
- Chelikani, P., Fita, I., and Loewen, P. C. (2004). Diversity of structures and properties among catalases. *Cell. Mol. Life Sci.* **61**, 192-208.

- Chen, C. J., Huang, H. S., Lee, Y. T., Yang, C. Y., and Chang, W. C. (1997). Characterization and purification of a lipoxygenase inhibitor in human epidermoid carcinoma A431 cells. *Biochem. J.* **327**, 193-198.
- Chen, C. J., Huang, H. S., Lin, S. B., and Chang, W. C. (2000). Regulation of cyclooxygenase and 12-lipoxygenase catalysis by phospholipids hydroperoxide glutathione peroxidase in A431 cells. *Prostaglandins Leukot. Essent. Fatty Acids* **62**, 261-268.
- Choresch, O., Loya, Y., Muller, W. E., Wiedenmann, J., and Azem, A. (2004). The mitochondrial 60-kDa heat shock protein in marine invertebrates: Biochemical purification and molecular characterization. *Cell Stress Chaperones* **9**, 38-48.
- Chu, F. F., Doroshov, J. H., and Esworthy, R. S. (1993). Expression, characterization, and tissue distribution of a new cellular selenium dependent glutathione peroxidase, GSHPx-GI. *J. Biol. Chem.* **268**, 2571-2576.
- Cikala, M., Wilm, B., Hobmayer, E., Bottger, A., and David, C. N (1999). Identification of caspases and apoptosis in the simple metazoan Hydra. *Curr. Biol.* **9**, 959-962.
- Clegg, J. S., Uhlinger, K. R., Jackson, S. A., Cherr, G. N., Rifkin, E., and Friedman, C. S. (1998). Induced thermotolerance and the heat shock protein-70 family in the Pacific oyster, *Crassostrea gigas*. *Mol. Marine Biol. Biotechnol.* **7**, 21-30.
- Cochrane, B. J., Irby, R. B., and Snell, T. W. (1991). Effects of copper and tributyltin on stress protein abundance in the rotifer *Brachionus plicatilis*. *Comp. Biochem. Physiol.* **98C**, 385-390.
- Colasanti, M., Venturini, G., Merante, A., Musci, G., and Lauro, G.M. (1997). Nitric oxide involvement in *Hydra vulgaris* very primitive olfactory-like system. *J. Neurosci.* **17**, 493-499.

- Coleman, J. S., Heckathorne, S. A., and Hallberg, R. L. (1995). Heat shock proteins and thermotolerance: Linking molecular and ecological perspectives. *Trends Ecol. Evol.* **10**, 305-306.
- Craig, E. A. (1985). The heat shock response. *CRC Crit. Rev. Biochem.* **18**, 239-280.
- Cramer, R., Faith, A., Hemmann, S., Jaussi, R., Ismail, C., Menz, G., and Blaser, K. (1996). Humoral and cell-mediated autoimmunity in allergy to *Aspergillus fumigatus*. *J. Exp. Med.* **184**, 265-270.
- David, C. N. (1973). A quantitative method for maceration of hydra tissue. *Roux' Archiv. Dev. Biol.* **171**, 259-268.
- David, C. N., and Campbell, R. D. (1972). Cell cycle kinetics and development of *Hydra attenuata*. I. Epithelial cells. *J. Cell Sci.* **11**, 557-568.
- de Haan, J. B., Bladier, C., Griffiths, P., Kelner, M., O'Shea, R. D., Cheung, N. S., Bronson, R. T., Silvestro, M. J., Wild, S., Zheng, S. S., Beart, P. M., Hertzog, P. J., and Kola, I. (1998). Mice with a homozygous null mutation for the most abundant glutathione peroxidase, Gpx1, show increased susceptibility to the oxidative stress-inducing agents paraquat and hydrogen peroxide. *J. Biol. Chem.* **273**, 22528-22536.
- De Petrocellis, L., Melck, D., Bisogno, T., Milone, A., and Di Marzo, V. (1999). Finding of the endocannabinoid signalling system in hydra, a very primitive organism: Possible role in the feeding response. *Neuroscience* **92**, 377-387.
- de Pomerai, D. (1996). Heat-shock proteins as biomarkers of pollution. *Hum. Exp. Toxicol.* **15**, 279-285.
- Del Razo, L. M., Quintanilla-Vega, B., Brambila-Colombres, E., Calderon-Aranda, E. S., Manno, M., and Albores, A. (2001). Stress proteins induced by arsenic. *Toxicol. Appl. Pharmacol.* **177**, 132-148.

- Demand, J., Luders, J., and Hohfeld, J. (1998). The carboxy-terminal domain of HSC70 provides binding sites for a distinct set of chaperone cofactors. *Mol. Cell. Biol.* **18**, 2023-2028.
- Di Giulio, R. T., Washburn, P. C., Wenning, R. J., Winston, G. W., and Jewell, C. S. (1989). Biochemical responses in aquatic animals: A review of oxidative stress. *Environ. Toxicol. Chem.* **8**, 1103-1123.
- Ditlow, C., Johansen, J. T., Martin, B. M., and Svendsen, I. (1982). The complete amino acid sequence of manganese-superoxide dismutase from *Saccharomyces cerevisiae*. *Carlsberg Res. Commun.* **47**, 81-91.
- Docampo, R., and Moreno, S. N. J. (1984). Free-radical intermediates in the antiparasitic action of drugs and phagocytic cells. In *Free Radicals in Biology* (W. A. Pryor, Ed.), pp. 243-288. Academic Press, New York.
- Downs, C. A., Fauth, J. E., Halas, J. C., Dustan, P., Bemiss, J., and Woodley, C. M. (2002). Oxidative stress and seasonal coral bleaching. *Free Radic. Biol. Med.* **33**, 533-543.
- Downs, C. A., Mueller, E., Phillips, S., Fauth, J. E., and Woodley, C.M. (2001). A molecular biomarker system for assessing the health of coral (*Montastraea faveolata*) during heat stress. *Mar. Biotechnol.* **2**, 533-544.
- Doyotte, A., Cossu, C., Jacquin, M. C., Babut, M., and Vasseur, P. (1997). Antioxidant enzymes, glutathione and lipid peroxidation as relevant biomarkers of experimental or field exposure in the gills and the digestive gland of the freshwater bivalve *Unio timidus*. *Aquat. Toxicol.* **39**, 93-110.
- Dunlap, D. Y., and Matsumura, F. (1997). Development of broad spectrum antibodies to heat shock protein 70s as biomarkers for detection of multiple stress by pollutants and environmental factors. *Ecotoxicol. Environ. Saf.* **37**, 238-244.

- Dunlap, W. C., Shick, J. M., and Yamamoto, Y. (1999). Sunscreens, oxidative stress and antioxidant functions in marine organisms of the Great Barrier Reef. *Redox Rep.* **4**, 301-306.
- Dunlap, W. C., Shick, J. M., and Yamamoto, Y. (2000). Ultraviolet (UV) protection in marine organisms I: Sunscreens, oxidative stress and antioxidants. In *Free Radicals in Chemistry, Biology and Medicine* (S. Yoshikawa, S. Toyokuni, *et al.*, Eds.), pp. 200-214. OICA Int., London.
- Dworniczak, B., and Mirault, M. E. (1987). Structure and expression of a human gene coding for a 71 kDa heat shock 'cognate' protein. *Nucleic Acids Res.* **15**, 5181-5197.
- Dyer, S. D., Brooks, G. L., Dickson, K. L., Sanders, B. M., and Zimmerman, E. G. (1993). Synthesis and accumulation of stress proteins in tissues of arsenite-exposed fathead minnows *Pimephales promelas*. *Environ. Toxicol. Chem.* **12**, 913-24
- Dyken, J. A., and Shick, J. M. (1982). Oxygen production by endosymbiotic algae controls superoxide dismutase activity in their animal host. *Nature* **297**, 579-585.
- Dyken, J. A., and Shick, J. M. (1984). Photobiology of the symbiotic sea anemone, *Anthopleura elegantissima* defenses against photodynamic effects, and seasonal photoacclimatization, *Biol. Bull.* **167**, 683-697.
- Dyken, J. A., Shick, J. M., Benoit, C., Buettner, G. R., and Winston, G. W. (1992). Oxygen radical production in the sea anemone *Anthopleura elegantissima* and its endosymbiotic algae. *J. Exp. Biol.* **168**, 219-241.
- Farr, S. B., Dari, R., and Touati, D. (1986). Oxygen-dependent mutagenesis in *E. coli* lacking superoxide dismutase. *Proc. Natl. Acad. Sci. U. S. A.* **83**, 8268-8272.
- Fattman, C. L., Schaefer, L. M., and Oury, T. D. (2003). Extracellular superoxide dismutase in biology and medicine. *Free Radic. Biol. Med.* **35**, 236-256.

- Feder, M. E., and Hofmann, G. E. (1999). Heat-shock proteins, molecular chaperones, and the stress response: Evolutionary and ecological physiology. *Annu. Rev. Physiol.* **61**, 243-82.
- Felsenstein, J. (1985). Confidence limits on phylogenies: An approach using the bootstrap. *Evolution* **39**, 783-791.
- Felsenstein, J. (1993). PHYLIP (PHYLogeny Inference Package) version 3.6a2. Department of Genetics, University of Washington, Seattle, WA.
- Field, K. G., Olsen, G. J., Lane, D. J., Giovannoni, S. J., Ghiselin, M. T., Raff, E. C., Pace, N., and Raff, R. A. (1988). Molecular phylogeny of the animal kingdom. *Science* **239**, 748-753.
- Fischer, D. (2000). Hybrid fold recognition: Combining sequence derived properties with evolutionary information. *Pac. Symp. Biocomput.* **5**, 116-127.
- Flaherty, K. M., DeLuca-Flaherty, C., and McKay, D. B. (1990). Three-dimensional structure of the ATPase fragment of a 70K heat-shock cognate protein. *Nature* **346**, 623-628.
- Forsyth, R. B., Candido, E. P. M., Babich, S. L., and Iwama, G. K. (1997). Stress protein expression in coho salmon with bacterial kidney disease. *J. Aquat. Anim. Health* **9**, 18-25.
- Frei, B., Stocker, R., and Ames, B. N. (1992). Small molecule antioxidant defenses in human extracellular fluids. In *Molecular Biology of Free Radical Scavenging Systems* (J. G. Scandalios, Ed.), pp. 23-45. Cold Spring Harbor Laboratory Press. New York.
- Fridovich, I. (1975). Superoxide dismutases. *Annu. Rev. Biochem.* **44**, 147-159.
- Fridovich, I. (1995). Superoxide radical and superoxide dismutases. *Annu. Rev. Biochem.* **64**, 97-112.

- Fujii, J., Nakata, T., Miyoshi, E., Ikeda, Y., and Taniguchi, N. (1994). Induction of manganese superoxide dismutase mRNA by okadaic acid and protein synthesis inhibitors. *Biochem. J.* **301**, 31-34.
- Fujii, J., and Taniguchi, N. (1991). Phorbol ester induces manganese-superoxide dismutase in tumor necrosis factor-resistant cells. *J. Biol. Chem.* **266**, 23142-23146.
- Fujii, M., Ishii, N., Joguchi, A., Yasuda, K., and Ayusawa, D. (1998). A novel superoxide dismutase gene encoding membrane-bound and extracellular isoforms by alternative splicing in *Caenorhabditis elegans*. *DNA Res.* **5**, 25-30.
- Fujisawa, T., and David, C. N. (1984). Loss of differentiating nematocytes induced by regeneration and wound healing in *Hydra*. *J. Cell Sci.* **68**, 243-255.
- Fukuhori, N., Kitano, M., and Kimura, H. (2005). Toxic effects of bisphenol A on sexual and asexual reproduction in *Hydra oligactis*. *Arch. Environ. Contam. Toxicol.* **48**, 495-500.
- Galaris, D., and Evangelou, A. (2002). The role of oxidative stress in mechanisms of metal-induced carcinogenesis. *Crit. Rev. Oncol. Hematol.* **42**, 93-103.
- Gamble, S. C., Goldfarb, P., Porte, C., and Livingstone, D. R. (1995). Glutathione peroxidase function in marine invertebrates. *Mar. Environ. Res.* **39**, 191-195.
- Garnier, J., Gibrat, J. F., and Robson, B. (1996). GOR secondary structure prediction method version IV. In *Methods in Enzymology* (R. F. Doolittle, Ed.) 540-553. Academic Press, New York.
- Gauchat, D., Escriva, H., Miljkovic-Licina, M., Chera, S., Langlois, M. C., Begue, A., Laudet, V., and Galliot, B. (2004). The orphan COUP-TF nuclear receptors are markers for neurogenesis from cnidarians to vertebrates. *Dev. Biol.* **275**, 104-123.

- Geiger, P. G., Thomas, J. P., and Girotti, A.W. (1991). Lethal damage to murine L1210 cells by exogenous lipid hydroperoxides: Protective role of glutathione-dependent selenoperoxidases. *Arch. Biochem. Biophys.* **288**, 671-680.
- Gellner, K., Praetzel, G., and Bosch, T. C. (1992). Cloning and expression of a heat-inducible hsp70 gene in two species of *Hydra* which differ in their stress response. *Eur. J. Biochem.* **210**, 683-691.
- Geret, F., Serafim, A., Barreira, L., and Bebianno, M. J. (2002). Effect of cadmium on antioxidant enzyme activities and lipid peroxidation in the gills of the clam *Ruditapes decussatus*. *Biomarkers* **7**, 242-256.
- Gething, M. J., and Sambrook, J. P. (1992). Protein folding in the cell. *Nature* **355**, 33-45.
- Getzoff, E. D., Tainer, J. A., Weiner, P. K., Kollman, P. A., Richardson, J. S., and Richardson, D. C. (1983). Electrostatic recognition between superoxide and copper, zinc superoxide dismutase. *Nature* **306**, 287-290.
- Ghyselinck, N. B., and Dufaure, J. P. (1990). A mouse cDNA sequence for epididymal androgen-regulated proteins related to glutathione peroxidase. *Nucleic Acids Res.* **18**, 7144.
- Golstein, P., Aubry, L., and Levraud, J. P. (2003). Cell-death alternative model organisms: Why and which? *Nat. Rev. Mol. Cell. Biol.* **4**, 798-807.
- Gourdon, I., Gricourt, L., Kellner, K., Roch, P., and Escoubas, J. M., (2000). Characterization of a cDNA encoding a 72 kDa heat shock cognate protein (Hsc72) from the Pacific oyster, *Crassostrea gigas*. *DNA Seq.* **11**, 265-270.
- Grens, A., Gee, L., Fisher, D. A., and Bode, H. (1996). CnNK-2, an NK-2 homeobox gene, has a role in patterning the basal end of the axis in hydra. *Dev. Biol.* **180**, 473-488.

- Grigoriev, N. G., Spafford, J. D., and Spencer, A. N. (1999). Modulation of jellyfish potassium channels by external potassium ions. *J. Neurophysiol.* **82**, 1728-1739.
- Grimmelikhuijzen, C. J., Graff, D., Koizumi, O., Westfall, J. A., and McFarlane, I. D. (1989). Neurons and their peptide transmitters in coelenterates. In *Evolution of the First Nervous Systems* (P.A.V. Anderson, Ed.), pp. 95-109. NATO Series, Serie A. Life Sciences, vol. 188, Plenum Press, New York.
- Grimmelikhuijzen, C. J., and Westfall, J. A. (1995). The nervous systems of cnidarians. *Experiment* **72**, 7-24.
- Guex, N., and Peitsch, M. C. (1997). SWISS-MODEL and the Swiss-PdbViewer: An environment for comparative protein modeling. *Electrophoresis* **18**, 2714-2723.
- Guindon, S., and Gascuel, O. (2003). A simple, fast, and accurate algorithm to estimate large phylogenies by maximum likelihood. *Syst. Biol.* **52**, 696-704.
- Hai, D. Q., Varga, S. I., and Matkovics, B. (1997). Organophosphate effects on antioxidant system of carp (*Cyprinus carpio*) and catfish (*Ictalurus nebulosus*). *Comp. Biochem. Physiol.* **117C**, 83-88.
- Halliwell, B., and Gutteridge, J. M. C. (1999). *Free Radicals in Biology and Medicine*. Oxford University Press, Oxford, England.
- Hand, S. C., and Hardewig, I. (1996). Down regulation of cellular metabolism during environmental stress: Mechanisms and implications. *Annu. Rev. Physiol.* **58**, 539-563.
- Harland, R., and Gerhart, J. (1997). Formation and function of Spemanns organizer. *Annu. Rev. Cell. Dev. Biol.* **13**, 611-667.

- Hart, P. J., Balbirnie, M. M., Ogihara, N. L., Nersissian, A. M., Weiss, M. S., Valentine, J. S., and Eisenberg, D. (1999). A structure-based mechanism for copper-zinc superoxide dismutase. *Biochemistry* **38**, 2167-2178.
- Hartl, F. U. (1996). Molecular chaperones in cellular protein folding. *Nature* **381**, 571-579.
- Hartl, F. U., and Neupert, W. (1990). Protein sorting to mitochondria: Evolutionary conservations of folding and assembly. *Science* **247**, 930-938.
- Hawkrigde, J. M., Pipe, R. K., and Brown, B. E. (2000). Localisation of antioxidant enzymes in the cnidarians *Anemonia viridis* and *Goniopora stokesi*. *Mar. Biol.* **137**, 1-9.
- Hayakawa, E., Fujisawa, C., and Fujisawa, T. (2004). Involvement of Hydra achaete-scute gene CnASH in the differentiation pathway of sensory neurons in the tentacles. *Dev. Genes Evol.* **214**, 486-492.
- Hayes, R. L., and King, C. M. (1995). Induction of 70 kDa heat shock protein in scleractinian corals by elevated temperature: Significance for coral bleaching. *Mol. Mar. Biol. Biotechnol.* **4**, 36-42.
- Hayward, D. C., Samuel, G., Pontynen, P. C., Catmull, J., Saint, R., Miller, D. J., and Ball, E. E. (2002). Localized expression of a dpp/BMP2/4 ortholog in a coral embryo. *Proc. Natl. Acad. Sci. U. S. A.* **99**, 8106-8111.
- Hearn, A. S., Stroupe, M. E., Cabelli, D. E., Ramilo, C. A., Luba, J. P., Tainer, J. A., Nick, H. S., and Silverman, D. N. (2003). Catalytic and structural effects of amino acid substitution at histidine 30 in human manganese superoxide dismutase: Insertion of valine C gamma into the substrate access channel. *Biochemistry* **42**, 2781-2789.
- Henkle-Duhrsen, K., Tawe, W., Warnecke, C., and Walter, R. D. (1995). Characterization of the manganese superoxide dismutase cDNA and

- gene from the human parasite *Onchocerca volvulus*. *Biochem. J.* **308**, 441-446.
- Hetherington, L. H., Livingstone, D. R., and Walker, C. H. (1996). Two-and one-electron dependent *in vitro* reductive metabolism of nitroaromatics by *Mytilus edulis*, *Carcinus maenas* and *Asterias rubens*. *Comp. Biochem. Physiol.* **113C**, 231-239.
- Hightower, L. E. (1993). A brief perspective on the heat-shock response and stress proteins. *Mar. Environ. Res.* **35**, 79-83.
- Hobmayer, B., Rentzsch, F., Kuhn, K., Happel, C. M., von Laue, C. C., Snyder, P., Rothbacher, U., and Holstein, T. W. (2000). Wnt signalling molecules act in axis formation in the diploblastic metazoan hydra. *Nature* **407**, 186-189.
- Hoffmeister-Ullerich, S. A., Herrmann, D., Kielholz, J., Schweizer, M., Schaller, H. C. (2002). Isolation of a putative peroxidase, a target for factors controlling foot-formation in the coelenterate hydra. *Eur. J. Biochem.* **269**, 4597-4606.
- Holdway, D. A., Lok, K., and Semaan, M. (2001). The acute and chronic toxicity of cadmium and zinc to two hydra species. *Environ. Toxicol.* **16**, 557-565.
- Holland, P. W. (1999). The future of evolutionary developmental biology. *Nature* **402**, C41-C44.
- Holley, S. A., Jackson, P. D., Sasai, Y., Lu, B., De Robertis, E. M., Hoffmann, F. M., and Ferguson, E. L. (1995). A conserved system for dorsal ventral patterning in insects and vertebrates involving sog and chordin. *Nature* **376**, 249-253.
- Hong Z., Kosman D. J., Thakur A., Rekosh D., and LoVerde P. T. (1992). Identification and purification of a second form of Cu/Zn superoxide dismutase from *Schistosoma mansoni*. *Infect. Immun.* **60**, 3641-3651.

- Huang, H. S., Chen, C. J., and Chang, W. C. (1999a). Inhibitory effect of phospholipid hydroperoxide glutathione peroxidase on the activity of lipoxygenases and cyclooxygenases. *Prostaglandins Other Lipid Mediat.* **58**, 65-75.
- Huang, Y., Wimler, K. M., and Carmichael, G. G. (1999b). Intronless mRNA transport elements may affect multiple steps of pre-mRNA processing. *EMBO J.* **18**, 1642-1652.
- Huebner, H. J., Mayura, K., Pallaroni, L., Ake, C. L., Lemke, S. L., Herrera, P., and Phillips, T. D. (2000). Development and characterization of a carbon-based composite material for reducing patulin levels in apple juice. *J. Food Prot.* **63**, 106-110.
- Hunt C., and Morimoto, R. I. (1985). Conserved features of eukaryotic hsp70 genes revealed by comparison with the nucleotide sequence of human hsp70. *Proc. Natl. Acad. Sci. U. S. A.* **82**, 6455-6459.
- Imlay, J. A., Chin, S. M., and Linn, S. (1988). Toxic DNA damage by hydrogen peroxide through the Fenton reaction *in vivo* and *in vitro*. *Science* **240**, 640-642.
- Ingolia, T. D., and Craig, E. A. (1982a). Drosophila gene related to the major heat shock-induced gene is transcribed at normal temperatures and not induced by heat shock. *Proc. Natl. Acad. Sci. U. S. A.* **79**, 525-529.
- Ingolia, T. D., Slater, M. J., and Craig, E. A. (1982b). *Saccharomyces cerevisiae* contains a complex multigene family related to the major heat shock-inducible gene of Drosophila. *Mol. Cell. Biol.* **2**, 1388-1398.
- Ishikawa, T., Ohta, Y., Takeda, T., Shigeoka, S., and Nishikimi, M. (1998). Increased cellular resistance to oxidative stress by expression of cyanobacterium catalase-peroxidase in animal cells. *FEBS Lett.* **426**, 221-224.

- Iyama, S., Okamoto, T., Sato, T., Yamauchi, N., Sato, Y., Sasaki, K., Takahashi, M., Tanaka, M., Adachi, T., Kogawa, K., Kato, J., Sakamaki, S., and Niitsu, Y. (2001). Treatment of murine collagen-induced arthritis by ex vivo extracellular superoxide dismutase gene transfer. *Arthritis Rheum.* **44**, 2160-2167.
- Jantzen, H., Hassel, M., and Schulze, I. (1998). Hydroperoxides mediate lithium effects on regeneration in *Hydra*. *Comp. Biochem. Physiol C Pharmacol. Toxicol. Endocrinol.* **119C**, 165-175.
- Jeziorski, M. C., Greenberg, R. M. and Anderson, P. A., (1999). Cloning and expression of a jellyfish calcium channel beta subunit reveal functional conservation of the alpha1-beta interaction. *Recept. Chann.* **6**, 375-386.
- Johansson, M. W., Holmblad, T., Thornqvist, P. O., Cammarata, M., Parrinello, N., and Soderhall, K. (1999). A cell-surface superoxide dismutase is a binding protein for peroxinectin, a cell-adhesive peroxidase in crayfish. *J. Cell Sci.* **112**, 917-925.
- Johnson, E. M., Gorman, R. M., Gabel, B. E., and George, M. E. (1982). The *Hydra attenuata* system for detection of teratogenic hazards. *Teratog. Carcinog. Mutagen.* **2**, 263-276.
- Jolly, C., and Morimoto, R. I. (2000). Role of the heat shock response and molecular chaperones in oncogenesis and cell death. *J. Natl. Cancer Inst.* **92**, 1564-1572.
- Jones, P. L., Kucera, G., Gordon, H., and Boss, J. M. (1995). Cloning and characterization of the murine manganous superoxide dismutase-encoding gene. *Gene* **153**, 155-161.
- Jones, P., and Wilson, I. (1978). *Catalases and Iron Complexes With Catalase-Like Properties*, Vol. 7. Marcel Dekker, New York.
- Kalafatic, M., Znidaric, D., and Lui, A. (1991a). Changes in *Hydra vulgaris* Pallas (Cnidaria) caused by the effect of Torak EC 24 insecticide. *Acta*

Hydrochimica. Et. Hydrobiologica **19**, 693-701.

- Kalafatic, M., Znidaric, D., Lui, A., and Wrischer, M. (1991b). Effect of insecticides (Dimilin WP 25, Torak EC 24 and Gamacid 20) on hydra (*Hydra vulgaris* Pallas). *Int. J. Dev. Biol.* **35**, 335-340.
- Kammenga, J. E., Dallinger, R., Donker, M. H., Kohler, H. R., Simonsen, V., Tribskorn, R., and Weeks, J. M. (2000). Biomarkers in terrestrial invertebrates for ecotoxicological soil risk assessment. *Rev. Environ. Contam. Toxicol.* **164**, 93-147.
- Karntanut, W., and Pascoe, D. (2000). A comparison of methods for measuring acute toxicity to *Hydra vulgaris*. *Chemosphere* **41**, 1543-1548.
- Karntanut, W., and Pascoe, D. (2002). The toxicity of copper, cadmium and zinc to four different Hydra (Cnidaria. Hydrozoa). *Chemosphere* **47**, 1059-1064.
- Karplus, K., Barrett, C., and Hughey, R. (1998). Hidden Markov models for detecting remote protein homologies. *Bioinformatics* **14**, 846-856.
- Kelly, K. A., Havrilla, C. M., Brady, T. C., Abramo, K. H., and Levin, E. D. (1998). Oxidative stress in toxicology. established mammalian and emerging piscine model systems. *Environ. Health Perspect.* **106**, 375-384.
- Kelley, L. A., MacCallum, R. M., and Sternberg, M. J. E. (2000). Enhanced genome annotation using structural profiles in the program 3D-PSSM. *J. Mol. Biol.* **299**, 501-522.
- Kiecker, C., and Niehrs, C. A. (2001). A morphogen gradient of Wnt/beta-catenin signalling regulates anteroposterior neural patterning in *Xenopus*. *Development* **128**, 4189-4201.
- Kingsley, R. J., Afif, E., Cox, B. C., Kothari, S., Kriechbaum, K., Kuchinsky, K., Neill, A. T., Puri, A. F., and Kish, V. M. (2003). Expression of heat shock

and cold shock proteins in the gorgonian *Leptogorgia virgulata*. *J. Exp. Zool. A Comp. Exp. Biol.* **296**, 98-107.

Kispert, A., Herrmann, B. G., Leptin, M., and Reuter, R. (1994). Homologs of the mouse brachyury gene are involved in the specification of posterior terminal structures in *Drosophila*, *Tribolium*, and *Locusta*. *Genes Dev.* **8**, 2137-2150.

Kitayama, K., Kitayama, M., and Togasaki, R. K. (1995). A cDNA clone encoding a manganese-superoxide dismutase (GenBank U24500) from *Chlamydomonas reinhardtii*. *Plant Physiol.* **108**, 1748.

Kohler, H. R., Triebkorn, R., Stocker, W., Kloetzel, P. M., and Alberti, G. (1992). The 70 kD heat shock protein (hsp 70) in soil invertebrates: A possible tool for monitoring environmental toxicants. *Arch. Environ. Contam. Toxicol.* **22**, 334-338.

Koizumi, O., Itazawa, M., Mizumoto, H., Minobe, S., Javois, L.C., Grimmelikhuijzen, C.J., and Bode, H.R. (1992). Nerve ring of the hypostome in hydra. I. Its structure, development, and maintenance. *J. Comp. Neurol.* **326**, 7-21.

Koljak, R., Olivier, B., Bih-Hwa, S., Nigulas, S., and Alan, R. B. (1997). Identification of a naturally occurring peroxidase-lipoxygenase fusion protein. *Science* **277**, 1994-1996

Kondo, H., and Watabe, S. (2004). Temperature-dependent enhancement of cell proliferation and mRNA expression for type I collagen and HSP70 in primary cultured goldfish cells. *Comp. Biochem. Physiol. Part A Mol. Integr. Physiol.* **138**, 221-228.

Kortschak, R. D., Samuel, G., Saint, R., and Miller, D. J. (2003). EST analysis of the cnidarian *Acropora millepora* reveals extensive gene loss and rapid sequence divergence in the model invertebrates. *Curr. Biol.* **16**, 2190-2195.

- Krasko, A., Scheffer, U., Koziol, C., Pancer, Z., Batel, R., Badria, F. A., and Müller, W. E. G. (1997). Diagnosis of sublethal stress in the marine sponge *Geodia cydonium*, application of the 70 kDa heat-shock protein and a novel biomarker, the Rab GDP dissociation inhibitor, as probes. *Aquat. Toxicol.* **37**, 157-168.
- Krishnan, A. V., Stathis, P., Permuth, S. F., Tokes, L., and Feldman, D. (1993). Bisphenol-A an estrogenic substance is released from polycarbonate flasks during autoclaving. *Endocrinology* **132**, 2279-2286.
- Krone, P. H., Blechinger, S. R., Evans, T. G., Ryan, J. A., Noonan, E. J., and Hightower, L. E. (2005). Use of fish liver PLHC-1 cells and zebrafish embryos in cytotoxicity assays. *Methods* **35**, 176-187.
- Kultz, D. (2005). Molecular and evolutionary basis of the cellular stress response. *Annu. Rev. Physiol.* **67**, 225-257.
- Lah, M. S., Dixon, M. M., Patridge, K. A., Stallings, W. C., Fee, J. A., and Ludwig, M. L. (1995). Structure-function in *Escherichia coli* iron superoxide dismutase: Comparisons with the manganese enzyme from *Thermus thermophilus*. *Biochemistry* **34**, 1646-1660.
- Laskowski, R. A., MacArthur, M. W., Smith, D. K., Jones, D. T., Hutchinson, E. G., Morris, A. L., Naylor, D., Moss, D. S., and Thornton, J. M. (1994). PROCHECK v.3.0 - Program to check the stereochemistry quality of protein structures - Operating instructions.
- Laukkanen, M. O., Kivela, A., Rissanen, T., Rutanen, J., Karkkainen, M. K., Leppanen, O., Brasen, J. H., and Yla-Herttuala, S. (2002). Adenovirus-mediated extracellular superoxide dismutase gene therapy reduces neointima formation in balloon-denuded rabbit aorta. *Circulation* **106**, 1999-2003.
- Leaver, M. J., and George, S. G. (1998). A piscine glutathione S-transferase which efficiently conjugates the end-products of lipid peroxidation. *Mar. Environ. Res.* **46**, 71-74.

- LeBlanc, G. A., Bain, L. J., and Wilson, V. S. (1997). Chronic toxicity of environmental contaminants. sentinels and biomarkers. *Environ. Health. Perspect. Suppl.* **105** (1), 65-80.
- Lee, H. J., and Gu, M. B. (2003). Construction of a *soda::luxCDABE* fusion *Escherichia coli*: comparison with a *katG* fusion strain through their responses to oxidative stresses. *Appl. Microbiol. Biotechnol.* **60**, 577-580.
- Legrand-Poels, S., Schoonbroodt, S., Matroule, J. Y., and Piette, J. (1998). NF-kappa B: An important transcription factor in photobiology. *J. Photochem. Photobiol. B* **45**, 1-8.
- Lemaire, P., and Livingstone, D. R. (1997). Aromatic hydrocarbon quinone-mediated reactive oxygen species production in hepatic microsomes of the flounder (*Platichthys flesus* L.). *Comp. Biochem. Physiol.* **117C**, 131-139.
- Lemaire, P., and Livingstone, D. R. (1993). Pro-oxidant/antioxidant processes and organic xenobiotic interactions in marine organisms, in particular the flounder *Platichthys flesus* and mussel *Mytilus edulis*. *Trends Comp. Biochem. Physiol.* **1**, 1119-1150.
- Lemaire, P., Viarengo, A., Canesi, L., and Livingstone, D. R. (1993). Pro-oxidant and antioxidant processes in gas gland and other tissues of cod (*Gadus morhua*). *J. Comp. Physiol.* **163**, 477-486.
- Lemke, S. L., Ottinger, S. E., Ake, C. L., Mayura, K., and Phillips, T. D. (2001). Deamination of fumonisin B₍₁₎ and biological assessment of reaction product toxicity. *Chem. Res. Toxicol.* **14**, 11-15.
- Lemmon, A., and Milinkovitch, M. (2002). The metapopulation genetic algorithm: An efficient solution for the problem of large phylogeny estimation. *Proc. Natl. Acad. Sci. U. S. A.* **99**, 10516-10521.

- Lin, F., Geiger, P. G., and Girotti, A. W. (1992). Selenoperoxidase mediated cytoprotection against merocyanine 540-sensitized photoperoxidation and photokilling of leukemia cells. *Cancer Res.* **52**, 5282-5290.
- Lindquist, S. (1986). The heat-shock response. *Annu. Rev. Biochem.* **55**, 1151-1191.
- Lindquist, S., and Craig, E. A. (1988). *The Heat Shock Proteins*. *Annu. Rev. Genet.* **22**, 631-677.
- Livingstone, D. R. (1991). Organic xenobiotic metabolism in marine invertebrates. In *Advances in Comparative and Environmental Physiology* (R. Gilles, Ed.), pp. 45-185. Springer, Berlin.
- Livingstone, D. R. (1998). The fate of organic xenobiotics in aquatic ecosystems: Quantitative and qualitative differences in biotransformation by invertebrates and fish. *Comp. Biochem. Physiol.* **120A**, 43-49.
- Livingstone, D. R., Chipman, J. K., Lowe, D. M., Minier, C., Mitchelmore, C. L., Moore, M. N., Peters, L. D., and Pipe, R. K. (2000). Development of biomarkers to detect the effects of organic pollution on aquatic invertebrates: Recent molecular, genotoxic, cellular and immunological studies on the common mussel (*Mytilus edulis* L.) and other mytilids. *Int. J. Pollut.* **13**, 56-91.
- Livingstone, D. R., Forlin, L., and George, S. (1994). Molecular biomarkers and toxic consequences of impact by organic pollution in aquatic organisms. In *Water Quality and Stress Indicators in Marine and Freshwater Systems: Linking Levels of Organization* (D. W. Sutcliffe, Ed.), pp. 154-171. Freshwater Biological Association, Ambleside, UK.
- Livingstone, D. R., Garcia Martinez, P., Michel, X., Narbonne, J. F., O'Hara, S., Ribera, D., and Winston, G. W. (1990). Oxyradical generation as a pollution-mediated mechanism of toxicity in the common mussel, *Mytilus edulis* L., and other molluscs. *Funct. Ecol.* **4**, 415-424.

- Lohmann, J. U., Endl, I., and Bosch, T. C. (1999). Silencing of developmental genes in Hydra. *Dev. Biol.* **214**, 211-214.
- Lowe, D. G., Fulford, W. D., and Moran, L. A. (1983). Mouse and Drosophila genes encoding the major heat shock protein (hsp70) are highly conserved. *Mol. Cell. Biol.* **3**, 1540-1543.
- Luedeking, A., and Koehler, A. (2004). Regulation of expression of multixenobiotic resistance (MXR) genes by environmental factors in the blue mussel *Mytilus edulis*. *Aquat. Toxicol.* **69**, 1-10.
- Lum, K. T., Huebner, H. J., Li, Y., Phillips, T. D., and Raushel, F. M. (2003). Organophosphate nerve agent toxicity in *Hydra attenuata*. *Chem. Res. Toxicol.* **16**, 953-957.
- Macario, A. J., Lange, M., Ahring, B. K., and De Macario, E. C. (1999). Stress genes and proteins in the archaea. *Microbiol. Mol. Biol. Rev.* **63**, 923-967.
- Maddipati, K. R., Gasparski, C., and Marnett, L. J. (1987). Characterization of the hydroperoxide-reducing activity of human plasma. *Arch. Biochem. Biophys.* **254**, 9-17.
- Maiorino, M., Chu, F. F., Ursini, F., Davies, K. J. A., Doroshov, J. H., and Eswortby, R. S. (1991). Phospholipid hydroperoxide glutathione peroxidase is the 18-kDa selenoprotein expressed in human tumor cell lines. *J. Biol. Chem.* **266**, 7728-7732.
- Malins, D. C., and Ostrander, G. K. (1991). Perspectives in aquatic toxicology. *Annu. Rev. Pharmacol. Toxicol.* **31**, 371- 399.
- Manduzio, H., Monsinjon, T., Rocher, B., Leboulenger, F., and Galap, C. (2003). Characterization of an inducible isoform of the Cu/Zn superoxide dismutase in the blue mussel *Mytilus edulis*. *Aquat. Toxicol.* **64**, 73-83.

- Mantonavi, A., and Dejana, E. (1989). Cytokines as communication signals between leukocytes and endothelial cells. *Immunol. Today* **10**, 370-375.
- Marklund, S. L. (1982). Human copper-containing superoxide dismutase of high molecular weight. *Proc. Natl. Acad. Sci. U. S. A.* **79**, 7634-7638.
- Marklund, S. L. (1992). Regulation by cytokines of extracellular superoxide dismutase and other superoxide dismutase isoenzymes in fibroblast. *J. Biol. Chem.* **267**, 6696-6701.
- Marres, C. A. M., Van Loon, A. P. G. M., Oudshoorn, P., Van Steeg, H., Grivell, L. A., and Slater, E. C. (1985). Nucleotide sequence analysis of the nuclear gene coding for manganese superoxide dismutase of yeast mitochondria, a gene previously assumed to code for the Rieske iron-sulphur protein. *Eur. J. Biochem.* **147**, 153-161.
- Martensson, J., and Meister, A. (1991). Glutathione deficiency decreases tissue ascorbate levels in newborn rats: Ascorbate spares glutathione and protects. *Proc. Natl. Acad. Sci. U. S. A.* **88**, 4656-4660.
- Mayura, K., Smith, E. E., Clement, B. A., and Phillips, T. D. (1991). Evaluation of the developmental toxicity of chlorinated phenols utilizing *Hydra attenuata* and postimplantation rat embryos in culture. *Toxicol. Appl. Pharmacol.* **108**, 253-266.
- Meinhardt, H. (1993). A model for pattern-formation of hypostome, tentacles, and foot in hydra: How to form structures close to each other, how to form them at a distance. *Dev. Biol.* **157**, 321-333.
- Meinhardt, H. (2002). The radial-symmetric hydra and the evolution of the bilateral body plan: An old body became a young brain. *Bioessays* **24**, 185-191.
- Meinhardt, H. (2004). Models for the generation of the embryonic body axes: Ontogenetic and evolutionary aspects. *Curr. Opin. Genet. Dev.* **14**, 446-454.

- Miljkovic-Licina, M., Gauchat, D., and Galliot, B. (2004). Neuronal evolution: Analysis of regulatory genes in a first-evolved nervous system, the hydra nervous system. *Biosystems* **76**, 75-87.
- Moradas-Ferreira, P., Costa, V., Piper, P., and Mager, W. (1996). The molecular defenses against reactive oxygen species in yeast. *Mol. Microbiol.* **19**, 651-658.
- Morales, A. E., Perez-Jimenez, A., Hidalgo, M. C., Abellan, E., and Cardenete, G. (2004). Oxidative stress and antioxidant defenses after prolonged starvation in *Dentex dentex* liver. *Comp. Biochem. Physiol. C Toxicol. Pharmacol.* **139**, 153-161.
- Morgan, R. W., Christmas, M. F., Jacobson, F. S., Storz, G., and Ames, B. (1986). Hydrogen peroxide inducible proteins in *Salmonella typhimurium* overlap with heat shock and other stress proteins. *Proc. Natl. Acad. Sci. U. S. A.* **83**, 8059.
- Mueller, W. E. G., Koziol, C., Kurelec, B., Dapper, J., Batel, R., and Rinkevich, B. (1995). Combinatory effects of temperature stress and nonionic organic pollutants on stress protein (hsp70) gene expression in the freshwater sponge *Ephydatia fluviatilis*. *Environ. Toxicol. Chem.* **14**, 1203-1208.
- Murphy, L. M., Strange, R. W., and Hasnain, S. S. (1997). A critical assessment of the evidence from XAFS and crystallography for the breakage of the imidazolate bridge during catalysis in CuZn superoxide dismutase. *Structure* **5**, 371-379.
- Nadeau, D., Corneau, S., Plante, I., Morrow, G., and Tanguay, R.M. (2001). Evaluation for Hsp70 as a biomarker of effect of pollutants on the earthworm *Lumbricus terrestris*. *Cell Stress Chaperones* **6**, 153-163.
- Nadler, V., Goldberg, I., and Hochman, A. (1986). Comparative study of bacterial catalases. *Biochim. Biophys. Acta* **882**, 234-241.

- Nasci, C., Da Ros, L., Campesan, G., and Fossato, V. U. (1998). Assessment of the impact of chemical pollutants on mussel, *Mytilus galloprovincialis*, from the Venice Lagoon, Italy. *Mar. Environ. Res.* **46**, 279-282.
- Nascimento, I. A., Dickson, K. L., and Zimmerman, E. G. (1996). Heat shock protein response to thermal stress in the Asiatic clam, *Corbicula fluminea*. *J. Aquat. Ecosystem Health* **5**, 231-238.
- Niehrs, C., Keller, R., Cho, K. W. Y., and De Robertis, E. M. (1993). The homeobox gene goosecoid controls cell-migration in *Xenopus* embryos. *Cell* **72**, 491-503.
- Nielsen, C. (1997). *Phylum Cnidaria: Animal Evolution Interrelationships of the Living Phyla*. Pp 53-60. Oxford University Press, Oxford.
- Nomura, K., Imai, H., Koumura, T., Arai, M., and Nakagawak, Y. (1999). Mitochondrial phospholipid hydroperoxide glutathione peroxidase suppresses apoptosis mediated by a mitochondrial death pathway. *J. Biol. Chem.* **274**, 29294-29302.
- Noramly, S., Freeman, A., and Morgan, B. A. (1999). B-catenin signaling can initiate feather development. *Development* **126**, 3509-3521.
- Nordstrom, U., Jessell, T. M., and Edlund, T. (2002). Progressive induction of caudal neural character by graded Wnt signaling. *Nat. Neurosci.* **5**, 525-532.
- O'Malley, K., Maunon, A., Barchas, J. D., and Kedes, L. (1985). Constitutively expressed rat mRNA encoding a 70-kilodalton heat shock-like protein. *Mol. Cell. Biol.* **5**, 3476-3483.
- Ogihara, N. L., Parge, H. E., Hart, P. J., Weiss, M. S., Goto, J. J., Crane, B. R., Tsang, J., Slater, K., Roe, J. A., Valentine, J. S., Eisenberg, D., and Tainer, J. A. (1996). Unusual trigonal-planar copper configuration revealed in the atomic structure of yeast copper-zinc superoxide dismutase. *Biochemistry* **35**, 2316-2321.

- Olinescu, R., and Smith, T. L. (2002). *Free Radicals in Medicine*. Nova Science Publishers, Inc., New York.
- Ostroumova, T. V., and Markova, L. N. (2002). The effects of dopamine synthesis inhibitors and dopamine antagonists on regeneration in the hydra *Hydra attenuata*. *Neurosci. Behav. Physiol.* **32**, 293-298.
- Ottinger, S. E., Mayura, K., Lemke, S. L., McKenzie, K. S., Wang, N., Kubena, L. F., and Phillips, T. D. (1999) Utilization of electrochemically generated ozone in the degradation and detoxification of benzo[a]pyrene. *J. Toxicol. Environ. Health A* **57**, 565-583.
- Oury, T. D., Day, B. J., and Crapo, J. D. (1996). Extracellular superoxide dismutase in vessels and airways of humans and baboons. *Free Radic. Biol. Med.* **20**, 957-965.
- Pan, S. M., Ye, J. S., and Hseu, R. S. (1997). Purification and characterization of manganese superoxide dismutase from *Ganoderma microsporum*. *Biochem. Mol. Biol. Int.* **42**, 1035-1043.
- Pardos, M., Benninghoff, C., Gueguen, C., Thomas, R., Dobrowolski, J., and Dominik, J. (1999). Acute toxicity assessment of Polish (waste) water with a microplate-based *Hydra attenuata* assay. a comparison with the Microtox test. *Sci. Total Environ.* **243-244**, 141-148.
- Parge, H. E., Hallewell, R. A., and Tainer, J. A. (1992). Atomic structures of wild-type and thermostable mutant recombinant human Cu, Zn superoxide dismutase. *Proc. Natl. Acad. Sci. U. S. A.* **89**, 6109-6113.
- Parr, B. A., and McMahon, A. P. (1995). Dorsalizing signal Wnt-7a required for normal polarity of D-V and A-P axes of the mouse limb. *Nature* **374**, 350-353.
- Pascoe, D., Carroll, K., Karntanut, W., and Watts, M. M. (2002). Toxicity of 17 α -ethinylestradiol and bisphenol A to the freshwater cnidarian *Hydra vulgaris*. *Arch. Environ. Contam. Toxicol.* **43**, 56-63.

- Pascoe, D., Karntanut, W., and Muller, C. T. (2003). Do pharmaceuticals affect freshwater invertebrates? A study with the cnidarian *Hydra vulgaris*. *Chemosphere* **51**, 521-528.
- Petersen, S. V., Oury, T. D., Ostergaard, L., Valnickova, Z., Wegrzyn, J., Thogersen, I. B., Jacobsen, C., Bowler, R. P., Fattman, C. L., Crapo, J. D., and Enghild, J. J. (2004). Extracellular superoxide dismutase (EC-SOD) binds to type I collagen and protects against oxidative fragmentation. *J. Biol. Chem.* **279**, 13705-13710.
- Piano, A., Valbonesi, P., and Fabbri, E. (2004). Expression of cytoprotective proteins, heat shock protein 70 and metallothioneins, in tissues of *Ostrea edulis* exposed to heat and heavy metals. *Cell Stress Chaperones* **9**, 134-142.
- Pierobon, P., Sogliano, C., Minei, R., Tino, A., Porcu, P., Marino, G., Tortiglione, C., and Concas, A. (2004). Putative NMDA receptors in Hydra: A biochemical and functional study. *Eur. J. Neurosci.* **20**, 2598-2604.
- Pispa, J., and Thesleff, I. (2003). Mechanisms of ectodermal organogenesis. *Dev. Biol.* **262**, 195-205.
- Plantivaux, A., Furla, P., Zoccola, D., Garelli, G., Forcioli, D., Richier, S., Merle, P. L., Tambutte, E., Tambutte, S., and Allemand, D. (2004). Molecular characterization of two CuZn-superoxide dismutases in a sea anemone. *Free Radic. Biol. Med.* **37**, 1170-1181.
- Pollino, C. A., and Holdway, D. A. (1999). Potential of two hydra species as standard toxicity test animals. *Ecotoxicol. Environ. Saf.* **43**, 309-316.
- Raff, R. A. (1996). Deep time and metazoan origins, In *The Shape of Life: Genes, Development and the Evolution of Animal Form* (R.A. Raff, Ed.), pp. 63-102. Chicago University Press, Chicago.
- Rand, G. (1995). *Fundamentals of Aquatic Toxicology: Effects, Environmental Fate, and Risk Assessment*. Taylor and Francis, London.

- Rathinam, A. V., Chen, T. T., and Grossfeld, R. M. (2000). Cloning and sequence analysis of a cDNA for an inducible 70 kDa heat shock Protein (Hsp70) of the American Oyster (*Crassostrea virginica*). *DNA Seq.* **11**, 261-264.
- Reed, D. J. (1990). Glutathione: Toxicological implications. *Annu. Rev. Pharmacol. Toxicol.* **30**, 603-631.
- Regoli, F., Hummel, H., Amiard-Triquet, C., Larroux C., and Sukhotin A. (1998a). Trace metals and variations of antioxidant enzymes in Arctic bivalve populations. *Arch. Environ. Contam. Toxicol.* **35**, 594-601.
- Regoli, F., Nigro, M., and Orlando, E. (1998b). Lysosomal and antioxidant responses to metals in the Antarctic scallop *Adamussium colbecki*. *Aquat. Toxicol.* **40**, 375-392.
- Richier, S., Furla, P., Plantivaux, A., Merle, P. L., and Allemand, D. (2005). Symbiosis-induced adaptation to oxidative stress. *J. Exp. Biol.* **208**, 277-285.
- Richier, S., Merle, P. L., Furla, P., Pigozzi, D., Sola, F., and Allemand, D. (2003). Characterization of superoxide dismutases in anoxia- and hyperoxia-tolerant symbiotic cnidarians. *Biochim. Biophys. Acta* **1621**, 84-91.
- Richter, H. E., and Loewen, P. C. (1982). Rapid inactivation of bacteriophage T7 by ascorbic acid is repairable. *Biochim. Biophys. Acta* **697**, 25-30.
- Rohrdanz, E., and Kahl, R. (1998). Alterations of antioxidant enzyme expression in response to hydrogen peroxide. *Free Radic. Biol. Med.* **24**, 27-38.
- Roise, D., Theiler, F., Horvath, S. J., Tomich, J. M., Richards, J. H., Allison, D. S., and Schatz, G. (1988). Amphiphilicity is essential for mitochondrial presequence function. *EMBO J.* **7**, 649-653.

- Rossi, S., and Snyder, M. J. (2001). Competition for space among sessile marine invertebrates: changes in HSP70 expression in two Pacific cnidarians. *Biol. Bull.* **201**, 385-393.
- Rost, B. (1995). In *The Third International Conference on Intelligent Systems for Molecular Biology (ISMB)* (C. Rawlings, D. Clark, *et al.*, Eds), pp. 314-321. AAAI Press, Cambridge.
- Rotruck, J. T., Pope, A. L., Ganther, H. E., Swanson, A. B., Hafeman, D. G., and Hoekstra, W. G. (1973). Selenium: Biochemical role as a component of glutathione peroxidase. *Science* **179**, 588-590.
- Ryan, J. A., and Hightower, L. E. (1994). Evaluation of heavy-metal ion toxicity in fish cells using a combined stress protein and cytotoxicity assay. *Environ. Toxicol. Chem.* **13**, 1231-140.
- Ryan, J. A., and Hightower, L. E. (1996). Stress proteins as molecular biomarkers for environmental toxicology. In *Stress-Inducible Cellular Responses* (U. Feige, R. I. Morimoto, I. Yahara, B. S. Polla, Eds.), pp. 411-424. Birkhäuser, Basel.
- Rudneva, I. I. (1997). Blood antioxidant systems of Black Sea elasmobranch and teleosts. *Comp. Biochem. Physiol.* **118C**, 255-260.
- Ruffin, P., Demuyne, S., Hilbert, J. L., and Dhainaut, A. (1994). Stress protein in the polychaete annelid *Nereis diversicolor* induced by heat shock or cadmium exposure. *Biochimie* **76**, 423-427.
- Rulifson, E. J., Micchelli, C. A., Axelrod, J. D., Perrimon, N., and Blair, S. S. (1996). Wingless refines its own expression domain on the Drosophila wing margin. *Nature* **384**, 72-74.
- Sali, A., and Blundell, T. L. (1993). Comparative protein modeling by satisfaction of spatial restraints. *J. Mol. Biol.* **234**, 779-815.

- Sambrook, J., Fritsch, E. F., and Maniatis, T. (1989). *Molecular Cloning: A Laboratory Manual*. Cold Spring Harbor Laboratory, Cold Spring Harbor, New York.
- Samuel, G., Miller, D.J., and Saint, R. (2001). Conservation of a DPP/BMP signaling pathway in the nonbilateral cnidarian *Acropora millepora*. *Evol. Dev.* **3**, 241-250.
- Sanders, B. M., and Dyer, S. D. (1994). Cellular stress response. *Environ. Toxicol. Chem.* **13**, 1209-1210.
- Sanders, B. M., and Martin, L. S. (1993). Stress proteins as biomarkers of contaminant exposure in archived environmental samples. *Sci. Total Environ.* **139-140**, 459-470.
- Sarras, M. P., Jr. Madden, M. E., Zhang, X. M., Gunwar, S., Huff, J. K., and Hudson, B. G. (1991). Extracellular matrix (mesoglea) of *Hydra vulgaris*. I. Isolation and characterization. *Dev. Biol.* **148**, 481-494.
- Schmitt, D. M., and Brower, D. L. (2001). Intron dynamics and the evolution of integrin beta-subunit genes: Maintenance of an ancestral gene structure in the coral, *Acropora millepora*. *J. Mol. Evol.* **53**, 703-710.
- Schnellhorn, H. E. (1994). Regulation of hydroperoxidase (catalase) expression in *Escherichia coli*. *FEMS Microbiol. Lett.* **131**, 113-119.
- Schubert, J., and Wilmer, J. W. (1991). Does hydrogen peroxide exist 'free' in biological systems? *Free Radic. Biol. Med.* **11**, 545-555.
- Segner, H., Caroll, K., Fenske, M., Janssen, C. R., Maack, G., Pascoe, D., Schafers, C., Vandenberg, G. F., Watts, M., and Wenzel, A. (2003). Identification of endocrine-disrupting effects in aquatic vertebrates and invertebrates: Report from the European IDEA project. *Ecotoxicol. Environ. Saf.* **54**, 302-314.

- Serra, V., von Zglinicki, T., Lorenz, M., and Saretzki, G. (2003). Extracellular superoxide dismutase is a major antioxidant in human fibroblasts and slows telomere shortening. *J. Biol. Chem.* **278**, 6824-6830.
- Sher, D., Knebel, A., Bsor, T., Nesher, N., Tal, T., Morgenstern, D., Cohen, E., Fishman, Y., and Zlotkin, E. (2005). Toxic polypeptides of the hydra: A bioinformatic approach to cnidarian allomones. *Toxicon* **45**, 865-879.
- Shick, J. M. (1991). *A Functional Biology of Sea Anemones*. Chapman and Hall, London.
- Shimizu, H., and Fujisawa, T. (2003). Peduncle of Hydra and the heart of higher organisms share a common ancestral origin. *Genesis* **36**, 182-186.
- Spafford, J. D., Spencer, A. N., and Gallin, W. J. (1999). Genomic organization of a voltage-gated Na⁺ channel in a hydrozoan jellyfish: Insights into the evolution of voltage-gated Na⁺ channel genes. *Recept. Channels* **6**, 493-506.
- Spencer, A. N. (1989). Chemical and electrical synaptic transmission in the cnidarian. In *Evolution of the First Nervous Systems* (P.A.V. Anderson, Ed.), pp. 33-53. NATO Series, Serie A. Life Sciences, Vol. 188. Plenum Press, New York.
- Spring, J., Yanze, N., Josch, C., Middel, A. M., Wünniger, B., and Schmid, V. (2002). Conservation of Brachyury, Mef2, and Snail in the myogenic lineage of jellyfish: A connection to the mesoderm of bilateria. *Dev. Biol.* **244**, 372-384.
- Stallings, W. C., Patridge, K. A., Strong, R. K., and Ludwig, M. L. (1984). Manganese and iron superoxide dismutases are structural homologs. *J. Biol. Chem.* **259**, 10695-10699.
- Stamatakis, A., Ludwig, T., and Meier, H. (2005). RAxML-III: A fast program for maximum likelihood-based inference of large phylogenetic trees. *Bioinformatics* **21**, 456-463.

- Steinert, S. A., and Pickwell, G. V. (1988). Expression of heat shock proteins and metallothionein in mussels exposed to heat stress and metal ion challenge. *Mar. Environ. Res.* **24**, 211-214.
- Steinert, S. A., Streib-Montee, R., and Sastre, M. P. (1998). Influence of sunlight on DNA damage in mussels exposed to polycyclic aromatic hydrocarbons. *Mar. Environ. Res.* **46**, 355-358.
- Stover, N. A., and Steele, R. E. (2001). Trans-spliced leader addition to mRNAs in a cnidarian. *Proc. Natl. Acad. Sci. U. S. A.* **98**, 5693-5698.
- Stralin, P., and Marklund, S. L. (1994). Effects of oxidative stress on expression of extracellular superoxide dismutase, CuZn-superoxide dismutase and Mn-superoxide dismutase in human dermal fibroblasts. *Biochem. J.* **298**, 347-352.
- Stralin, P., Karlsson, K., Johansson, B. O., and Marklund, S. L. (1995). The interstitium of the human arterial wall contains very large amounts of extracellular superoxide dismutase. *Arterioscler. Thromb. Vasc. Biol.* **15**, 2032-2036.
- Struhl, G., and Basler, K. (1993). Organizing activity of wingless protein in *Drosophila*. *Cell* **72**, 527-540.
- Sukenaga, Y., Ishida, K., Takeda, T., and Takagi, K. (1987). cDNA sequence coding for human glutathione peroxidase. *Nucleic Acids Res.* **15**, 7178.
- Sun, W., Van Montagu, M., and Verbruggen, N. (2002). Small heat shock proteins and stress tolerance in plants. *Biochim. Biophys. Acta* **19**, 1-9.
- Sunde, R. A. (1990). Molecular biology of selenoproteins. *Annu. Rev. Nutr.* **10**, 451-474.

- Tainer, J. A., Getzoff, E. D., Beem, K. M., Richardson, J. S., and Richardson, D. C. (1982). Determination and analysis of the 2 Å structure of copper, zinc superoxide dismutase. *J. Mol. Biol.* **160**, 181-217.
- Takeda, Y., and Avila, H. (1986). Structure and gene expression of the *E. coli* Mn-superoxide dismutase gene. *Nucleic Acids Res.* **14**, 4577-4589.
- Technau, U., and Bode, H. R. (1999). HyBra1, a brachyury homologue, acts during head formation in Hydra. *Development* **126**, 999-1010.
- Thomas, J. P., Maiorino, M., Ursini, F., and Girotti, A. W. (1990). Protective action of phospholipid hydroperoxide glutathione peroxidase against membrane-damaging lipid peroxidation: *In situ* reduction of phospholipid and cholesterol hydroperoxides. *J. Biol. Chem.* **265**, 454-461.
- Thomsen, S., Till, A., Wittlieb, J., Beetz, C., Khalturin, K., and Bosch, T. C. (2004). Control of foot differentiation in hydra: *in vitro* evidence that the nk-2 homeobox factor cnkn-2 autoregulates its own expression and uses pedibin as target gene. *Mech. Dev.* **121**, 195-204.
- Tom, M., Douek, J., Yankelevich, I., Bosch, T. C., and Rinkevich, B. (1999). Molecular characterization of the first heat shock protein 70 from a reef coral. *Biochem. Biophys. Res. Commun.* **262**, 103-108.
- Tsolis, R. M., Baumler, A. J., and Heffron, F. (1995). Role of *Salmonella typhimurium* Mn-superoxide dismutase (SodA) in protection against early killing by J774 macrophages. *Infect. Immun.* **63**, 1739-1744.
- Ulrich, H., and Tarnok, A. (2005). Quantification of cell-cycle distribution and mitotic index in Hydra by flow cytometry. *Cell Prolif.* **38**, 63-75.
- Ursini, F., Maiorino, M., and Gregolin, C. (1985). The selenoenzyme phospholipid hydroperoxide glutathione peroxidase. *Biochim. Biophys. Acta* **839**, 62-70.

- Valko, M., Morris, H., and Cronin, M. T. D. (2005). Metals, toxicity and oxidative stress. *Curr. Med. Chem.* **12**, 1161-1208.
- van de Wetering, M., Cavallo, R., Dooijes, D., van Beest, M., van Es, J., Loureiro, J., Ypma, A., Hursh, D., Jones, T., Bejsovec, A., Peifer, M., Mortin, M., and Clevers, H. (1997). Armadillo coactivates transcription driven by the product of the *Drosophila* segment polarity gene dTCF. *Cell* **88**, 789-799.
- Van Dyk, T. K., Majarian, W. R., Konstantinov, K. B., Young, R. M., Dhurjati, P. S., and LaRossa, R. A. (1994). Rapid and sensitive pollutant detection by induction of heat shock gene-bioluminescence gene fusions. *Appl. Environ. Microbiol.* **60**, 1414-120.
- Van Veld, P. A. (1990). Absorption and metabolism of dietary xenobiotics by the intestine of fish. *Rev. Aquat. Sci.* **2**, 185-203.
- Vayssier, M., Leguerhier, F., Fabien, J. F., Philippe, H., Vallet, C., Ortega-Pierres, G., Soule, C., Perret, C., Liu, M., Vega- Lopez, M., and Boireau, M. P. (1999). Cloning and analysis of a *Trichinella britovi* gene encoding a cytoplasmic heat shock protein of 72 kDa. *Parasitology* **119**, 81-93.
- Veldhuizen Tsoerkan, M. B., Holwerda, D. A., van der Mast, C. A., and Zandee, D. I. (1991). Synthesis of stress proteins under normal and heat shock conditions in gill tissue of sea mussels (*Mytilus edulis*) after chronic exposure to cadmium. *Comp. Biochem. Physiol.* **100C**, 699-706.
- Viarengo, A., Canesi, L., Garcia Martinez, P., Peters, L. D., and Livingstone, D. R. (1995). Pro-oxidant processes and antioxidant defense systems in the tissues of the Antarctic scallop (*Adamussium colbecki*) compared to the Mediterranean scallop (*Pecten jacobaeus*). *Comp. Biochem. Physiol. B Biochem. Mol. Biol.* **111**, 119-126.
- Vijayan, M. M., Pereira, C., Forsyth, R. B., Kennedy, C. J., and Iwama, G. K. (1997). Handling stress does not affect the expression of hepatic heat shock protein 70 and conjugation enzymes in rainbow trout treated with beta-naphthoflavone. *Life Sci.* **61**:117-27

- Visner, G. A., Dougall, W. C., Wilson, J. M., Burr, I. A., and Nick, H. S. (1990). Regulation of manganese superoxide dismutase by lipopolysaccharide, interleukin-1, and tumor necrosis factor: Role in the acute inflammatory response. *J. Biol. Chem.* **265**, 2856-2864.
- Walker, C. H., Hopkin, S. P., Sibley, R. M., and Peakall, D. B. (1996). *Principles of Ecotoxicology*. Taylor and Francis, London.
- Wan, X. S., Devalajara, M. N., and St. Clair, D. K. (1994). Molecular structure and organization of the human manganese superoxide dismutase gene. *DNA Cell. Biol.* **13**, 1127-1136.
- Warchalowska-Sliwa, E., Niklinska, M., Gorlich, A., Michailova, P., and Pyza, E. (2005). Heavy metal accumulation, heat shock protein expression and cytogenetic changes in *Tetrix tenuicornis* (L.) (Tetrigidae, Orthoptera) from polluted areas. *Environ. Pollut.* **133**, 373-381.
- Weisiger, R. A., and Fridovich, I. (1973). Mitochondrial superoxide dismutase: Site of synthesis and intra-mitochondrial localization. *J. Biol. Chem.* **248**, 4793-4796.
- Weitzel, F., Ursini, F., and Wendel, A. (1990). Phospholipid hydroperoxide glutathione peroxidase in various mouse organs during selenium deficiency and repletion. *Biochim. Biophys. Acta* **1036**, 88-94.
- Werner, I., and Nagel, R. (1997). Stress proteins HSP60 and HSP70 in 3 species of amphipods exposed to cadmium, diazinon, dieldrin and fluoranthene. *Environ. Toxicol. Chem.* **16**, 2393-403.
- Westfall, J. A. (1996). Ultrastructure of synapses in the first-evolved nervous systems. *J. Neurocytol.* **25**, 735-746.

- Wiederrecht, G., Shuet, D. J., Kibbe, W. A., and Parker, C. S. (1987). The *Saccharomyces* and *Drosophila* heat shock transcription factors are identical in size and DNA binding properties. *Cell* **48**, 507-515.
- Wieser, R., Adam, G., Wagner, A., Schuller, C., Marchler, G., Ruis, H., Krawiec, Z., and Bilinski, T. (1991). Heat-shock-factor independent heat control of transcription of the *CTT1* gene encoding the cytosolic catalase T of *Saccharomyces cerevisiae*. *J. Biol. Chem.* **266**, 12406.
- Winston, G. W., and Di Giulio, R. T. (1991). Prooxidant and antioxidant mechanisms in aquatic organisms. *Aquat. Toxicol.* **19**, 137-161.
- Winterbourn, C. C. (1994). Superoxide as an intracellular radical sink. *Free Radic. Biol. Med.* **14**, 85-92.
- Wong, G. H., and Goeddel, D. V. (1988). Induction of manganous superoxide dismutase by tumor necrosis factor: Possible protective mechanism. *Science* **242**, 941-944.
- Wood, L. A., Brown, I. R., and Youson, J. H. (1998). Characterization of the heat shock response in the gills of sea lampreys and a brook lamprey at different intervals of their life cycles. *Comp. Biochem. Physiol. Part A* **120**, 509-518.
- Yagi, K., Komura, S., Kojima, H., Sun, Q., Nagata, N., Ohishi, N., and Nishikimi, M. (1996). Expression of human phospholipid hydroperoxide glutathione peroxidase gene for protection of host cells from lipid hydroperoxide-mediated injury. *Biochem. Biophys. Res. Commun.* **219**, 486-491.
- Yakovleva, I., Bhagooli, R., Takemura, A., and Hidaka, M. (2004). Differential susceptibility to oxidative stress of two scleractinian corals: Antioxidant functioning of mycosporine-glycine. *Comp. Biochem. Physiol. B. Biochem. Mol. Biol.* **139**, 721-730.
- Yang, Y. G., Mayura, K., Spainhour, C. B., Jr. Edwards, J. F., and Phillips, T. D. (1993). Evaluation of the developmental toxicity of citrinin using *Hydra*

attenuata and postimplantation rat whole embryo culture. *Toxicology* **85**, 179-198.

Yost, H. J., Petersen, R. B., and Lindquist, S. (1990). RNA metabolism: Strategies for regulation in the heat shock response. *Trends Genet.* **6**, 223-227.

Zelko, I. N., Mariani, T. J., and Folz, R. J. (2002). Superoxide dismutase mutigene family: A comparison of the CuZn-SOD (SOD1), Mn-SOD (SOD2), and EC-SOD (SOD3) gene structures, evolution, and expression. *Free Radic. Biol. Med.* **33**, 337-349.

Zinoni, F., Birkmann, A., Stadtman, T. C., and Bock, A. (1986). Nucleotide sequence and expression of the selenocysteine-containing polypeptide of formate dehydrogenase (formate-hydrogen-lyase-linked) from *Escherichia coli*. *Proc. Natl. Acad. Sci. U. S. A.* **83**, 4650-4654.

Zou, P. J., Borovok, I., de Orue Lucana, D. O., Muller, D., and Schrempf, H. (1999). The mycelium-associated *Streptomyces reticuli* catalase-peroxidase, its gene and regulation by FurS. *Microbiology* **145**, 549-559.

Supplemental sources consulted

Ali, M. B., Hahn, E. J., and Paek, K. Y. (2005). Effects of temperature on oxidative stress defense systems, lipid peroxidation and lipoxygenase activity in *Phalaenopsis*. *Plant Physiol. Biochem.* **43**, 213-223.

Altschul, S. F., Madden, T. L., Schaffer, A. A., Zhang, J., Zhang, Z., Miller, W., and Lipman, D. J. (1997). Gapped BLAST and PSI-PLAST: A new generation of protein database search programs. *Nucleic Acids Res.* **25**, 3389-3402.

Asayama, K., Hayashibe, H., Dobashi, K., Niitsu, T., Miyao, A., and Kato, K. (1989). Antioxidant enzyme status and lipid peroxidation in various tissues of diabetic and starved rats. *Diabetes Res.* **12**, 85-91.

- Baum, J. A., and Scandalios, J. G. (1982). Isolation and characterization of the cytosolic and mitochondrial superoxide dismutases of maize. *Arch. Biochem. Biophys.* **206**, 249-264.
- Culi, J., and Modolell, J. (1998). Proneural gene self-stimulation in neural precursors -an essential mechanism for sense organ development that is regulated by Notch signalling. *Genes Dev.* **12**, 2036-2047.
- Damen, W. G. M., Weller, M., and Tautz, D. (2000). Expression patterns of hairy, even-skipped, and runt in the spider *Cupiennius salei* imply that these genes were segmentation genes in a basal arthropod. *Proc. Natl. Acad. Sci. U. S. A.* **97**, 4515-4519.
- Elstner, E. F. (1982). Oxygen activation and oxygen toxicity. *Annu. Rev. Plant Physiol.* **33**, 73-96.
- Finzel, B. C., Poulos, T. L., and Kraut, J. (1984). Crystal structure of yeast cytochrome c peroxidase refined at 1.7-Å resolution. *J. Biol. Chem.* **259**, 13027-13036.
- Fridovich, I. (1978). The biology of oxygen radicals. *Science* **201**, 875-880.
- Fukumori, Y., Fujiwara, T., Okada-Takahashi, Y., Mukohata, Y., and Yamanaka, T. (1985). Purification and properties of a peroxidase from *Halobacterium halobium* L-33. *J. Biochem.* **98**, 1055-1061.
- He, H. J., Yuan, Q. S., Yang, G. Z., and Wu, X. F. (2002). High-level expression of human extracellular superoxide dismutase in *Escherichia coli* and insect cells. *Protein Expr. Purif.* **24**, 13-17.
- Heck, D. E., Vetrano, A. M., Marian T. M., and Laskin J. D. (2003). UVB light stimulates production of reactive oxygen species: Unexpected role for catalase. *J. Biol. Chem.* **278**, 22432-22436.

- Hidalgo, M. C., Exposito, A., Palma, J. M., and de la Higuera, M. (2002). Oxidative stress generated by dietary Zn-deficiency: Studies in rainbow trout (*Oncorhynchus mykiss*). *Int. J. Biochem. Cell Biol.* **34**, 183-193.
- Ivancich, A., Barynin, V. V., and Zimmermann, J. L. (1995). Pulsed EPR studies of the binuclear Mn (III) Mn (IV) center in catalase from *Thermus thermophilus*. *Biochemistry* **34**, 6628-6639.
- Klotz, M. G., Klassen, G. R., and Loewen, P. C. (1997). Phylogenetic relationships among prokaryotic and eukaryotic catalases. *Mol. Biol. Evol.* **14**, 951-958.
- Klotz, M. G., and Loewen, P. C. (2003). The molecular evolution of catalatic hydroperoxidases: Evidence for multiple lateral transfer of genes between prokaryota and from bacteria into eukaryota. *Mol. Biol. Evol.* **20**, 1098-1112.
- Kono, Y., Yamamoto, H., Takeuchi, M., and Komada, H. (1995). Alterations in superoxide dismutase and catalase in *Fusarium oxysporum* during starvation-induced differentiation. *Biochim. Biophys. Acta* **1268**, 35-40.
- Kono, Y., and Fridovich, I. (1983). Isolation and characterization of the pseudocatalase of *Lactobacillus plantarum*. *J. Biol. Chem.* **258**, 6015-6019.
- Kwon, S. I., and An, C. S. (1999). Isolation and characterization of mitochondrial manganese superoxide dismutase (MnSOD) from *Capsicum annuum* L. *Mol. Cells.* **9**, 625-630
- Langley, S. C., and Kelly, F. J. (1992). Effect of food restriction on hyperoxia-induced lung injury in preterm guinea pig. *Am. J. Physiol.* **263**, L357-L362.
- Li, M., Hu, C., Zhu, Q., Chen, L., Kong, Z., and Liu, Z. (2005). Copper and zinc induction of lipid peroxidation and effects on antioxidant enzyme activities in the microalga *Pavlova viridis* (Prymnesiophyceae). *Chemosphere* [Epub ahead of print]

- Lombardo, M. F., Ciriolo, M.R., Rotilio, G., and Rossi, L. (2003). Prolonged copper depletion induces expression of antioxidants and triggers apoptosis in SH-SY5Y neuroblastoma cells. *Cell. Mol. Life Sci.* **60**, 1733-1743.
- Magliozzo, R. S., and Marcinkeviciene, J. A. (1997). The role of Mn (II) - peroxidase activity of mycobacterial catalase-peroxidase in activation of the antibiotic isoniazid. *J. Biol. Chem.* **272**, 8867-8870.
- Marczuk-Krynicka, D., Hryniewiecki, T., Piatek, J., and Paluszak, J. (2003). The effect of brief food withdrawal on the level of free radicals and other parameters of oxidative status in the liver. *Med. Sci. Monit.* **9**, BR131-35.
- Nicholls, P., Fita, I., and Loewen, P. C. (2001). Enzymology and structure of catalases. *Adv. Inorg. Chem.* **51**, 51-106.
- Mario, S., Huijun, W., Ralf, L., and Reinhard, F. (2002). *Aspergillus nidulans* catalase-peroxidase gene (*cpea*) is transcriptionally induced during sexual development through the transcription factor StuA. *Eukaryot. Cell* **1**, 725-735.
- Meinhardt, H. (1983). A boundary model for pattern formation in vertebrate limbs. *J. Embryol. Exp. Morphol.* **76**, 115-137.
- Matters, G. L., and Scandalios, J. G. (1986). Effect of the free radical-generating herbicide paraquat on the expression of the superoxide dismutase (Sod) genes in maize. *Biochim. Biophys. Acta* **882**, 29-38.
- Oberegger, H., Zadra, I., Schoeser, M., and Haas, H. (2000). Iron starvation leads to increased expression of Cu-Zn-superoxide dismutase in *Aspergillus*. *FEBS Lett.* **485**, 113 -116.
- Parvatiyar, K., Alsabbagh, E. M., Ochsner, U. A., Stegemeyer, M. A., Smulian, A. G., Hwang, S.H., Jackson, C. R., McDermott, T. R., and Hassett, D. J.

- (2005). Global analysis of cellular factors and responses involved in *Pseudomonas aeruginosa* resistance to arsenite. *J. Bacteriol.* **187**, 4853-4864.
- Reveillaud, I., Kongpachith, A., Park, R., and Fleming, J. E. (1992). Stress resistance of *Drosophila* transgenic for bovine CuZn superoxide dismutase. *Free Radic. Res. Commun.* **17**, 73-85.
- Reveillaud, I., Niedzwiecki, A., Bensch, K. G., and Fleming, J. E. (1991). Expression of bovine superoxide dismutase in *Drosophila melanogaster* augments resistance of oxidative stress. *Mol. Cell. Biol.* **11**, 632-640.
- Saez, J. C., Kessler, J. A., Bennett, M. V., and Spray, D. C. (1987). Superoxide dismutase protects cultured neurons against death by starvation. *Proc. Natl. Acad. Sci. U. S. A.* **84**, 3056-3059.
- Sanders, B. M., Hope, C., Pascoe, V. M., and Martin, L. S. (1991). Characterization of the stress protein response in two species of *Collisella limpets* with different temperature tolerances. *Physiol Zool.* **64**, 1471-1489.
- Sevinc, M. S., Switala, J., Bravo, J., Fita, I., and Loewen, P. C. (1998). Truncation and heme pocket mutation reduce production of functional catalase HP11 in *Escherichia coli*. *Protein Eng.* **11**, 549-555.
- Smith, M. W., and Doolittle, R. F. (1992). A comparison of evolutionary rates of the two major kinds of superoxide dismutase. *J. Mol. Evol.* **34**, 175-184.
- Sumner, E. R., Shanmuganathan, A., Sideri, T. C., Willetts, S. A., Houghton, J. E., and Avery, S. V. (2005). Oxidative protein damage causes chromium toxicity in yeast. *Microbiology* **151**, 1939-1948.
- Sundaramoorthy, M., Kishi, K., Gold, M. H., and Poulos, T.L. (1994). The crystal structure of manganese peroxidase from *Phanerochaete chrysosporium* at 2.06-Å resolution. *J. Biol. Chem.* **269**, 32759-32767.

- Tripathi, B. N., Mehta, S. K., Amar, A., and Gaur, J. P. (2005). Oxidative stress in *Scenedesmus* sp. during short- and long-term exposure to Cu^{2+} and Zn^{2+} . *Chemosphere* [Epub ahead of print].
- Welinder, K. G. (1991). Bacterial catalase-peroxidases are gene duplicated members of the plant peroxidase superfamily. *Biochem. Biophys. Acta* **1080**, 215-220.
- Wilczek, G. (2005). Apoptosis and biochemical biomarkers of stress in spiders from industrially polluted areas exposed to high temperature and dimethoate. *Comp. Biochem. Physiol. C Toxicol. Pharmacol.* **141**, 194-206.

VITA

Bhagirathi Dash

428 VMRB . College of Veterinary Medicine and Biomedical Sciences . College
Station . TX 77843 . (979) 862-4976

Educational Background

Doctor of Philosophy in Toxicology, Texas A&M University at College Station,
December 2005

Master of Science in Entomology, Punjab Agricultural University at Ludhiana,
December 1999

Bachelor of Science in Agriculture, Orissa University of Agriculture and
Technology at Bhubaneswar, August 1997

Professional Experience

Dept. of Veterinary Integrative Biosciences, Texas A&M University
Graduate Research Assistant, January 2003 – December 2005

Dept. of Entomology, Texas A&M University
Graduate Research Assistant, September 2001 – December 2002

Dept. of Entomology, Indian Agricultural Research Institute at New Delhi
Senior Research Fellow, May 2000 – November 2000

Dept. of Entomology, Punjab Agricultural University
Junior Research Fellow, September 1997 – December 1999

Related Publications

Dash, B., Metz, R., Huebner, H. J., Porter, W., and Phillips, T. D. Molecular cloning and characterization of a heat shock protein 70 from *Hydra vulgaris*. In preparation.

Dash, B., Metz, R., Huebner, H. J., Porter, W., and Phillips, T. D. Molecular cloning and characterization of two superoxide dismutase genes (MnSOD and EC-SOD) from *Hydra vulgaris*. In preparation.

Dash, B., Metz, R., Huebner, H. J., Porter, W., and Phillips, T. D. Molecular cloning and characterization of a phospholipid hydroperoxide glutathione peroxidase and a monofunctional catalase from *Hydra vulgaris*. In preparation.